Synthesis, Formulation and Biological Evaluation of Novel Cationic Lipid Bio-conjugates for Potential Therapeutic Gene Delivery

THESIS

Submitted in partial fulfilment of the requirement

For the Degree of

DOCTOR OF PHILOSOPHY

(In Chemistry)

To

NATIONAL INSTITUTE OF TECHNOLOGY

WARANGAL

By

RAVULA VENKATESH

(Roll No. 716189)

Research supervisor

PROF. P. V. SRILAKSHMI

DEPARTMENT OF CHEMISTRY
NATIONAL INSTITUTE OF TECHNOLOGY, WARANGAL-506004
INDIA

NOVEMBER – 2021

DECLARATION

I hereby declare that the matter embodied in this thesis entitled **"Synthesis, Formulation and Biological Evaluation of Novel Cationic Lipid Bio-conjugates for Potential Therapeutic Gene Delivery"** is based entirely on the results of the investigations and research work carried out by me under the supervision of **Prof. P. V. Srilakshmi**, Department of Chemistry, National Institute of Technology, Warangal. I declare that this work is original and has not been submitted in part or full, for any degree or diploma to this or any other university.

I declare that this written submission represents my ideas in my own words and where others' ideas or words have been included, I have adequately cited and referenced the original sources. I also declare that I have adhered to all principles of academic honesty and integrity and have not misrepresented or fabricated or falsified any idea/data/fact/source in my submission. I understand that any violation of the above will be a cause for disciplinary action by the Institute and can also evoke penal action from the sources which have thus not been properly cited or from whom proper permission has not been taken when needed.

Date: 16-11-2021 (RAVULA VENKATESH**)**

Place: NIT Warangal **Roll Number: 716189**

Prof. P. V. Srilakshmi
Professor
Tel: +91-870-2462675
Fax: +91-870-2459547
Email: patrisrilakshmi@nitw.ac.in

Department Chemistry
National Institute of Technology
Warangal - 506 004,
Telangana, India.

CERTIFICATE

I certify that **Mr. RAVULA VENKATESH**, a bonafide student of Ph. D degree in National Institute of Technology, Warangal, has carried out research work under my direct supervision. The investigations, observations and the conclusions reported by him in this thesis entitled "**Synthesis, Formulation and Biological Evaluation of Novel Cationic Lipid Bio-conjugates for Potential Therapeutic Gene Delivery**" being submitted for the award of Ph. D degree in Chemistry are his original contributions to the Chemical Sciences. It is also certified that he has not submitted the same in part or in full to this or any other University for the award of a degree or diploma.

Date: 16-11-2021
Place: **Warangal**

(Prof. P. V. Srilakshmi)

DEDICATED TO MY BELOVED

FAMILY

ACKNOWLEDGEMENTS

My soul feels elevated with gratification, heart feels happy with emotions, and mind feels light with revelation of truth to thank all those who helped me to sail through this long journey to achieve the most cherished dream of my life. The journey would not have been completed without the efforts and help from my co-workers, friends and well-wishers who have been an integral part of this saga. I would like to thank every person whom I have encountered in my life, whose dreams have been part of my dreams and whose advice, respect, love and appreciation have been an important motivation in my career.

First and foremost, I am truly indebted and I express my earnest gratitude for my research supervisor **Prof. P. V. Srilakshmi**, Department of Chemistry, National Institute of Technology Warangal, for her inestimable expertise and astute guidance. Her unabated enthusiasm, which stems from her absolute command over the subject, has been a constant source of inspiration for me to work hard and the outcome is expressed in the form of this thesis. I will be forever thankful to her for her valuable guidance and constant encouragement.

I express my sincere thanks to **Prof. N. V. Ramana Rao**, Director, NIT Warangal, for giving me the opportunity to carry out my research work and for providing instrumentation facilities. I greatly acknowledge **Ministry of Education, Government of India,** for the financial support in the form of fellowship.

I wish to express my sincere gratitude to **Prof. Li-Fang Wang,** Department of Medicinal and Applied Chemistry, Kaohsiung Medical University (KMU), Taiwan, for her constant guidance, valuable suggestions and providing facilities to carry out a part of my research work at her lab during my doctoral research. I greatly acknowledge **TEEP@Asian Plus** for selecting me for a **Short term research internship program** at Kaohsiung Medical University, Taiwan.

I express my gratitude to the Doctoral Scrutiny Committee members: **Dr. Vishnu Shanker**, Chairman and Head, Department of Chemistry, **Prof. V. Rajeswar Rao**, Department of Chemistry, **Dr. B. Srinivas,** Department of Chemistry, and **Dr. Asit Kumar Khanra**, Department of Metallurgical and Materials Engineering, NIT Warangal, for their detailed review, constructive suggestions and excellent advice during the progress of this research work.

My sincere thanks to Prof. V. Rajeshwar Rao, Prof. K. V. Gobi, and Prof. P.V. Srilakshmi, Former Heads of the Department of Chemistry during the period of my research work. I would like to thank all the faculty members from Chemistry Department Prof. K. Laxma Reddy, Prof. A. Ramachandraiah, Dr. D. Kasinath, Dr. N. Venkatathri, Dr. Raghu Chitta, Dr. K. Hari Prasad, Dr.S. Nagarajan, Dr. M. Raghasudha, Dr. CH. Jugun Prakash, Dr. Ravinder Pawar, Dr. Mukul Pradhan Dr. Rajeshkhanna Gaddam Dr. V. Rajeshkumar for their cooperation and encouragement.

I would like to express my profound sense of gratitude and thanks to all my teachers who shaped my career right from the school.

I take this opportunity to thank all those scientists who guided me during my initial research career; Dr. Sridevi Annapurna Singh, Dr. Lalitha R. Gowda and Late Dr. K. Srinivasan from CSIR-CFTRI and Dr. Galla V. Karunakar form CSIR-IICT.

I convey my special thanks from the bottom of my heart to my seniors and juniors, Dr. Mallikarjun Gosangi, Dr. Venkanna Muripiti, R. Hithavani, M. Shireesha and Akash Kumar, for their continuous support and encouragement in each and every step of my research work.

I express my sincere gratitude to Dr. Yu-Lun Lo, for teaching me all the *in vitro* biological experiments during this doctoral research. My special thanks to all the members of Prof. Wang's lab, Dr. Ming-Fong Tsai, S. Yugendhar, Siva Shankari, Richa, Yi-Ting, Terry, Timmy, Jordan, Aly and Shawn, for being amazing friends and co-workers.

The unconditional love and untiring moral support extended towards me by my best friends over the years, Hari, Manoj, Dr. Subash, Dr. Geethinka, Vishnupriya, Dr. Anudeep, Dr. Dhanasree, Dr. Vidya, Dr. Yashaswini, Dr. Lalitha, Dr. Chinmayee, Dr. Safiya Nisar, Dhanasri, Dr. Mahendra Jadhav, Swathi and Dr. Huishen Ooi (San) is gratefully acknowledged. I wouldn't have come this far without the love, care, encouragement of these wonderful friends.

Many friends have helped me stay sane through these difficult years. With all happiness, I acknowledge the cheerful assistance rendered by all my research colleagues, Dr. K. Vimal Kumar**,** Mr. K. Sathish, Mr. A. Naveen Reddy, Mr. Ch. Raju, Mr. G. Ambedkar, Dr. K. Shekar, Dr. Chirra Suman, Dr. S. Suresh, Mr. T. Dhanunjaya rao, Mr. A. Ramesh, Dr. T. Sanjeeva, Ms. P. Sowmya, Mr. N. Satyanarayana, Mr. G. Srinath, Mr. G. Sripal Reddy, Mr. Karingula Sampath, Dr. M. Srikanth, Mr. K. Vijender Reddy, Mr. A. Bhargav sai, Ms. G. Sivaparvathi, Ms. T. Shirisha, Ms. B. Sravanthi, Mr. P. Venkatesham, Mr. B. Prashanth, Mr. R. Varaprasad, , Dr. J. Parameshwara Chary, Dr. V. Sunil Kumar, Dr. A. Ajay Kumar, Dr. K. Yugender, Dr. G. Ramesh, Dr. S. Nagaraju, Dr. B. Papalal, Dr. N.V. Bharath, Dr. A. Varun, Dr. K. Sujatha, Dr. K. Ramaiah, Dr. P. Vinay, Dr. P. Babji, Mr. R. Arun, Ms. Akanksha, Mr. B. Anjaiah, Mr. Madhu, Mr. Naik, Mr. B. Srikanth, Ms. Tohira Banoo, Ms. Khushboo Agarwala, Mr. Vijay, Mr. Subir and Dr. Vinay Raj (CSE).

I sincerely acknowledge the assistance provided by all the supporting staff, Department of Chemistry, NIT-Warangal.

The most pleasant part of this acknowledge is that it gives me a unique opportunity to thank my parents, **Shri. Ravula Lachaiah** and **Smt. Yadhamma,** and my beloved sister **Ms. Pravalika,** whose love and sacrifices have made me come this far**.** My deepest gratitude goes to my relatives and well-wishers for their unflagging love and unconditional support throughout my life and my studies.

(Ravula Venkatesh)

ABBREVIATIONS

Antp	:	Antennapedia
BBB	:	Blood-brain barrier
Boc	:	di-tert-butyl-pyrocarbonate
CLSM	:	Confocal laser scanning microscopy
CVC	:	Critical vesicular concentration
CPZ	:	chlorpromazine
DMAP	:	4-dimethylaminopyridine
DMF	:	Dimethylformamide
DMSO	:	dimethyl sulfoxide
DCM	:	Dichloromethane
DMEM	:	Dulbecco's modified Eagles medium
DMRIE	:	1,2-Dimyristyloxypropyl-3-dimethyl-hydroxyethyl ammonium bromide
DORIE	:	1,2-Dioleyloxypropyl-3-dimethyl-hydroxyethyl ammonium bromide
DOSPA	:	2,3-dioleyloxy-N-[2(sperminecarboxamidolethyl]-N,N-di-methyl-l-propanaminium trifluoroacetate
DOTMA	:	*N*-[1-(2,3-Dioleyloxy)propyl]-*N*,*N*,*N*-trimethyl ammonium chloride
DOTIM	:	1-[2-(9-(Z)-octadecenoyloxy)ethyl]-2-(8-(Z)-heptadecenyl)-3-(hydroxyethyl)imidazolinium chloride
DDAB	:	Dimethyldioctadecylammonium bromide
DOTAP	:	1,2-Dioleoyloxy-3-(trimethylammonio)propane
DC-Chol	:	3β-[*N*-(*N',N'*-dimethylaminomethane) carbamoyl] cholesterol
DOPE	:	1,2-dioleoyl-*sn*- glycero-3-phosphoethanolamine
DOPC	:	1,2-dioleoyl-*sn*- glycero-sn-3-phosphatidylcholine
DMDHP	:	(±)-*N*,*N*-[Bis(2-hydroxyethyl)]-*N*-[2,3-bis (tetradecano yloxy) propyl] ammonium chloride
ECL	:	Enhanced Chemi-Luminescence

EA	:	Ethylacetate
EDTA	:	Ethylenediaminetetraacetic acid
EDCI	:	1-(3-dimethylaminopropyl)-3-ethyl carbodi imide
FBS	:	Fetal bovine serum
FADD	:	Fas-associated death domain
FACS	:	Fluorescence-activated cell sorting
GFP	:	Green fluorescence protein
GSH	:	Glutathione
HOBt	:	1-hydroxybenzotriazole
LUV	:	Large unilamellar vesicle
ESIMS	:	Electrospray Ionisation Mass Spectroscopy
ONPG	:	*o*-nitrophenyl-β-D-galactopyranoside
Lipofect	:	LipofectAmine-2000
MTT	:	3-(4,5-Dimethylthiazol-2-yl)-2,5-diphenyl-tetrazolium bromide
NMR	:	Nuclear magnetic resonance
OD	:	optical density
OPG	:	Osteoprotegerin
PBS	:	Phosphate buffered saline
Pr	:	Propyl
pTRAIL		plasmid encoded TRAIL
r.t	:	room temperature
SAINT	:	1-methyl-4(dioleoyl)methyl-pyrimidinium chloride
TAT	:	Trans-activating transcriptional activators
TRAIL	:	Tumor necrosis factor (TNF)-related apoptosis-inducing ligand
TFA	:	Trifluorocetic acid
TMS	:	Trimethylsilyl
THF	:	Tetrahydrofuran
TLC	:	Thin Layer Chromatography
UV	:	Ultra Violet
X-SCID	:	X-linked severe combined immunodeficiency

TABLE OF CONTENTS

CHAPTER-I

INTRODUCTION

CHAPTER I
INTRODUCTION

1.1. GENE THERAPY: A PROMISING THERAPEUTIC STRATEGY

The knowledge that a genetic material can be delivered into particular cell types and its expression can lead to therapeutic outcome, has improved the patients' quality of life substantially. In view of this, the gene, which acts as a drug in the case of gene therapy, is packed within a vector to facilitate its entry into the patients' cells. In general, the notion of gene therapy is referred to as a therapeutic method which involves the use of a nucleic acid to genetically manipulate the patients' cells. Fundamentally, there are three kinds of gene therapy: *ex vivo*, *in vivo*, and *in situ*.[1] *Ex vivo* gene therapy involves removing the target cells from the patient's body and engineering them with the therapeutic gene or other genetic alterations that allow the disease's phenotype to be corrected. After that, the "corrected" cells are re-infused into the patient. This sort of treatment is also known as in vitro gene therapy, and it is particularly useful in the treatment of blood cancers. *Ex vivo* gene therapy is not necessarily the desired type of remedial treatment, depending on the tissue of interest. If the target organ is the liver, brain, spinal canal or vascular system, for example, another type of therapy called *in vivo* gene therapy is used. In this case, the therapeutic vector is delivered systemically to the patient's blood circulation or cerebral fluid, depending on the condition. Finally, there is a type of gene therapy in which the therapeutic gene is delivered *in situ*, that is, to a specific organ or area in the patient's body, either through direct injection, such as into the tumour or into appropriate brain areas, or through the insertion of a catheter in the case of the heart. Thus, *in situ* gene therapy can be considered as a branch of *in vivo* gene delivery. The procedure is chosen fully based on the type of indication, the afflicted tissue, and the cell type that needs to be corrected.[2]

The original purpose of gene therapy was to replace a faulty gene with a healthy one or to repair a damaged gene, hence confiscating disease symptoms. However, researchers have

expanded their focus beyond inherited genetic disorders to include additional ailments.[3-5] Initially, the DNA transfer was expected to be primarily used as a corrective/supplementary treatment for inherited genetic problems. Over the previous four decades, the possibility for treating a patient with gene transfer has grown exponentially in tandem with developments in molecular biology, but it has also suffered major obstacles and unforeseen complexity.[6-9] Aside from cancer, which is the most common experimental use of gene therapy, other acquired health conditions such as HIV and cardiovascular ailments are also being researched.[9] Multiple therapeutic techniques are being used to treat cancer, including augmenting tumour suppressor genes, triggering apoptosis, using suicide genes to kill tumour cells, and transferring replicative viruses. Currently, about 76% of all gene therapy clinical trials are directed towards cancer (65%) and inherited monogenic diseases (11%).[10] Other new gene therapy attempts are focusing on ailments such as diabetes, Alzheimer's disease, arthritis, and heart disease, which are all linked to genetic susceptibility to illness. Gene therapists are attempting to reduce or eliminate this risk. Gene therapy may one day help elderly people regain muscle strength and enhance the pumping capacity of their aged hearts.

Accepting both the benefits and drawbacks of gene therapy is a prerequisite for taking a position. Gene therapy will undoubtedly have an impact on the future of genetics. Interfering with evolution is a misguided worry. Gene therapy is one of the most promising ways being developed by researchers to produce a better society for future generations.

1.2. THERAPEUTIC GENES USED IN GENE THERAPY

In human gene therapy experiments, a wide range of gene types have been employed (**Figure 1.1**). Cancer has been the most frequently treated disease through gene therapy. The most often transferred gene types (antigens, tumor suppressors, cytokines, and suicide enzymes), as one might anticipate, are those utilised to fight cancer. These types account for 47.5 percent of trials, though it's worth noting that pathogen-specific antigens are also employed

in vaccinations.[10] In 7.0 percent of trials, growth factors were transferred, with many of these trials focusing at cardiovascular disorders. In 8.5 percent of studies, deficiency genes were employed, while in 11.6 percent, receptor genes were used (most frequently used for cancer gene therapy). In 2.1 percent of studies, marker genes were transferred, while in 3.7 percent of trials, replication inhibitors were utilised to combat HIV infection. In 2.0% of studies, oncolytic viruses (rather than specific therapeutic genes) were used to kill cancer cells, while 1.1 percent of trials used antisense or short interfering RNA to prevent the expression of a target gene.

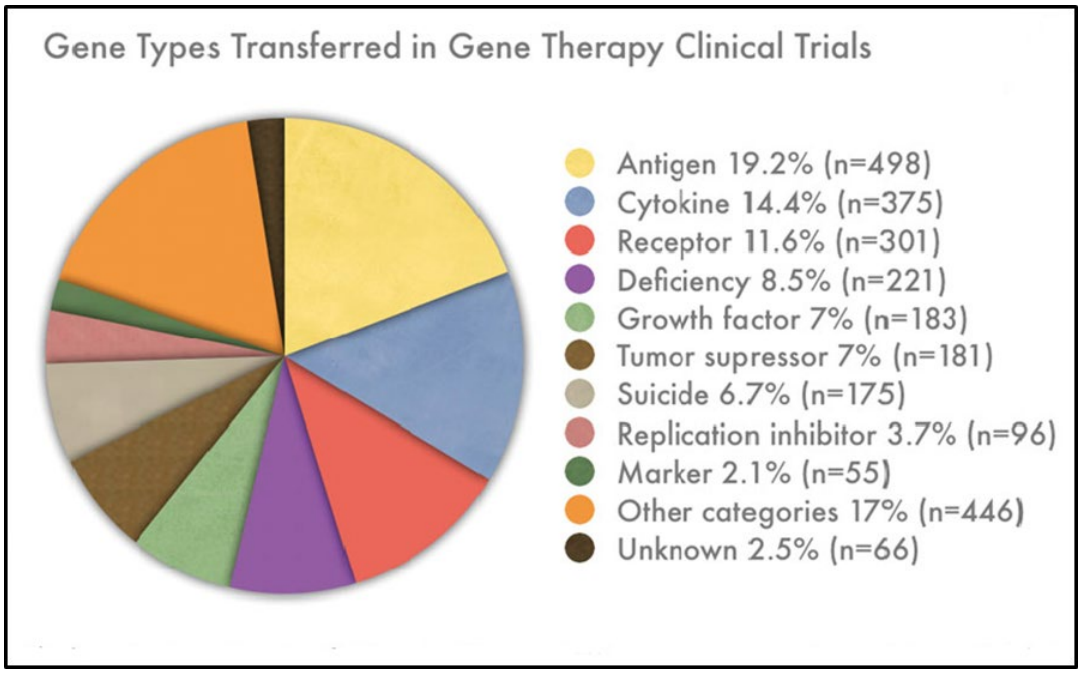

Figure 1.1: *Types of genes transferred in gene therapy clinical trials (Adopted from Ref. 10)*

Marker genes were transferred in 2.1% of trials, whereas 3.7% of trials used replication inhibitors to target HIV infection. Apart from these gene types, oncolytic viruses to destroy cancer cells and short interfering RNA to block the expression of specific gene, were used in minor studies.[10]

Despite the fact that the biological and clinical trial outcomes in monogenetic disease are well defined, scientific and technological advancements in recent decades, together with promising clinical evidence, have made cancer one of the most important disease targets for gene therapy. Several potential strategies for targeting cancer with gene therapy are currently

being investigated, including: (a) apoptosis induction through specific gene expression or elevating tumour sensitivity to traditional drug/radiation therapy; (b) introducing a wild type tumour-suppressor gene to recompense for its loss/deregulation; and (c) using an antisense (RNA/DNA) method to block the expression of an oncogene.; and (d) increasing the tumor's immunogenicity in order to enhance immune cell recognition.

The motivation for gene therapy to target the apoptotic mechanism stems from defective apoptotic signalling caused by mutations or abnormalities in the expression of pro- and anti-apoptotic genes, ensuing resistance to apoptosis in malignant cells. One of the most prevalent ways used in cancer gene therapy is to induce apoptosis by adding genes encoding an inducer, mediator, or executer of apoptosis.[11] Tumour necrosis factor-related apoptosis inducing ligand (TRAIL) is a type of apoptosis-inducing ligand that has been shown to destroy a wide range of tumour cells with low toxicity towards normal cells.[12] Another example of an apoptosis-inducer gene is melanoma differentiation associated gene-7 (mda-7), commonly known as Interleukin-24 (IL-24), belongs to IL-10 gene family that selectively induces apoptosis in various malignancies without causing harm to normal tissue.[13] Caspases and other apoptosis executioner genes work on cancer cells independently of the state of the apoptosis mechanism. Specific siRNA or microRNAs mediate the silencing of anti-apoptotic genes in cancer cells in a way to sensitise them to pro-apoptotic reagents or radiotherapy, which are common cancer gene therapy treatment approaches.[14]

The hypothesis that cancer is a genetic disease that develops through a multistage process in which inherited and somatic mutations in two classes of genes; proto-oncogenes and tumour suppressor genes, play major contributing roles, is now supported by overwhelming evidence based on familial, epidemiological, and cytogenetic studies.[15] Several tumour suppressor genes have been identified, including p53 (controls apoptosis and cell cycle),[16, 17] Rb (regulates cell cycle and differentiation),[18] p16INK/CDKN2 (controls cell cycle), and PTEN

(controls cell survival), and many attempts have been made to transport these genes explicitly to cancer cells.[19]

1.2.1. pTRAIL: A tumour-selective therapeutic gene

Tumour necrosis factor (TNF) is a crucial component of the immune system's homeostatic regulation.[20] TNF-related apoptosis-inducing ligand (TRAIL) belongs to the TNF superfamily that activates the pro-apoptotic death receptors, DR4 and DR5 to cause tumour-selective cell death. This type II transmembrane protein can be released in soluble form from the cell surface by proteolysis.[21] Normal cells are unaffected by soluble TRAIL, and healthy adult plasma contains a trace quantity of endogenous TRAIL (100 pg/mL).[22, 23] TRAIL has gotten a lot of attention lately, thanks to its capacity to induce tumor-selective apoptosis in multiple human cancer cell lines. In physiological setting, For TRAIL, there are five homologous human receptors: i) DR4 (TRAIL-R1) and ii) DR5 (TRAIL-R2), both of which are the full-length intracellular death domain (DD)-containing receptors; iii) the decoy receptor 1 (DcR1 or TRAIL-R3), which lacks an intracellular domain; iv) DcR2 (TRAIL-R4), which holds a truncated DD; and v) the soluble receptor osteoprotegerin (OPG).[24] Only the binding of TRAIL to DR4 or DR5, because of their integrated intracellular structure, can produce an apoptotic response. DR5 also has the strongest TRAIL affinity.[25] The death inducing signalling complex (DISC) is formed when the localized DDs of DR4 or DR5 bind to TRAIL and engage Fas-associated death domain (FADD) and procaspase-8. The activation of caspase-8 is triggered by the oligomerization and autocatalysis of procaspase-8, which results in the cleavage of the effector caspases-3/- 7/-9, causing apoptosis. In type II cells, caspase-8 also promotes the release of cytochrome c, resulting in intrinsic apoptosis via the mitochondrial pathway. Caspases 8 activates caspase-3 in type I cells, triggering apoptosis via the extrinsic pathway.[24] The mechanism of TRAIL-induced apoptosis is summarized in **Figure 1.2**.

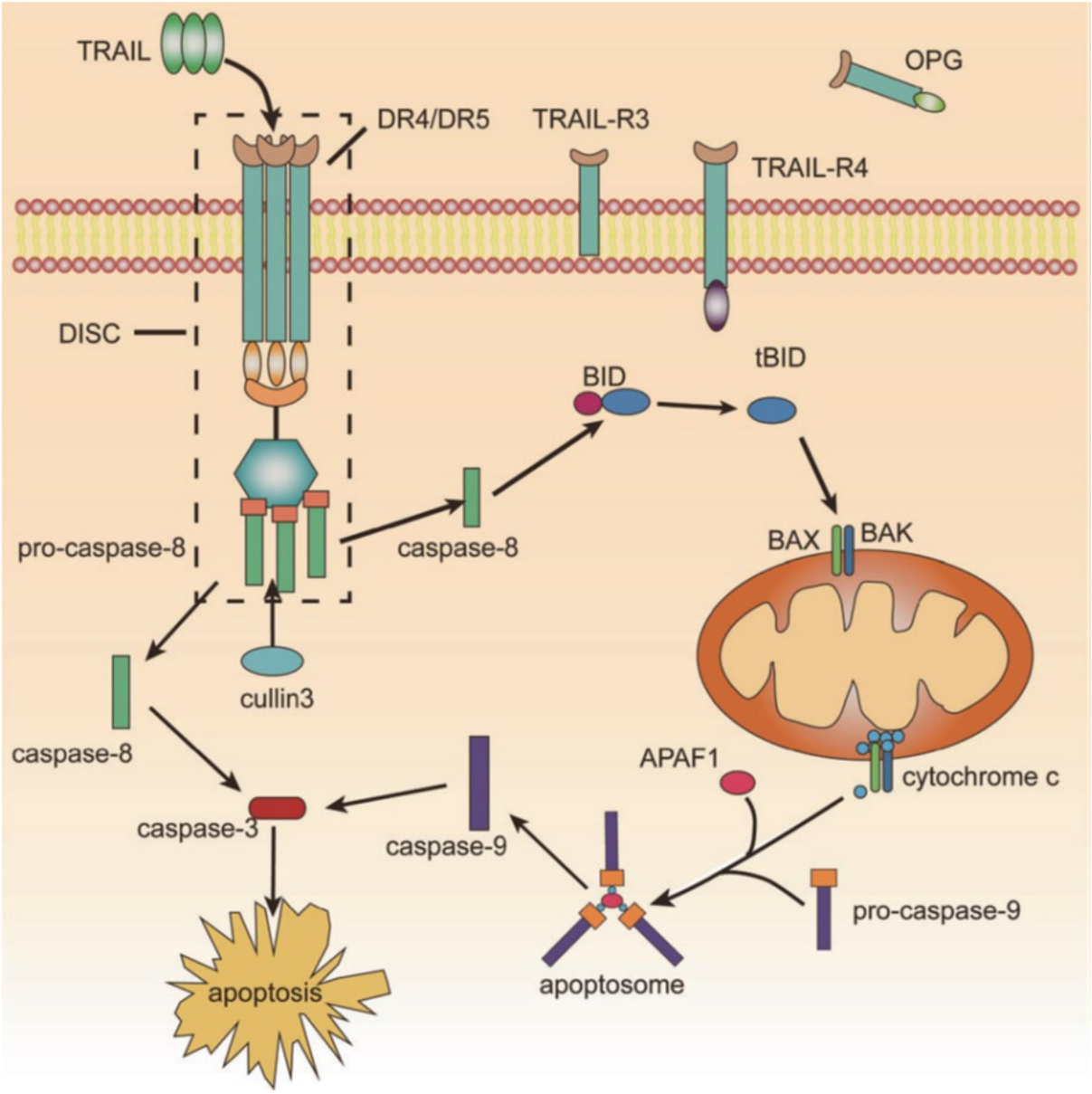

Figure 1.2: TRAIL-induced apoptosis pathway (adapted from Ref. 22)

The capacity of TRAIL's tumor-specific action to trigger cancer cell apoptosis while sparing normal cells is appealing, making TRAIL signalling a viable therapeutic target. However, TRAIL-based therapy has been hindered by three key drawbacks: a limited in vivo half-life, low tumor-targeting efficacy, and resistance to TRAIL monotherapy. Vector mediated TRAIL delivery could improve TRAIL stability and lengthen its half-life in the bloodstream, transport TRAIL to specific target areas, and overcome TRAIL resistance.[26] In comparison to direct TRAIL protein administration, TRAIL gene therapy has the distinct advantage of

delivering TRAIL-encoding DNA into tumour cells, allowing the TRAIL protein to be secreted locally on the membrane or in the tumour microenvironment, overpowering the disadvantages of recombinant TRAIL protein. Concerning TRAIL-based therapies, viral vectors are predominantly utilised for cell therapy, while non-viral vectors transport plasmid encoded TRAIL (pTRAIL) to targets.

1.3. GENE DELIVERY METHODS

Gene therapy relies on the introduction of exogenous nucleic acids into a cell to restore missing genes or mute overexpressed genes, allowing nearly any gene to be regulated with high specificity and efficiency. Therefore, employing nucleic acids as treatment has inherent advantages in terms of selectively drugging genetic targets which are otherwise very difficult to target by conventional protein or small molecule therapeutics.[27] However, due to its instability in physiological conditions and inability to penetrate the plasma membrane, direct delivery of nucleic acid is severely limited. This gives rise to the need for efficient gene delivery vectors to systematically carry and deliver the gene in controlled manner. Based on the use of the delivery vectors, the gene delivery methods can be categorized into following types (**Figure 1.3**).

1 Viral gene delivery

2 Non-viral gene delivery

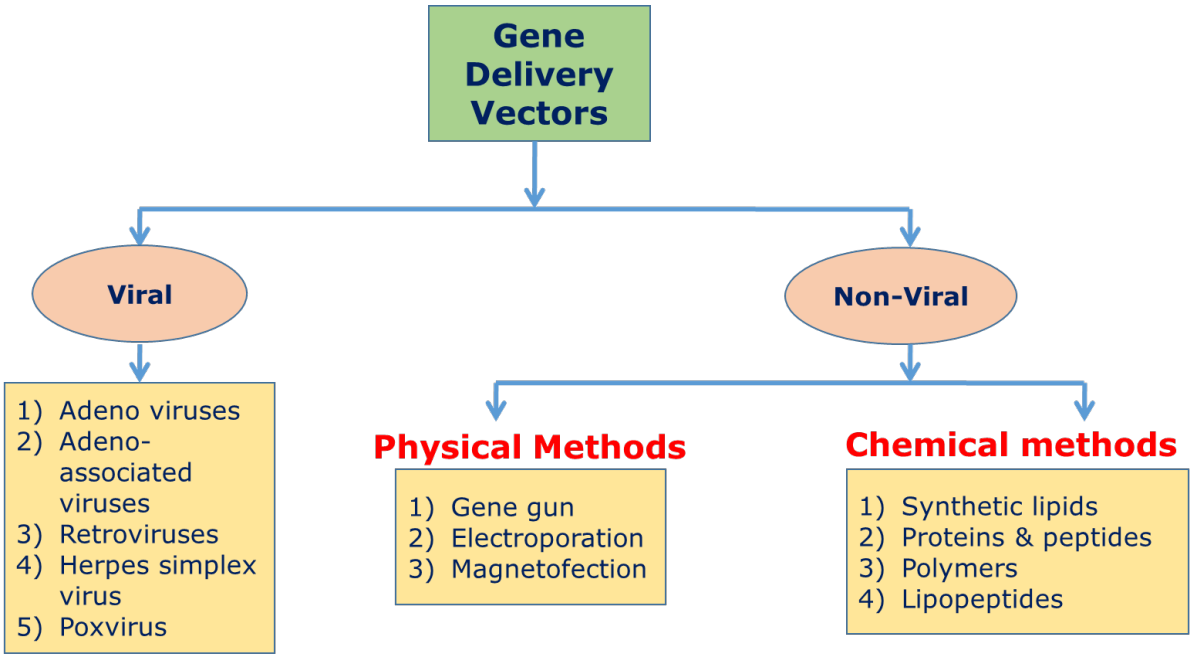

Figure 1.3: *Categorization of gene delivery vectors*

1.3.1. Viral gene delivery

Viruses are highly specialised obligatory intra-cellular parasites that have evolved to infect cells, typically with exceptional specificity to a certain cell type. They're usually quite good in transfecting their own DNA into the host cell, which is then expressed to make more viral particles. As a result, they're ideal for use as gene transfer vectors. Given the hundreds of clinical experiments that have been undertaken to date, it is clear that the vast majority of them have used genetically modified viruses to deliver nucleic acids to the target cells.[28] The recombinant viral vectors can transduce the cell type it would normally infect by replacing non-essential genes with foreign genes of interest during the replication phase of their life cycle. Non-essential genes are delivered in trans, either incorporated into the genome of the packaging cell line or on a plasmid, to construct such recombinant viral vectors. Because viruses developed as parasites, they all provoke an immunological response from the host. Despite the fact that a variety of viruses have been produced, the focus has been on four types: adenoviruses, adeno-associated viruses, retroviruses (includes gammaretroviruses and lentiviruses), and herpes

simplex virus type 1. The majority of clinical trials now being conducted around the world are based on these four kinds.[28-30]

Although the notion of viral gene therapy appears simple and uncomplicated, there are various issues and hazards that prevent the use of viral vectors in gene therapy. Viruses can frequently infect multiple cell types. As a result, when viral vectors are utilised to deliver genes into the body, they may infect both healthy and malignant cells. Another risk is that the new gene will be placed in the wrong spot in the DNA, potentially resulting in damaging DNA alterations or even cancer. The first death of a patient in clinical trials related to viral gene therapy was occurred due to a severe immunological reaction to the viral vector.[31] In what was thought to be the first big clinical stride forward for gene therapy, eleven individuals with X-linked severe combined immunodeficiency (X-SCID) responded very well.[32] Later research, however, found that four of the patients got leukaemia as a result of retroviral integration near an oncogene, which resulted in its upregulation.[33] Improper chromosomal integration results in either disrupted tumour suppressor gene expression or increased oncogene expression, resulting in cell malignancy. Purification and sequence verification of recombinant vectors are also time-consuming operations. Size limitation of the genetic material to be conveyed is also an added disadvantage when using viral vectors. As a result of these issues, viral gene therapy has been heavily scrutinised, prompting a rush to find safer alternatives to viral vectors. Scientists have been working on non-cytotoxic, effective non-viral techniques as a result of the problems associated with viral vectors.

1.3.2. Non-viral gene delivery

Naked DNA, particle-based, and chemical-based vectors are collectively called as non-viral vectors. They can be administered directly (plasmid DNA/Naked DNA), chemically, or physically. Non-viral vectors provide a significant safety benefit over viral vectors due to their reduced pathogenicity, low cost, and ease of manufacture. The bio-safety of non-viral vectors

is a big advantage. However, because of their poor delivery effectiveness and thus limited transient expression of their transgenes, non-viral gene transfer has been overlooked for a long time.[34] Because of their lower immunotoxicity, non-viral vectors have gotten a lot of interest. During the past decade, the use of non-viral vectors in clinical trials has increased significantly.[35] Because of improvements in efficiency, specificity, duration of gene expression, and safety, more non-viral vector products are entering clinical trials.

1.3.2.1. Physical Methods

Physical methods employ physical force to overcome the cell's membrane barrier, allowing genetic material to be delivered intracellularly. The introduction of simple DNA into local tissues or the systemic circulation utilising specialised tools or physical procedures is referred to as naked DNA delivery. The following has been described in terms of the devices and physical procedures utilised in delivery.

a. **Gene Gun:** Another physical form of DNA transfection is particle bombardment, sometimes known as the gene gun. DNA is coated with inorganic particles and loaded into a device that provides a force to allow the DNA/particles to penetrate the cells in this method. This procedure is quick, easy, and safe, and it has been used to deliver nucleic acids to cultured cells as well as cells *in vivo*, with particular success in gene transfer to skin and superficial wounds.[36]
b. **Electroporation:** Electroporation is a technique for forming temporary openings in cell membranes that allow DNA molecules to pass through. In cell culture, a high voltage of electric brief pulses is employed to cause pore creation but also a high rate of cell death. This approach can be used to transfect even the most challenging cell types. Because of the high incidence of cell death in this application, clinical trials are limited.[37]
c. **Magnetofection:** In this method, genetic material complexes with magnetic nanoparticle and the complex is introduced to the cells in culture plate. The field gradient created by rare

earth electromagnets placed beneath cell culture accelerates complex sedimentation and transfection. The therapeutic gene-magnetic particle complex is administered intravenously in the case of *in vivo*. The complex is captured and held at the target using powerful high gradient external magnets. The release of genetic material occurs through charge interaction, enzymatic cleavage of the cross-linkers, or matrix degradation. This technique is preferably used in *in vitro* setting to transfect primary cells and difficult-to-transfect cells.[38-40]

d. Sonoporation: Sonoporation is a noninvasive site-specific approach that uses ultrasound waves to permeabilize the cell membrane momentarily, allowing DNA to be taken up by the cells. The genetic material of interest is encapsulated in a tiny bubble and injected into the bloodstream. Following that, ultrasound is applied externally. The ultrasonic wave cavitates a micro bubble within the target tissue's microcirculation, causing physiological effects that culminate in targeted therapeutic gene transfection.[41]

e. Microinjection: In this procedure, the DNA is injected straight into the nuclei of particular cells using a thin glass needle under a microscope. Although this strategy is straightforward, it is the most challenging to put into practise in clinical settings. Though this technique of gene transfer is approximately 100% efficient, it is difficult and laborious, with just a few hundreds of cells (e.g., 500) can be transfected in each experiment.[42]

Apart from the abovementioned physical methods, there are methods like photoporation, hydroporation and mechanical massage which however, are scarcely documented.[43] The naked DNA delivery technologies have a slew of drawbacks that make them unsuitable for clinical use. The size, shape, and polyanionic charge of systemically injected naked DNA may affect the cell permeability of DNA. Every physical method relies on a specific type of apparatus to transport the DNA, which is responsible for a significant amount of cell death in almost all approaches. Another significant issue that prevents physical approaches from being used *in vivo* is DNA degradation.

1.3.2.2. Chemical Methods

Chemical methods of non-viral gene therapy have received the great attention and are currently under the most extensive investigations. These methods generally involve the use of chemically modified carriers or vectors to deliver gene to the desired cells. Chemical vectors are broadly categorized into inorganic particles, polymer based, peptide based, and lipid based. These non-viral approaches have a number of advantages over viral methods, including ease of large-scale synthesis, low host immunogenicity, and no limit on insert size. Brief introduction to each type of chemical non-viral vectors is given below,

a. **Inorganic particles**: They are nanoparticles that can be fabricated to escape from the reticuloendothelial system or to shield an entrapped molecule from degradation by altering their size, shape, and porosity. The most investigated materials in this category are quantum dots, magnetic nanoparticles, carbon nanotubes, silica, and gold nanoparticles.
b. **Quantum dots:** Quantum dots are nanoscale materials that generate fluorescence when exposed to light and electricity, making them extremely useful for labelling and tracking proteins inside cells.[44] Although fluorescently labelled DNA complexes can demonstrate the interaction of the carrier and DNA, pinpointing the point of separation is difficult since the two components must disperse a given distance before being recognised as separate entities. The donor-acceptor separation distances in quantum dot-based FRET analysis of protein are smaller than 100 nm, demonstrating the possibility of monitoring the unpacking of DNA nanoplexes following endocytosis.[45]
c. **Magnetic Nanoparticles:** An external magnetic field could be used to boost cellular uptake of magnetic nanoparticle-containing gene vectors *in vitro* and increase transfection efficiency to targeted tissues/organs *in vivo*. Magnetic nanoparticle-based gene carriers can be made from superparamagnetic iron oxide nanoparticles, which have good biocompatibility and superparamagnetism. Magnetic nanoparticles have distinct benefits

over conventional gene delivery technologies, such as fast transfection, magnetic targeting, isolation/positioning of transfected cells, and molecular imaging.[46]

d. Carbon nanotubes: Carbon nanotubes predominantly consist two classes of nanomaterials, including single-wall carbon nanotubes and multiwalled carbon nanotubes. These nanomaterials have some positive attributes such as substantial strength, high surface area, needle-like structure, high drug loading capacity, flexible interaction with cargo, outstanding optical and electrical features, high stability, and ability to release therapeutic agents at targeted sites. On the other hand, their toxicity due to lack of biodegradability has been severely hindering effective applications.[47]

e. Silica: The most often utilised silica as a gene delivery agent is generated by functionalizing nanoparticles with amino silicanes. Their advantages over the organic nanosystems are generally their stability in physiological settings and easily modifying surface. Its lower delivery effectiveness in the presence of serum-containing medium is a primary limiting factor due to serum protein interactions.[48]

f. Gold nanoparticles: Researchers were drawn to gold nanoparticles because of their ease of synthesis, unrestricted surface characterization, and inert nature. Gold nanoparticles absorb light in the infrared spectrum. Near infrared light has the ability to penetrate deep into tissues. The photo thermal effect can be utilised to transfect a cell by modifying the surface of gold with DNA. The photo thermal effect causes thermal denaturation, which serves to control gene release. *In vitro* studies have shown that gold transfection efficiency is comparable to that of lipoplexes. However, because of its great chemical stability, it is difficult to dissolve in cells, resulting in particle accumulation that might impair cell growth.

Other inorganic nanomaterials including, calcium phosphate particles, fullerenes (soluble carbon molecules), and supramolecular systems have also showed promise in in *in vitro* and animal models. These inorganic nanoparticles' surfaces can be coated to aid DNA binding. Small particles, according to the theory, can readily bypass most physiological and cellular

barriers, resulting in increased transfection efficiency. To accelerate their clinical application, more research is needed on long-term safety, surface functionalization, and the effect of size, shape and type on transfection efficiency.

g. Polymeric based vectors: Cationic polymers are a viable alternative vectors for viral gene therapy that are relatively safe, predictable and biodegradable. Endocytosis-based delivery could be achieved via synthetic polymer-based carriers coupled to the targeted gene or other biological molecules.[49, 50] As a result, chitosan, PEI, polylysine, polyamino ester, and other polymers have been studied for gene delivery.[51, 52] Cationic polymers combine with DNA to generate polyplexes, which are nanoscale complexes. Natural and synthetic polymers are the two types of polymers used in gene therapy.

Natural- proteins, peptides, polysaccharides.

Synthetic- Polyethylene mine (PEI), Dendrimers, and Polyphosphoesters. Some of the majorly studied polymeric gene vectors are discussed below.

i. Polyethylenimine (PEI): PEI is regarded as the gold standard for gene transfer *in vivo* and *in vitro*. Cationic polymers possess high-density amine moieties that act as a protein sponge, preventing acidification of endosomal pH. This causes an influx of chloride into the compartment and an increase in osmotic pressure, causing endosomal membrane thickening and rupture.

ii. Chitosan: It's a cationic polysaccharide-based natural polymer which is one of the most extensively researched non-viral vectors. Even at large concentrations, it shows low toxicity. It is a glucosamine-based linear cationic polysaccharide. Chitosan's positive charge electrostatically attaches to DNA's negative charge. Chitosan/DNA polyplexes are frequently employed in oral and nasal gene therapy due to their mucoadhesive characteristics. Chitosan is conjugated to folic acid to successfully evade intracellular obstacles.

iii. **Poly (DL - Lactide) (PLA) and Poly (DL -Lactide- co- glycoside) (PLG A):** They're biodegradable polyesters that go through bulk hydrolysis to provide long-term delivery. The citric acid cycle removes the breakdown products. The FDA has approved PLGA as a protein delivery vehicle. They are easily phagocytosed by antigen presenting cells and cause an immunological response since they are less than 10 m in size.

iv. **Dendrimers:** Dendrimer molecules have symmetrical size and form, as well as functional terminal groups. When positively charged peripheral groups interact with nucleic acids at physiological pH, it attaches to genetic material. It can interact well with cell membranes, proteins and organelles, because of its nanometric size. The toxicity profile is determined by the terminal amino group and positive charge density.

v. **Polymethacrylate:** Polymethacrylates are a vinyl-based polymers capable of reducing polynucleotides to nanometer-sized particles. However, due to their restricted capacity to interact with membranes, transfection is limited.

vi. **Proteins and Peptides:** Proteins and peptides provide a one-of-a-kind approach of delivering genetic materials by direct conjugation to olegonucleotides, with excellent efficiency and cell specificity. Because peptide vectors use short sequences of basic amino acid residues that may easily traverse the plasma membrane, they have high efficiency. Protein transduction domains, also known as cell-penetrating peptides, are split into two categories: (1) lysine-rich peptides (e.g. MPG peptide and transportan) and (2) arginine-rich peptides (e.g. antennapedia (Antp), trans-activating transcriptional activators) (TAT).[53] The peptide is usually covalently bonded to the oligonucleotide construct rather than complexed via electrostatic interactions in peptideoligonucleotide delivery techniques. Several methods are used to make these peptideoligonucleotide complexes. Haralmbidis et al. were the first to use solid phase synthesis methods to create peptide-oligonucleotide constructs.[54]

h. Lipid based vectors: Cationic lipids, structural analogues of surfactants, have an interesting property to self-assemble in aqueous solution to produce bilayer membrane type vesicles. These artificially manufactured vesicles comprised of lipid bilayers are called as liposomes. Liposomes are biomimetic membranes that can easily diffuse across cell membranes and into the cytoplasm. Liposomes have multiple qualities that may be beneficial in a variety of applications due to their chemical composition, structure, and colloidal size, all of which can be easily controlled via preparation procedures. Colloidal size, or rather homogenous particle size distributions in the range of 20 nm to 10 μm is one of the most essential attributes. On the other hand, specific membrane and surface features such as bilayer mechanical characteristics, phase behaviour, permeability, charge density, and the attachment of specific ligands, altogether make liposome an attractive nanomaterial for drug/gene delivery. Liposomes are also effective solubilizing systems for a variety of chemicals due to their amphiphilic nature. Liposomes have several unique biological traits, including selective interactions with biological membranes and diverse cells, in addition to the physical qualities.

1.4. LIPOSOMES: NATURE'S NANOTECHNOLOGY!

Liposomes are lipid spheres or spherical bilayers made up of individual lipids with an aqueous centre. Liposomes have long been regarded as biocompatible gene/drug delivery reagents due to their structural similarities to cell membranes. Each lipid has a polar hydrophilic head group that is linked to a hydrophobic domain via a linker. Above a certain critical vesicular concentration (CVC), these amphiphiles spontaneously form huge spherical structures known as liposomes when exposed to an aqueous environment. Lipids are organised in bilayers within the sphere, with the polar hydrophilic group facing outwards, shielding the hydrophobic portion from the aqueous medium. Liposomes can be unilamellar (made of a single bilayer) or multilamellar (consisting of many bilayers). Upon sonication and repeated extrusion of

multilamellar vesicles (MLV) through polycarbonate membranes with predetermined pore sizes, they shrink to the size of a small unilamellar vesicles (SUV, 30-100 nm) or a large unilamellar vesicle (LUV, 150-250 nm) (**Figure 1.4**).

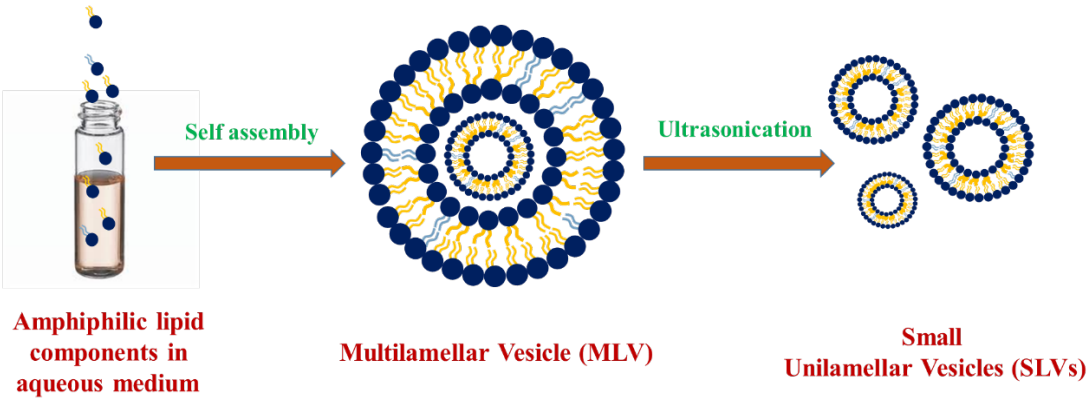

Figure 1.4: *Schematic representation of liposome formation*

Hydrophilic molecules can be encapsulated in hydrophilic portion inside a hydrophobic membrane of a liposome and the dissolved hydrophilic solutes cannot easily flow through the lipids. Liposomes may carry both hydrophobic and hydrophilic molecules because amphiphilic self-assembled structures. The lipid bilayer can fuse with other bilayers, such as the cell membrane, to transfer the molecules to the areas of action, therefore delivering the liposomal contents. Liposomes can deliver plasmid DNA, RNA, DNA-RNA chimaeras, oligonucleotides, antisense molecules, synthetic ribozymes, and other biomolecules. Cationic liposomes could also accomplish targeted distribution through covalent conjugation of receptor-specific ligands to the liposomal surface. Encapsulating DNA into ordinary liposomes could be a technical challenge, because of the plasmid size, leading to poor transfection. In this context, a new technology based on cationic lipids and PE was introduced in the late 1980s.[55]| To condense plasmids more efficiently and transfer DNA into cells, positively charged lipids were used to neutralize the negative charge of plasmids. In general, this is a straightforward method that

involves combining cationic lipids with DNA and injecting them into cells. Aggregates of DNA and cationic lipids form as a result of this process.

Felgner et al. were the first to describe non-viral cationic lipid mediated gene transfer using the cationic lipid DOTMA.[55] This lipid creates multilamellar vesicles (MLV) that can be sonicated to form small unilamellar vesicles when used alone or in conjunction with other neutral lipids (SUV). DNA spontaneously forms lipoplexes with DOTMA, with 100 percent of the DNA getting attached. Complex formation is thought to be the result of electrostatic interactions between DOTMA's positively charged head group and DNA's negatively charged phosphate groups. DOTMA is sold as a one-to-one mixture with DOPE (Lipofectin., Gibco-BRL, Gaithersburg, MD) and has been widely used to transfect a range of cells.[56-58] In order to minimise DOTMA's cytotoxicity, a variety of metabolizable quaternary ammonium salts with effectiveness comparable to Lipofectin in combination with DOPE have been created.[59]

1.4.1. Lipofection Pathway: Mechanism of lipoplex mediated transfection

Lipofection is a method of inserting desired functional material into cells, such as active nucleotide, by passing liposomal vesicles through the cell membrane. The process involves steps such as, (a) formation of lipoplex (lipid-DNA complex); (b) lipoplex binding to the surface of cell; (c) internalization of the lipoplex through endocytosis; (d) endosomal escape of lipoplex to the cytosol; (e) passage of the released DNA from endosome to the nucleus and its transgene expression **(Figure 1.5)**. Each stage in the lipofection pathway encounters obstacles, reducing the overall efficiency of the process.

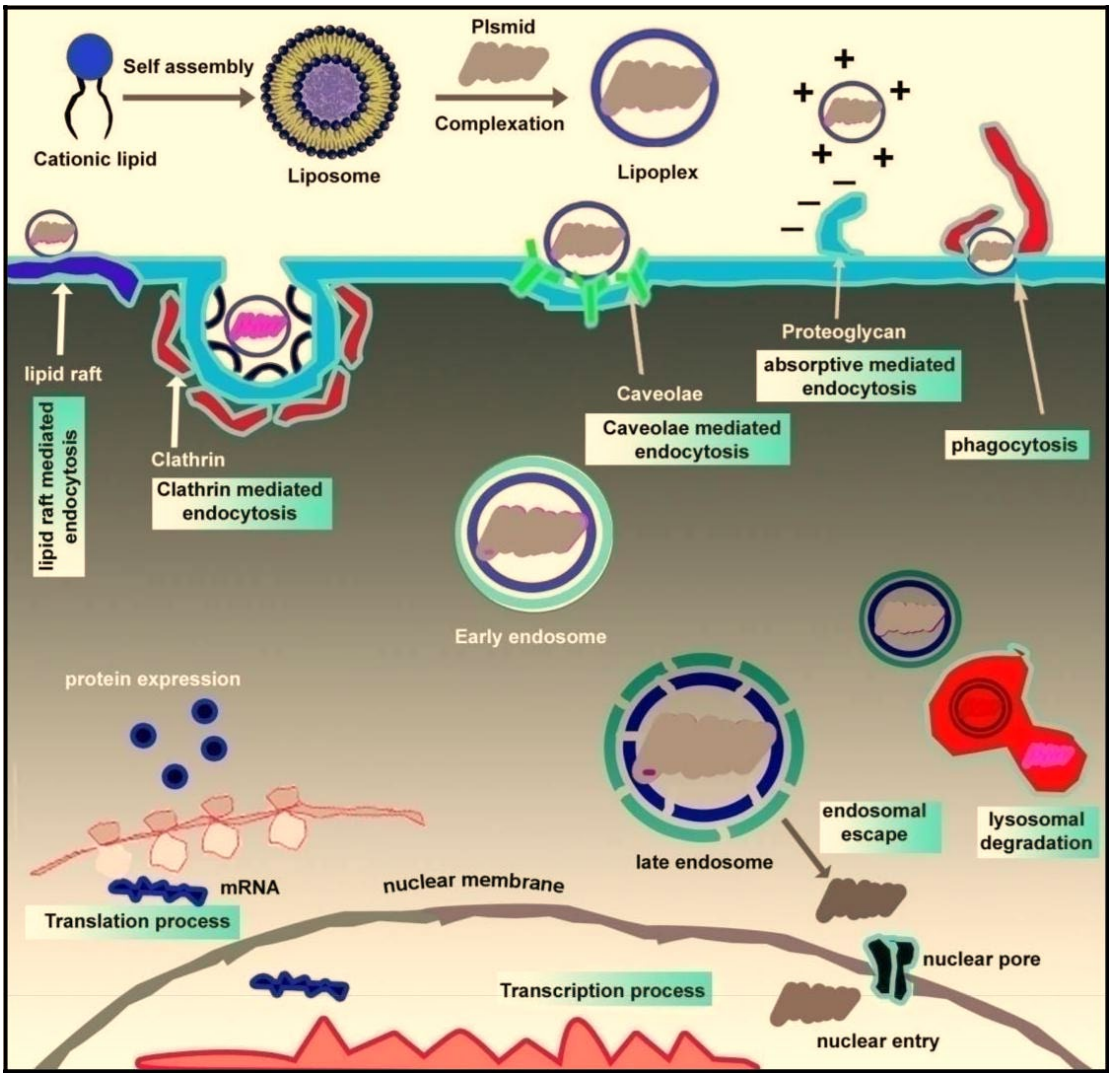

Figure 1.5: *Schematic of lipofection pathway*

Step (a). Formation of lipoplex

Lipoplexes are supramolecular complexes formed by the ionic attraction of positively charged lipid vesicles to plasmid DNA's negative termini. Initially, it was thought that many liposomes would bind to a single plasmid molecule, neutralizing its charge and condensing the DNA to form a tiny dense lipoplex.[60] However, electron microscopy examinations have revealed pictures of lipoplexes having macromolecular structures with widths ranging from 100 to 200 nm.[61-63] The lipoplexes' small size is assumed to be owing to DNA complexation or condensation, which results in elongated, 'spaghetti'-shaped lipoplexes that are thought to represent DNA sandwiched between the lipid bilayer and the bilamellar layer.[64] Large

aggregates, sometimes known as 'meatball' lipoplexes, have been discovered and are thought to contain many lipid and DNA molecules. It's unclear which of these reflects the proportion with the highest transfection efficiency.

Step (b). lipoplex binding to the surface of cell

Because of the large concentration of glycoproteins and glycolipids with negatively charged sialic acid residues, the cell membrane is negatively charged. The binding of the lipid-DNA complex to the cell membrane is mostly electrostatic in the absence of a receptor-specific targeting ligand. Internalization of the lipid-DNA complexes occurs mostly by endocytosis, according to electron microscopic investigations.[65] In the peri-membranous area, the lipid-DNA complex is absorbed by lower pH compartments known as "early endosomes." However, the possibility of membrane fusion playing a role in cellular absorption cannot be totally dismissed. DOPE and other co-lipids aid cellular absorption by facilitating fusion with cell membranes.[66]

Step (c). Internalization of the lipoplex through endocytosis

Non-viral vector produced lipoplexes were engulfed by the bilayered plasma membrane by endocytosis, according to studies on cell entrance and intracellular trafficking.[67] Few endocytotic pathways, such as caveolae-mediated endocytosis via caveolae vesicles and/or lipid-raft,[68] clathrin-mediated endocytosis via coated pits, adsorptive mediated endocytosis via proteoglycan fusion,[69] macropinocytosis, and phagocytosis, have been recognised and thoroughly described.

Lipoplexes can be uptaken by any of the above-mentioned mechanisms or by many pathways, as shown in **Figure 1.5**. Each endocytotic mechanism interacts with a variety of proteins and propels the lipoplexes into the early endosome phase, where the inner pH is greater than 5. Much of molecular biology research has been successful in identifying inhibitors that selectively suppress the expression of specific proteins, resulting in the blockage of the corresponding pathway. While clathrin-mediated endocytosis is inhibited by chlorpromazine (CPZ), caveolae-mediated endocytosis is inhibited by methyl— cyclodextrin (m—CD) or

filipin-III.[68] Cytochalasin D inhibits macropinocytosis by affecting actin polymerization and membrane ruffling.[70] Vesicle trafficking is aided by Wortmannin, a PI 3-kinase inhibitor that promotes vesicle fusion.[71] Nocodazole has been shown to limit the build-up of complexes in endosomes by blocking the transfer of complexes from endosomes to lysosomes.[72] Bafilomycin A1 is a potent inhibitor of vacuolar ATPase, a key enzyme in lysosome acidification.[73] Cholesterol sequestration with nystatin was also employed to assess the manner of internalisation. **Table 1.1** lists all of the inhibitors that correlate to specific endocytosis routes, as well as their effective concentrations.

Step (d). Endosomal escape of lipoplex to the cytosol

Endosome rupture or unfolding releases packed DNA material into the cytoplasm prior to destruction in the lysosome, which is one of the important steps in determining transfection efficiency. Following internalisation, the coated vesicle becomes an early endosome, which is followed by acidification of the vesicular lumen, eventually leading to the late endosome stage. Although the mechanism of DNA release from the endosome to the cytosol is unknown, several hypotheses have been developed to explain the mechanistic understanding. Local endosomal membrane instability is caused by electrostatic interactions between cationic lipoplex and anionic lipids of the endosomal membrane, which cause anionic lipids to be displaced from the cytoplasm and form a charge neutral ion pair with the cationic lipid, according to Xu & Szoka.[74] By way of the so-called flip-flop process, this can trigger destabilisation of the endosome membrane, which leads to decomplexation of the DNA. Non-cationic helper lipids, such as neutral DOPE, may also assist membrane fusion and speed up the pace of endosomal membrane destabilization.[75-77] DOPE does have a tendency to produce an inverted hexagonal phase, which is frequently observed when membranes are fused.

Table 1.1*: Inhibitors of the endocytosis pathway and their optimal doses*

	Inhibitor	**Pathway**	**Concentration**
1	Chlorpromazine	Clathrin	10 g/ml
2	Filipin-III	Caveolae	5 g/ml
3	Cytochalasin D	Actin	5 M
4	Wortmannin	Macropinocytosis	25M
5	Nystatin	Caveolae	25 g/ml
6	Methyl-β-cyclodextrin	Clathrin and caveolae	7.5 M
7	Nocadazole	Microtubules	10 M
8	Bafilomycin A1	Vacuolar-type H(+)-ATPase	2.5 nM

Step (e): Passage of the released DNA from endosome to the nucleus and its transgene expression

The most significant stumbling block to effective gene transfer may be the transit of DNA from the cytoplasm to the nucleus. After escaping endosomes, the nucleic acid must travel through the cytoplasm and into the nucleus, overcoming obstacles such as cytoplasmic nuclease destruction and limited cytoplasmic DNA mobility. Two alternative ideas exist for how cytoplasmic pDNA enters the nucleus: cytoplasm mixing following the loss of the nuclear membrane during mitosis[78] and direct entry via the nuclear pore complex.[79] Mitotic activity for the lipoplexes has consistently been shown to greatly enhance gene transfer in cultured cells. This could imply that tumour cells are more targetable due to their multiple mitosis, but non-dividing cells, such as healthy brain cells, are rarely transfected. Nuclear localization sequences (NLS) can be introduced into DNA complexes to transfer the plasmid into the nucleus for delivery to non-dividing cells. NLS are short peptide sequences (5–25 amino acids) that are required and sufficient for nuclear protein localisation.[79] These sequences can be integrated into

cationic lipid complexes,[80] or they can be connected directly to the plasmid.[81] Despite this, the transfection outcomes of nondividing endothelium cells with and without the addition of a NLS are 5 percent and 80 percent positive, respectively.[80]

1.4.2. Structural aspects of cationic lipids and their role in lipofection

A hydrophobic domain, linker functionality, and a cationic head-group make up the molecular architecture of cationic transfection lipids. It's vital to remember that the transfection efficiency is governed by a combination of factors, not just one element of the cationic lipid. The overall structure of the lipid determines the properties of the head group, hydrophobic moiety, and linker regions that define efficient gene transfer. Different forms of lipids may have unrelated structural requirements for transfection when it comes to the optimal length of hydrocarbon chains, polar head groups, and chemical nature of linkages. As a result, a modular approach is beneficial when planning and designing new vectors. The effect of alterations in the chemical structures of the cationic lipids can be used to determine trends in liposome aggregation capabilities. The understanding of the structure–activity relationship (SAR) and systematic adjustment of each portion are crucial variables for achieving optimal performance.

a. **Hydrophobic region:** Cationic transfection lipids' hydrophobic domains are mostly made up of simple aliphatic hydrocarbon chains or steroid. The majority of commonly used cationic transfection lipids, such as DOTMA[55] and SAINT,[82] have two linear aliphatic chains in their hydrophobic domains. In general, lipids with one hydrocarbon chain tend to form micelles, transfect poorly, and are toxic. On the other hand, cationic lipids with three aliphatic chains tend to transfect poorly in comparison with lipids of two hydrocarbon chains.[83] In contrast, a variety of cationic lipids with either a single cholesterol or a tocopherol moiety in hydrophobic areas have been described as the best transfecting agents, with enough hydrophobic regions to participate in self-assembly and generate unilamellar vesicles.

b. **Head group region:** Cationic transfection lipids with positively charged nitrogen head groups attached to hydrophobic tails often have a single quaternary ammonium group (DOTMA, **Figure 1.7**), polyamine moieties (DOSPA,[84] **Figure 1.8**), and guanidinium salts (BGBH,[85] **Figure 1.9**). Several cationic lipids with heterocyclic head groups (e.g., pyridinium, piperizine, imidazolium (SAINT,[82] NCC10[86] & (C16Im2)C2,[87] **Figure 1.7 & 1.8**) as well as amino acid head-groups (e.g., lysine, arginine, ornithine, Histidine, and tryptophan) have also been described.

c. **Linker moieties**: The type of the linker bond that connects the cationic head group and the hydrocarbon anchor determines their relative orientation. A cationic amphiphile's conformational flexibility, degree of stability, biodegradability, and thus gene transfer effectiveness are all controlled by the linker group. Ethers (e.g., DOTMA, **Figure 1.7**) are chemically stable yet non-biodegradable, and have been found to provide greater transfection efficacies while producing toxicities due to their long-term persistence. Esters (for example, DOTAP,[88] **Figure 1.7**) are biodegradable and less poisonous, although they are not chemically stable. The hydration level of a lipid is determined by the length of the linker. The incorporation of ester function as a linker in tocopherol-derived lipids was done in order to develop less toxic and more powerful transfecting reagents. The phosphate di-ester bond (as found in DOPE) is biodegradable and has a chemical stability that is higher than that of esters but lower than that of amides. Phosphonates, on the other hand, are more hydrolytically stable than phosphates and are likely biodegradable.[89]

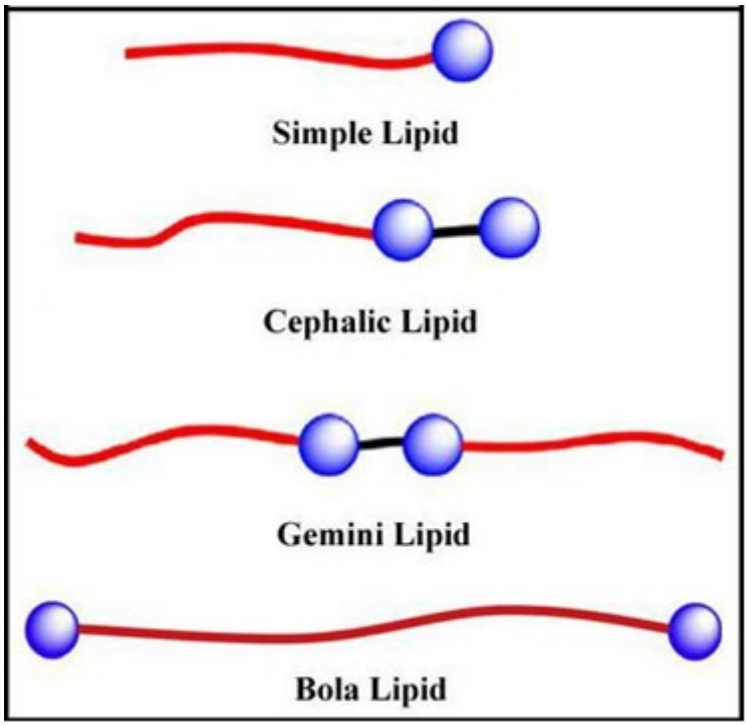

Figure 1.6: *Types of cationic lipids*

1.4.3. Types of Cationic Transfection Lipids

The discovery of cationic liposomes-based formulations for transfecting cultured cells by Felgner et al.[55] sparked the creation of a wide spectrum of cationic lipid-based reagents for gene therapy.[90, 91] Depending on the type of the head group, hydrocarbon anchor, or linker bonds, cationic transfection lipids can be divided into several categories and sub-groups. They can be neatly categorised into the following groups based on the orientation of the head group in relation to structural features: (**Figure 1.6**):

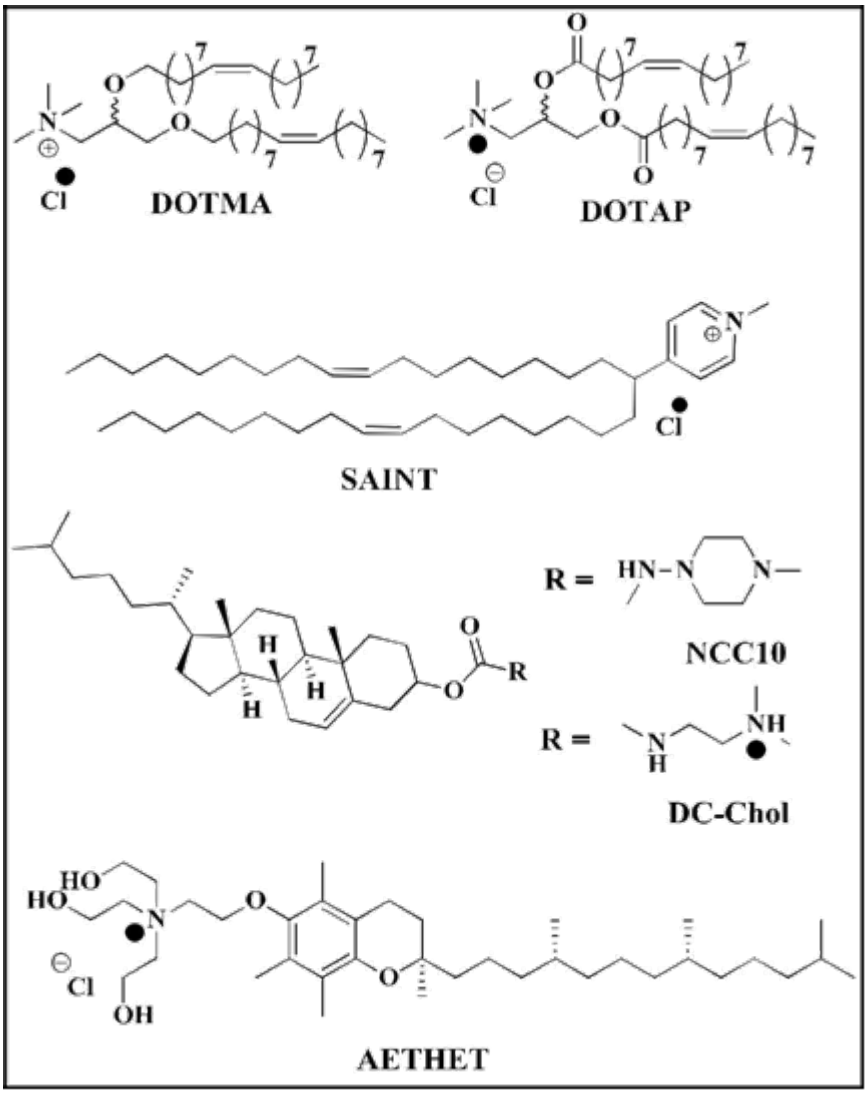

Figure 1.7: *Chemical structures of simple lipids with mono cationic head groups in the form of quaternary ammonium cations (DOTMA,DOTAP, DC-Chol & AETHET) or delocalizable cation (SAINT) while their hydrophobic anchoring groups made up of aliphatic long alkyl chain (DOTMA, SAINT) or cholesterol (NCC10, DC-Chol) or tocopherol (AETHET).*

a. **Simple cationic lipids:** Simple surfactants that can able to produce bilayer membrane vesicles while expose to hydration, commonly made up of from one cationic charge either simple (DOTMA) or delocalized (SAINT) as hydrophilic head group connects to a hydrophobic back bone usually arises from dialkyl long aliphatic chain or one steroidal skeleton from cholesterol (NCC10, DC-Chol) or vitamin-E[92-94] (AETHET)[92] considered as simple cationic lipids (**Figure 1.7**).

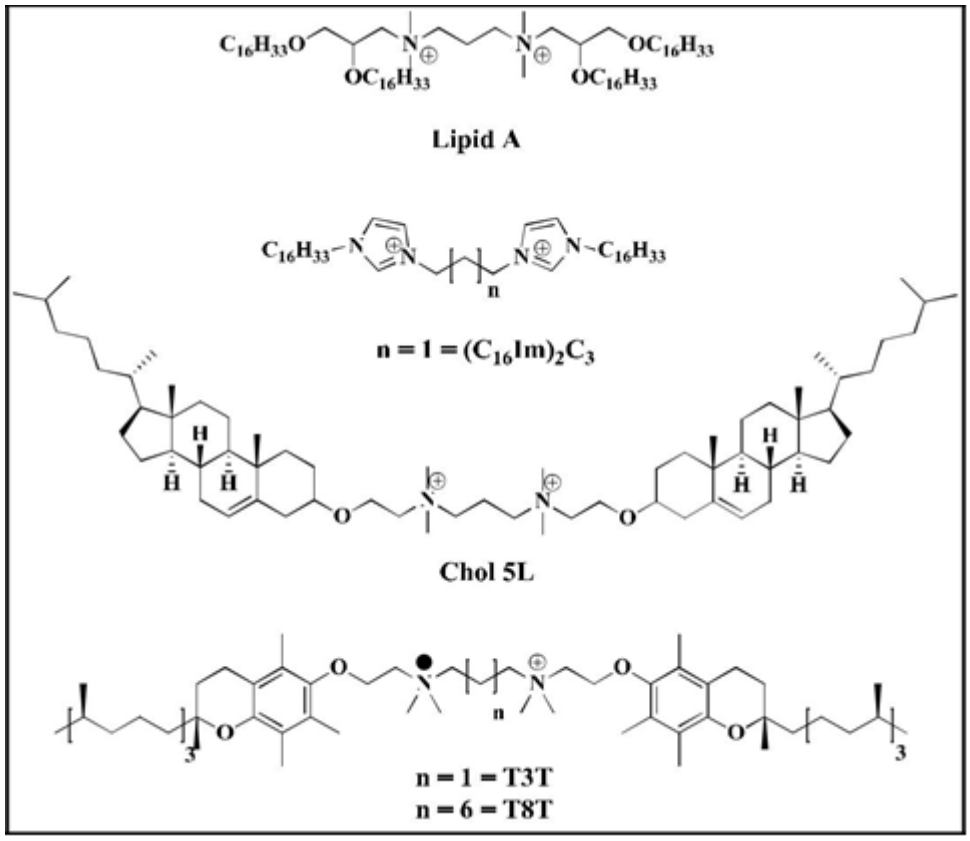

Figure 1.8: *Chemical structures of cationic gemini lipids with simple quaternary ammonium cation (lipid A) or delocalizable cationic ($(C_{16}Im)_2C_3$) head groups, while their hydrophobic anchoring groups made up of long aliphatic alkyl chains (lipid A, $(C_{16}Im)_2C_3$) or cholesterol (Chol 5L) or tocopherol (T3T, T8T).*

b. **Gemini cationic lipids:** There are several lipids, that have been developed as better transfection reagents with the name of gemini cationic lipids, which is a term used to refer a dimeric lipid generated from two similar lipid molecules that are connected each other by a spacer functionality at their head group region.[95] The structural entity which is helpful to connect two similar lipid molecules plays crucial role in determining transfection along with the other common lipid constituents. Some of the achievements using this kind of lipid molecules towards gene delivery mentioned in **Figure. 1.8** such as cardiolipin analogue based gemini surfactants (lipid A),[96] cholesterol based gemini lipids (Chol 5L)[97] and tocopherol as anchoring group (T3T, T8T & DTEC)[98, 99] with localized positive charge

density whereas the (C16Im)2C3[100] gemini lipid is made up of from delocalized charge density using imidazolium cation.

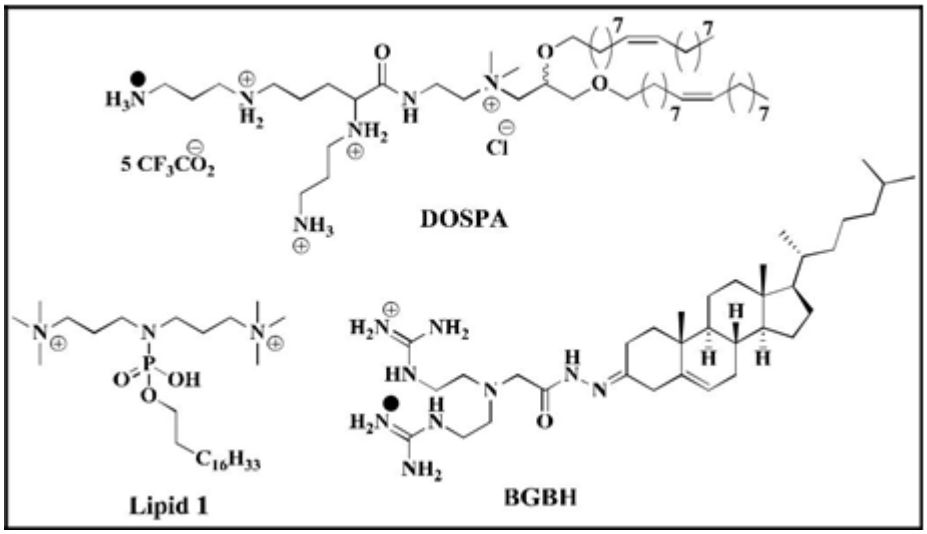

Figure 1.9: *Chemical structures of multi-charged cationic lipids (protonated amines: DOSPA, guanidinium:BGBH, and trimethylammonium: lipid 1) while their hydrophobic anchoring groups made up of aliphatic hydrocarbon chains or cholesterol.*

c. **Polycephalic lipids:** Cephalic lipids are nothing but simple lipids which have more than one cationic head groups either of similar or dissimilar in structure. Increase in number of cationic head groups can facilitate the strong charge-charge interactions with less amount of lipid and provide better transfection results. Usually two or more number of cationic head groups connect to a single hydrophobic back bone generates bicephalic and poly cephalic lipids respectively. **Figure 1.9** represents the structures of cationic lipids having multiple cations in their head groups generated from simple protonated amines (DOSPA), trimethyl amines (lipid 1) and guanidinum groups (BGBH).[85]

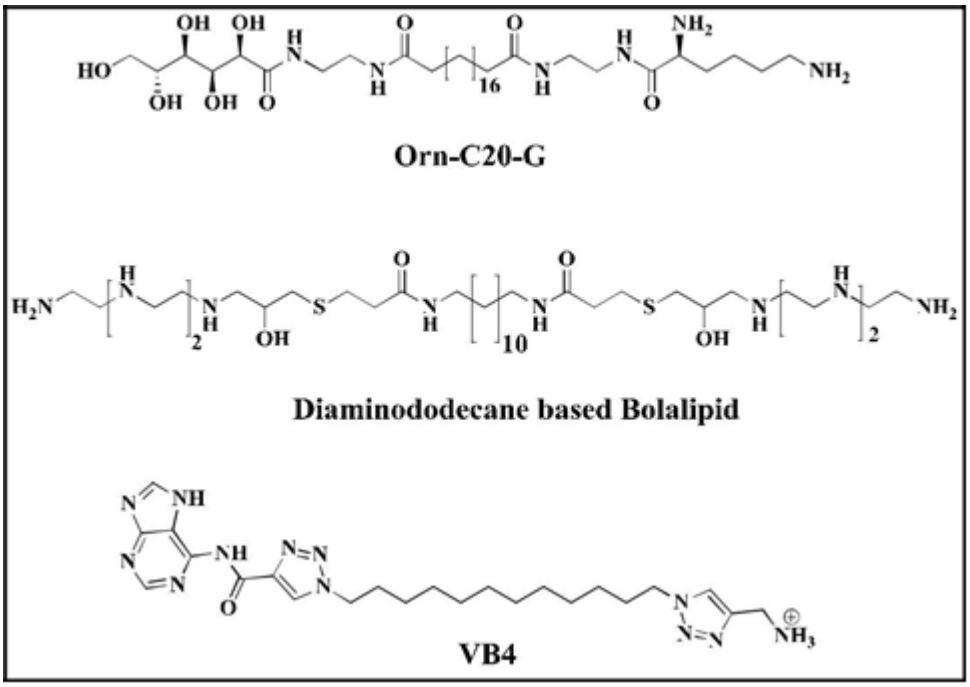

Figure 1.10: *Chemical structures of bolaamphiphilic cationic lipids with symmetrical (Diaminododecane based bolalpid) or unsymmetrical (Orn-C20-G and VB4) hydrophilic head groups.*

d. **Bolaamphiphile:** Surfactants, which consist of two hydrophilic centres with similar or distinct structures connected by a long hydrophobic chain and are known as bolaamphiphiles or bolalipids, have been used in several recent reports to improve transfection efficacy.[101] Different types of aggregations can be made from bolalipids such as nano fibers, hydrogelators, and monolayered membrane vesicles, which can be useful in efficacious transfer of olegonucleotides to cells.[102] Surfactants' significant qualities of developing chemically stable aggregations leads to correct packing and unwrapping of DNA when moving from extracellular to intracellular settings, respectively, account for their quick use in cutting-edge medication and gene delivery advances. Some of the successful applications of bolamphiphiles in gene delivery in recent times include, an asymmetrical bolaamphiphile, Orn-C20-G (Jain, N.et al,[103] **Figure 1.10**), diaminododecane based bolaamphiphiles with symmetrical multi-charged head group (Khan, M. et al,[104] **Figure 1.10**) and vitamin B derived asymmetrical bolalipid (Patil, S. P. et al,[105] **Figure 1.10**).

In conclusion, significant effort has been made to create ever-more-effective systems that enable the delivery of nucleic acids into a variety of cells. Lipid-based non-viral vectors have become the most effective delivery systems for this purpose, however only a small number of them have started clinical studies. There is still a long way to go in order to live up to the higher expectations, notwithstanding early enthusiasm for the usage of these vectors. Some of the major challenges that are still persisting are, low transfection, biological barriers, biocompatibility and targeted delivery. Sadly, there is still no universal agreement on the qualities that a lipidic vector needs to possess in order to be effective. Instead, particular cell types and applications benefit more from particular cationic lipid compositions. A systematic design of lipoplex formulations is thus necessary to create functional particles with accurate and reproducible physico-chemical characteristics and increased biological activity. The present thesis tried to address some of the existing challenges by developing transfection agents having the ability to overcome biological barriers such as Blood brain barrier (BBB). Amino acids, sugars or peptides with cell penetrating functional groups in the head group region have been incorporated in lipid design to help reduce cytotoxicity and improve cellular uptake. Gene delivering lipopeptides with cancer specific cytotoxicity have been introduced in liposomal formulations.

1.5. PRESENT THESIS

The present thesis work focuses on synthesis of cationic lipids and developing better transfection reagents to address some of the biological challenges that hinder the efficiency of gene therapy, for example, selective gene delivery and crossing blood brain barrier. Biomimetic small molecules such as amino acids, sugars and short peptides as the cationic head groups were employed in enhancing transfection while keeping low cytotoxicity. The thesis also demonstrates the design of novel gene carriers with special properties in the form of lipopeptide and cationic lipids with new hydrophobic domain.

Chapter I:

This chapter deals with the background of gene therapy and introduction of therapeutic genes, gene delivery methods, cationic lipids and their structural aspects.

Chapter II:

Because of its unique properties, arginine stands out among the several amino acids used in the synthesis of cationic lipids. Liposomes containing arginine showed higher transfection while having lower cytotoxicity than those lacking arginine, according to early studies on amino acid-based cationic lipids.[106] In comparison to other amino acids, cationic liposomes with an arginine-rich periphery had better serum stability.[107] Arginine, the main component of cell penetrating peptides (CPPs), is vital for receptor binding. Bioconjugation of tiny molecules like amino acids or vitamins to lipid-like organic molecules, has resulted in new gene delivery vehicles.[106, 108] Amino acids, in particular, facilitate the formation of natural cationic head groups, while their carboxylic acid terminals can be employed to conjugate hydrophobic moieties. Vitamin E, also known as -tocopherol, is a naturally occurring antioxidant that is membrane soluble.[109] Since nearly a decade, tocopherol as a lipid backbone has made a significant contribution to liposomal gene/drug delivery studies.[92, 110-112] Tocopherol's lipophilic nature and membrane protectiveness, as well as a variety of other biological features, may improve its biocompatibility,[110] making it a desirable delivery carrier.

To illustrate the role of the arginine moiety on pTRAIL gene expression in glioma cells, **Chapter II** demonstrates the design, synthesis and biological evaluation of two cationic lipids derived from arginine and glycine as cationic head groups, and vitamin E as the hydrophobic domain. The cationic lipids AT and GT were synthesized through the bio-conjugation of amino acids with α-tocopherol through cleavable ester bonds as shown in **Scheme 1**. These vitamin-amino acid conjugates turned out to be safe as established by their natural characteristics. Keeping glycine-derived lipid as control, arginine's selectivity was investigated exploiting its cell penetrating ability.

Scheme 1: *Synthesis of arginine-conjugated tocopherol (AT) and glycine-conjugated tocopherol (GT) lipids*

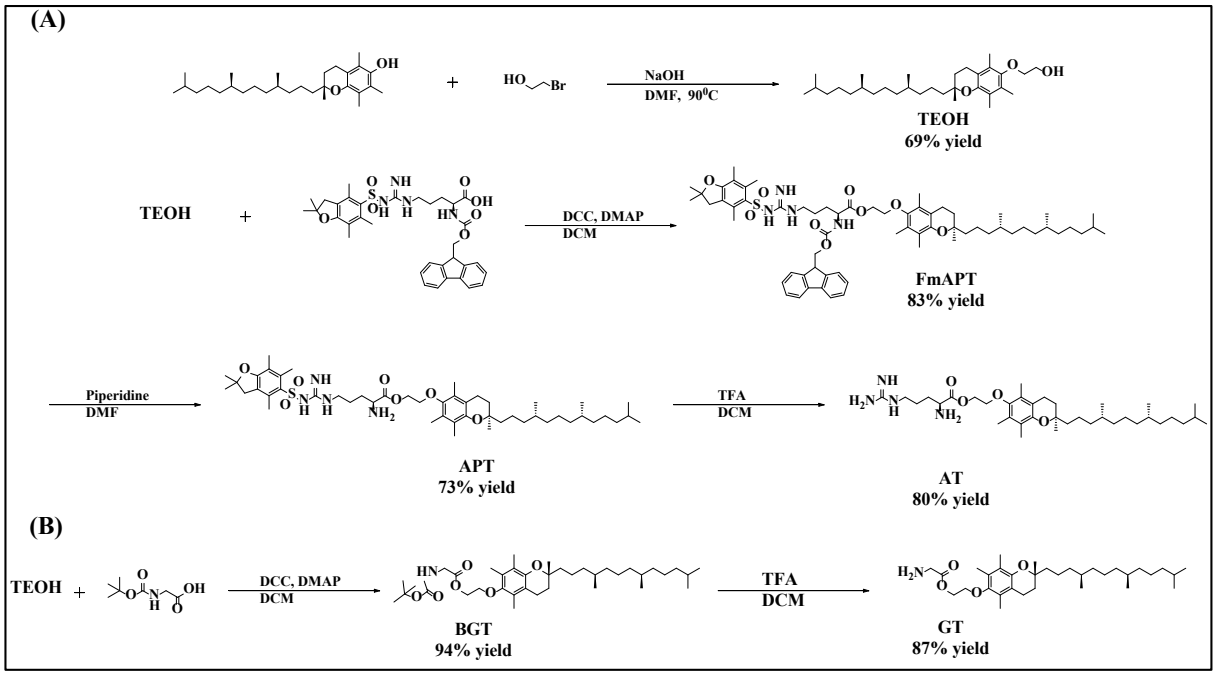

Reagents and solvents. *NaOH: Sodium Hydroxide, DMF: N,N-Dimethylformamide, DCC: Dicyclohexylcarbodiimide, DMAP: 4-dimethylaminopyridine, TFA: Trifluoroacetic acid.*

Chapter III

Cationic gemini lipopeptides are a relatively new class of amphiphilic compounds to be used for gene delivery. Through the possibility of incorporating short peptides with cell penetrating functionalities, these lipopeptides may be advantageous over traditional cationic lipids. Cationic gemini lipopeptides contain two monomeric peptide-lipid conjugates are connected by a spacer.[113, 114] These new types of molecules along with other conventional lipopeptides have been utilized for antimicrobial testing[115, 116] but their use in gene delivery is very rare. Damen et al. utilized an ultrashort (serine-proline-lysine-arginine) peptide containing lipopeptide to deliver DNA and siRNA.[117] Zheng et al. synthesized a lysine-based gemini lipopeptide for siRNA delivery.[118] In spite of these examples, the cationic gemini lipopeptides are less explored for their gene delivery and anticancer properties.

Scheme 2: *Synthesis of cationic gemini lipopeptide* ***(ATTA).***

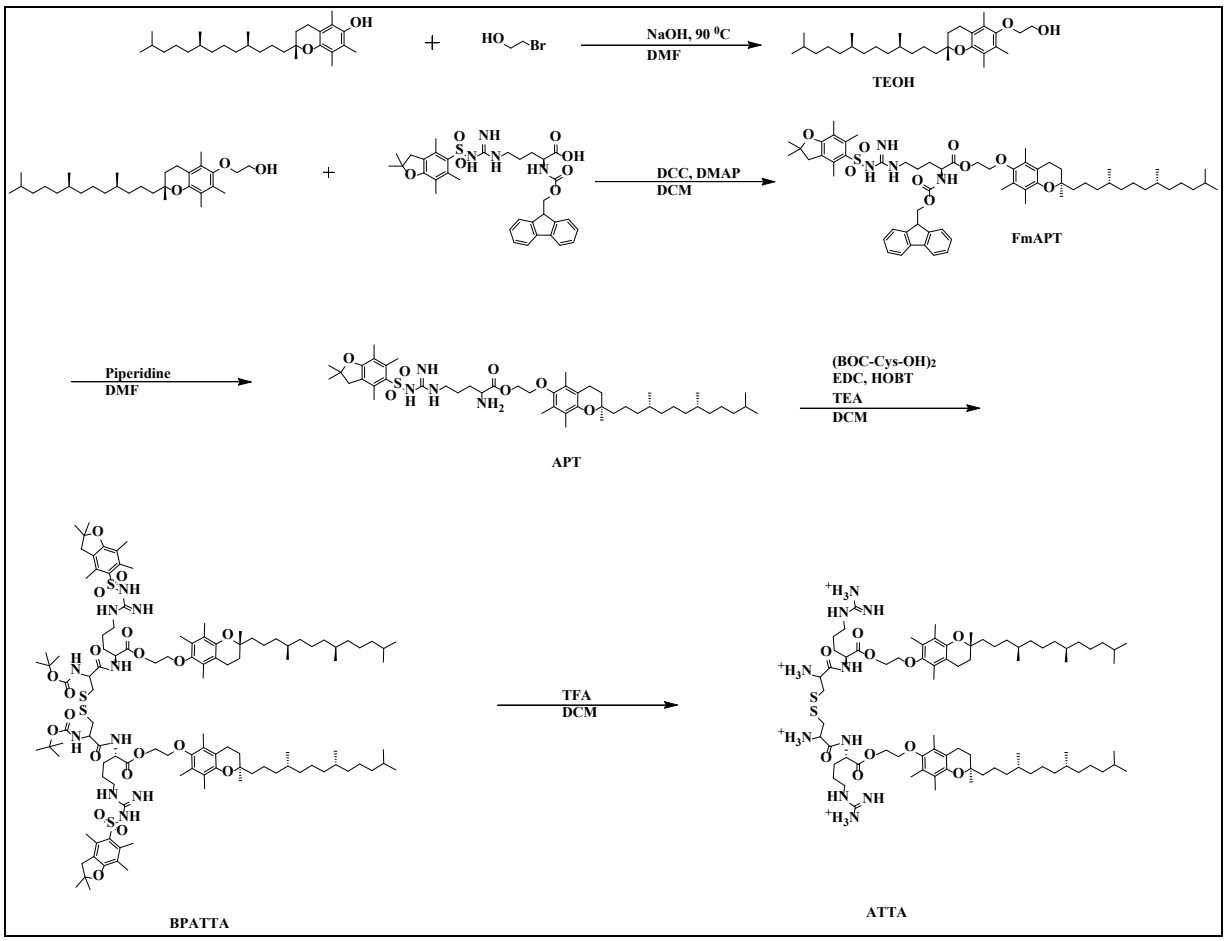

Reagents and solvents. *NaOH: Sodium hydroxide, DMF: N,N-Dimethylformamide, DCC: Dicyclohexylcarbodiimide, DMAP: 4-Dimethylaminopyridine, (BOC-Cys-OH)$_2$: Nα,Nα'-di-Boc-L-cysteine, EDC: N-(3-Dimethylaminopropyl)-N'-ethylcarbodiimide hydrochloride, 1-HOBT: Hydroxybenzotriazole, TEA: Triethylamine, DCM: Dichloromethane, TFA: Trifluoroacetic acid.*

To this end, C**hapter III** describe the design, synthesis **(Scheme 2)** and application of a novel cationic gemini lipopeptide for gene delivery. An ultrashort peptide, containing four amino acids, arginine-cysteine-cysteine-arginine, serves as cationic head group and two α-tocopherol moieties as hydrophobic anchoring groups. The new lipopeptide (ATTA) is formulated at different molar ratios into liposomes with conventional lipids, 1,2-dioleoyl-3-trimethylammonium-propane (DOTAP) and 1,2-dioleoyl-sn-glycerol-3-phosphoethanolamine (DOPE). The formulated liposomes are characterized and screened for better transfection efficiency.

Transfection activity in multiple human cell lines from cancerous and non-cancerous origins, indicates that the inclusion of optimal ratio of ATTA in the liposomes substantially

enhances transfection efficiency superior to a traditional liposome, DOTAP-DOPE. Cytotoxicity of ATTA-containing formulations against multiple cell lines indicates potentially distinct activity between cancer and non-cancer cell lines.

CHAPTER IV

Structural modifications on the cationic head groups,[119] incorporating cell penetrating peptides[120] and variations in hydrophobic chain lengths[121] are some of the strategies used for improved liposomal transfection. Although improvements were achieved, majority of these strategies have still outplayed by the transfection of commercial transfection reagents Lipofectamine 2000 (L2K) and Lipofectamine 3000 (L3K). L2k and L3k on the other hand cause significant cytotoxicity in variety of cell lines while transfecting. Thus, investigations on competent transfection reagents with better safety must be continued to improve cationic liposome-mediated gene delivery. Along with structural variations, formulation changes may hold promise to enhance transfection.

Amino acid based cationic lipids have long been considered as safe gene delivery vectors owing to their biocompatibility. **Chapter IV** described the new formulations for efficient transfection consisting of new amino acid based cationic lipids with DOTAP and the results indicate some of these formulations are comparatively safer and better at transfection than L2k in specific cell lines. Arginine-based cationic lipid AT and cystine based dimeric lipid CTT while incorporated with DOTAP in liposomal formulations have shown promising transfection results. Cationic lipid AT was synthesized as describe in Chapter I, whereas CTT was synthesized following the reaction **scheme 3**. For all the liposomal formulations, the average size of the particles was found to be in the range of 100 nm – 180 nm. Incorporation of DOTAP in the formulations apparently reduced the particle size as revealed by the sizes of DtATD and DtCTTD formulations.

Scheme 3: *Synthesis of Cationic Lipid CTT*

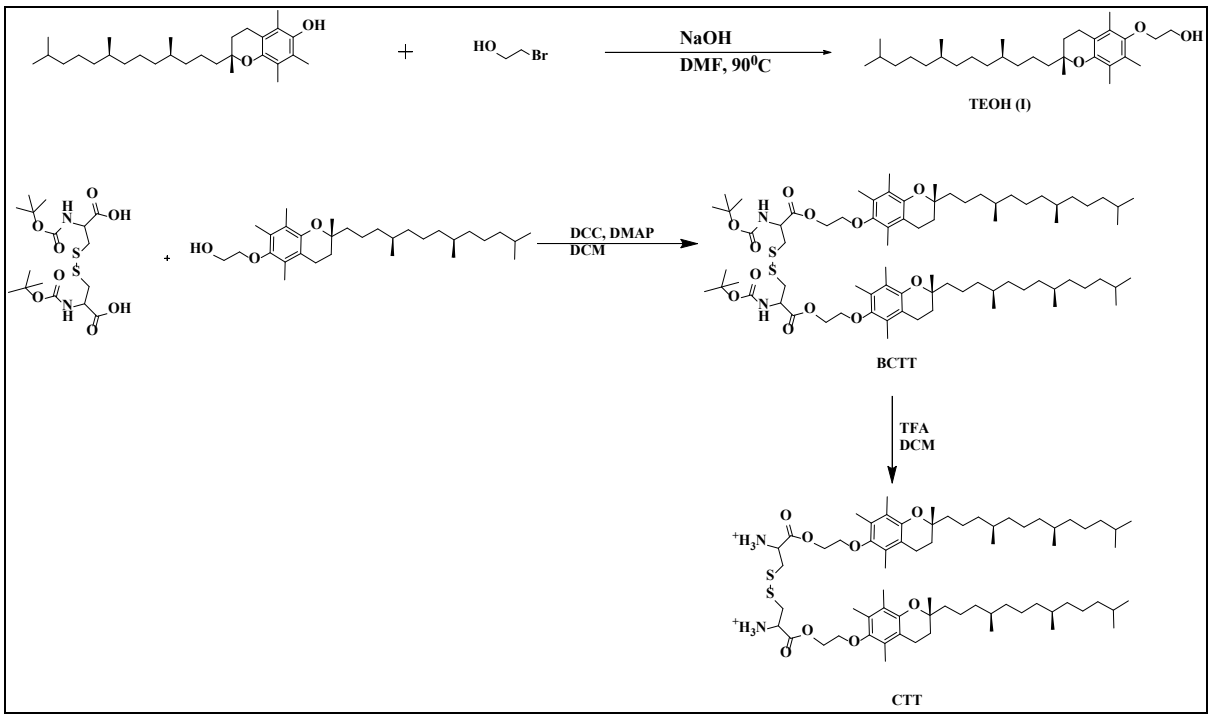

Four types of liposomes (CTTD, ATD, DtATD and DtCTTD) were combined with pEGFP-C1 plasmid to give lipid-DNA complexes. The gene de-livery experiments revealed that cationic lipid AT-containing lipid-DNA complexes (ATD and DtATD) attained maximum transfection at N/P ratio of 5, while the cationic lipid CTT-containing lipid complexes (CTTD and DtCTTD) have shown their best transfection at N/P ratio of 9. It can be noted that the complexes of DtCTTD, at the N/P ratio of 9 exhibited superior transfection activity over other test formulations. Interestingly, in PC3 cell line, DOTAP-containing DtCTTD has resulted in 2-fold higher transfection efficiency than commercial transfection reagent, L2K. On the other hand, cytotoxicity of DOTAP incorporated formulations at optimal N/P ratio was lower than that of L2K. The obtained results here show the importance of formulation changes of amino acid based liposomes to improve physicochemical properties as well as transfection with respect to conventional formulations.

CHAPTER V

Sugar based cationic lipids are promising carriers of nucleic acids into various cells. Particularly, abundant hydroxyl functional groups in the sugar-like moieties are believed to

enhance target oriented uptake as well as biocompatibility. Introduction of hydroxyethyl functional groups on the quaternary ammonium head group has resulted in enhanced transfection efficacy. It was believed that hydrophilic hydroxyethyl functional groups in the head group region modulate the hydration level and inter-lipidic interaction of liposomes. **Chapter V**, describes the development of three new cationic lipid analogues with or without sugar-like multi-hydroxyl functional head groups for non-viral gene delivery as given in **Schemes 4-6**. Liposomal formulations are developed by mixing these lipids with helper lipid, DOPC. All of the lipid formulations were thoroughly characterized by means of DNA binding ability, size and zeta potential. Characterization of liposomes revealed that, lipids containing sugar like moieties attained smaller liposomal size and reduced cationic charge which in turn favoured low cytotoxicity of the sugar based cationic lipids. Optimal N/P ratios of each lipid-DNA complex were elucidated by their transfection efficiency in HEK-293 cells. Sugar-mimicking cationic lipids, TS1 and TS2, exhibited superior transfection properties in HEPG2 cell line, whereas this property was reversed in the case of U87 cell line. The results point out that the transfection efficiencies of sugar alcohol-based cationic lipids are cell-dependant. Cytotoxicity of the lipid complexes through MTT based assay revealed that the sugar-mimicking cationic lipids are non-toxic towards the tested cell lines. Cationic lipid, TS1 with open chain sugar-like head group may have potential for hepatocellular targeted gene delivery. In conclusion, the current work adds knowledge on the sugar based cationic lipids and reiterates that these lipids could yield potential applications towards liver targeted gene delivery.

Scheme 4: *Synthesis of Control Lipid (TA)*

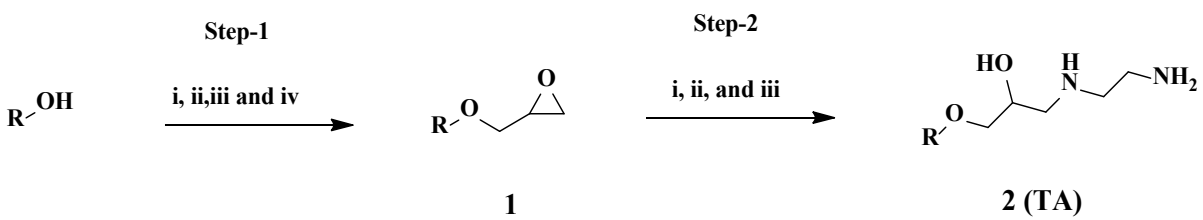

1 **2 (TA)**

Reagents: *R= tocopheryl; Step1: i) Epichlorohydrin, ii) NaOH solution, iii) tetrabutylammonium hydrogen sulfate, iv) Refluxed 16h, Step2: i) Ethylenediamine ii) Methanol, iii) Refluxed 16h.*

Scheme 5: *Synthesis of Cationic Lipid TS1*

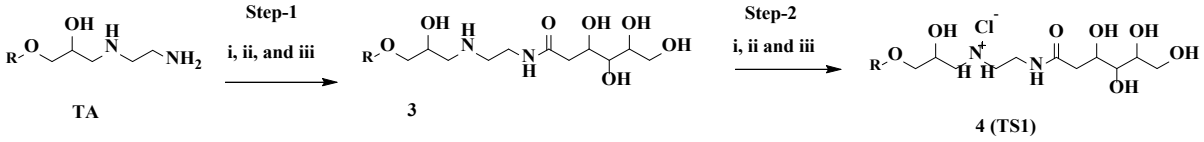

Reagents: *R= tocopheryl ; Step1: i) Methanol, ii) 1,4 gluconic γ-lactone, iii) Refluxed 16h, Step2: i) 6N HCl in Dioxane ii) RT 12h.*

Scheme 6: *Synthesis of Cationic Lipid TS1*

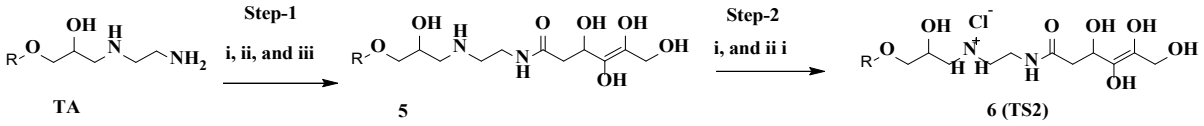

Reagents: *R= tocopheryl ; Step1: i) Methanol, ii) ascorbic acid, iii) Refluxed 16h, Step2: i) 6N HCl in Dioxane ii) RT 12h.*

CHAPTER VI

The configuration of the hydrophobic region in cationic lipid regulates the key factors in gene delivery. Factors such as phase transition temperature of liposome, fluidity of the bilayer, stability of liposomes, the endosomal escape, protection of DNA from nucleases, the release of DNA from lipoplex and the nuclear uptake are all influenced by the structure of hydrophobic moiety. On the other hand, hydrophobic domain also take part in determining the toxicity of lipid.[122] Thus, similar to other components of cationic lipids, the hydrophobic groups influence almost every step in the process of gene delivery.

In general, shorter chain length, unsaturation and branching on aliphatic chain are collectively bestows the better transfection properties to gene delivery vectors. In spite of these

evidences, the research on cationic lipids fulfilling all these requirements is scarce. Over the years, major attention has been given to the head group evolution to enhance the gene delivery ability of cationic lipids. More exploration on the hydrophobic region seems necessary, in order to establish the competent gene delivery vectors.

Farnesol is a natural 15-carbon acyclic sesquiterpene alcohol with tri-unsaturated C12 aliphatic chain and branch like methyl groups adjacent to unsaturation. Structurally, farnesol appears to be interesting molecule to fabricate into cationic lipid with branched structure, short chain length, higher unsaturation than regular cationic lipids. Farnesol has been reported to inhibit tumor cell proliferation in vitro[123, 124] as well as in vivo.[124, 125] Additionally, pharmacological studies revealed that farnesol has chemo-preventative, anti-inflammatory antioxidant, analgesic and neuroprotective properties .[126-130] Over the past two decades, several patents were registered studying the pharmaceutical potential of farnesol.[131] Given the wide variety of pharmoclogical applications coupled with its promising structural features, it's worthwhile to design farnesol based cationic lipids for gene delivery applications.

In view of the above mentioned aspects, the **Chapter VI** discusses the synthesis of a new class of farnesol based cationic lipids for carrying nucleic acids in to desired cell lines. The cationic lipids of the current design generally contain a quarternary amine head group and a farnesol moiety as hydrophobic tail connected through a pyrazenone ring as a linker. The general synthetic scheme of newly designed cationic lipids in this chapter is given as Scheme 7. All the intermediate compounds and final lipids were thoroughly characterized. The newly developed cationic lipids can find potential applications in drug/gene delivery when formulated with neutral lipids.

Scheme 7: General scheme of synthesis of cationic lipids, NTMDPF, NEDMDPF, NMDEDPF and NTEDPF

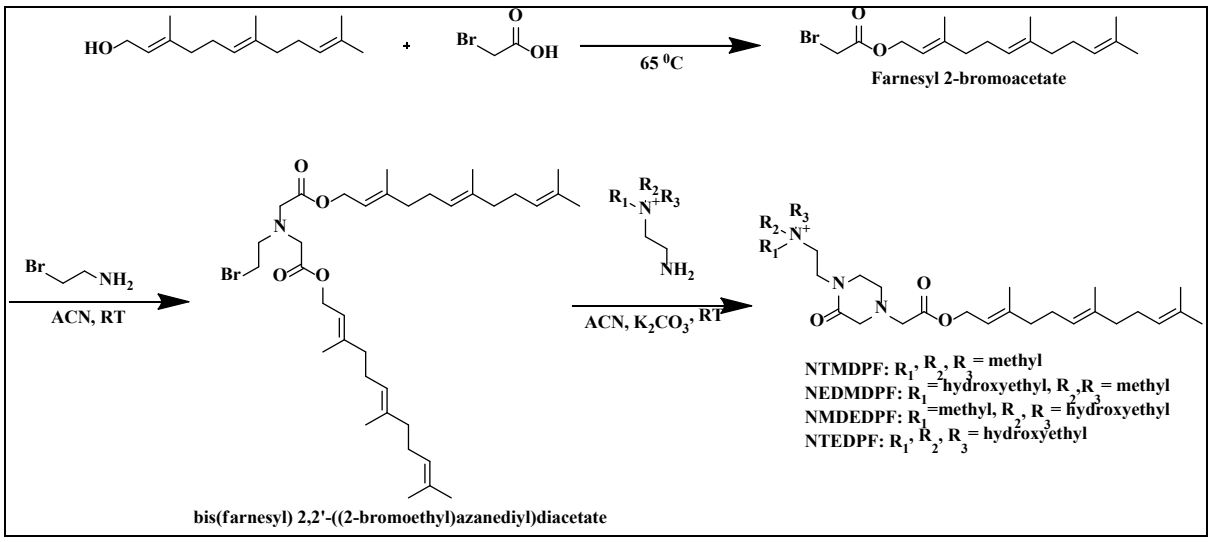

Reagents and Conditions. ACN: Acetonitrile, K2CO3: Potassium carbonate, RT: Room temperature

CHAPTER-II

ARGININE-TOCOPHEROL BIOCONJUGATED LIPID VESICLES FOR SELECTIVE PTRAIL DELIVERY AND SUBSEQUENT APOPTOSIS INDUCTION IN GLIOBLASTOMA CELLS

CHAPTER II

ARGININE-TOCOPHEROL BIOCONJUGATED LIPID VESICLES FOR SELECTIVE PTRAIL DELIVERY AND SUBSEQUENT APOPTOSIS INDUCTION IN GLIOBLASTOMA CELLS

2.1. INTRODUCTION

Gene therapy has been a promising therapeutic approach as evidenced by recent clinical trials.[132] Success of gene therapy is relied on the vectors that can incorporate the therapeutic gene at the disease site. Delivered gene, either by expressing therapeutic protein or by counteracting the malfunctioning gene, achieves the therapeutic effect.[132] Liposomal gene delivery is a well-established research field and attracts several researchers' attention to developing efficient gene delivery vehicles based on cationic liposomes.[133, 134] Advantages of cationic liposomes are due to their relatively low immunogenic response, feasibility to structural modification and bulk production possibility. However, most efficient cationic lipids are associated with low biosafety.[135] Lipofectamine 2000 and 1,2-dioleoyl-3-trimethylammonium-propane (DOTAP) for example are commercial liposomes with decent transfection ability but have shown substantial cytotoxicity. Cytotoxicity of cationic liposomes is mainly attributed to its cationic charge density, though the other components such as hydrophobic tail and linkers also contributing to their cytotoxicity.[136, 137] To overcome this issue, the use of bio-based natural products to build cationic liposomes seems a solution with high transfection without compromising on the safety.

Bioconjugation of small molecules such as amino acids or vitamins to lipids like organic molecules has resulted in new delivery vehicles for gene delivery.[106, 108, 138] Particularly, amino acids facilitate natural cationic head groups while their carboxylic acid ends can be used for conjugation to hydrophobic moieties. Out of the many amino acids used in synthesis of cationic lipids, arginine stands out with superior properties. Early studies on amino acid-based cationic lipids demonstrate that arginine containing liposomes exhibited higher transfection while

maintaining low cytotoxicity in comparison with those without arginine.[106] Cationic liposomes with arginine rich periphery also display greater serum stability in comparison with other amino acids.[107] Arginine was also used to modify carbon dots in order to achieve high cellular uptake and biocompatibility.[139] Arginine being the major component in cell penetrating peptides (CPPs) plays an important role in binding to various receptors. The guanidine moiety of arginine is crucial for the interaction between CPPs and the surface of the cell membrane. The mechanism involves bidentate hydrogen-bonding between guanidine portion and phosphate groups on cell surface facilitating internalization.[140] These studies highlight the outstanding transmembrane functions of arginine. On the other hand, vitamin E or α-tocopherol is a natural antioxidant which is known to be membrane soluble.[109] Tocopherol as lipid backbone has enormously contributed to liposomal gene/drug delivery research since nearly a decade.[92, 110-112] Tocopherol's lipophilic nature and membrane protectiveness along with numerous other biological properties are possibly enhancing its biocompatibility[110] which in turn making it an attractive delivery vehicle.

Glioblastoma is aggressive and the most common tumor type related to central nervous system with high mortality and fewer effective therapies.[141] Selective and efficient approaches are thus direly needed to treat glioblastoma. Arginine auxotroph dependent arginine deprivation selectively induce cytotoxicity in glioblastoma cells as reported by previous studies .[142, 143] Arginine metabolising enzyme arginase 1 is highly expressed in glioblastoma[144] making the cells starve for arginine. These findings, in combination with the guanidino dependent cell penetrating ability of arginine, make it a suitable candidate for designing therapeutic agents with selectivity.

One of the highly potent anticancer therapeutic genes, pTRAIL encoding tumor necrosis factor (TNF)-related apoptosis-inducing ligand (TRAIL) is of particular interest due to its selective apoptosis induction in cancer cells.[145, 146] TRAIL induces apoptosis and necrosis in cancer cells by specifically binding to death receptors like DR4 and DR5.[147, 148] The selective

apoptotic activity of TRAIL is explained by the fact that these receptors (DR4 and DR5) expressed highly in cancer cells but not in normal cells.[149] TRAIL's binding to the death receptors leads to the formation of death inducing signaling complex (DISC) which activates caspase-8 and finally inducing apoptosis and necrosis.[150, 151] Although the anticancer effect of TRAIL is limited by its short half-life and presence of cancer cells resistant to TRAIL, the nanocarriers mediated TRAIL expressing gene delivery has shown promise for cancer therapy.[26] Since most of the anticancer agents are toxic to normal cells and are poorly bio-available, TRAIL can be an alternative anticancer agent with cancer specific cytotoxicity.

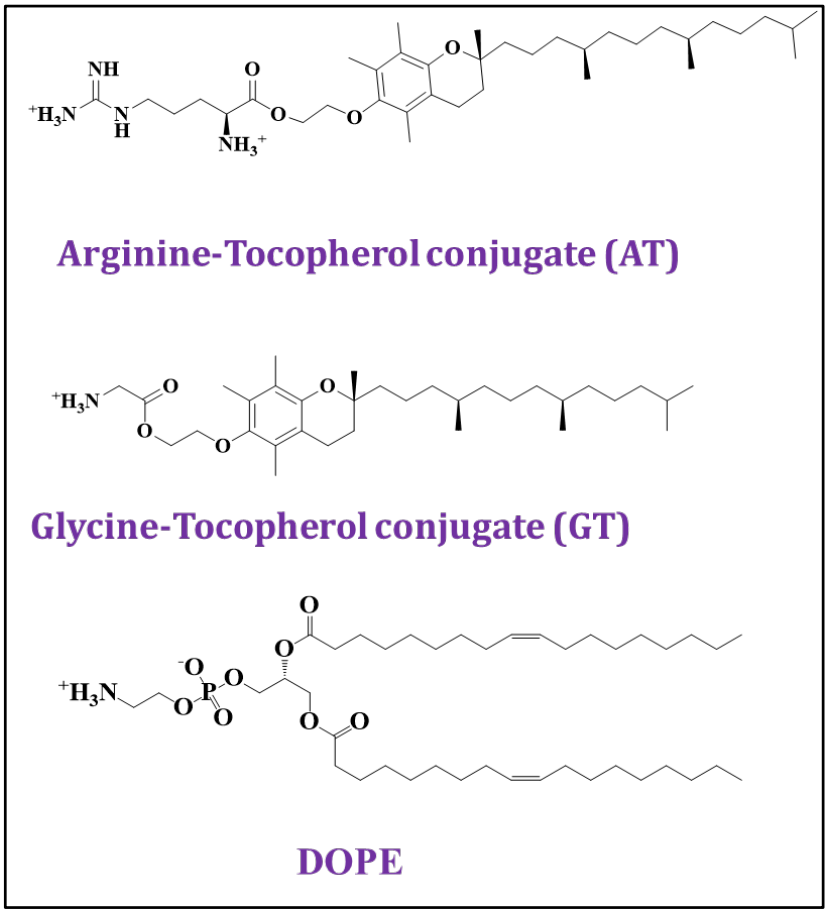

Figure 2.1: *Chemical structure of cationic lipid and colipid (DOPE) used in this study*

To illustrate the role of the arginine moiety on pTRAIL gene expression in glioma cells, we designed two cationic lipids derived from arginine and glycine as cationic head groups, and vitamin E as the hydrophobic domain. These vitamin-amino acid conjugates turned out to be

safe as established by their natural characteristics. Keeping glycine-derived lipid as control, arginine's selectivity was investigated exploiting its cell penetrating ability. The newly formed liposomes combined with TRAIL expressing plasmid can be an effective and safe therapeutic system.

2.2. RESULTS AND DISSCUSSION

2.2.1. Design, Synthesis and Characterization: Cationic lipids with amino acids in the head group region have shown promising transfection efficiencies with low cytotoxicity. A recent study demonstrated that the presence of arginine in the head group region resulted in enhanced cellular uptake and serum compatibility.[152] The use of α-tocopherol as hydrophobic anchor in cationic liposomes has been studied substantially by our and other groups previously.[111, 112, 152, 153] In this study, we synthesized two new lipids by using arginine or glycine as a cationic head group and α-tocopherol as a hydrophobic group (**Figure 2.1**). The cationic lipids AT and GT were synthesized through the bio-conjugation of amino acids with α-tocopherol through cleavable ester bonds as shown in **Scheme 2.1**.

Scheme 2.1: *Synthesis of arginine-conjugated tocopherol* ***(AT)*** *and glycine-conjugated tocopherol* ***(GT)*** *lipids*

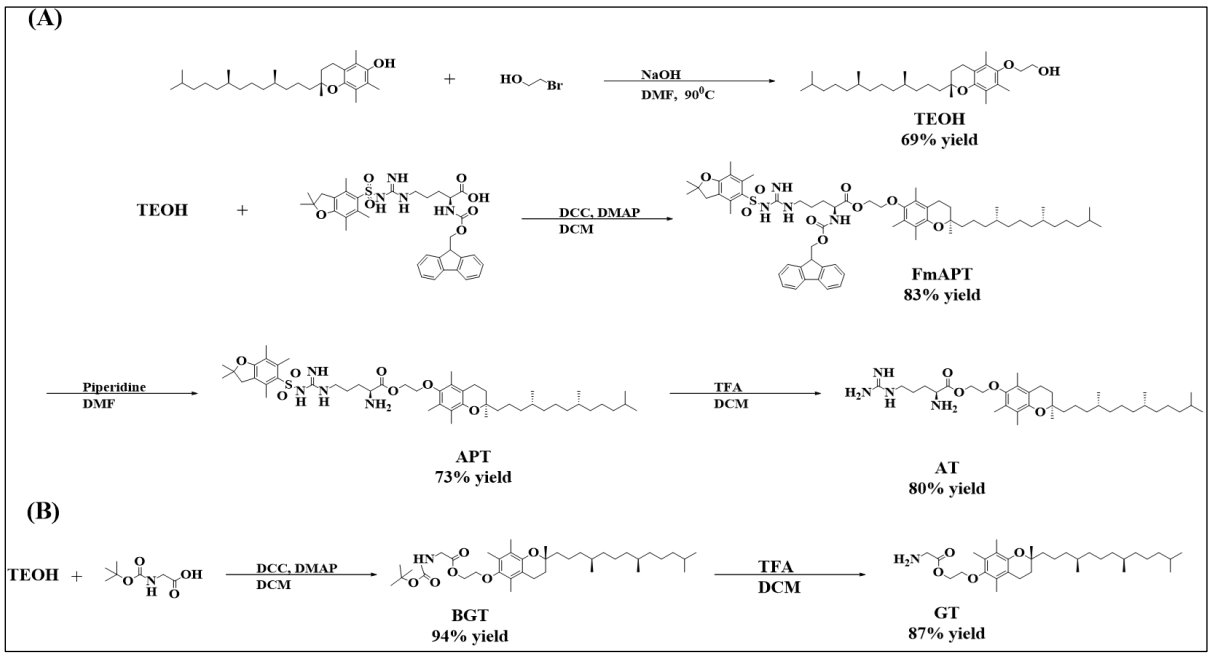

Reagents and solvents. *NaOH: Sodium Hydroxide, DMF: N,N-Dimethylformamide, DCC: Dicyclohexylcarbodiimide, DMAP: 4-dimethylaminopyridine, TFA: Trifluoroacetic acid.*

The ester linkage offers stable lipids in extracellular environment but hydrolizable by cellular esterase, facilitating the release of gene.[154] Since the phenolic esters are not sufficiently stable, the hydroxyl group of tocopherol was initially treated with 2-bromoethanol in order to extend the hydroxyl functionality away from bulky methyl groups on aromatic ring. This facilitates the easy coupling with an amino acid as well as working as a spacer between the hydrophilic and hydrophobic groups. AT was synthesized by coupling of amine protected arginine, Fmoc-Arg(pbf)-OH with tocopheryloxyethanol in the presence of DCC and DMAP. Sequential removal of Fmoc and pbf groups yielded the target lipid AT. Fmoc-Arg(pbf)-OH is relatively less expensive compared with other amine protected arginine products and also allows controlled deprotection of amine groups. GT was synthesized by coupling Boc-glycine with tocopheryloxyethanol. Removal of protecting group using TFA yielded the lipid GT. All the lipid intermediates and final compounds were characterized by NMR and mass spectrometry.

2.2.2. Physicochemical Characterization: Towards the physicochemical characterization of two new lipids developed, the size, shape, morphology and stability of these liposomes were studied using DLS, TEM and DNA electrophoretic mobility assay. The liposomal formulations of the synthesized lipids were prepared using DOPE as a co-lipid at different molar ratios of lipid:DOPE (1:1, 2:1 and 1:2). DOPE, a zwitterionic phospholipid is used as a helper lipid in most of the studies because of its fusogenic nature and nonbilayer structure formation that helps to disrupt the endosomal membrane after the cellular uptake of lipoplex into cytoplasm. Our previous studies also show that tocopherol-based lipids with DOPE as co-lipid resulted in promising gene transfection.[108, 153] The particle size measurements using DLS revealed that both types of liposomes at lipid:DOPE ratio of 1:1 formed stable particles with the size <200 nm (**Figure 2.2A**).

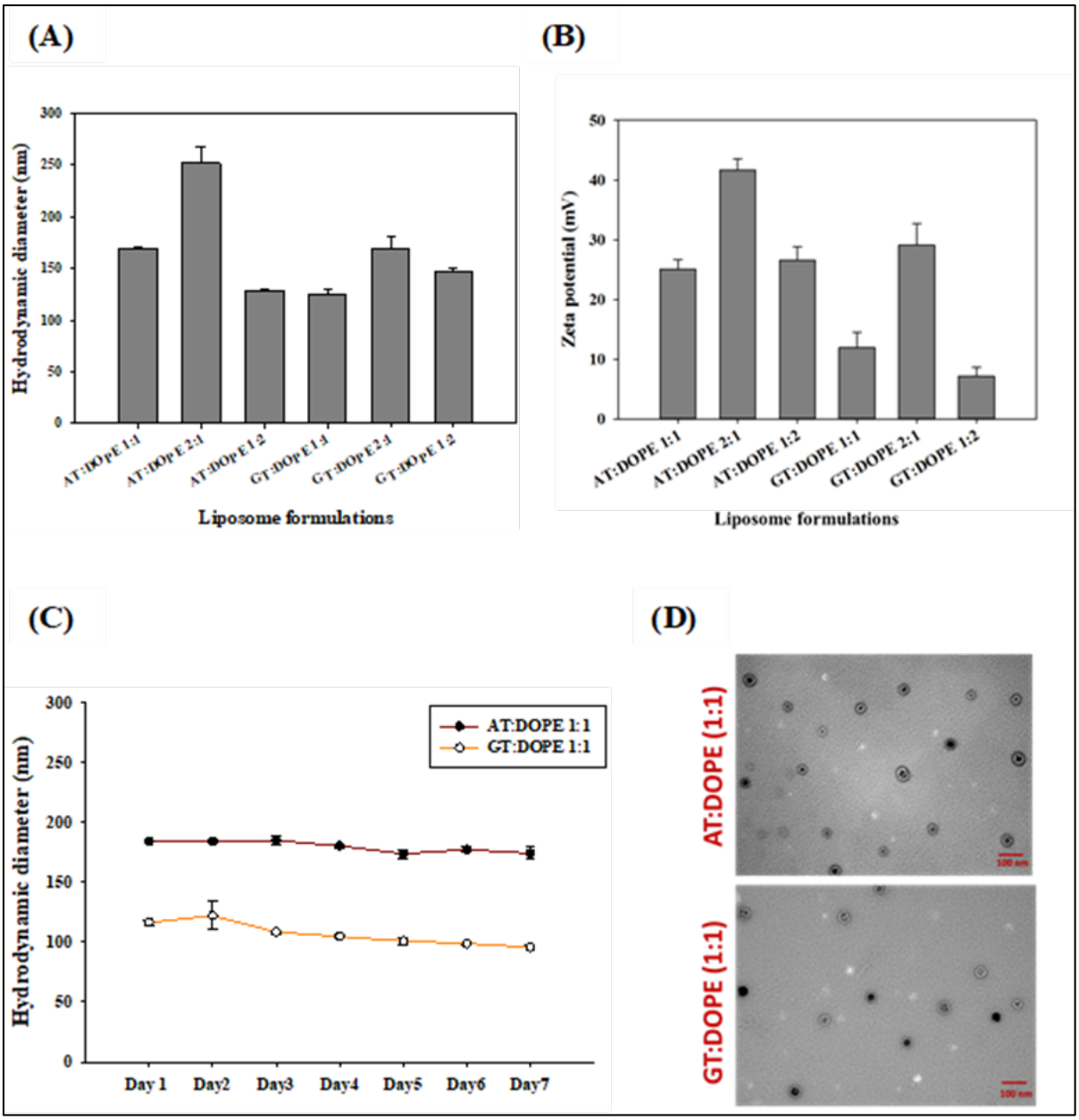

Figure 2.2: *Characterization of liposomes. (A) Hydrodynamic diameters of liposomes at different lipid:DOPE ratios; (B) Zeta potentials of liposomes at different lipid:DOPE ratios; (C) Size stability of liposomes at lipid:DOPE ratio 1:1 over 7 days; (D) Transmission electron microscopic images of liposomes at lipid:DOPE ratio 1:1.*

Although the formulation AT:DOPE at molar ratio 1:1 had slightly larger particle size than that of 1:2, the storage stability of the formulation AT:DOPE at 1:1 ratio is higher, as there is no significant change in particle size was observed over 28 days when stored at 4 ^{0}C (**Figure 2.3**). Having a simple glycine head group with a single cationic charge, GT-DOPE liposomes

at 1:1 formed vesicles with smaller hydrodynamic diameters (124 ± 6 nm) than AT-DOPE liposomes (169 ± 2 nm).

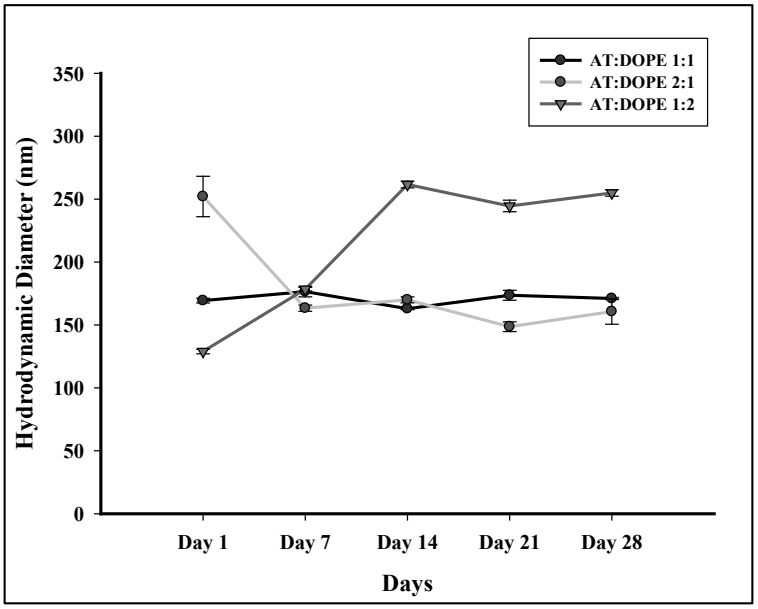

Figure 2.3: *Size stability of liposomes at different AT:DOPE ratios over 28 days*

The zeta potential values of all liposomal formulations are shown in **Figure 2.2**B**,** where AT-based liposomes at all three lipid:DOPE ratios showed moderate to high positive net surface charge. With moderate positive charge and appropriate size range, the stability of AT-based and GT-based liposomes at 1:1 lipid:DOPE ratio was evaluated over 7 days and found no considerable size change of liposomes (**Figure 2.2C**). The morphologies of liposomes of both the lipids at molar ratio 1:1, were also visualized under transmission electron microscope (TEM), showing double circular imaging with a uniform size distribution (**Figure 2.2D**). The TEM images of liposomes revealed that the sizes of the dehydrated lipid vesicles were varied from the hydrodynamic diameters of the same. The dried lipid vesicles of AT-based liposomes attained the size (~60 nm) similar to that of GT-based liposomes (~55 nm).

The electrostatic interactions of positively-charged liposomes and negatively-charged DNA, were a parameter to determine gene transfection efficacy. The ratio of effective binding between lipid and DNA was evaluated using gel retardation electrophoresis assay. The DNA binding ability of the AT and GT-based liposomes found to be efficient in binding with DNA. The DNA

retardation was initiated by both types of liposomes at N/P ratio as low as 1:1 and complete binding was achieved at N/P ratio of 3:1 and above, as shown in **Figure 2.4A**. The change in the size and surface zeta potential of liposomes upon addition of DNA was assessed by DLS. AT-based and GT-based lipoplexes followed a similar pattern, the sizes increased initially then decreased as N/P ratio increases (**Figure 2.4B**). It is believed that as the N/P ratio increases, large lipoplexes might be formed when lipoplexes are charge neutralized. Large aggregates are likely to be formed through electrostatic and hydrophobic interaction. Further increase in the N/P ratio could result in smaller sized lipoplexes due to electrostatic repulsion of lipoplexes with net positive charge.[155, 156] Surface charges of lipoplexes increased positively and almost saturated above N/P ratio 7:1 (**Figure 2.4**C). The results imply that both AT-based and GT-based liposomes were effectively condensed the DNA.

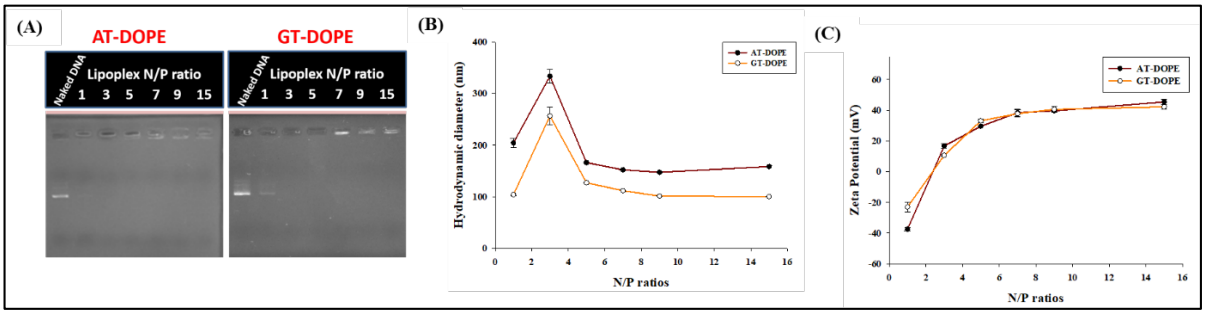

Figure 2.4: *Characterization of lipoplexes. (A) Gel retardation images of lipoplexes at different N/P ratios; (B) Variations in the hydrodynamic diameters of lipoplexes after complexation with pDNA at different N/P ratios; (C) Variations in the zeta potentials of lipoplexes after complexation with pDNA over different N/P ratios.*

2.2.3. Cell Viability: Cytotoxicity is one of the major limitations for cationic lipid-based gene delivery system.[111, 157, 158] Thus, cytotoxicities of liposomes and lipoplexes were investigated by MTT assay. AT-based and GT-based liposomes showed negligible cytotoxicities in test concentrations of 0.5-100 µg/mL against 293T, U87, and PC-3 cells (**Figure 2.5A and B**). The cell viabilities of lipoplexes were also tested against these three cell lines at various N/P ratios of 5:1–15:1. For cytotoxicity and transfection experiments, 1µg of pDNA was complexed with calculated amount of liposome solution as per their N/P ratios. Both of the AT-DOPE/pDNA

lipoplex and GT-DOPE/pDNA lipoplex treated cells showed higher viabilities than did the Lipofectamine and PEI polyplex treated cells (**Figure 2.5D-E**). The cell viabilities of AT- and GT-formed lipoplexes were higher than 85% in all the three cell lines but those of Lipofectamine were about 63% in U87, 68% in 293T, and 54% in PC-3 cells. The lower cytotoxicity of AT- and GT-formed lipoplexes implies that they are safer gene carrier candidates than PEI and Lipofectamine. The formulation of Lipofectamine is the mixture of cationic lipid, 2,3-dioleyloxy-N-[2(sperminecarboxamido)ethyl]-N,dimethyl-1-propanaminium trifluoroacetate (DOSPA) and neutral lipid DOPE at a weight ratio of 3:1. DOSPA contains highly cationic density of a quaternary ammonium group, two secondary amine groups, and two primary amine groups.[159]

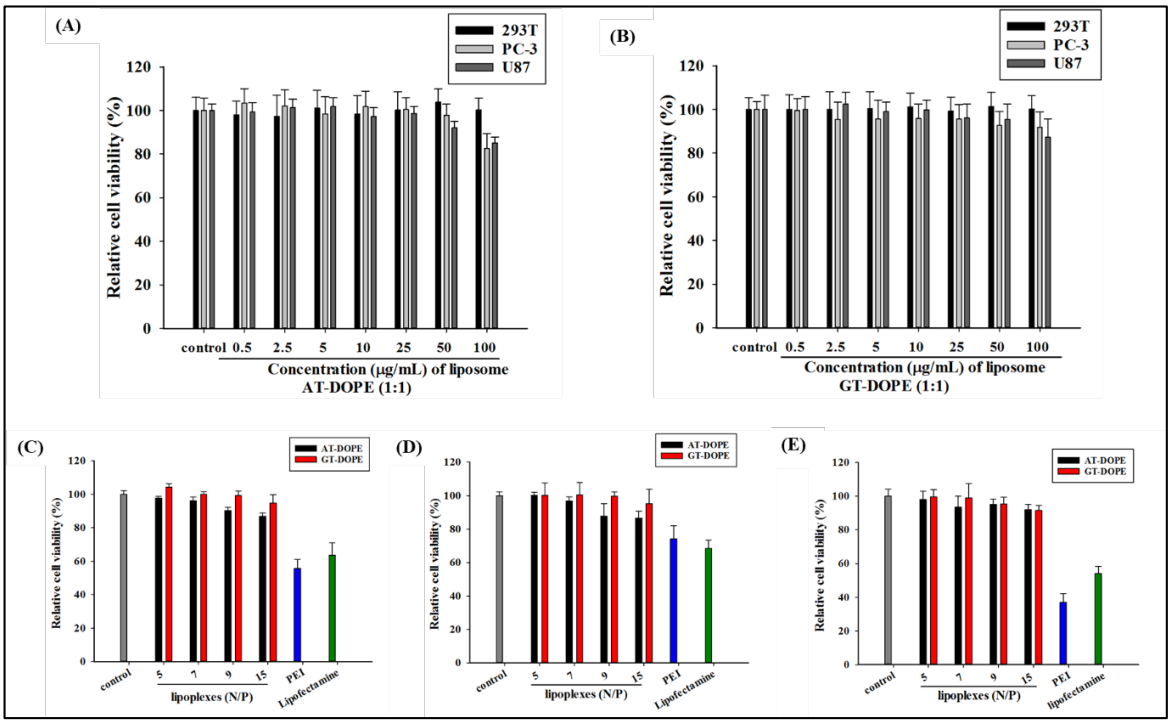

Figure 2.5: *Relative cell viabilities of liposomes and lipoplexes. (A) AT-based and (B) GT-based liposomes at various concentrations of 0.5-100 μg/mL against 293T, PC-3, and U87 cells (n=8). AT-DOPE/pDNA and GT-DOPE/pDNA lipoplexes prepared at various N/P ratios for 48-h post-incubation respectively against (C) U87, (D) 293T, and (E) PC-3 cells (n=3). PEI/pDNA polyplex was prepared at an N/P ratio of 10 and Lipofectamine/pDNA was prepared according to the manufacturer's protocol.*

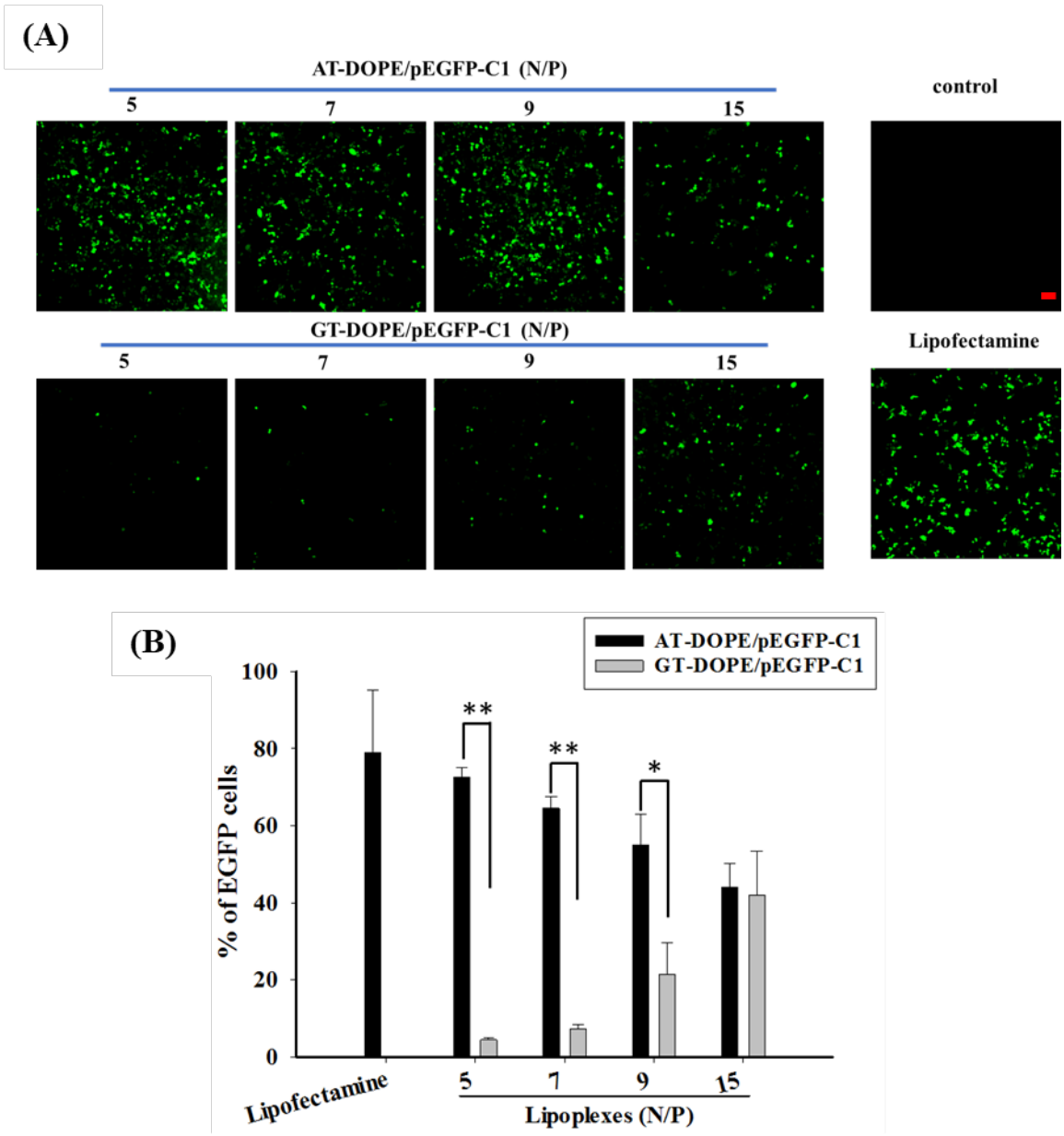

Figure 2.6: *(A) GFP expression in 293T cells using AT-DOPE/pDNA and GT-DOPE/pDNA lipoplexes at various N/P ratios. Lipofectamine/pDNA lipoplex was used as a positive control and prepared according to the manufacturer's protocol. The scale bar is 100 µm. (B) GFP expression in 293T cells transfected with AT-DOPE/pDNA and GT-DOPE/pDNA lipoplexes at various N/P ratios and analyzed by flow cytometry. (n=3, *p<0.05).*

2.2.4. Transfection and Cellular Uptake: After ensuring low cytotoxicity, AT- and GT-based liposomes were first evaluated for transfection efficiency by GFP expression. AT-DOPE and GT-DOPE liposomes at 1:1 ratio were complexed with pEGFP-C1 at various N/P ratios of 5:1-15:1, and commercial gold-standard Lipofectamine was used as the positive control. AT-

DOPE/pDNA lipoplexes showed obviously higher GFP expression than GT/pDNA lipoplexes and similar to Lipofectamine in 293T cells (**Figure 2.6A**). In addition to qualitative fluorescent microscope observation, GFP expression was quantitatively analyzed by flow cytometry as well. In **Figure 2.6**B, GFP-expressed analysis of AT-DOPE/pDNA at the N/P ratio of 5:1 showed the highest GFP expression (72±2.5%) and close to that of Lipofectamine (79±16.1%). GT-DOPE/pEGFP-C1 showed the highest GFP expression at the N/P ratio of 15:1 (42±11.4%), which was much lower than those of AT-DOPE and Lipofectamine. During gene delivery, it is essential to attain high transfection while maintaining minimum cytotoxicity. In accordance with previous studies,[106, 160] our current transfection results reiterate that arginine based cationic lipids are better at achieving high transfection and low cytotoxicity. Our previous reports[92, 111] show that the tocopherol-based lipids are highly potential in transfecting pDNA even in the presence of high concentrations of serum (50%). Similarly, arginine on liposomal periphery is known to endow serum compatibility to the liposomes.[107] Hence it is anticipated that the arginine-tocopherol based liposomes can be efficiently used in systemic delivery as well.

AT-DOPE/pDNA at the N/P ratio of 5:1 and GT-DOPE/pDNA at the N/P ratio of 15:1 were adopted for further GFP expression studies. In **Figure 2.7A and B**, of AT- and GT-formed lipoplexes was evaluated against 293T, U87 and PC-3 cell lines. In both 293T and U87 cells, AT-formed lipoplexes showed remarkably higher GFP expression than GT-formed lipoplexes but similar expression observed in PC-3 cells. Besides, transfection efficiencies of several glioma cell lines, namely, C6, 9L, F98 and ASTC1S1 cells were also assayed to demonstrate higher transfection efficacy of AT-based lipoplex than that of GT-based lipoplex (**Figure 2.8**).

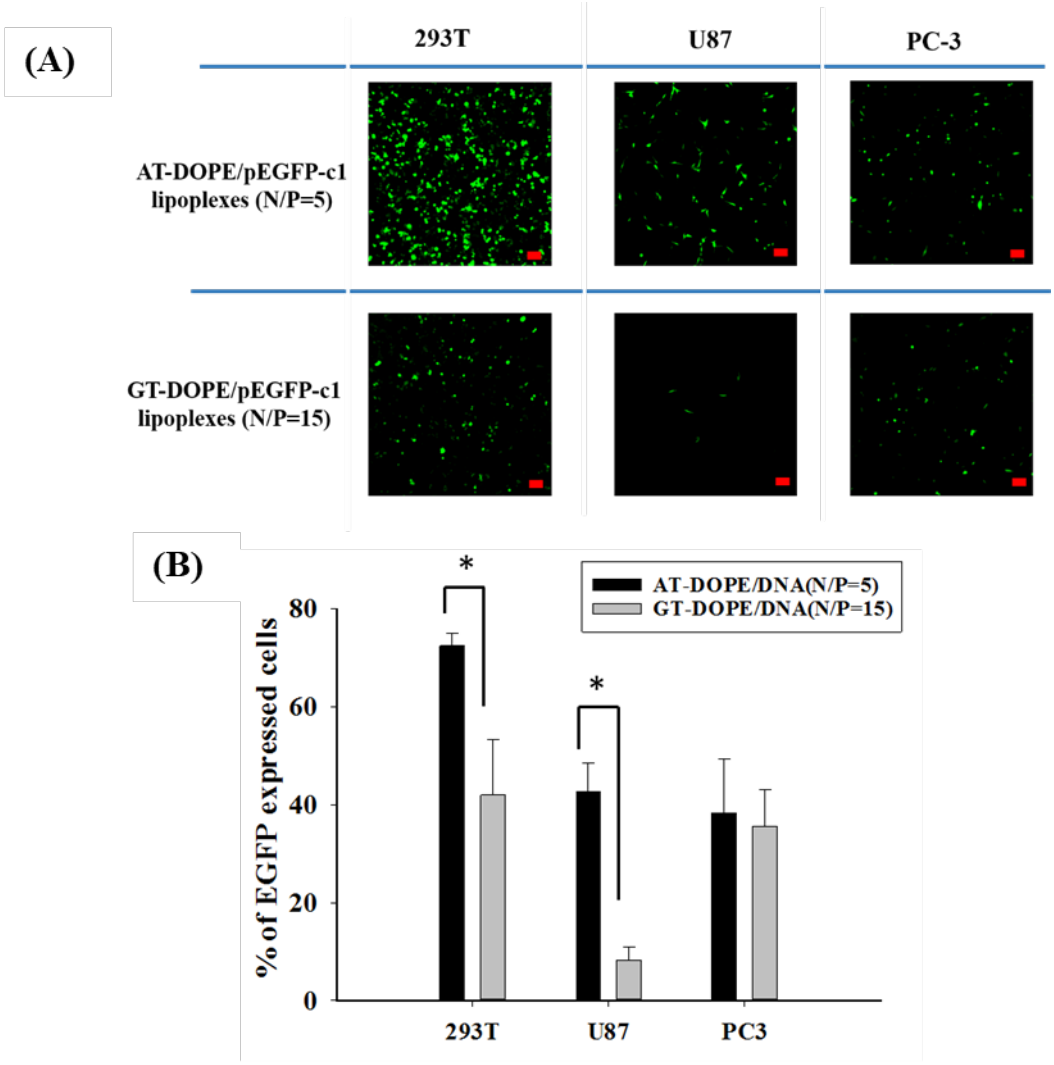

Figure 2.7: *(A) GFP expression in 293T, U87, and PC-3 cells exposed to AT-DOPE/pDNA at the N/P ratio of 5 and GT-DOPE/pDNA at the N/P ratio of 15. The scale bar is 100 µm. (B) Percentage of GFP-positive cells analyzed by flow cytometry (n=3, *p<0.05).*

Because of malignant glioma dependence on exogenous arginine due to metabolic characteristic,[161-163] U87 cells were thus selected to verify if the arginine-conjugated liposome could be a potential candidate for glioma-targeting gene delivery vector. To demonstrate the difference of transfection efficiency between AT-DOPE and GT-DOPE, plasmid pGL3-control was labeled with a Cy-5 dye and complexed with AT-DOPE or GT-DOPE and co-incubated with U87 cells for 2 h. Interestingly, the intracellular uptake of Cy5-labeled pDNA in red fluorescence is clearly seen significantly higher in AT-DOPE/Cy5-pDNA than in GT-DOPE/Cy5-pDNA in U87 cells (**Figure 2.9**).

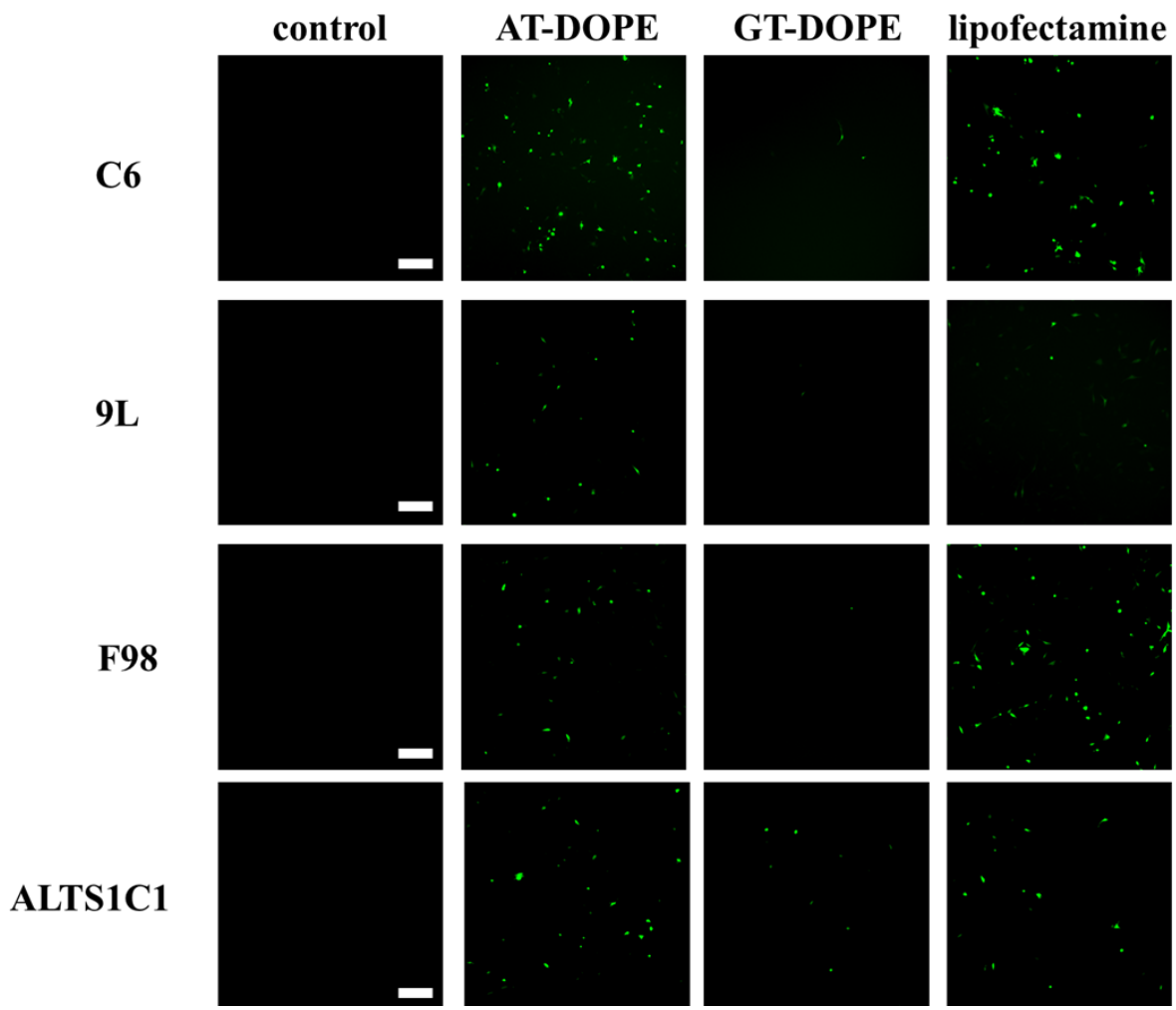

Figure 2.8: *Green fluorescence protein (GFP) expression in different glioma cells: C6, 9L, F98 and ALTS1C1 cells exposed to AT-DOPE/pDNA at the N/P ratio of 5 or GT-DOPE/pDNA at the N/P ratio of 15. The scale bar is 200 µm.*

As described previously, glioma U87 cells endowed arginine auxotrophic characteristics;[142, 161-163] thus, it is expected that AT-DOPE facilitates higher transfection efficiency specifically in glioma cell lines in comparison with GT-DOPE. Transfection efficiency majorly depends on the cell type, although many other factors also take part. Different cell lines react differently to transfecting reagents.[164] In case of PC3 cells in the current study, no selectivity was observed between AT-DOPE and GT-DOPE liposomes. This indicates that the interaction and mechanism of transfection of AT and GT based liposomes might be similar in PC-3 cells. On the other hand, significant difference in transfection efficiency of AT-DOPE and GT-DOPE was evident in case of HEK-293, U87 and other glioma cells. Particularly, in case of U87, 4-

fold higher transfection efficiency of AT-DOPE over GT-DOPE (**Figure 2.7**B) clearly indicates that the internalization was selective towards AT-DOPE. This was further confirmed by the cellular uptake study as shown in **Figure 2.9**. The confocal laser scanning microscopic (CLSM) images of U87 cells exposed to AT-DOPE/Cy5-labeled pDNA at the N/P ratio of 5 indeed displayed higher pDNA internalization than those exposed to GT-DOPE/Cy5-labeled pDNA at the N/P ratio of 15.

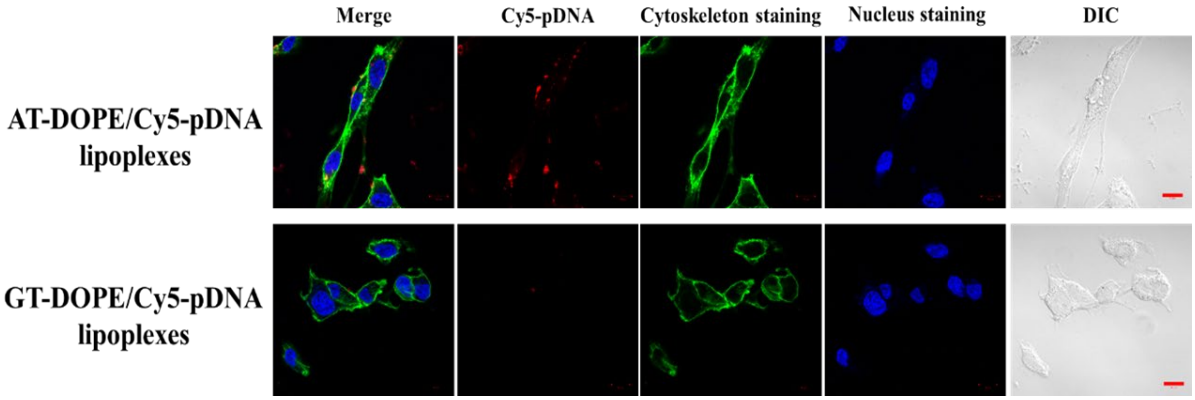

Figure 2.9: *CLSM images of U87 cells exposed to AT-DOPE/Cy5-labeled pDNA (2μg/well) at the N/P ratio of 5 or GT-DOPE/Cy5-labeled pDNA at the N/P ratio of 15. Blue: nuclei stained by DAPI; Green: cytoskeletal actin stained by Alexa Fluor 488; Red: pGL3-control plasmid stained with Cy-5. The scale bar is 10 μm.*

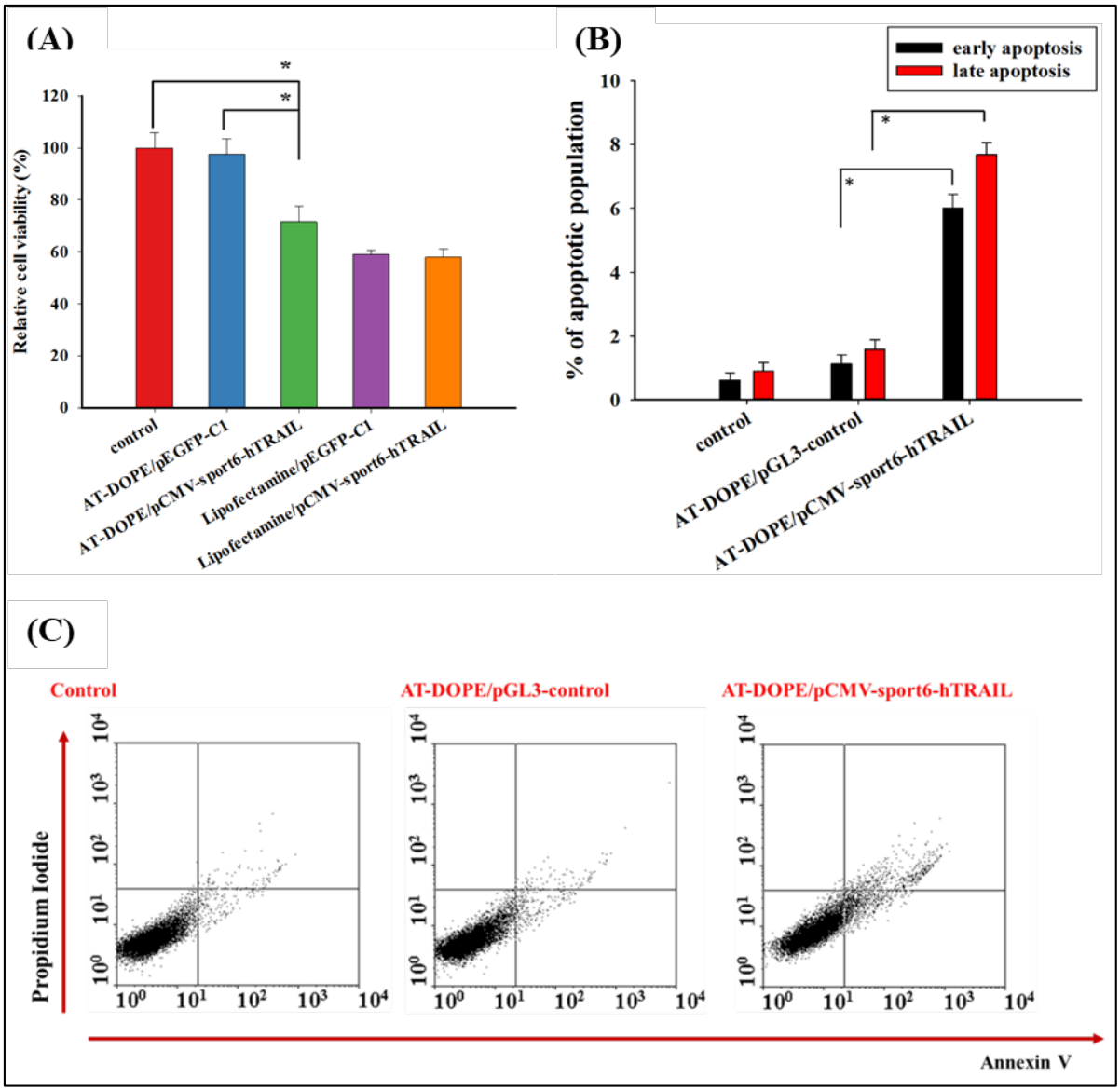

Figure 2.10: *Induction of apoptosis in U87 cells exposed to AT-DOPE/pTRAIL. (A) Cytotoxicity measured by MTT assay. Plasmid pEGFP-C1 was used as a negative control (n=8, *p<0.05). (B) Apoptotic percentage positive cells summed from the late apoptosis (upper right quadrant) and the early apoptosis (lower right quadrant) of Figure 7B (n=3, *p<0.05). (C) Representative flow cytometry histograms of apoptotic of U87 cells exposed to AT-DOPE/pTRAIL using Annexin V-Propidium iodide dual-staining assay.*

2.2.5. In Vitro TRAIL Expression-Induced Cell Apoptosis: As a proof of concept, the therapeutic potential of AT-DOPE/pCMV-sport6-hTRAIL (pTRAIL) lipoplex was used to demonstrate its efficiency of inducing apoptotic behavior against U87 cells. AT-DOPE/pTRAIL was prepared at the optimum N/P ratio of 5, and TRAIL-transfection induced

apoptosis was preliminarily evaluated by MTT assay. **Figure 2.10A** shows ~70% cell viability for U87 cells transfected with AT-DOPE/pTRAIL and ~98% cell viability for the cells transfected with AT-DOPE/pEGFP-C1. The cell viabilities of Lipofectamine/pTRAIL and Lipofectamine/pEGFP-C1 were ~60%; no difference in cytotoxicity was observed in the use of pTRAIL or pEGFP as a plasmid. Since Lipofectamine showed higher cytotoxicity than AT-DOPE in U87 cells (**Figure 2.5C**), the cellular morphology of U87 cells was directly observed using an optical microscope. Compared with cells alone, the morphology of U87 cells appeared irregular or rounded with a decrease in cell density after the cells were transfected with pTRAIL, independent of using AT-DOPE or Lipofectamine as the gene vector (**Figure 2.11**). Nevertheless, U87 cells shrank to rounded shape when the cells were transfected with Lipofectamine/pEGFP-C1 but remained intact when transfected with AT-DOPE/pEGFP-C1. This fact also explained the higher cytotoxicity of Lipofectamine than AT-DOPE. The cause of U87 cell death may also arise from Lipofectamine in lieu of pTRAIL alone.

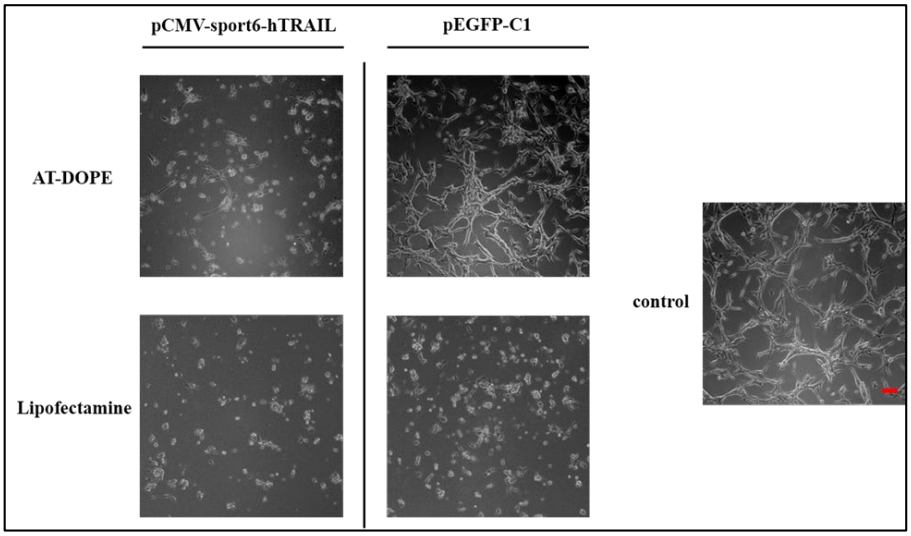

Figure 2.11: *Cellular morphology observed by optical microscopy. U87 cells were transfected with AT-DOPE/pCMV-sport6-hTRAIL or pEGFP-c1 at the N/P ratio of 5 for 48-h post-incubation. The scale bar is 100 μm.*

Apoptotic activity of AT-DOPE/pTRAIL was further evaluated by Annexin-V/PI dual staining assay (**Figure 2.10B and C**). Late apoptotic cells that were stained with PI and

Annexin V in the upper right quadrant and early apoptotic cells that were stained with Annexin V in the lower right quadrant, summed up to account for the percentage of apoptotic cells. Due to the ambiguous apoptotic activity and inadequate amounts of cells available owing to the cytotoxicity of Lipofectamine, Annexin-V/PI dual staining assay was unsuccessful on Lipofectamine/pTRAIL treated cells. **Figure 2.10B** is the bar graph of apoptotic cells associated with the upper right quadrant and lower right quadrant of **Figure 2.10C**. AT-DOPE/pTRAIL showed higher level of apoptotic cells in early and late apoptotic phase than AT-DOPE/pGL3.

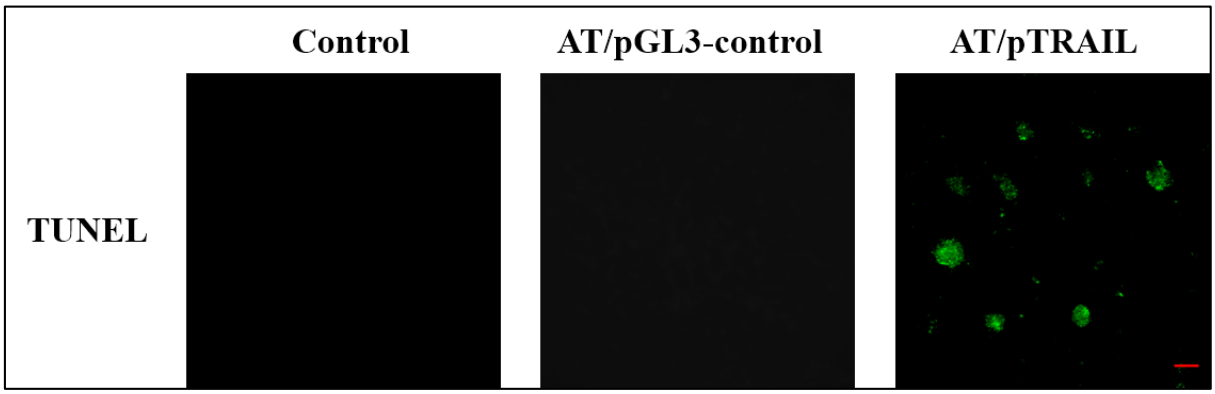

Figure 2.12: *Apoptosis induction of U87 cells treated with lipoplexes. TUNEL assay of U87 cells transfected with AT-DOPE/pCMV-sport6-hTRAIL or AT-DOPE/pGL3-control at the N/P ratio of 5 for 48-h post-incubation. The scale bar is 100 μm.*

In addition, apoptotic activity of AT-DOPE/pTRAIL was also evaluated with TUNEL assay (**Figure 2.12**). The increased TUNEL green fluorescence was clearly observed in the cells transfected with AT-DOPE/pTRAIL as compared with the cells transfected with AT-DOPE/pGL3-control. Significant improvement in cell-killing effect was found in the cells transfected with pTRAIL. A similar apoptotic result induced by pTRAIL has been reported using dendrimers as a gene delivery vector.[165, 166] Besides, it is believed that caspase-8 and caspase-3 play key roles of extrinsic apoptotic pathway. Thus, activation of caspase-8 and caspase-3 was detected in AT-DOPE/pTRAIL (N/P=5) and GT-DOPE/pTRAIL (N/P=15) lipoplexes transfected U87 cells. The fluorescence-activated cell sorting (FACS) results showed higher level of caspase-8 (**Figure 2.13A**) and caspase-3 (**Figure 2.13B**) activation in AT-

DOPE/pTRAIL lipoplex than GT-DOPE/pTRAIL lipoplex. Percentages of the caspase activities analyzed by CXP analysis software were included in **Figure 2.13C**. It implied that AT-DOPE/pTRAIL lipoplex induced higher apoptotic activity in U87 cells than GT-DOPE/pTRAIL. This fact is in accordance with the transfection results.

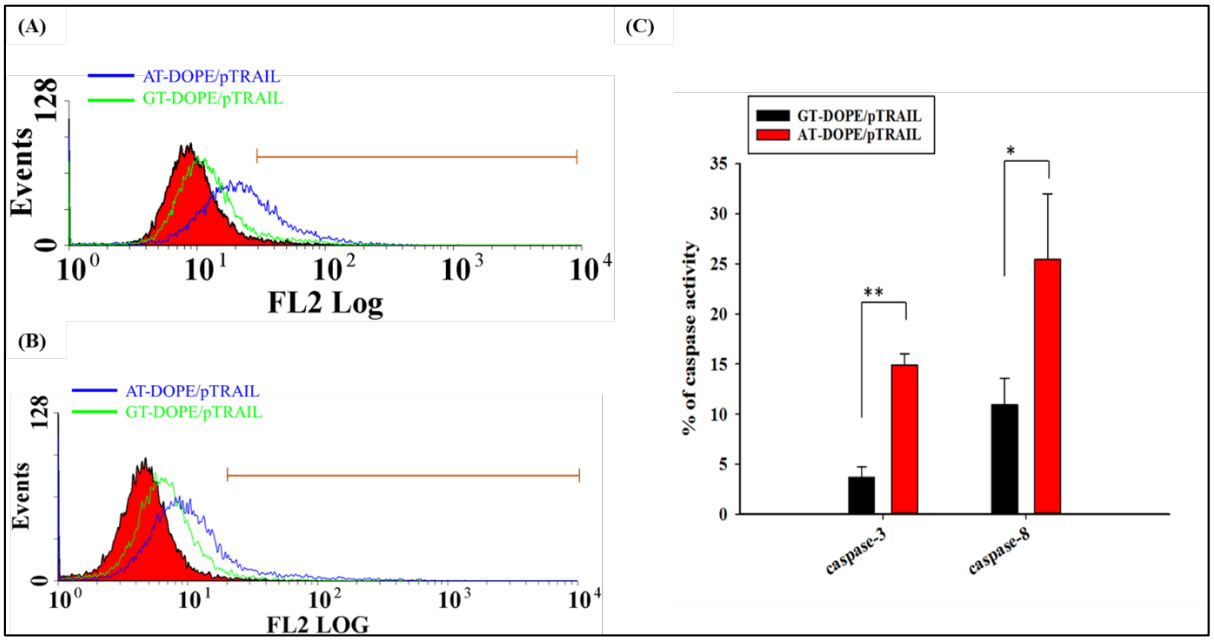

Figure 2.13: *Apoptosis induction of U87 cells treated with lipoplexes. (A) Caspase-8 activity and (B) Caspase-3 activity of pTRAIL-transfected U87 cells using AT-DOPE or GT-DOPE as vectors by flow cytometry. (C) Percentages of caspase activities analyzed by CXP analysis software (n=3, *P<0.05, **P<0.01).*

2.2.6. Increment of TRAIL Expression Upregulated Death Receptors and Apoptosis Signaling Pathway: pTRAIL induced TRAIL protein expression was initially visualized by immunofluorescence staining assay using CLSM. As shown in **Figure 2.14A**, cytoplasmic fluorescence in red was apparently observed in U87 cells transfected with AT-DOPE/pTRAIL but not with AT-DOPE/pGL3-control, implying a successful delivery of pTRAIL and TRAIL protein expression in AT-DOPE/pTRAIL transfected cells. The TRAIL protein expression was also examined by western blot analysis in U87 cells. As shown in **Figure 2.14B**, U87 cells were transfected with TRAIL-expressing plasmid using AT-DOPE as a vector. The TRAIL protein expression level was obviously seen in the pTRAIL plasmid-treated cells. The expression of

pTRAIL induced upregulation of DRs and apoptosis signaling pathway was further examined by western blot analysis in U87 cells. Previous studies show that TRAIL expression was associated with death receptors (DRs) and apoptosis signaling pathway.[26, 167, 168] Thus, U87 cells were transfected with AT-DOPE/pTRAIL at the N/P ratio of 5:1. **Figure 2.14C** displays that the target protein of DR4 and DR5 and apoptosis pathway which included cleaved caspase-9, cleaved caspase-3, cleaved PARP were all involved in AT-DOPE/pTRAIL-treated cells.

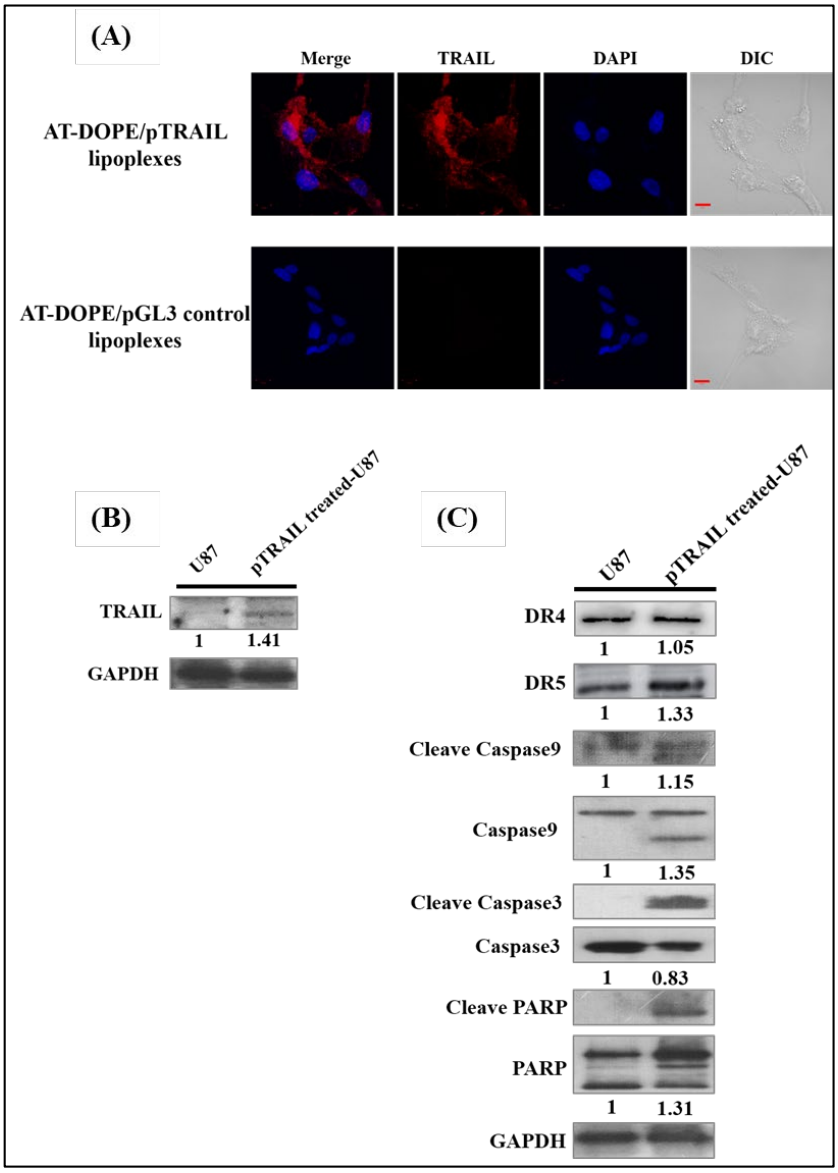

Figure 2.14: *The expression of TRAIL protein and regulation of death receptors and apoptosis signaling proteins of U87 cells transfected with AT-DOPE/pTRAIL. (A) Detection of TRAIL expression by immunofluorescence staining of U87 cells. U87 cells were transfected with AT-DOPE/pTRAIL or AT-DOPE/pGL3-control at the N/P ratio of 5. Red: TRAIL expression; Blue: DAPI-stained cell nuclei. The scale bar is 10 μm. (B) The level of TRAIL protein assayed by*

western blot. U87 cells were transfected with AT-DOPE/pTRAIL for 4 h. Protein lysates were obtained after 48-h post-incubation. (C) The effect of AT-DOPE/pTRAIL on death receptors and apoptosis signaling pathway evaluated by western blot. The death receptors include DR4 and DR5, and the factors of apoptosis pathway contain caspase9, cleaved caspase9, caspase3, cleaved caspase3, PARP, cleaved PARP. The GAPDH was used to normalize the levels of protein. The ratios of protein expression which were relative to non-treated U87 cells were calculated from western blot images using ImageJ software (n=2).

A significant upregulation of DR5 expression was noticed in the AT-DOPE/pTRAIL-treated cells compared with cells alone. Out of the two well-known TRAIL receptors (DR4 and DR5), DR5 is believed to be present on the cancer cell surface before TRAIL stimulation, however internalized into the cytoplasm upon adding TRAIL.[169] Recent studies on different cancer cell lines also prove that the significant high DR5 expression is noticeable upon TRAIL delivery.[170, 171] In addition, it was also reiterated by Kang et al. that DR5, but not DR4, was essential in inducing apoptosis mediated by TRAIL.[169] In accordance with these studies, our current results indicate that DR5 may be predominant in inducing apoptosis through subsequent activation of caspases. Receptor mediated apoptosis essentially involves caspases, as emphasized by previous mechanistic studies.[172-174] TRAIL induced apoptosis can be proceeded by either extrinsic or intrinsic pathways, however mediated by capsase-8, capsase-9 and capsase-3.[172] Although caspase-8 has been considered to be an initiator caspase, subsequent amplification of apoptotic signal lead by caspase-9[175] and the executioner caspase, caspase-3.[176, 177] Caspase-3 is considered as the main caspase responsible to execute apoptosis in various cell types.[177] TRAIL binding to DR4 or DR5 which are its cognate agonistic receptors leads to the formation of DISC (Death-Inducing Signaling Complex) which ultimately activates caspase-3.[176] Reduced expression of caspase-3 which in turn increases the expression of activated caspase-3 is one of the indications of induced cell death [57].[166] At the same time, TRAIL expression upregulates proapoptotic cleaved caspase-3 which contributes to programmed cell death.[178] Significant expression of cleaved caspase-9 and cleaved caspase-3 in the present study infers

that the cell death was possibly induced by TRAIL delivery. Our results imply that, compared with the control group, the high expression of DRs using AT-DOPE as the vector indeed induced the downstream of apoptosis pathway for triggering apoptotic cell death. It is also noted that while using AT-DOPE/pTRAIL system, the apoptosis in U87 cells is predominantly due to the delivered pTRAIL but not due to that vector related cytotoxicity which might be the case with the Lipofectamine.

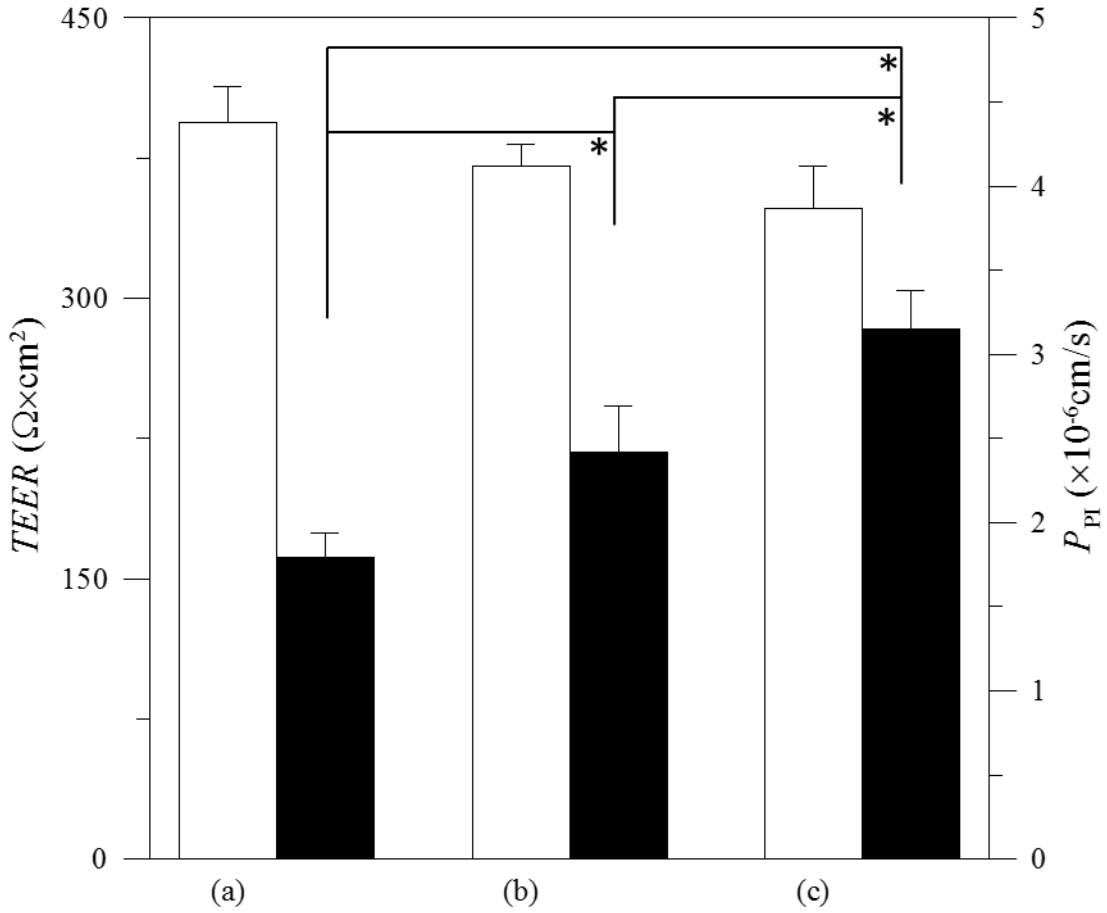

Figure 2.15: *The PET membrane with the cocultured human brain microvascular endothelial cells, human astrocytes, and human brain vascular pericytes (HBMECs/HAs/HBVPs) established as a BBB model to analyze the efficacy of lipoplexes entering the brain. The transendothelial electrical resistance (TEER) and propidium iodide (PI) permeability of (a) control, (b) GT/pDNA lipoplex, (c) AT/pDNA lipoplex, (n=3, *p<0.05). White bar for TEER (left axis); black bar for BBB permeability of PI (right axis).*

2.2.7. Permeability across the blood-brain barrier (BBB): The transendothelial electrical resistance (TEER) and PI permeability were assayed to illustrate the penetration ability of the

BBB. It is known that the α-tocopherol moiety could across the BBB and enhance accumulation in the nanomedicine containing α-tocopherol in the brain.[179] To test the permeability across the BBB, TEER and PI permeability values of AT- and GT-based lipoplexes were measured. The *ex vivo* BBB model was established by co-culture of human brain microvascular endothelial cells, human astrocytes, and human brain vascular pericytes (HBMECs/HAs/HBVPs). As shown in **Figure 2.15**, the AT-DOPE/pDNA lipoplex exhibited the highest level of PI penetration (3.15±0.23) as compared with control (1.79±0.15) and GT-DOPE/pDNA lipoplex (2.42±0.27). Nevertheless, there is insignificant difference in TEER level. This result implied that both AT- or GT-based lipoplex passed the BBB via receptor-mediate transcytosis rather than disrupted the tight junction of HBMECs according to previous publication[180] and the arginine conjugates with α-tocopherol indeed enhance the transport across the BBB.

2.3. CONCLUSIONS

Two new cationic lipids were successfully synthesized conjugating the natural biomolecules, arginine or glycine with α-tocopherol. Liposomal formulations of cationic lipids with fusogenic helper lipid DOPE yielded storage stable co-liposomes with favorable size and surface charge for transfection. Positively charged nanosized macromolecular assemblies were formed after successful binding of DNA with liposomes. The formulations either as free liposomes or as lipoplexes combined with pEGFP-C1, have shown high cell viabilities in several cell lines signifying that these nano carriers are safe for delivery applications. Transfection efficiencies were optimized over the different N/P ratios using pEGFP-C1 while qualitatively and quantitatively determined by fluorescence microscopy and flow cytometry, respectively. Transfection and cellular uptake studies discovered that arginine containing AT-based lipoplexes attained selectively high internalization in U87 glioblastoma cells. The AT-based lipoplex showed higher level of permeability than GT-based lipoplex using the *ex vivo* BBB model. Furthermore, considering the low cytotoxicity and high transfection capability,

AT-DOPE liposomes emerged as a healthier transfection reagent than commercial Lipofectamine-2000. AT-DOPE liposomes were further utilized to complex and deliver the therapeutic gene pTRAIL into U87 and PC3 cancer cell lines. Interestingly, the apoptosis activity through TRAIL mediated cytotoxicity was significantly high in U87 glioblastoma cells, substantiating the preliminary transfection results. Apoptosis induction of AT-DOPE/pTRAIL lipoplex in U87 cells was verified by Annexin-V/PI dual staining, TUNEL, caspase-8 and caspase-3 activity assays. TRAIL binding DR stimulates apoptosis pathway which was corroborated by western blot analysis. The results indicate that the AT-DOPE/pTRAIL lipoplexes selectively penetrated into glioblastoma cells and induced apoptotic cell death after intracellular pTRAIL delivery. Given that pTRAIL is a cancer cell specific anticancer agent and AT-DOPE being the biocompatible nanocarrier system, we envisage that AT-DOPE/pTRAIL biomacromolecular assembly can be an effective and safe non-viral therapeutic candidate for glioblastoma gene therapy.

2.4. EXPERIMENTAL SECTION

2.4.1. Materials. α-tocopherol, 2-bromoethanol, Boc-glycine, Fmoc-Arg(pbf)-OH and 1,2-dioleoyl-sn-glycerol-3-phosphoethanolamine (DOPE) were purchased from Sigma (Sigma-Aldrich Co., Ltd.). Lipofectamine-2000 was purchased from Invitrogen Life Technologies. Unless otherwise mentioned, different organic solvents and reagents including, piperidine, sodium hydroxide (NaOH), dimethyl formamide (DMF), methanol, methylene chloride (DCM), trifluoroacetic acid (TFA), N, N′ -dicyclohexylcarbodiimide (DCC) and 4-dimethylaminopyridine (DMAP) were procured from Sigma, Alfa Aesor and Finar at highest purity and were utilised without further purification. Silica gel thin-layer chromatography plates (0.25 mm) were used to monitor reaction progress. Column chromatography separation of compounds was performed with silica gel (60-120 mesh, Acme Synthetic Chemicals, India). ^{1}H and ^{13}C NMR spectral data were recorded on a Varian FT400 MHz NMR spectrometer.

Mass spectral data were obtained using a commercial LCQ ion trap mass spectrometer equipped with an ESI source (Thermo Finnigan, SanJose, CA, U.S.). 3-(4,5- Dimethylthiazol-2-yl)-2,5-diphenyl-tetrazolium bromide (MTT) was obtained from MP Biomedicals. Dulbecco's Modified Eagle Medium (DMEM), Phosphate buffer saline (PBS), Roswell Park Memorial Institute (RPMI) 1640 Medium, fetal bovine serum (FBS) and trypsin−EDTA were purchased from Invitrogen. pTRAIL plasmid was a gift from Prof. Chien-Wen Chang. In brief, the pTRAIL vector was prepared by cloning TRAIL gene (Costumed synthesis by Genedirex) into the downstream of CMV promoter of pcDNA3 (Invitrogen) vector.

Synthesis. Two new cationic amphiphiles were synthesized using the strategies described in **Scheme 2.1**. Characterization of the final lipids and their precedent intermediates was done by NMR (Supporting Information) and mass spectrometry.

2.4.2. Synthesis of Arginine-α-tocopherol Lipid (AT)

Synthesis of 2-Tocopheryloxyethanol (TEOH). TEOH was synthesized by previously described method in the literature with slight modification.[181] Briefly, α-tocopherol (1.0 eq, 1.0 g) in anhydrous DMF (5 mL) was taken in round bottom flask. 2-Bromoethanol (1.25 eq, 0.22 mL) and NaOH (1.5 eq, 0.14 g) were added to the flask and stirred for 16 h at 90°C. The reaction was cooled to room temperature and added with water (50 mL). The crude product was extracted with diethyl ether (30 mL × 3). The organic layer was collected, dried over sodium sulfate and concentrated under vacuum. The crude was subjected to silica gel column chromatography for further purification using petroleum ether (PE) and ethyl acetate (EA) as mobile phase (PE: EA = 9:1). Yield: 0.75g (69%). ^{1}H NMR [δ/ppm] (400 MHz, $CDCl_3$) 3.95-3.93 (t, 2H, OCH_2CH_2OH), 3.80-3.78 (t, 2H, OCH_2CH_2OH), 2.58 (t, 2H, tocopheryl), 2.18 (s, 3H, CH_3), 2.14 (s, 3H, CH_3), 2.09 (s, 3H, CH_3), 1.80 (m, 2H, tocopheryl), 1.61-1.04 (m, 24H, tocopheryl), 0.87-0.83 (m, 12H, tocopheryl, 4 × CH_3). MS: calculated: 474.41, found: 475.42 $[M + H]^+$, 497.40 $[M + Na]^+$.

Synthesis of 2-Tocopheryloxyethyl 2-((fmoc)amino)-5-(3-(pbf)guanidino)pentanoate (FmAPT). TEOH (1.0 eq, 0.474 g), Fmoc-Arg(pbf)-OH (1.1 eq, 0.713 g,), DMAP (0.15 eq, 0.018 g,) and DCC (1.5 eq, 0.31 g,) were added to round bottom flask with 10 mL of dry DCM at 0 $^{\circ}$C. The solution was stirred at 0 ^{0}C for 30 minutes followed by stirring at room temperature for another 24 h. Dicyclohexylurea (DCU) formed was filtered off and the remaining filtrate was concentrated by vacuum evaporation. The concentrated content was added with 50 mL of EA and washed with brine (2×50 mL) and water (2×50 mL). The organic phase was dried over Na_2SO_4 and concentrated. Chromatographic purification with 2% methanol in chloroform as mobile phase yielded white solid as product. Yield: 0.915 (83%). ^{1}H NMR [δ/ppm] (400 MHz, $CDCl_3$) 7.78-7.76 (d, 2H, Fmoc-4-H-, 5-H-), 7.60-7.59 (d, 2H, Fmoc-1-H-, 8-H-), 7.40-7.38 (m, 2H, Fmoc-3-H-, 6-H-), 7.33-7.30 (m, 2H, Fmoc-2-H-, 7-H-), 4.43 (m, 2H, Fmoc-CH_2-), 4.42 (m, 2H, TEOH, CO(O)CH_2), 4.21 (t, 1H, Fmoc-CH-), 4.18-4.12 (m, 1H, Arginine-CH-), 3.90 (m, 2H, TEOH-OCH_2-), 3.30-3.22 (dm, 2H, Arg -CH_2-), 2.93 (s, 2H, pbf -CH_2-), 2.59-2.52 (m, 8H, pbf, 2 × CH_3-, tocopheryl-CH_2-), 2.16 (s, 3H, pbf- CH_3), 2.12-2.07 (t, 9H, tocopheryl, 3 × CH_3-), 1.80 (m, 2H, tocopheryl), 1.95 (m, 2H, Arg -CH_2-), 1.66 (m, 2H, Arg -CH_2-), 1.55 (m, 2H, tocopheryl -CH_2-), 1.45 (s, 9H, pbf , 2 × CH_3-, tocopheryl -CH_3), 1.34-1.10 (m, 18H, tocopheryl), 0.90-0.86 (m, 12H, tocopheryl, 4 × CH_3-). MS: calculated: 1104.66, found: 1105.88 $[M + H]^+$, 1127.87 $[M + Na]^+$.

Synthesis of 2-Tocopheryloxyethyl 2-Amino-5-(3-(pbf)guanidino)pentanoate (APT). Deprotection of Fmoc group was carried out using piperidine (20 % in DMF). Briefly, FmAPT (0.68 g, 0.62mmol) was dissolved in 5 mL of DMF and 1.5 mL of piperidine was added. The mixture was stirred at room temperature for 3 h while monitoring the reaction progress by TLC. After complete deprotection, 50 mL of EA was added to the reaction mixture and washed with brine (2 × 50 mL) and water (2 × 50 mL). Organic phase was dried over Na_2SO_4 and concentrated under vacuum. Chromatographic purification with 3% methanol in chloroform yielded pure product (APT). Yield: 0.4g (73%). ^{1}H NMR [δ/ppm] (400 MHz, $CDCl_3$) 6.37 (s,

2H, NH2), 4.47-4.39 (m, 2H, TEOH -CH_2-), 4.18 (m, 1H, Arginine -CH-), 3.85 (m, 2H, TEOH -CH_2-), 3.23 (m, 2H, Arg -CH_2-), 2.93 (s, 2H, pbf -CH_2-), 2.95-2.88 (t, 2H, tocopheryl -CH_2-), 2.55(s, 3H, pbf -CH_3), 2.49 (s, 3H, pbf -CH_3), 2.13 (s, 3H, pbf -CH_3), 2.09 (s, 3H, tocopheryl -CH_3), 2.06 (s, 6H, tocopheryl 2 × CH_3-), 1.88-1.71 (m, 4H, tocopheryl -CH_2-, Arg -CH_2-), 1.66 (m, 2H, Arg -CH_2-), 1.55 (m, 2H, tocopheryl -CH_2-), 1.45 (s, 9H, pbf 2 × CH_3-, tocopheryl -CH_3), 1.34-1.10 (m, 18H, tocopheryl), 0.87-0.83 (m, 12H, tocopheryl, 4 × CH_3-). MS: calculated: 880.59, found: 881.60 $[M + H]^+$.

Synthesis of 2- Tocopheryloxyethyl 2-Amino-5-guanidinopentanoate (AT). Deprotection of pbf group was achieved by trifluoroacetic acid (TFA) in DCM. APT (0.3 g, 0.34 mmol) in 2 mL of DCM was added with 2 mL of TFA slowly at 0 ^{0}C. After addition, the ice bath was removed and the reaction mixture was stirred for 1 h. After deprotection of pbf, TFA and DCM were evaporated under vacuum and the crude product was washed with diethyl ether which provided pure arginine-tocopherol conjugate as greasy solid. Yield: 0.18g (80%), ^{1}H NMR [δ/ppm] (400 MHz, DMSO-D6) 4.47-4.39 (m, 2H, TEOH -CH_2-), 4.05 (t, 1H, Arg -CH-), 3.83 (m, 2H, TEOH -CH_2-), 3.13 (m, 2H, Arg -CH_2-), 2.0 (s, 3H, tocopheryl -CH_3), 2.06 (s, 3H, tocopheryl -CH_3), 1.99 (s, 3H, tocopheryl -CH_3), 1.88-1.73 (m, 2H, tocopheryl –CH_2),1.73 (t, 2H, Arg -CH_2-), 1.54-1.46 (m, 4H, tocopheryl -CH_2-, Arg -CH_2-), 1.37 (s, 3H, tocopheryl -CH_3), 1.23-1.06 (m, 18H, tocopheryl), 0.84-0.81 (m, 12H, tocopheryl, 4 × CH_3). MS: calculated: 630.51, found: 631.55 $[M + H]^+$.

2.4.3. Synthesis of Glycine-α-tocopherol Lipid (GT)

Synthesis of 2-Tocopheryloxyethyl 2-((boc)amino)acetate (BGT). TEOH (1.0eq, 0.1 g), Boc-glycine (1.1 eq, 0.041 g), DMAP (0.15 eq, 0.004 g) and DCC (1.5 eq, 0.065 g) were added to round bottom flask with 5 mL of dry DCM at 0 ^{0}C. The reaction mixture was stirred at 0 ^{0}C for 30 minutes followed by stirring at room temperature for another 24 h. DCU was filtered off and the remaining filtrate was concentrated by vacuum evaporation. The reaction mixture was

added with 30 mL of EA and washed with brine (2×30 mL) and water (2×30 mL). The organic phase was dried over Na_2SO_4 and concentrated. Chromatographic purification with 10% EA in hexane as mobile phase yielded the product as white waxy solid. Yield: 0.125 g (94 %). ^{1}H NMR [δ/ppm] (400 MHz, $CDCl_3$) 4.48-4.44 (t, 2H, TEOH -CO(O)CH_2), 4.02-3.99 (m, 2H, TEOH -CH_2O), 3.90-3.86 (m, 2H, glycine -CH_2-), 2.59-2.53 (t, 2H, tocopheryl -CH2-), 2.16 (s, 3H, tocopheryl -CH_3), 2.12 (s, 3H, tocopheryl -CH_3), 2.07 (s, 3H, tocopheryl -CH_3), 1.77 (m, 2H, tocopheryl), 1.59 (m, 5H, CH_2, tocopheryl, 3 × CH-), 1.46 (s, 9H, Boc, 3 × CH_3-), 1.34-1.10 (m, 18H, tocopheryl), 0.88-0.85 (m, 12H, tocopheryl, 4 × CH_3-). MS: calculated: 631.48, found: 632.46 $[M + H]^+$, 654.43 $[M + Na]^+$.

Synthesis of 2-Tocopheryloxyethyl 2-Aminoacetate (GT). BGT (0.115g, 0.182 mmol) was dissolved in 2 mL of DCM and 0.5 mL of TFA was added dropwise. The reaction mixture was stirred for 1 h at 0^0C. After deprotection of Boc group, TFA and DCM were evaporated under vacuum and the crude mixture was further purified by silica gel column chromatography. Pure product GT was eluted using 6–8 % methanol in dichloromethane as greasy solid. Yield: 0.102g (87%), ^{1}H NMR [δ/ppm] (400 MHz, $CDCl_3$) 4.48 (m, 2H, TEOH -CO(O)CH_2), 3.92-3.83 (m, 4H, TEOH -CH_2O, Glycine -CH2-), 2.53 (m, 2H, tocopheryl -CH2-), 2.21-2.04 (m, 9H, tocopheryl, 3 × CH_3-), 1.74 (m, 2H, tocopheryl–CH2), 1.55-1.07 (m, 24H), 0.87-0.84 (m, 12H, tocopheryl -CH_3). MS: calculated: 531.43, found: 532.38 $[M + H]^+$.

2.4.4. Preparation of Liposomes and Lipoplexes: Each cationic lipid and co-lipid (DOPE) in chloroform solutions at required molar ratios were mixed in clean and dried Wheaton glass vials. Solvent was removed by a slow stream of moisture-free nitrogen gas initially, to make a thin film on the wall. The film was placed under high vacuum for 3 h to remove chloroform residue. The dried-up lipid film was added with deionized (Milli-Q) water for hydration of lipid film so as to make the final lipid concentration of 1 mg/mL. After hydrating the thin film overnight at room temperature, the vial was repeatedly subjected to vortex and bath sonication

to make turbid solution containing multi-lamellar vesicles. Finally, the solution was sonicated using a probe sonicator (pulse mode, 6 s on/off, 25% Amplitude) until homogenous colloidal solution obtained in an ice bath. These visibly clear liposomal stock solutions were stored at 4 °C for further use. No visible aggregation was detected, even after 30 days of storage. To form lipoplexes, pDNA concentration was kept constant at 0.3 µg/50 µL for gel retardation assay and 1 µg/50 µL for other studies. Liposomal stock solution was further diluted in sterile deionized water at various concentrations and added with 50 µL of DNA solution under medium vortex. The liposome/DNA mixture was vortexed vigorously for 30 seconds and incubated at room temperature for 20-30 minutes. The lipoplexes formed at different N/P ratios were investigated for their size, zeta potential, DNA binding ability, cytotoxicity and transfection efficiency.

2.4.5. Characterization of Liposomes and Lipoplexes

Hydrodynamic diameters and net surface charges (zeta potentials) of liposomes and lipoplexes were determined at room temperature using dynamic light scattering (DLS) zeta-sizer (ELSZ-2000, Otsuka Electronics). Samples were prepared in deionized water and measured at solution refractive index and viscosity of 1.33 and 0.89, respectively. The instrument calibration was done using polystyrene nanospheres (−50 mV, 220 ± 6 nm). Light scattering analysis with a laser beam of 633 nm was performed at a 90° scattering angle. All measurements were taken in triplicates and graphs were plotted with mean values. Samples were prepared and analyzed in a dust free condition.

The particle-size dispersion and aggregation pattern of the liposomes/lipoplexes were examined using a transmission electron microscope (TEM, HT7700, Hitachi). Briefly, a 200-mesh copper specimen grid (carbon coated) was glow-discharged for 90 seconds. Four microliters of liposomal suspension were dropped on a copper grid and kept at room

temperature to dry for a week. TEM Images were observed and captured using a CCD camera at 60 Kev acceleration voltage (DC voltage).

Agarose Gel Electrophoresis. The DNA complexation of liposomes was assessed by typical agarose gel electrophoresis assay. Cationic lipids (AT and GT) and their corresponding liposomes (lipid:DOPE at 1:1 ratio) were mixed with 0.3 μg of pDNA. Lipoplexes were formulated at different N/P ratios (1-15) by varying liposome concentrations and keeping a constant amount (0.3 μg) of pEGFP-N3 plasmid in 50 μL of de-ionized Milli-Q water. Complexes, after 30 minutes' incubation at room temperature, were added to the 0.8 % agarose gel. The electrophoresis was carried out at a current of 100 V for 20 min in Tris-acetate EDTA (TAE) buffer with ethidium bromide (EtBr) (1 mg/mL). The DNA retention pattern was observed under UV light at 365 nm.

2.4.6. Cell Experiments

U87 cells (a human glioblastoma cell line) were cultivated and maintained at 37 °C under humidified 5% CO_2 in MEM, supplemented with 10% fetal bovine serum (FBS), 1% sodium pyruvate and 100 μg/mL penicillin-streptomycin. 293T cells (a human embryonic kidney cell line) were cultivated in DMEM, supplemented with 10% fetal bovine serum (FBS) and 100 μg/mL penicillin-streptomycin. PC-3 cells (a human prostate cancer cell line) were cultivated in Roswell Park Memorial Institute medium-1640 (RPMI-1640), supplemented with 10% fetal bovine serum (FBS) and 100 μg/mL penicillin-streptomycin. The medium was replenished every two or three days, and the cells were sub-cultured after they had reached 90% confluence. ALTS1C1 cells (a murine astrocytoma cell) were obtained from the courtesy of Dr. Hsin-Cheng Chiu, Department of Biomedical Engineering and Environmental Sciences at National Tsing Hua University, Taiwan. F98, 9L, and C6 cells (originally purchased from ATCC®) were obtained from Dr. Ren-Jei Chung, Department of Chemical Engineering and Biotechnology at National Taipei University of Technology, Taiwan. These glioma cells were cultivated and

maintained at 37 °C under humidified 5% CO2 in DMEM, supplemented with 10% fetal bovine serum (FBS) and 100 μg/mL penicillin-streptomycin.

Cell viability. The cell viability of liposomes or lipoplexes were evaluated by MTT assay. The cytotoxicities of liposomes were examined for incubation with various concentrations of AT-DOPE liposome or GT-DOPE liposome liposomes (0.5–100 μg of liposome/mL). 293T, PC-3, and U87 cells were seeded in 96-well tissue culture plates at a density of 5×10^3/well in their corresponding medium containing 10% FBS. The relative of cell viability of lipoplexes were examined at various N/P ratios (5-15) of AT/DNA lipoplexes or GT/DNA lipoplexes for 48 h of post-incubation after they had been incubated at 37 °C for 4 h. The total lipid concentration for the cytotoxicity study of lipoplexes was same as that used for transfection studies. For N/P ratios 5, 7, 9 and 15, the total lipid concentration in each well was 10, 15, 19 and 32 μg/mL while 1 μg of pEGFP DNA was complexed with lipid. PEI-25K/DNA was prepared at an N/P ratio of 10 (10 μg/mL of PEI) and Lipofectamine/pDNA was prepared according to the manufacturer's protocol. The number of viable cells was determined by estimating their mitochondrial reductase activity using a tetrazolium-based colorimetric method.[182]

In vitro transgene expression. In vitro transgene expression was done in U87, PC-3 and 293T cells at a density of 5×10^4/well in 24-well plates and incubated in MEM or RPMI or DMEM medium containing 10% FBS for 24 h before transfection. Lipoplexes with N/P ratios of 5 -15 were prepared using various amounts of AT-DOPE or GT-DOPE liposome and a fixed DNA (pEGFP-C1 plasmid) amount of 1 μg to a final volume of 100 μL, which were added into MEM/RPMI/DMEM-maintained cells. Following 4h of incubation, the medium was replaced with fresh complete-medium and the cells were incubated for 48 h of post-transfection. Green fluorescence protein (GFP) expression was directly visualized using fluorescent microscopy (*Leica DMi8*; Leica Microsystems, Wetzlar, Germany). Moreover, after using fluorescence

microscopy to visualize GFP expression, the transfection efficiency was also analyzed by flow cytometry (Cytomics™ FC 500; Brea, CA, USA).

For a TRAIL expression, the procedures stated above were repeated to determine the transfection efficiency in glioma cell lines. To quantify the TRAIL expression, the transfected cells were twice rinsed gently with PBS, added to a 200-μL/well of RIPA buffer (Promega, Madison, WI, USA), and allowed to stand overnight at −20 ℃.

Confocal laser scanning microscope (CLSM). The protocol was followed previously publications.[182, 183] Briefly, the cellular uptake of lipoplexes was observed using a CLSM (LSM 700 Zeiss Confocal Microscopy, Stockholm, Sweden). U87 cells were seeded at a density of 1.0×10^5/well in 12-well plates containing one glass coverslip/well in MEM supplemented with 10% FBS, and incubated for 24 h. The AT or GT lipoplexes were prepared at optimum ratio of 5 or 15 respectively and the Cy5-labeled pGL3-control plasmid (Cy5 labeling kit; Mirus Bio LLC, Madison, WI, USA). The cells were exposed to the fluorescent lipoplexes at 37 °C for 4h. And then, the medium containing the lipoplexes was removed and washed gently with PBS. Next, the cell was fixed with 3.7% paraformaldehyde and rinsed with PBS three times. After that, the cell cytoskeleton was stained with Alexa Fluor 488 Phalloidin (Thermo Fisher Scientific, Waltham, MA, USA) and wash again. Subsequently, the cells on a coverslip were washed 3 times with PBS and directly mounted with a Fluoromount-G medium (Southern Biotech, Birmingham, AL, USA) on a glass slide. Cell images were captured and analyzed using Zeiss CLSM software.

CLSM was also used to observe immunofluorescence staining of pTRAIL transfected U87 cells. The staining protocol was followed previously publications. [183] U87 cells were seeded onto the glass coverslip in 12-well plate and transfected with AT-DOPE/pCMV-sport6-hTRAIL or AT-DOPE/pGL3-control at N/P ratio of 5 for 2 days post-incubation. Transfected cells were washed with PBS and fixed with 4% paraformaldehyde for 10 min at room temperature and then rinsed with PBS three times. Subsequently, cells on coverslips were treated with 0.2% triton X-100

(Sigma Aldrich) for 10 min, and then washed with PBS three times again. Non-specific reaction was blocked with blocking buffer (4% BSA in PBS) for 1 h at room temperature. After blocking, the buffer was removed, and cells were then incubated with Anti-TRAIL monoclonal primary antibody (1:400, Cell Signaling Technology, MA, USA) at 4°C overnight. After washing three times with PBS, cells were stained with Alexa Fluor 594-tagged secondary antibody (1:1000, Cell Signaling Technology) for 1 h at room temperature. After washing with PBS for three times, the coverslip with cells was directly mounted with a Fluoromount-G medium (Southern Biotech, Birmingham, AL, USA) on a glass slide and observed for confocal laser scanning microscopy (CLSM) observation (LSM 700 Zeiss Confocal Microscopy, Stockholm, Sweden).

Annexin-V/PI (propidium iodide) dual staining assay. Briefly, U87 cells were seeded in 24-well plates at 5×10^4 cells per well and incubated at 37 °C for 24 h before being transfected to AT-DOPE/pCMV-sport6-hTRAIL or negative-control plasmid. At N/P ratio of 5 of AT-DOPE/pDNA lipoplex was exposed to cells for 4h, and then medium was replaced the fresh medium. Following 48 h post-incubation, the Annexin-V/PI staining kit (Strong Biotech) was utilized to examine apoptotic activity according to previous publication. [184] Subsequently, the cells were collected, washed with PBS and resuspended in binding buffer with both Annexin-V and PI dye at 37°C for 30 min. After staining, the TRAIL-transfected U87 cells were washed with PBS again and analyzed using flow cytometer (Epics XL-MCL, Beckman Coulter). The experiment was repeated three times.

Western blot analysis. Cell lysates were extracted from TRAIL-expressing plasmid -treated cells at 2 days of incubation, washed twice with 1× PBS, and resuspended in radioimmunoprecipitation assay (RIPA) buffer (71009; Merck, Darmstadt, Germany). Western blotting was performed as previously described.[183] The membranes were blocked for 1 h at room temperature with Trident Universal Protein Blocking Reagent (GeneTex, California, USA) and incubated with primary antibodies at 4°C overnight. Primary antibodies were against

TRAIL antibody (1:1,000; GeneTex California, USA), GAPDH antibody (1:10,000; GeneTex California, USA), caspase-9 antibody (1:1,000; Cell signaling technology, USA), cleaved caspase-9 antibody (1:1,000; Cell signaling technology, USA), caspase-3 antibody (1:1,000; Cell signaling technology, USA), cleaved caspase-3 antibody (1:1,000; Cell signaling technology, USA), PARP antibody (1:1,000; Cell signaling technology, USA), cleaved PARP antibody (1:1,000; Cell signaling technology, USA), DR4 antibody (1:1,000; GeneTex California, USA) and DR5 antibody (1:1,000; GeneTex California, USA). The signals of chemiluminescent protein detection were detected using the Enhanced Chemi-Luminescence (ECL) western blotting reagent (Perkin-Elmer, Waltham, MA, USA).

TUNEL assay. Briefly, U87 cells were seeded in 12-well plates at density of 10^5 cells per well and incubated at 37 °C for 24 h before being transfected to AT-DOPE/pCMV-sport6-hTRAIL or negative-control pGL3-control plasmid. AT-DOPE/pDNA lipoplex at an N/P ratio of 5 was exposed to cells for 4 h, and then medium was replaced with the fresh medium. Following 2-day post-incubation, the In Situ Cell Death Detection Kit, Fluorescein (Roche) was utilized to examine apoptotic activity according to manufacturer's protocol. The cells were washed with PBS and fixed with 4% paraformaldehyde for 15 min. The cells were treated with permeabilization solution (0.1% Triton X-100 and 0.1% sodium citrate) for 2 min on ice. The cells were rinsed twice with PBS and incubated with TUNEL reaction solution for 60 min at 37 °C. Subsequently, the cells were analyzed under fluorescent microscopy (*Leica DMi8*; Leica Microsystems, Wentzler, Germany).

Caspase-8 and caspase-3 assay. U87 cells were transfected to AT-DOPE/pCMV-sport6-hTRAIL at an N/P ratio of 5 and GT-DOPE/pCMV-sport6-hTRAIL at an N/P ratio of 15. Following 2-day post-incubation, pTRAIL-transfected cells were harvested, washed with PBS, and fixed with 4% paraformaldehyde. Subsequently, the cells on coverslips were treated with 0.1% triton X-100 (Sigma Aldrich) for 10 min, and then washed with PBS three times and blocked with blocking buffer (4% BSA in PBS) at room temperature. Following blocking, the

cells were incubated with anti-caspase-8 or anti-caspase-3 monoclonal primary antibody or (1:400, Cell Signaling Technology) at 4°C for 2 h. After washing three times with PBS, the cells were stained with Alexa Fluor 594-tagged secondary antibody (1:1000, Cell Signaling Technology) 4°C for 1 h at room temperature. After washing three times with PBS, the cells were analyzed for flow cytometry (Cytomics™ FC 500). The quantitative analysis was analyzed by CXP software.

Ex vivo blood-brain barrier (BBB) assay. For establishing a BBB model, the transwell cell culture inserts with polyethylene terephthalate (PET) membrane (BD Falcon, CA, USA) were placed in the 24 well plate. Human brain microvascular endothelial cells (HBMECs, Sciencell Research Laboratories, CA, USA), human astrocytes (HAs, Sciencell Research Laboratories, CA, USA), and human brain vascular pericytes (HBVPs, Sciencell Research Laboratories, CA, USA) were co-cultured on PET membrane according to literature. [180, 185, 186] One hundred μL of AT/pDNA or GT/pDNA lipoplex containing 1 μg pDNA were added into the upper chamber of the transwell cell to measure the transendothelial electrical resistance (TEER, $\Omega \times cm^2$) using an electrical resistance system (Millipore, Billerica, MA, USA). The TEER value was measured as $TEER = (R_{sample} - R_{blank}) \times Am$, where Am is the area of the PET membrane in the transwell. In addition, the permeability of propidium iodide (PI, Sigma Aldrich) across the BBB was evaluated by treating culture medium containing PI (0.25 mg/mL) in the upper chamber of the HBMECs/HAs/HBVPs co-culture on the inserts after treatment with AT-DOPE/pDNA or GT-DOPE/pDNA lipoplex for 4 h. The permeated PI in the lower chamber was determined by fluorescent plate reader (Bio-tek, Winooski, VT, USA) at excitation and emission wavelengths of 485 and 590 nm, respectively.

SPECTRA

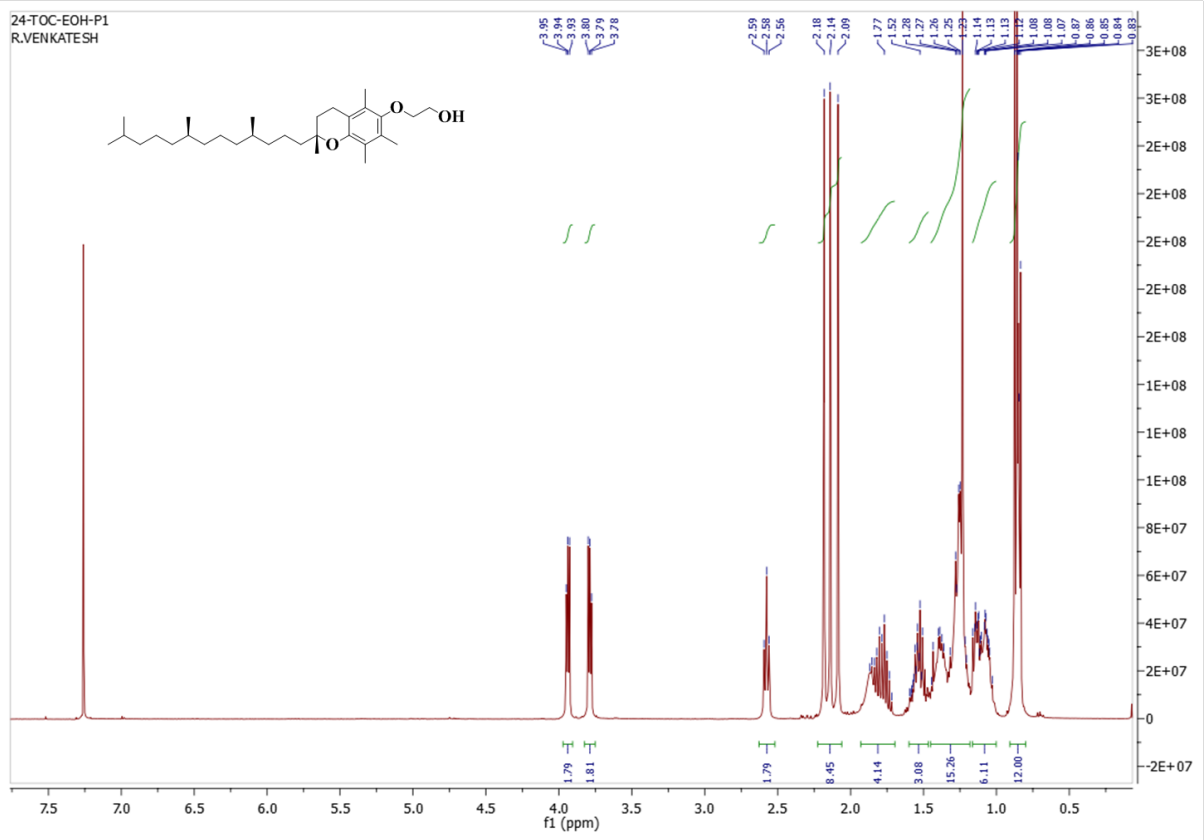

^{1}H NMR spectrum of TEOH (I) in $CDCl_3$

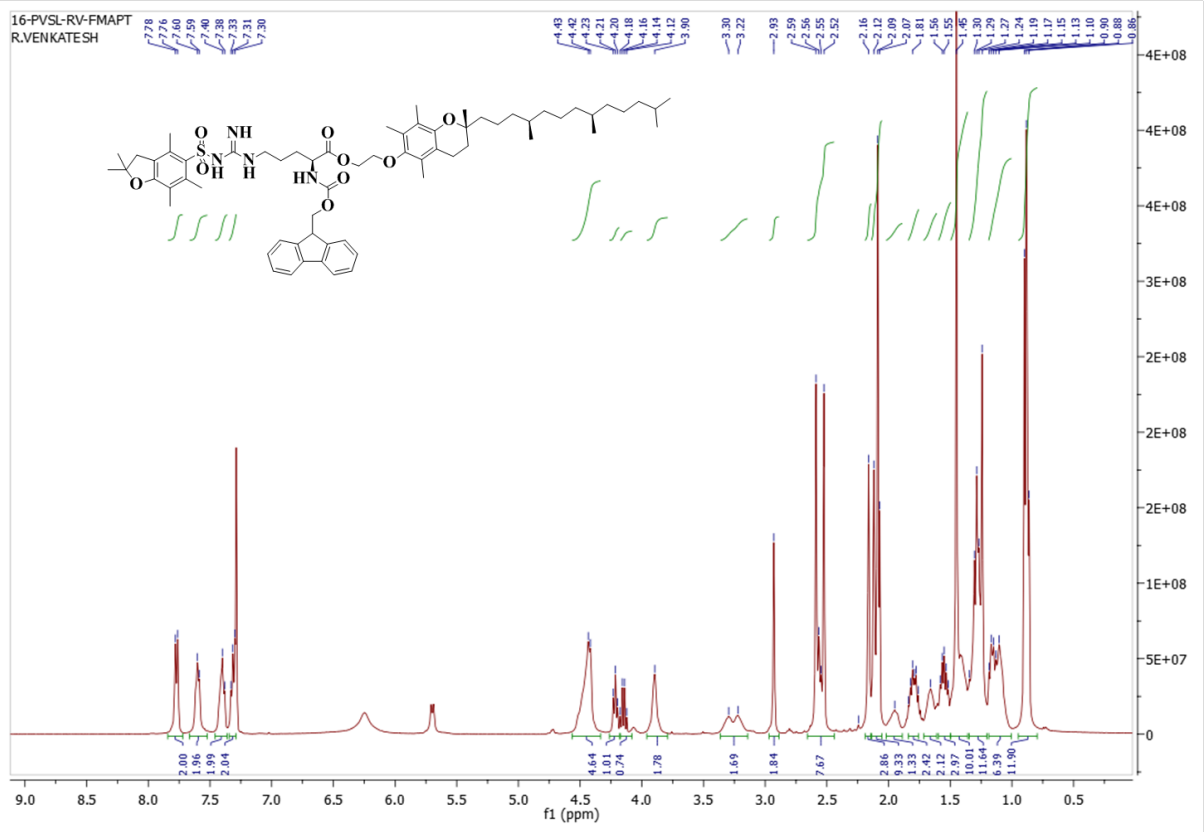

^{1}H NMR spectrum of FmAPT in $CDCl_3$

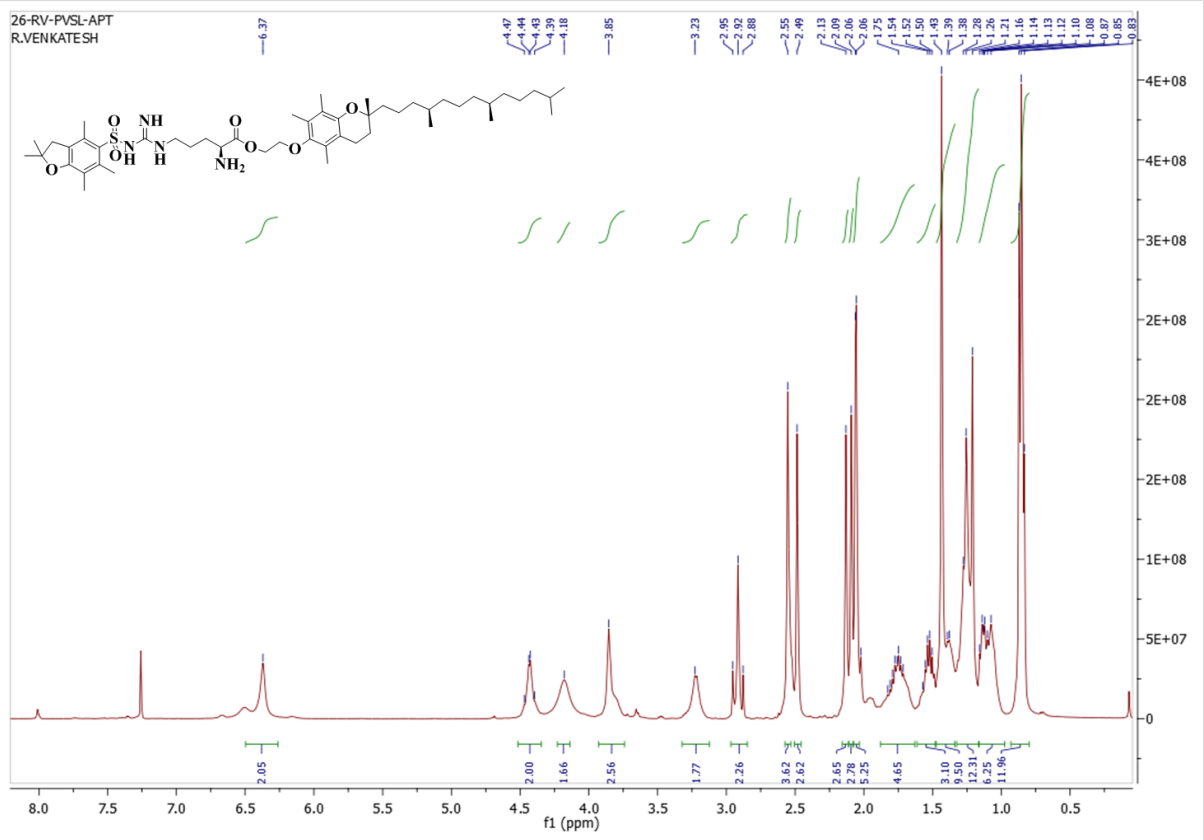

^{1}H NMR spectrum of APT in $CDCl_3$

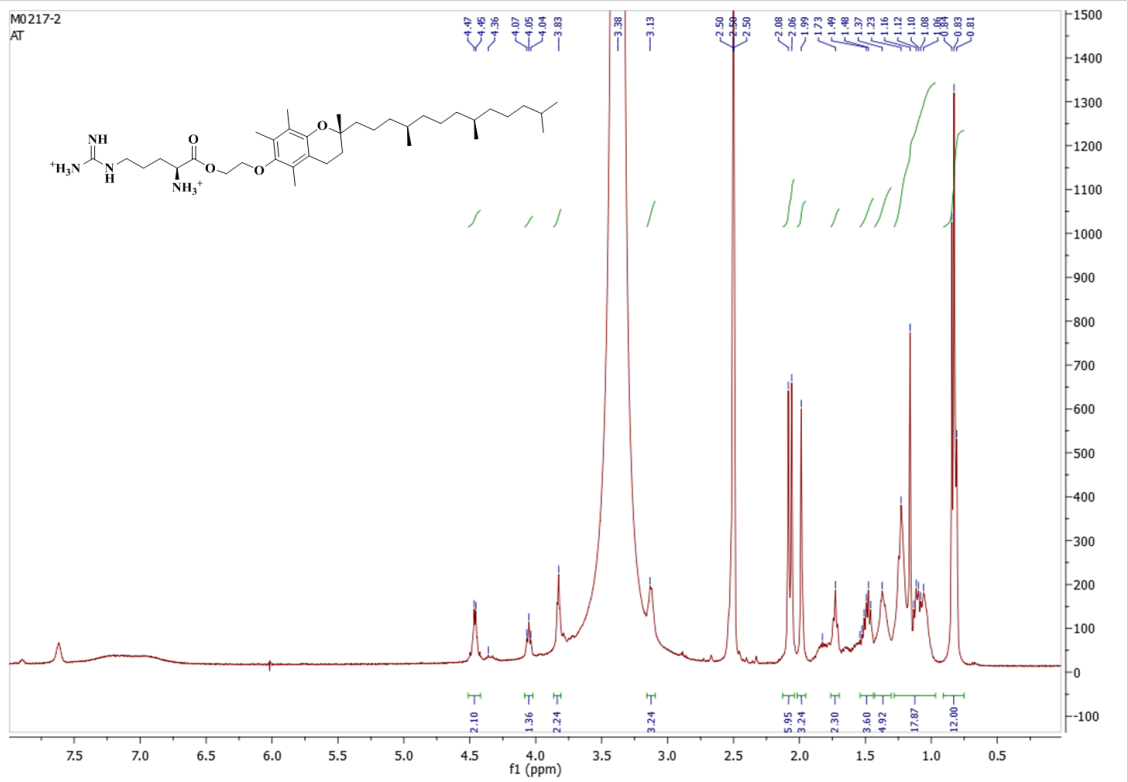

^{1}H NMR spectrum of AT in DMSO-*D_6*

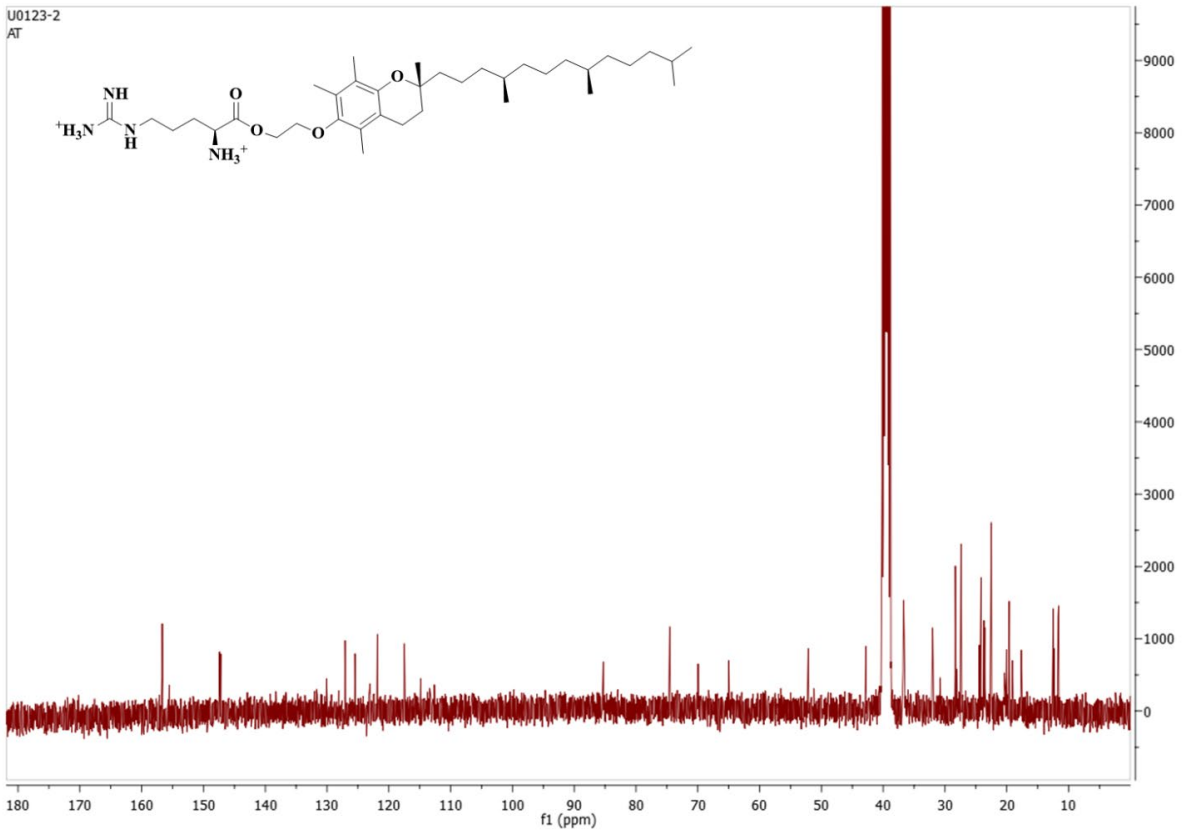

^{13}C NMR spectrum of AT in DMSO-*D*$_6$

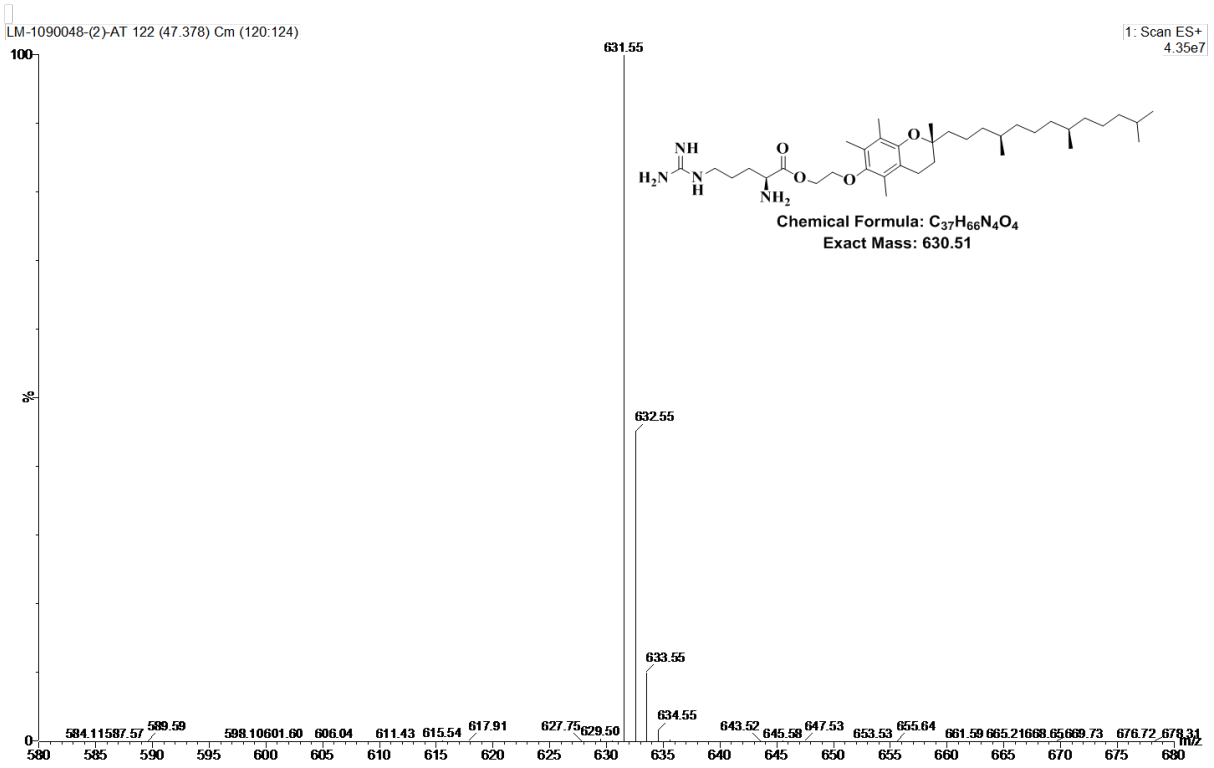

Mass spectrum of AT

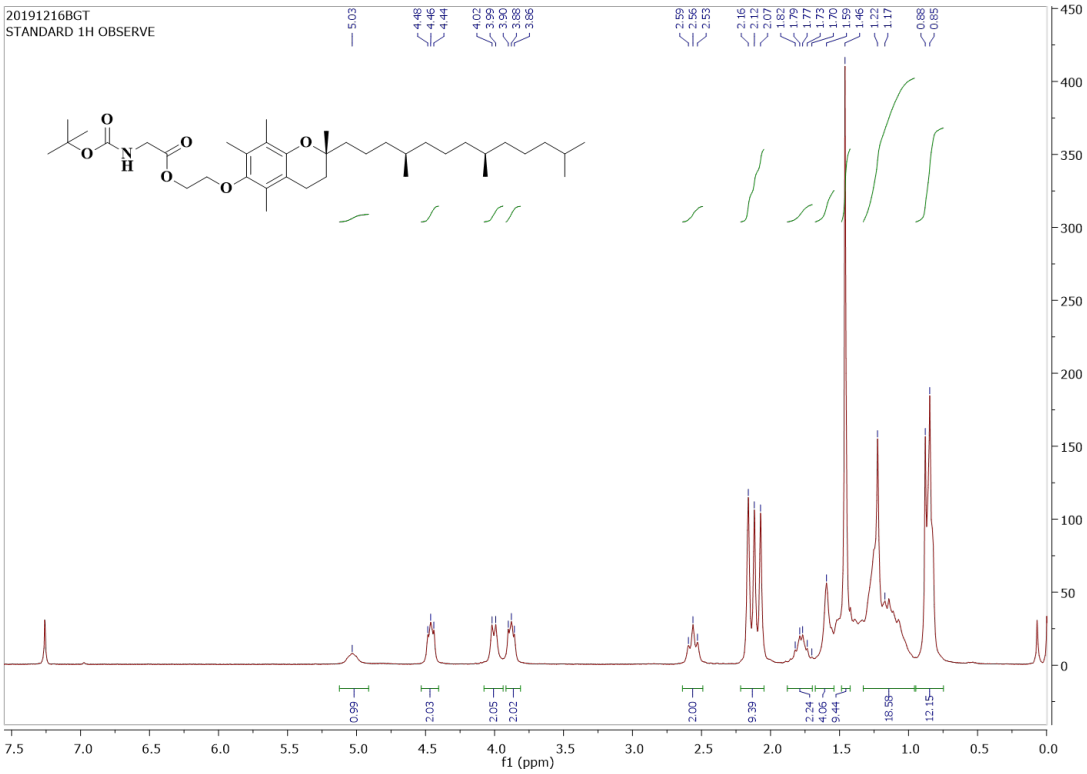

^{1}H NMR spectrum of BGT in $CDCl_3$

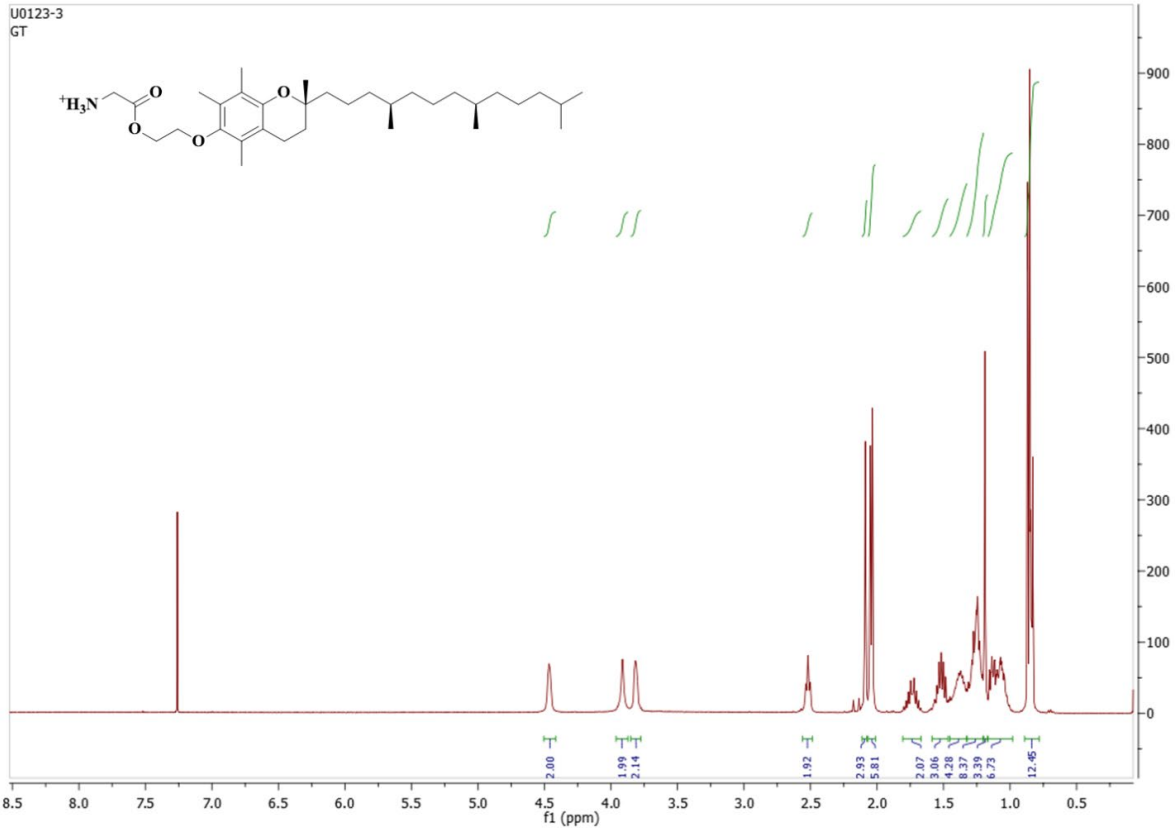

^{1}H NMR spectrum of GT in $CDCl_3$

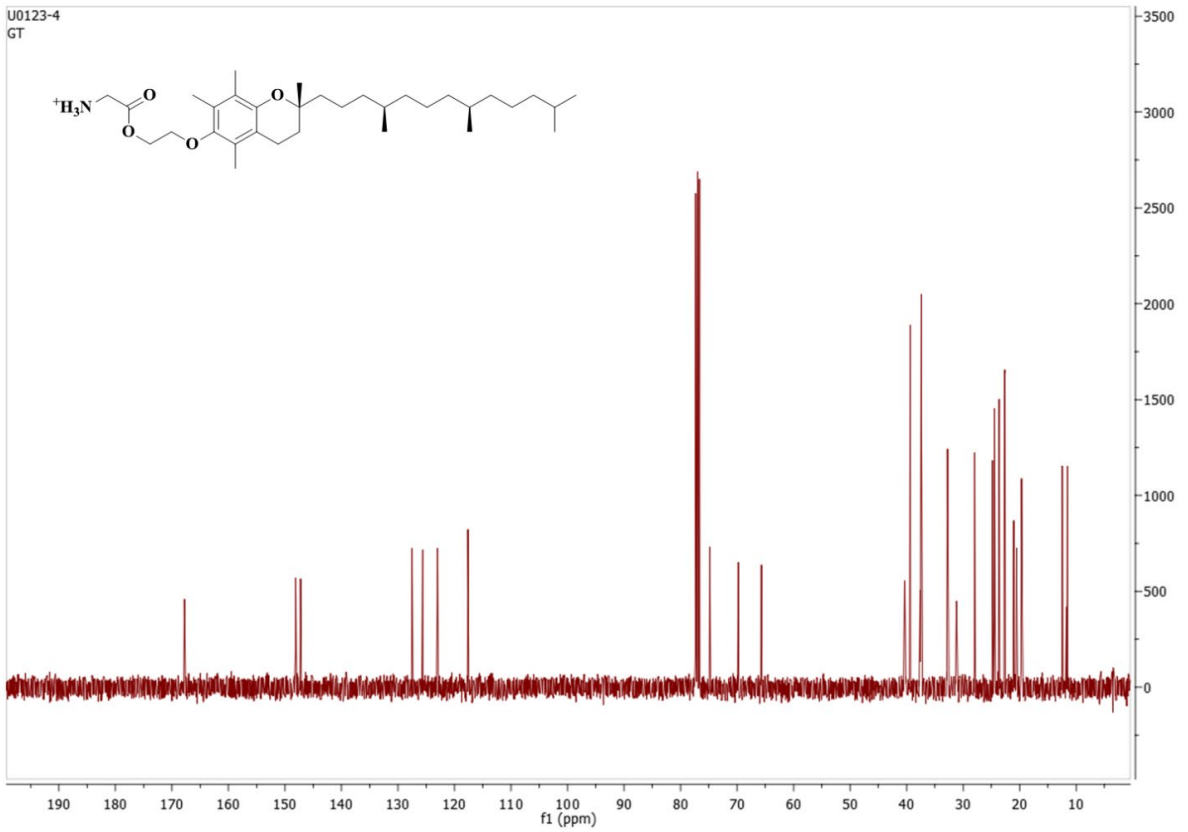

^{13}C NMR spectrum of GT in $CDCl_3$

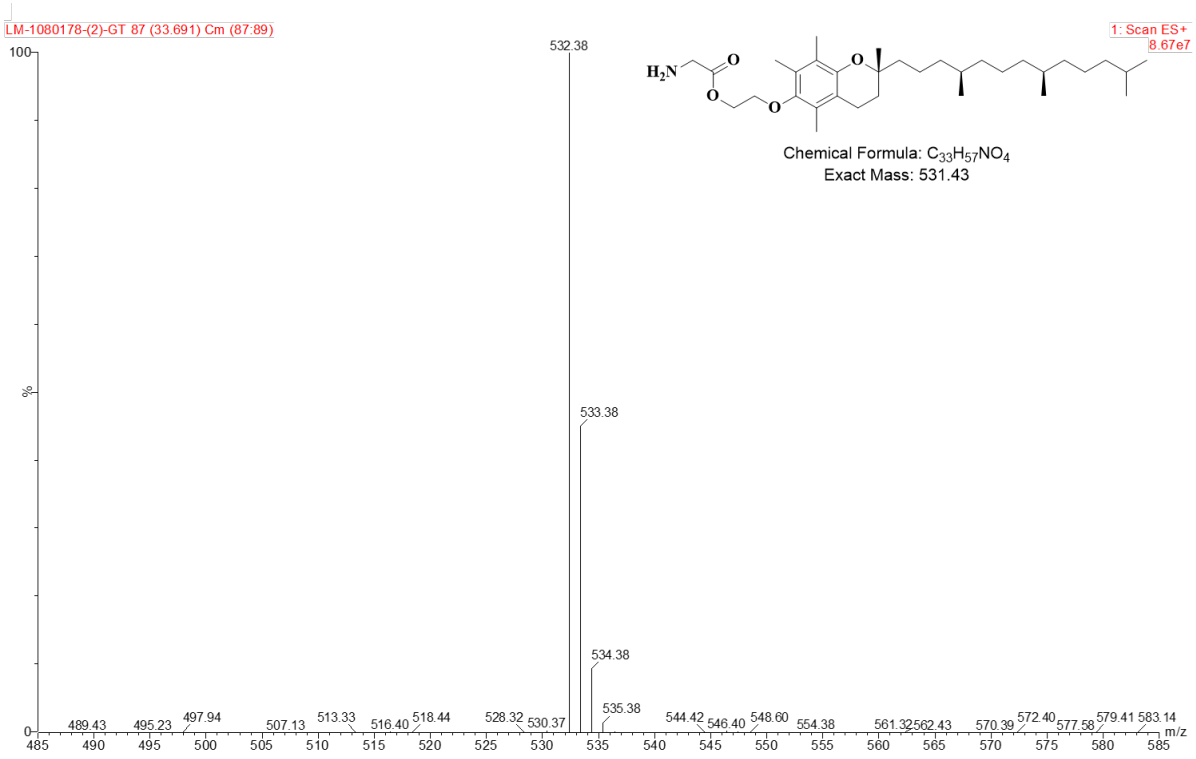

Mass spectrum of GT

CHAPTER III

ENHANCED TRANSFECTION EFFICIENCY AND CANCER-CELL-SPECIFIC CYTOTOXICITY BY NOVEL CATIONIC GEMINI LIPOPEPTIDE BEARING AN ULTRASHORT PEPTIDE

CHAPTER III

ENHANCED TRANSFECTION EFFICIENCY AND CANCER-CELL-SPECIFIC CYTOTOXICITY BY NOVEL CATIONIC GEMINI LIPOPEPTIDE BEARING AN ULTRASHORT PEPTIDE

3.1. INTRODUCTION

Gene therapy offers a promising strategy for treatment of several cancers by suppressing the cancer-associated gene expression and/or by increasing the therapeutic gene expression.[187, 188] However, naked genes cannot accomplish the desired results for the reason that their rapid clearance, low cellular internalization and non-specific biodistribution hinder their effect. Delivery vectors are essential to carry these genes safely to the desired site. Development of biosafe delivery vectors is the major challenge for implementing gene therapy at clinic level. Over the years, several viral and non-viral delivery vectors have been reported. Non-viral vectors such as lipid-based and polymer-based vectors have been frequently preferred in recent times due to their easily tunable chemistry structures, less risk of immunogenicity, complexation capability with wide range of oligonucleotides, flexibility and large scale production.[189, 190] Cationic lipids such as 1,2-di-O-octadecenyl-3-trimethylammonium propane (DOTMA), DOTAP are amphiphilic structures that were developed during the early research on lipid-based gene delivery. These lipids typically possess quaternary ammonium head groups, thus enormous research has been inspired from these lipids and several cationic lipids have been developed over the years.[119, 191, 192] Most of these traditional cationic lipids extensively studied by numerous researchers are largely limited by the challenges during the several steps of gene delivery. Transfection efficiency and dose dependant cytotoxicity have been major barriers that hinder the expansion of cationic lipid-based gene delivery beyond research purpose.[193] Therefore, a certain focus on the improvement of the efficacy and safety of the delivery vectors which carry the therapeutic genes to a particular target tissue is direly needed. Towards this end, a number of previous reports including ours have demonstrated that amino acid- or peptide

head- based lipids help improving biosafety while still providing desired transfection efficiency.[106, 194-197] Among several amino acids that have been studied, arginine-based gene delivery systems have been widely accepted for their transfection efficiancy.[198] Lipid-based delivery vectors with stimuli-responsive linker moieties which are enzyme cleavable,[199] pH[200] or redox responsive,[99] have grabbed certain interest of researchers for their obvious beneficial results. Owing to the high levels of glutathione (GSH), which is an intracellular reducing agent in the tumour microenvironment, redox responsive delivery vectors have been efficiently utilized to target tumors.[201, 202] Most recently, gemini like cationic lipids have been sought after, attributed to their excellent complexation ability with DNA and RNA facilitating better transfection efficacies while being low toxic.[112, 203-205] We have recently reported that transfection efficiency in cationic gemini lipids with heterocyclic head groups is spacer dependant.[205] Despite several efforts have been made as to develop efficacious liposomal formulations for gene delivery, still there exists a strong and persistent need of novel gene carriers which address the issues affecting the safe and efficient cellular delivery. Cationic gemini lipopeptides are a relatively new class of amphiphilic structures, where two monomeric peptide-lipid conjugates are connected by a spacer.[114, 206] These new types of molecules along with other conventional lipopeptides have been utilized for antimicrobial testing[115, 116] but their use in gene delivery is very rare. Damen et al. utilized an ultrashort (serine-proline-lysine-arginine) peptide containing lipopeptide to deliver DNA and siRNA.[117] Zheng et al. synthesized a lysine-based gemini lipopeptide for siRNA delivery.[207] In spite of these examples, the cationic gemini lipopeptides are less explored for their gene delivery and anticancer properties.

In this **chapter III**, we report the synthesis and application of, a novel gemini type cationic lipopeptide bearing a reduction responsive and ultrashort peptide, towards gene delivery. Taking into the consideration of above mentioned criteria, the molecular structure of this gemini lipopeptide contains Arg-Cys-Cys-Arg peptide in the head group region with a reducible disulphide linker. Two α-tocopherol moieties act as hydrophobic tails of the gemini

lipid. The new lipopeptide is formulated with conventional lipid-colipid pair: DOTAP-DOPE with the aim of enhancing the transfection efficiency of conventional formulations. The results indicate a remarkable enhancement in transfection efficiency using the newly developed gemini lipopeptide as compared with the conventional liposome system, DOTAP-DOPE. Moreover, the new formulation also shows potential for the cancer cell specific cytotoxicity while being nontoxic to normal cells. Further mechanistic studies may help elucidating the mechanism behind its cell specificity.

Scheme 3.1: *Synthesis of cationic gemini lipopeptide* ***(ATTA).***

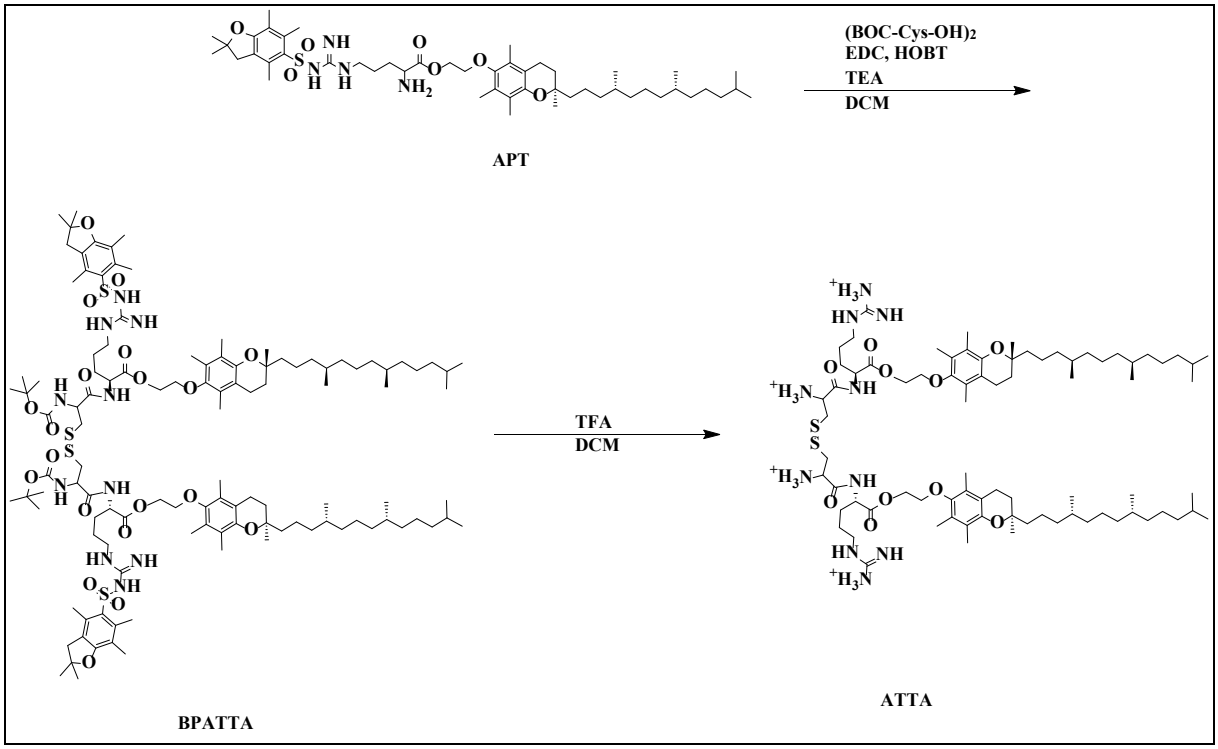

Reagents and solvents. *EDC: N-(3-Dimethylaminopropyl)-N'-ethylcarbodiimide hydrochloride, 1-HOBT: Hydroxybenzotriazole, TEA: Triethylamine, DCM: Dichloromethane, TFA: Trifluoroacetic acid.*

3.2. RESULTS AND DISCUSSION

3.2.1. Design and synthesis of dimeric lipid

The dimeric cationic lipopeptide in the current study was synthesized using bioconjugation strategy as shown in **Scheme 3.1**. In tandem with our recent experience with arginine-tocopherol conjugates which have shown significant transfection and selectivity,[197] the current dimeric cationic lipid was hypothesized to be an effective mediator for selective gene

therapy. The newly developed lipopeptide molecule contains multiple intracellularly labile bonds which may help in release of genetic material intracellularly. The reduction responsive disulphide bond can be cleaved by intracellular reducing agents such as GSH while the ester bonds can be broken by enzymatic action of esterase to facilitate gene delivery.[154] The role of disulphide bridge on nano-vesicles appears to be prominent as reported previously where increased release of siRNA by lipid nano-vesicles with two lysine moieties bridged by disulphide liker was observed.[207, 208] Arginine-tocopherol conjugate (APT) was synthesized initially as reported previously,[197] with guanidine group still protected. The free amine on APT was reacted with the two carboxylic acid groups of cystine molecule to make peptide linker. The resultant dimeric lipid with acid labile protecting groups was deprotected using trifluoroacetic acid (TFA) to yield the final lipid/lipopeptide ATTA. Two α-tocopherol moieties serve as membrane anchoring groups, while a short peptide Arg-Cys-Cys-Arg functions as multi cationic head group to interact with DNA. All the reaction intermediates and the final lipid were produced in good yields (69-93 %). Successful synthesis of final lipopeptide, ATTA, was confirmed by ^{1}H nuclear magnetic resonance (NMR), ^{13}C NMR and Mass spectral data.

3.2.2. Optimization and characterization of liposome formulations

Lipid components in required molar ratios were mixed in aqueous solutions as described in experimental section to form a series of liposomal formulations. The chemical structures of lipid components used in this study were depicted in **Figure 3.1**. Cationic lipid DOTAP and helper lipid DOPE at 1:1 lipid:DOPE molar ratio form a well-known transfection reagent.

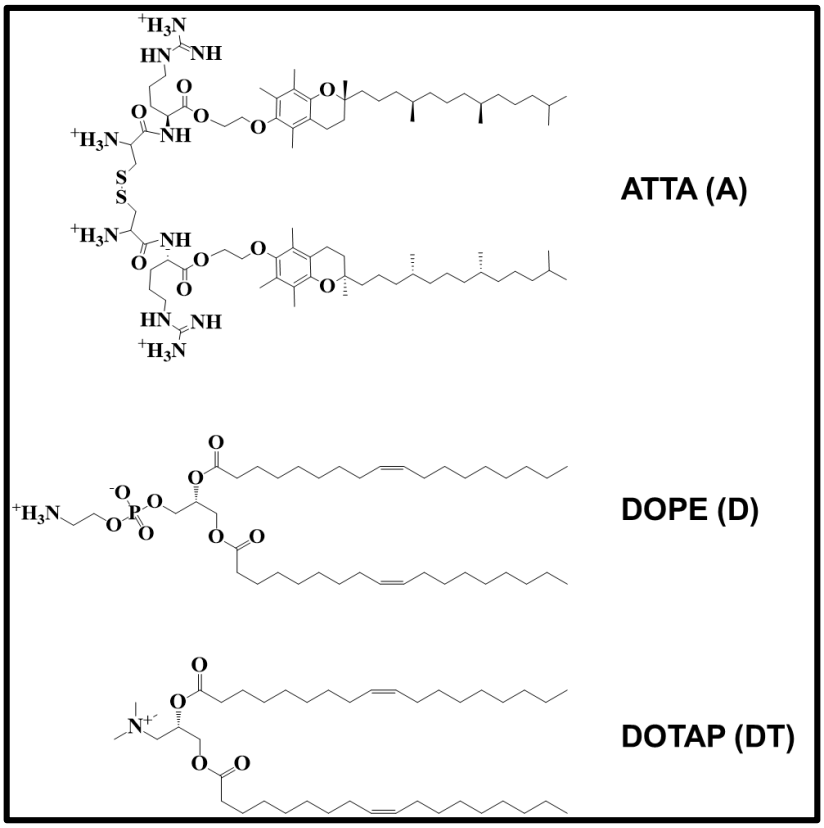

Figure 3.1: *Chemical structures of cationic lipids (ATTA and DOTAP) and neutral lipid (DOPE).*

In the current study, DOTAP:DOPE at lipid:DOPE ratio of 1:1 was formulated, labelled as "DTD 11" and used to compare the transfection efficiency of new formulations. Initially, peptide containing multi cationic lipid ATTA was formulated with DOPE at various lipid:DOPE ratios. However, this formulation resulted in non-homogenous aggregations. Nevertheless, mixing ATTA at various concentrations to DOTAP:DOPE formulation resulted in homogeneous colloidal solutions. Keeping DOTAP:DOPE molar ratio at 1:1, various ratios of ATTA ranging from 0.5 to 4 were mixed to form liposomal solutions. The formulations namely, DTD 11, DTDA 110.5, DTDA 111, DTDA 112 and DTDA 114 were characterised and optimized with regards to their size, zeta potential, stability and transfection efficiency. As shown in **Figure 3.2A**, the sizes of liposome particles were in the range of 100-350 nm with DTD 11, DTDA 110.5 and DTDA 111 attaining favourable size below 150 nm.

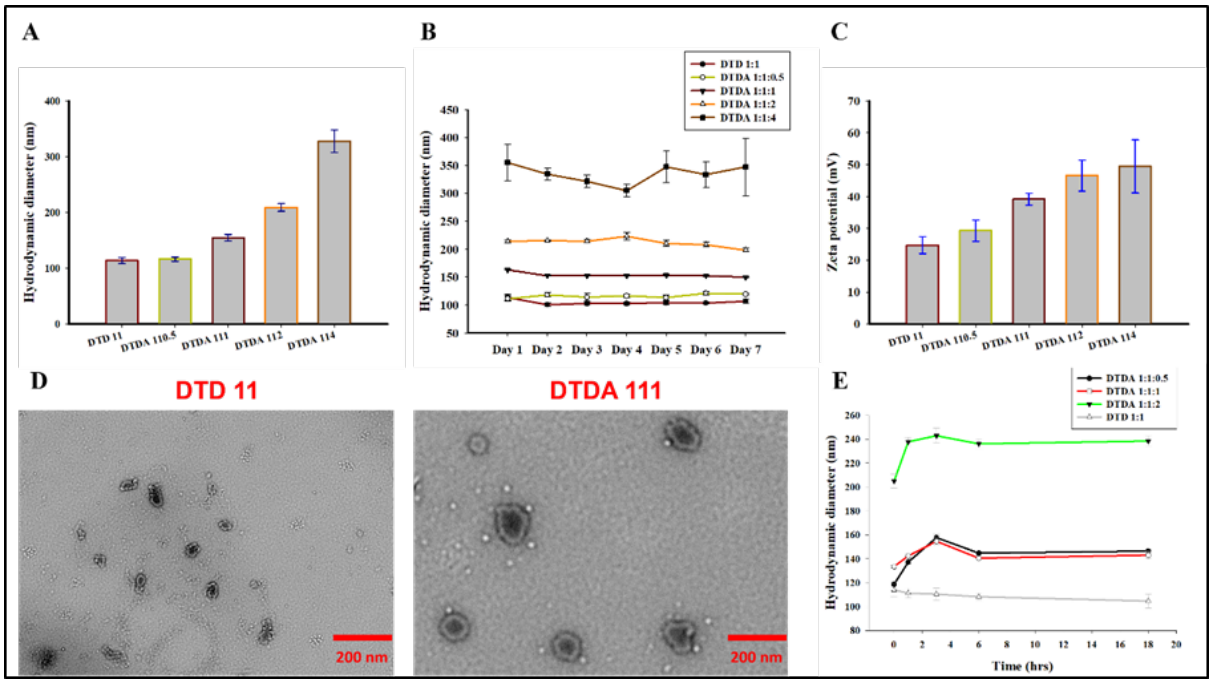

Figure 3.2: *Physicochemical characterization and reduction responsive stability test of liposomal formulations. A) Hydrodynamic diameters of liposomes at different lipid molar ratios (n=3). B) Stability of hydrodynamic diameters of liposomes over the period of 7 days (n=3). C) Zeta potentials of liposomes at different lipid molar ratios (n=3). D) TEM images of DTD 11 and DTDA 111. E) Time-dependent relative size variations of DTDA 110.5, DTDA 111, DTDA 112 and DTD 11 with 10 mM Dithiothreitol (DTT) treatment (n=3).*

The storage stability of the particles was assessed for a week (**Figure 3.2B**), where all the formulations exhibit high stability. Increase in the zeta potential was noted as the ratio of ATTA increases from DTD 11 to DTDA 114 as shown in **Figure 3.2C**. Owing to their favourable low particle sizes and moderate zeta potential values, DTD 11, DTDA 110.5 and DTDA 111 were presumed to show maximum gene delivery efficacy. Transmission electron microscopy observation confirmed the vesicular formation of lipid particles of DTD 11 and DTDA 111 as shown in **Figure 3.2D**. The reduction responsiveness of the lipid vesicles was analysed by the treatment of liposomes with dithiothreitol (DTT). Disulphide possessing liposomes are predicted to destabilise in liposomal structure by the action of reducing agents such as DTT and GSH. This may result in the variation of liposome size.[209] Slight increase in the size of ATTA containing liposomes was noted upon incubation with 10 mM concentration

of DTT. This is probably due to the disintegration of lipid components by the action of DTT. Although it is a common reducing agent used in demonstrating disulphide breakage, DTT is highly unstable in aqueous solutions.[210] Reverse oxidation may occur as the intermediates formed by DTT reduction are non-stable.[211] In the current study, maximum increase in the liposomal size was seen at 3h incubation time with DTT. Thus, 3h incubation time was considered to further examine DNA release from liposomes using gel retardation assay.

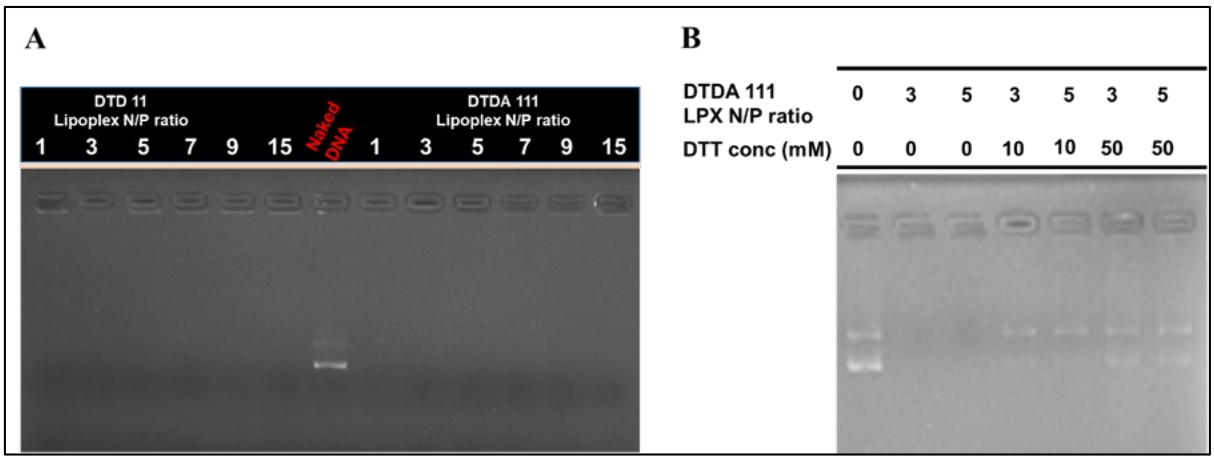

Figure 3.3: *(A) Gel retardation images of lipoplexes at different N/P ratios ranging from 1 to 15. B) Reduction responsive DNA (pEGFP-C1) release from DTDA 111 lipoplexes with DTT (10 mM or 50 mM) treatment.*

3.2.3. DNA binding and reduction responsive release

The surface charge of lipid vesicles measured by zeta potential in turn determines the DNA binding ability of the same. As depicted in **Figure 3.3A**, the electrophoretic mobility of DNA was completely inhibited by both the liposomes DTD 11 and DTDA 111 at various N/P ratios ranging from 1-9. Due to the high net positive charge and stability of the liposome particles, it was expected to show good DNA binding by the tested lipid particles. Besides, arginine rich periphery is reported to be favouring greater DNA binding and transfection even at low N/P ratios.[196] However, the compromise in lipid/DNA complex is essential for the release of DNA at the targeted site. This destabilization can be sometimes brought by stimuli responsive linkers in the lipid vesicles.[212] Disulphide bonds in the lipid structure can act as

redox responsive sites as they can be cleaved by intracellular reducing agents such as GSH, helping in release of genetic material that they are carrying.[196] In the present study, the redox responsive release of DNA was monitored by gel electrophoresis assay of DTDA111/DNA complexes incubated in DTT containing solution at pH 8.0. As represented in **Figure 3.3B**, the discrete fluorescent DNA bands observed in DTT treated complexes indicate slight release of DNA by the action of DTT. Although several factors influence the intracellular DNA release, the current results indicate that reduction sensitive bonds may reinforce the DNA releasing effect intracellularly.

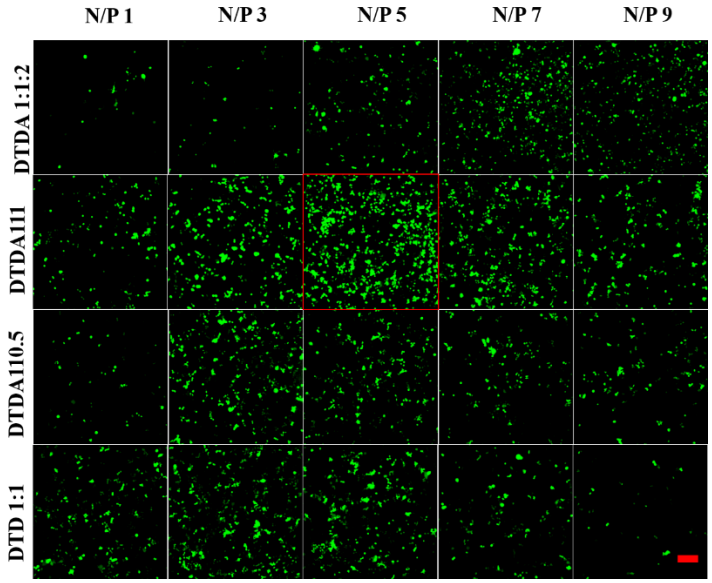

Figure 3.4: *GFP expression in HEK-293 cells exposed to various lipoplex formulations at N/P ratios ranging from 1 to 9. The highlighted image in the middle by red outline represents the optimal formulation and N/P ratio with superior expression. The scale bar is 200 µm.*

3.2.4. Transfection efficiency

Selected liposomal formulations, DTD 11, DTDA 110.5, DTDA 111 and DTDA 112 were further optimised in terms of transfection efficiency. HEK-293 (a human embryonic kidney cell line) cells were treated with lipoplexes derived from the above liposomal formulations and pEGFP-C1 plasmid. For cytotoxicity and transfection experiments, 1µg of pDNA was complexed with calculated amount of liposome solution as per their N/P ratios. Out of all the formulations and the N/P ratios ranging from 1-9, DTDA 111 at N/P ratio 5, shows

maximum transfection efficiency as observed by fluorescence microscopy (**Figure 3.4**). It was also confirmed that among the ATTA containing formulations, DTDA 111 has the superior potential to deliver pDNA. DTD 11, containing commercial lipids DOTAP and DOPE, exhibited maximum transfection at N/P ratio 3. Thus, further comparison of transfection efficiencies of DTD 11 and DTDA 111 with another most common transfection reagent, Lipofectamine2000, was presented in **Figure 3.5**. The ratio of the fluorescence intensity of DTDA 111 and Lipofectamine treated groups to the fluorescence intensity of DTD 11 treated groups was determined as relative transfection efficiency.[213] The relative transfection efficiency of the formulations (**Figure 3.5B**) at their respective N/P ratios was quantified from the fluorescence intensity observed from **Figure 3.5A**. Fluorescence intensity of each group quantified from ImageJ software was given in **Figure 3.5C**. DTDA 111 has brought remarkable enhancement in transfection efficiency in comparison with DTD 11.

For over the last two decades, cell penetrating peptides (CPPs) have been utilized as coherent biological tools to attain better cellular uptake during cargo delivery.[214] Several organic[215-217] and inorganic[218-220] biomaterials have been developed using CPPs, which proved that the peptide based delivery vectors are highly efficient in achieving adequate transfection. Especially, guanidinylation of delivery vector's surface has proved to impact drug or gene delivery significantly.[221, 222] ATTA lipid in DTDA 111 contains two guanidine cations on arginine moieties and two ammonium cations on cysteine moieties. The guanidine moiety in arginine plays a pivotal role in improving the transfection ability of arginine based delivery systems.[198] Arginine has been thought to be a key component of CPPs which involves in binding to many cellular receptors. Guanidine moiety in arginine is especially known to interact with phosphate groups on cell membrane enabling internalization of arginine containing CPPs.

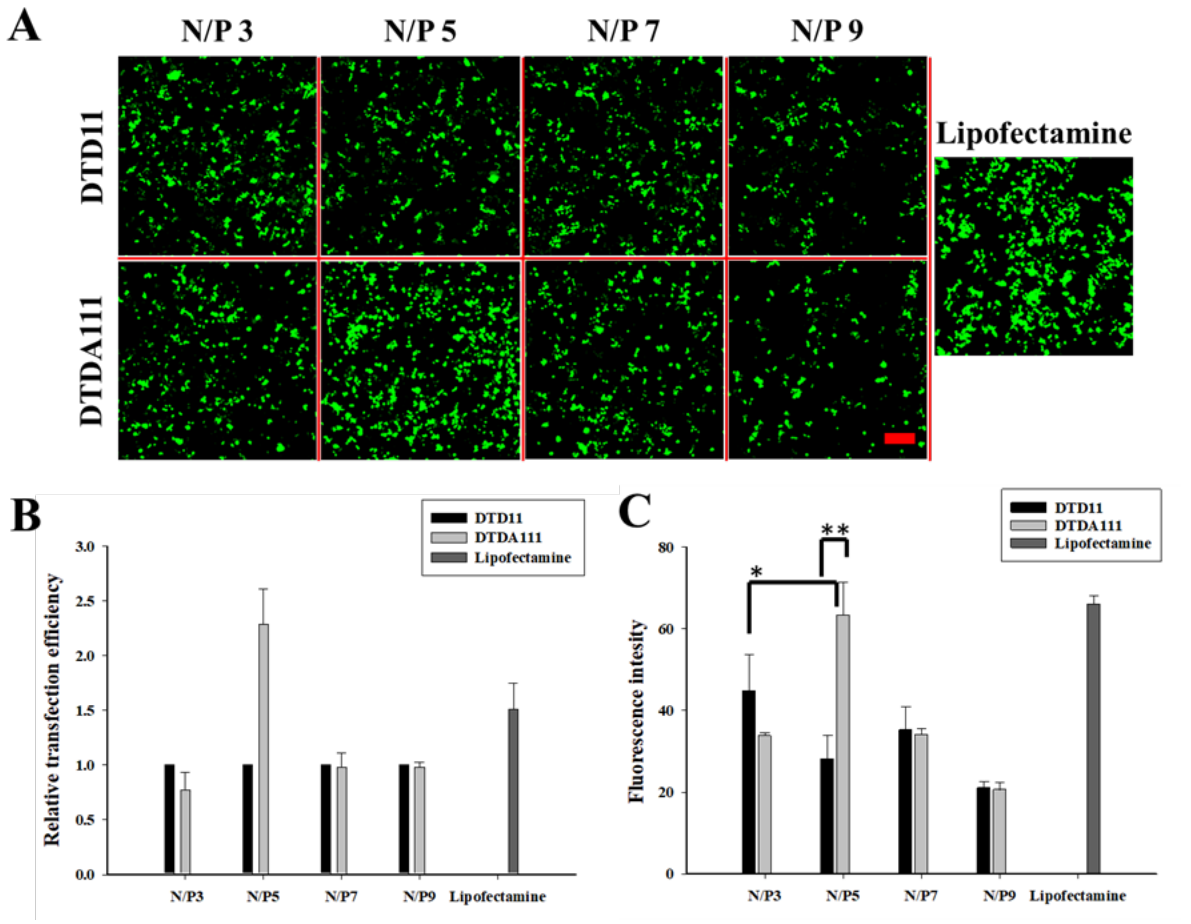

Figure 3.5: *In vitro pEGFP gene transfection efficiency mediated by DTDA 111 compared with DTD 11 and lipofectamine in HEK-293 cells. A) Representative fluorescence microscopy images after pEGFP gene transfection mediated by DTD 11, DTDA 111 at various N/P ratios ranging from 3 to 9. Scale bar is 200 µm. B) Relative transfection efficiencies of various lipid formulations quantified from the fluorescence intensities of images (A) using ImageJ software. Ratio of fluorescence intensity of DTDA 111 to the fluorescence intensity of DTD 11 at a given N/P ratio was calculated. Ratio of fluorescence intensity of Lipofectamine to the fluorescence intensity of DTD 11 at N/P ratio 3 was considered for Lipofectamine value. C) Fluorescence intensities of pEGFP transfected cells by various lipid formulations as quantified using ImageJ software (n=3, *P < 0.05, **P < 0.01).*

The mechanism of interaction of CPPs and cell membrane involves bidentate hydrogen-bonding among guanidine moieties and phosphate groups on the surface of the cell, helping the improved uptake inside the cell.[140] Similarly, in the case of the present study the improved transmembrane function of the lipopeptide, ATTA, through guanidine rich arginine periphery, is believed to enhance transfection of DTDA 111 over DTD 11 In order to further evaluate the

enhanced transfection efficiency and to confirm the effective N/P ratio, another non-cancer cell line HEL-299 (human embryonic lung cell line) was employed. Notably, very low transfection was detected by DTD 11-based lipoplexes (**Figure 3.6A**) in HEL-299 cells. On the other hand, DTDA 111 containing ATTA exhibited superior transfection efficiency at all given N/P ratios (**Figure 3.6B**). At the N/P ratio of 5, DTDA 111 proved to be better than Lipofectamine as evidenced by their fluorescence intensity values (**Figure 3.6C**). These results demonstrate that inclusion of ATTA in the liposomal formulations significantly enhances the transfection efficiency of DTDA 111 liposomes.

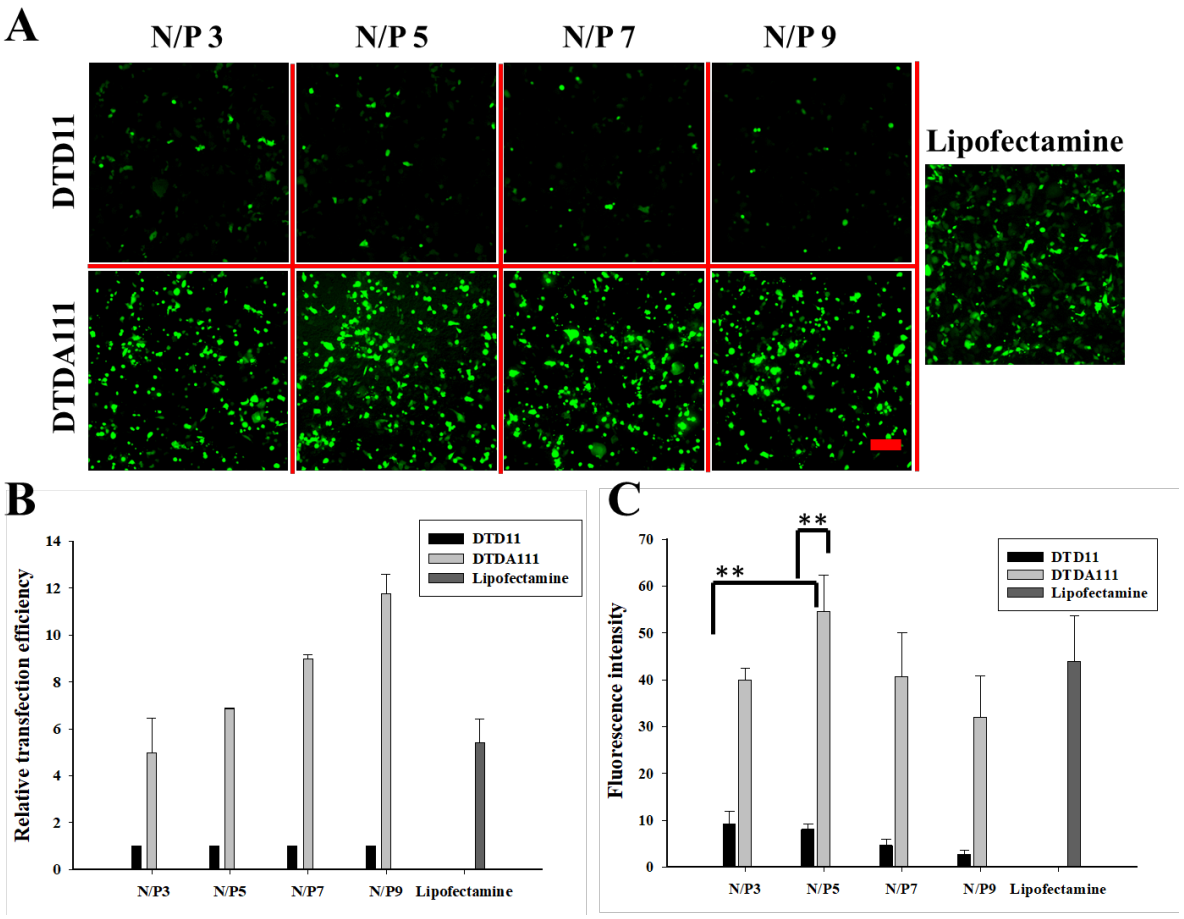

Figure 3.6: *In vitro pEGFP gene transfection efficiency mediated by DTDA 111 compared with DTD 11 and lipofectamine in HEL-299 cells. A) Representative fluorescence microscopy images after pEGFP gene transfection mediated by DTD 11, DTDA 111 at various N/P ratios ranging from 3 to 9. Scale bar is 200 µm. B) Relative transfection efficiencies of various lipid formulations quantified from the fluorescence intensities of images (A) using ImageJ software. Ratio of fluorescence intensity of DTDA 111 to the fluorescence intensity of DTD 11 at a given*

*N/P ratio was calculated. Ratio of fluorescence intensity of Lipofectamine to the fluorescence intensity of DTD 11 at N/P ratio 3 was considered for Lipofectamine value. C) Fluorescence intensities of pEGFP transfected cells by various lipid formulations as quantified using ImageJ software (n=3, **P < 0.01).*

After screening the effective N/P ratios of the liposomal formulations, we further evaluated the application of these formulations on various cancer cell lines where gene delivery may be essential. PC3 (a human prostate cancer cell line), U87 (a human glioblastoma cell line) and A549 (a human lung carcinoma cells) cell lines were employed to compare the ability of DTD 11 and DTDA 111 in terms of transfection. Representative fluorescence images of three cancer cell lines treated by various formulations are presented in **Figure 3.7A**. Clearly, in these cancer cell lines, DTDA 111 showed greater transfection ability than DTD 11, substantiating the earlier results (**Figure 3.7B**). DTDA 111 demonstrated competitive transfection efficiency in comparison with commercial transfection reagent Lipofectamine, except for A549 cell line. On the other hand, the percentage of GFP positive cells in the above mentioned cell lines revealed that, DTDA 111 has transfected significantly more number of cells than DTD 11 and Lipofectamine, except for A549 cell line. In the case of A549 cell lines, although DTDA 111 was highly significant when compared with DTD 11, Lipofectamine was dominant in transfection. It is to be noted that Lipofectamine has yielded intense transgene expression in transfected cells, which sometimes is the reason for its cytotoxicity, irrespective of the cell line. The practical effectiveness of transfecting reagent can be improved by enabling a moderate but uniform expression of the transgene with a high percentage of transfected cells.[223] Contrary to Lipofectamine, DOTAP based transfection reagent, DTD 11 has transfected much lower number of cells with less gene expression. The results suggest that the short peptide bearing multi cationic lipid ATTA plays a crucial role in the enhancement of transfection efficiency.

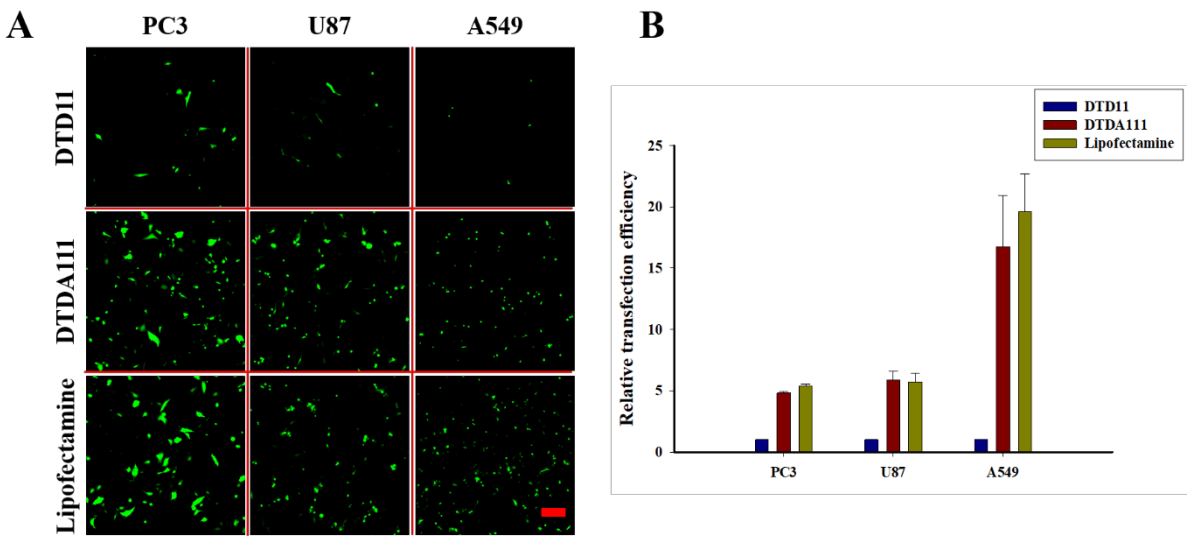

Figure 3.7: *In vitro pEGFP gene transfection efficiency mediated by DTDA 111 compared with DTD 11 and lipofectamine in three cancer cell lines (PC3, U87 and A549). A) Representative fluorescence microscopy images after pEGFP gene transfection mediated by DTD 11 (at N/P ratio 3), DTDA 111 (at N/P ratio 5) and Lipofectamine. Scale bar is 200 µm. B) Relative transfection efficiencies of DTD 11, DTDA 111 and Lipofectamine, quantified from the fluorescence intensities of images (A) using ImageJ software.*

3.2.5. Cell viability

The most effective liposomal formulations DTD 11 and DTDA 111 were assayed for their *in vitro* cytotoxicity against multiple normal and cancer cell lines (**Figure 3.8**). Through the MTT based cell viability assay, it was interesting to note that DTDA 111 has shown no cytotoxicity against the normal cells HEK-293 even at 100 µg/mL concentration (**Figure 3.8A**). Also, the cell viability of DTDA 111 against the normal cell line HEK-293 is much greater than Lipofectamine (**Figure 3.9**). To validate this result, several cancer cell lines from various cancer tissues (PC3, U87, A549 and MDAMB (a human breast cancer cell line)) and another non-cancer cell line HEL-299 were tested against the same formulations. In the case of HEL-299 cells as well, significantly higher cell viabilities were observed in cells treated with DTDA 111 than with DTD 11. Nevertheless, some cytotoxicity was noted at high concentration (100 µg/mL) of DTDA 111 with 68.83 ± 10.1 cell viability (**Figure 3.8B**). It was anticipated that, similar to HEK-293 and HEL-299, DTDA111 may show better cell viabilities than DTD 11

and Lipofectamine in other cell lines tested. However, against all the cancer cell lines tested, PC3 (**Figure 3.8C**), U87 (**Figure 3.8D**), A549 (**Figure 3.8E**) and MDA-MB-231 (**Figure 3.8F**), the newly developed liposomal formulation DTDA 111 has apparently exhibited higher cytotoxicity than DTD 11. As the x-axis of **Figure 3.8** represents the total concentrations of liposomes, it is understood that at any given concentration the amount of DOTAP is lower in DTDA 111 than DTD 11. It clearly demonstrates that DOTAP in DTD 11 has non selective cytotoxicity. Thus, minimising the DOTAP concentration and increasing ATTA concentration favors the transfection as well as selective cytotoxicity. Although DOTAP helps in keeping liposomal integrity, excess concentration of DOTAP in the liposomes negatively affect the transfection and cytotoxicity. The data also infers that the cell-selective cytotoxicity of DTDA 111 has arrived from lipopeptide, ATTA, but not from DOTAP. Ultrashort peptide containing lipopeptides have been investigated and demonstrated for their antimicrobial activity in the literature.[224-226] However, due to the non-selective cytotoxicity of these lipopeptides, the studies on their anticancer activities are very rare. The effect of DTDA 111 being more cytotoxic in cancer cells was particularly seen at above concentrations of 50 μg/mL irrespective of cell line. Further investigations may be required to determine the mechanism behind the cancer cell specific cytotoxicity of DTDA 111. Several naturally occurring lipopeptides known to show toxicity against mammalian cells are, however, non-cell-selective.[115, 224] Most recently, there is a report of arginine rich synthetic cationic lipopeptides showing selective cytotoxicity against cancer cells.[116] Previous studies also informed that the combination of cationic and amphiphilic structures are critical to exhibit potent anticancer activity.[227, 228] Typically, in a single molecule, a ratio of 1:2 for a cationic group and hydrophobic residues was summarized to display potent cytotoxicity against cancer cells.[227] Gemini lipopeptides typically contains two hydrophobic groups per a cationic peptide, which may help these compounds to achieve cancer specific cytotoxicity. Moreover, a short tetrapeptide, hydrophobicity and disulfide linkers are found to be favoring factors for cancer specific cytotoxicity.[116, 228]

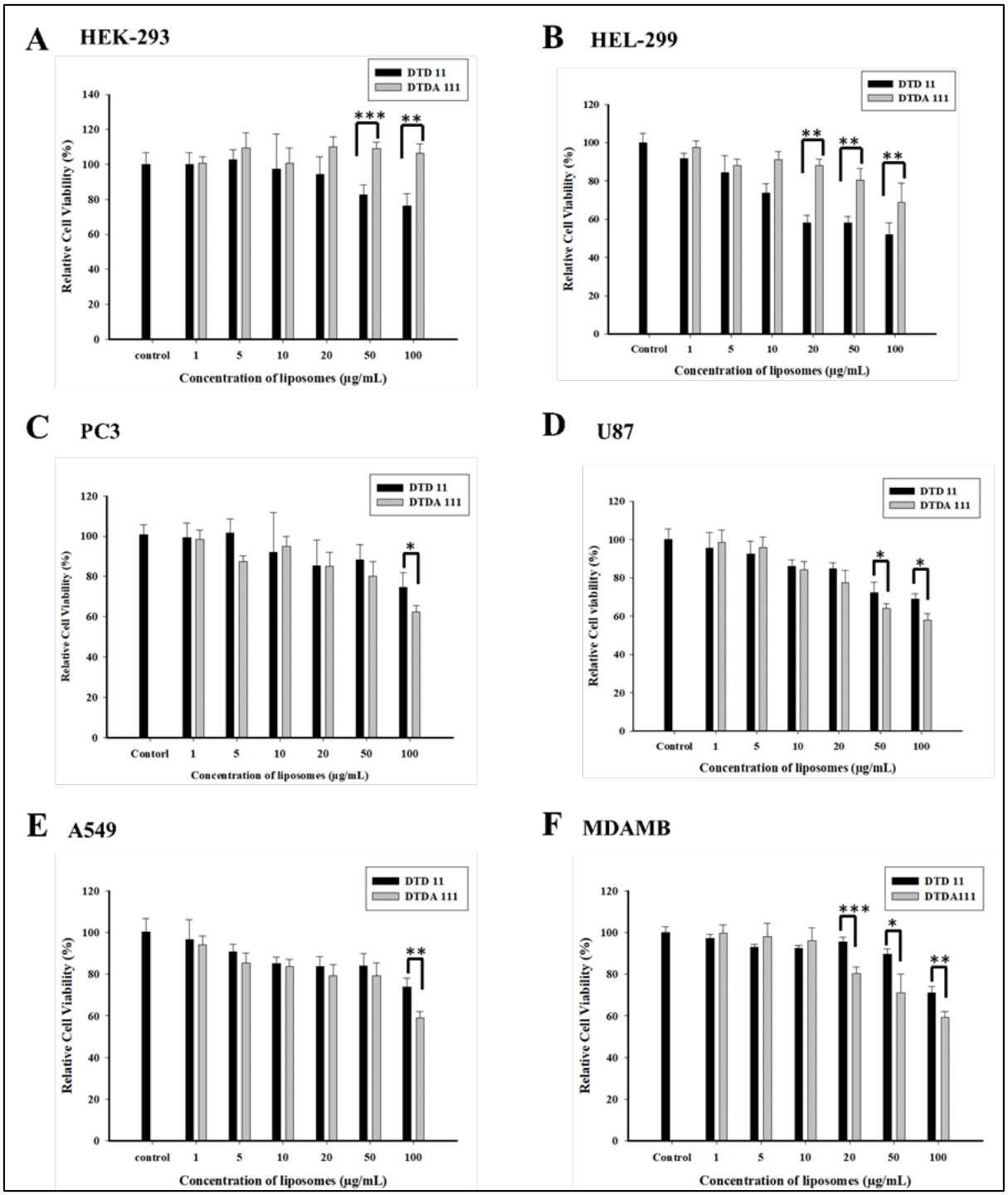

Figure 3.8: *Relative cell viabilities of liposomes. DTD 11 and DTDA 111 based liposomes at various concentrations of 1-100 µg/mL against A) HEK-293, B) HEL-299, C) PC3, D) U87, E) A549 and F) MDAMB cells (n = 6, *P < 0.05, **P < 0.01, ***P < 0.001).*

The cytotoxicity of pEGFP-C1 derived lipoplexes against HEK-293 and HEL-299 were in accordance with cytotoxicity of liposomes **(Figure 3.9)**. Higher cell viabilities were noted by

DTDA 111/pEGFP system compared to DTD 11 and Lipofectamine in HEK-293 and HEL-299 cell lines.

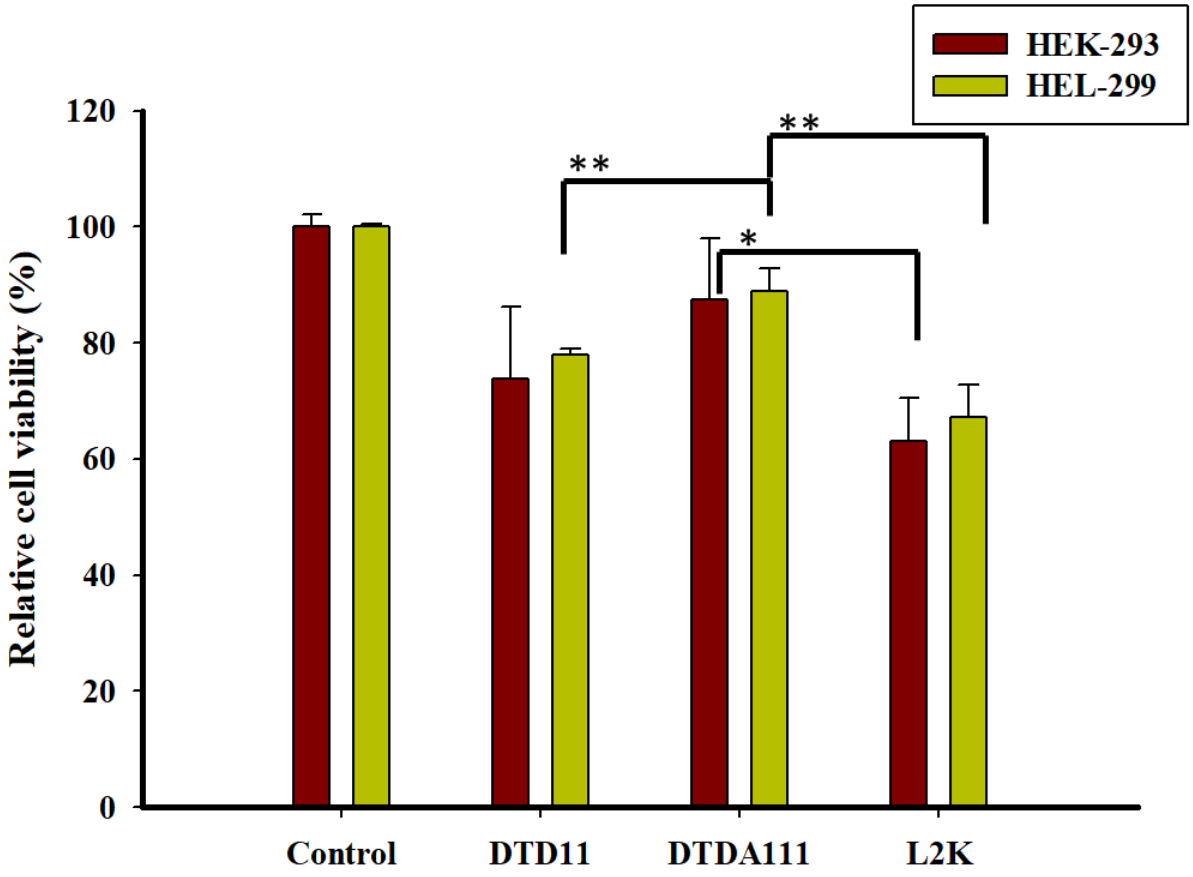

Figure 3.9: *Comparison of relative cell viabilities of transfection optimised lipoplexes derived from pEGFP plasmid using DTD 11(total lipid concentration =26µg/mL) DTDA 111(total lipid concentration = 22 µg/mL), and Lipofectamine (L2K concentration as per manufacturers protocol) formulations against non-cancer HEL-293 and Hel-299 cells (n=3, *P < 0.05, **P < 0.01).*

The corresponding lipoplexes of DTD 11 and DTDA 111, with either control pEGFP-C1 gene or anti-cancer pTRAIL gene, were tested for their cytotoxicity against selected cancer cell lines (**Figure 3.10**). In comparison with DTD 11 based lipoplexes, either with pEGFP-C1 or with pTRAIL gene, there was a significant decrease in cell viability of the cells treated with DTDA 111 based lipoplexes. In the case of PC3 cells, DTDA 111/pTRAIL system effectuated 42.7 ± 2.1 percentage of cell viability whereas DTD 11/pTRAIL system could cause 52.2 ± 3.1 percentage of cell viability (**Figure 3.10A**). Similarly, DTDA 111/pTRAIL system caused nearly

49 % cell viability in U87 cells while DTD 11/pTRAIL system resulted in ~ 60 % viable cells as shown in **Figure 3.10B**. Large variation in cell viability of pTRAIL derived lipoplexes of DTD 11 and DTDA 111 was witnessed in case of A549 cells. In the case of A549 cell line, no obvious variation in cell viability was detected in cells treated either with DTD 11/pTRAIL or DTD 11/pEGFP system with over 80 % of viable cells in both treatments (**Figure 3.10C**). This was probably due to the very poor transfection ability of DTD 11 in A549 cell line as evidenced by transfection results (**Figure 3.7**). In contrast, A549 cells treated with DTDA 111/pTRAIL system resulted in 51.4 ± 0.9 percentage of cell viability indicating the high cytotoxicity inducing ability caused by transfection. In each of these cancer cell lines, even the control DTDA 111/pEGFP system could induce significantly ($P < 0.05$) higher cytotoxicity than DTD 11/pEGFP system (**Figure 3.10**). Nevertheless, as expected, Lipofectamine was more cytotoxic irrespective of cell lines tested. In the current study, the optimal N/P ratio for transfection of DTDA based lipoplexes was 5, where the concentration of liposomes was calculated to be ~35 µg/mL. Data shown in Figures 8A, 8B and 8C indicate that the control DTDA 111/pEGFP lipoplexes at N/P 5 have induced certain level of cytotoxicity which is significant when compared to DTD 11/pEGEP lipoplexes. It also infers that increasing N/P ratio further, may result in enhanced selective cytotoxicity but affect the transfection efficiency. The cytotoxicity results were also substantiated through optical imaging of U87 cells displayed in **Figure 3.10D**. Normal cell morphologies and good confluence were observed in control naked DNA-treated U87 cells. However, DTDA 111/pTRAIL-treated cells showed significantly lesser cell numbers and their disrupted cell morphology was similar to Lipofectamine treated cells. Anti-cancer activity of lipopeptides, often determined by their cell membrane interactions as membrane profiles of cancer cells differ from normal cells.[229] Several anticancer peptides or lipopeptides are shown to be inducing cytotoxicity primarily by disrupting plasma membrane of the cells.[227] Membranolytic nature of cationic, amphiphilic peptides was reported previously demonstrating that the accumulation of these peptides on the cell membrane leads to their internalization,

either by making pores on the membrane or by completely dissolving the membrane through detergent-like activity.[230] Although these membrane activities of cationic lipopeptides and peptoids are establishing them as promising anticancer agents, their intracellular activity must not be overlooked. The mechanism of action of lipopeptides against cancer cell lines was not fully understood so far. Structurally variant lipopeptides act differently to induce cytotoxicity in cancer cell lines.[116, 228] Apoptotic, as well as non-apoptotic pathways are possibly taking part in the anticancer activities of lipopeptides.[231] In the present work, ATTA being equipped with the structural characteristics as described by previous studies to destabilize the anionic cell membranes, these interaction of ATTA with cancer cells may have a role to play in its selective cytotoxicity. However, we understand that the intracellular pathways cannot be ruled out and further explorations will be focused in that direction. Most importantly, ATTA, with its high efficiency to transfer therapeutic genes, offers an attractive combinatorial effect to gene therapy.

The current results indicate that the newly synthesized lipopeptide may have the potential to induce cell selective cytotoxicity. Further detailed mechanistic studies may help understanding the specificity of the lipopeptide and to probe enhancement of cancer specific cytotoxicity. Due to the non-selective cytotoxicity of Lipofectamine and low transfection of DOTAP:DOPE in many cancer cell lines, the new lipopeptide, ATTA, may be advantageous for improving transfection and cytotoxicity properties. Moreover, ATTA can be formulated with other conventional liposomes to enhance the delivery of therapeutic gene as well as to reinforce its therapeutic activity.

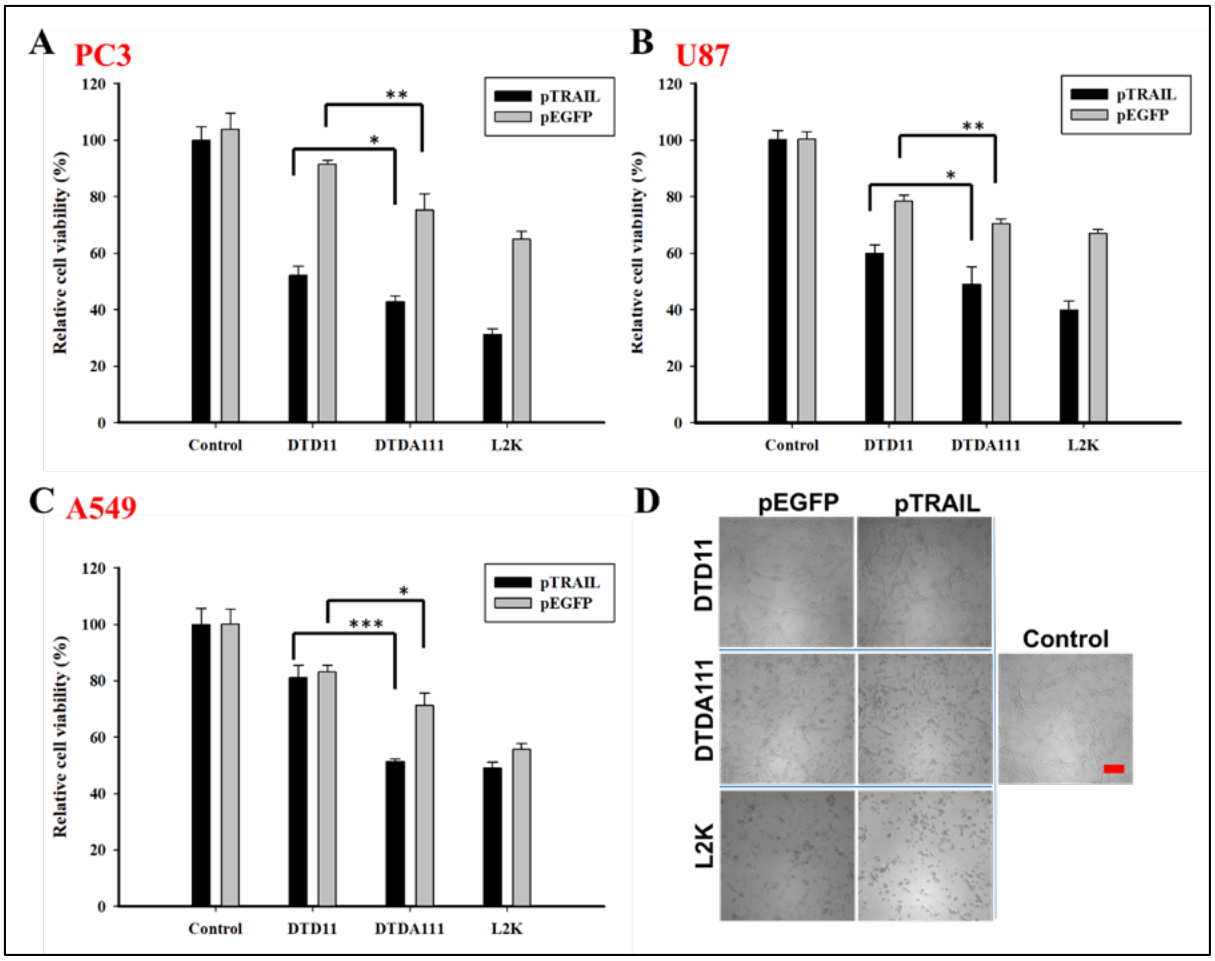

Figure 3.10: *Comparison of relative cell viabilities of lipoplexes derived from control pEGFP plasmid and therapeutic pTRAIL plasmid using DTD 11, DTDA 111 and Lipofectamine formulations against A) PC3, B) U87 and C) A549 cells (n = 3, *P < 0.05, **P < 0.01, ***P < 0.001). D) Microscopy observation of variations in U87 cell morphologies upon transfection with various lipoplexes based on control pEGFP plasmid and therapeutic pTRAIL plasmid. Scale bar is 200 µm.*

3.3. CONCLUSIONS

Short peptide containing cationic gemini lipopeptide (ATTA) was rationally synthesized using bioconjugation strategy. Various formulations resulting from ATTA mixed liposomes and N/P ratios of their corresponding lipoplexes were characterized and systematically optimized for better gene delivery properties. Optimal formulations with favourable size and zeta potentials as determined by dynamic light scattering were further utilized to analyze transfection efficiency. Moreover, reduction response of the optimal

formulations was verified by gel electrophoresis assay after incubation in reducing conditions. Substantial enhancement of transfection activity was observed with ATTA based formulation irrespective of cell lines. Distinct cytotoxicity of formulations was noted between various human cell lines due to the presence of ATTA in the formulations. Cationic lipopeptides are known to be cytotoxic towards mammalian cell lines. However, information on self-assembly, gene delivery and cytotoxicity of new synthetic lipopeptides is scarce. Extensive studies on cationic gemini lipopeptides may help designing efficient gene vectors with anticancer properties.

3.4. EXPERIMENTAL SECTION

3.4.1. Materials: α-Tocopherol, $(BOC\text{-}Cys\text{-}OH)_2$, 2-bromoethanol, Fmoc-Arg(pbf)-OH, DOPE and DOTAP were purchased from Sigma (Sigma-Aldrich Co., Ltd.). Lipofectamine2000 was supplied by Invitrogen Life Technologies. If not mentioned otherwise, other reagents and organic solvents i.e., trifluoroacetic acid (TFA), sodium hydroxide (NaOH), piperidine, N, N′-dicyclohexylcarbodiimide (DCC), methylene chloride (DCM), N-(3-dimethylaminopropyl)-N′-ethylcarbodiimide hydrochloride (EDC), 4-dimethylaminopyridine (DMAP), 1-hydroxybenzotriazole (HOBt), dimethyl formamide (DMF) and methanol were acquired from Sigma, Finar Alfa and Aesor at their maximum purity which were utilised without additional purification. Reaction progress was monitored on silica gel thin-layer chromatography (TLC) plates (0.25 mm). Silica gel (60-120 mesh, Acme Synthetic Chemicals, India) column chromatography was applied for the separation of compounds. Spectral data (^{1}H and ^{13}C NMR) were obtained using a Varian FT400MHz NMR spectrometer. Mass spectrometry data were recorded on a commercial ion trap LCQ mass spectrometer (Thermo Finnigan, SanJose, CA, U.S.) fitted with an ESI source. Dulbecco's Modified Eagle Medium (DMEM), Minimum Essential Medium (MEM), Fetal Bovine Serum (FBS), Phosphate Buffer Saline (PBS), trypsin−EDTA and Roswell Park Memorial Institute (RPMI) 1640 Medium were

procured from Invitrogen. 3-(4,5-Dimethylthiazol-2-yl)-2,5-diphenyl-tetrazolium bromide (MTT) was acquired from MP Biomedicals. pTRAIL plasmid was gifted by Prof. Chien-Wen Chang. Briefly, the pTRAIL vector was obtained by cloning TRAIL gene (synthesis protocol by Genedirex) into the downstream of CMV promoter of pcDNA3 (Invitrogen) vector.

Synthesis. Novel gemini cationic lipopeptide bearing ultrashort peptide was synthesized using the bioconjugation strategies described in **Scheme 3.1**. Arginine-tocopherol conjugate (APT) was synthesized initially as reported in our previous method.[197] Intermediate APT was then conjugated to $(BOC\text{-}Cys\text{-}OH)_2$ using peptide chemistry approach. Intermediate compounds and the final lipopeptide were characterized by nuclear magnetic resonance (NMR) and mass spectrometry.

3.4.2. Synthesis of Arginine-tocopherol Lipopeptide (ATTA)

Synthesis of bis(tocopheryloxyethyl) 2,2'-((3,3'-disulfanediylbis(2-(BOC)amino) propanoyl))bis(azanediyl))bis(5-(3-(Pbf)guanidino)pentanoate) (BPATTA).

2-Tocopheryloxyethyl 2-Amino-5-(3-(pbf)guanidino)pentanoate (APT, 2.2 eq, 0.5 g) dissolved in 10 mL of dry DCM in a round bottom flask was added with $(BOC\text{-}Cys\text{-}OH)_2$ (1.0 eq., 0.113 g,), HOBt (2.3 eq., 0.082 g,), EDC (2.3 eq., 0.115 g,) and trimethylamine (2.3 eq., 0.06 g) at 0° C. The mixure was stirred at 0° C for half an hour followed by stirring for another 24 h at room temperature. The solvent was evaporated under reduced pressure using rotary evaporator. 50 mL of ethyl acetate (EA) was added to the concentrated residue and washed with brine (3×50 mL) and water (3×50 mL). The organic layer was collected, dried over Na_2SO_4 and concentrated. Further purification on column chromatography using 2:98 methanol:chloroform as mobile phase produced white solid as product (BPATTA). Yield: 0.418 g (75%). ^{1}H NMR [δ/ppm] (400 MHz, $CDCl_3$) 4.64 (t, 4H, 2 X -COO-**CH_2**), 4.46-4.41 (q, 4H, 4 X -NH-**CH**-), 3.86 (t, 4H, 2 X -**CH2**-O-), 3.22-3.17 (m, 8H, 2 X –NH-**CH_2**-, 2 X –S-**CH_2**-), 2.93 (s, 4H, 2 X –**CH_2**- (Pbf)), 2.55-2.48 (ds, 14H, 4 X –CH_3 (Pbf), -Ar-**CH_2**-), 2.14-2.07 (m, 24H, 4 X –**CH_3**), 1.76-1.65 (m, 28H, 4 X –

CH_2- (arginine), 3 X –**CH_2-** (tocopherol)), 8 X –**CH-**, 2 X –**CH_3**), 1.56-1.43 (m, 30H, 10 X –**CH_3**), 1.25-1.08 (m, 32H, 16 X –**CH_2-**) , 0.88-0.85 (m, 24H, 8 X –**CH_3**).

Synthesis of 1,1'-((3,3'-disulfanediylbis(2-ammoniopropanoyl))bis(azanediyl))bis (tocopheryloxyethoxy)pentane-4,1-diyldiguanidinium (ATTA).

Deprotection of pbf and BOC groups from the above intermediate was done using 50 % trifluoroacetic acid (TFA) in DCM. BPATTA (0.3 g, 0.14 mmol) was dissolved in 2 mL of DCM and 2 mL of TFA was dropped slowly at 0° C. After complete addition of TFA, the reaction mixture was slowly warmed up to room temperature while stirring for 3 h. Then, the TFA and DCM were removed under vacuum condition and the residue with crude product was washed thrice using diethyl ether which yielded pure target produt, arginine-tocopherol conjugated lipopeptide (ATTA) as white solid. Yield: 0.25 g (93%). ^{1}H NMR [δ/ppm] (400 MHz, DMSO-D_6 + $CDCl_3$) 4.42-4.36 (m, 8H, 2 X -COO-**CH_2**, 4 X -NH-**CH**-), 3.81 (t, 4H, 2 X -**CH2**-O-), 3.13 (m, 4H, 2 X –S-**CH_2-**) , 2.18-2.08 (ts, 24 H, 6 X –**CH_3**, 3 X –**CH_2-**), 2.02-1.98 (m, 4H, **-CH_2-** (arginine)), 1.75-1.65 (m, 8H, 2 X –**CH_2-** (arginine), 2 X –**CH_2-** (tocopherol)), 8 X –**CH-**, 2 X –**CH_3**), 1.51-1.48 (m, 6H, 6 X –**CH-**), 1.38 (m, 8 H, 2 X –**CH_2-** (tocopherol), 2 X –**CH_2-** (arginine)), 1.24-1.18 (m, 38H, 2 X –**CH_3**, 16 X –**CH_2-**) , 0.88-0.85 (m, 24H, 8 X –**CH_3**). ^{13}C NMR [δ/ppm] (400 MHz, DMSO-D_6 + $CDCl_3$) 171.4, 168.4, 167.7, 157.7, 147.6, 127.6, 125.9, 122.5, 117.9, 74.7, 70.5, 70.3, 64.6, 64.4, 37.3, 32.6, 31.3, 31.0, 27.8, 24.6, 24.3, 23.9, 22.9, 22.8, 20.9, 20.6, 20.0, 19.9. ESI-MS: m/z Calculated for $[M]^{4+}/2$: 732.49 Found: 733.85.

3.4.3. Formulation of Liposomes and Lipoplexes. Chloroform solutions of DOTAP and co-lipid (DOPE) at equimolar ratios were taken in a Wheaton glass vial which was cleaned and dried previously. A thin film of the mixed lipids was made by drying the lipid mixture initially by a gentle flow of moisture-free nitrogen gas. Further, to remove traces of chloroform the film was dried-up under high vacuum for at least 3 h. To this, 2 mL of deionized water (Milli-Q)

was added to rehydrate the lipid film. The concentration of individual lipids after hydration was 0.5 mM. The vials were left overnight for hydration at room temperature, followed by recurrent vortex and bath sonication resulted in turbid suspension comprising liposomal multi-lamellar vesicles. Lastly, the solution was subjected to sonication using probe sonicator (pulse mode, 6 s on/off, 25% Amplitude) in an ice bath until homogenous colloidal solution was obtained. These visibly clear DOTAP + DOPE containing liposomal stock solutions were labelled as "DTD 11" and stored at 4 °C for further use. "DT" represents DOTAP, "D" represents DOPE and the numerical values represent their molar ratios in order. A series of DTDA liposomes were prepared similarly by adding the lipid ATTA (in chloroform) in required molar ratio to the glass vial during the first step. Four new liposomal formulations, namely DTDA 110.5, DTDA 111, DTDA 112 and DTDA 114 were prepared where "A" represents the new lipid ATTA and the last numerical represents its molar ratio in the solution. Except for "DTDA 114", all the liposomal formulations were attained with no apparent aggregation even later than 30 days of storage. Formation of lipoplexes was carried out using the liposomal stock at various concentrations in 50 µL of sterile deionized water, mixed with 50 µL of DNA solution under medium vortex. For gel electrophoresis assay, 0.3 µg/50 µL of pDNA and for the transfection or cystotoxicity studies, 1 µg/50 µL of pDNA was added to each liposomal formulation. After addition of liposome and pDNA, the complex was subjected to vigorous vortex for 30 seconds and incubated for 20-30 minutes at room temperature. DNA complexation ability, redox responsive DNA release, transfection efficiency and cytotoxicity of the lipoplexes formulated at various N/P ratios were examined.

3.4.4. Particle Size and Zeta Potential Measurements

Liposomal particle sizes and zeta potentials (net surface charges) were measured at 25° C using dynamic light scattering (DLS) zeta-sizer (ELSZ-2000, Otsuka Electronics). Deionized water was used as sample medium and measured at viscosity and solution refractive index of

0.89 and 1.33, respectively. The instrument was calibrated in advance with polystyrene nanospheres (−50 mV, 220 ± 6 nm). Analysis of light scattering at a scattering angle of 90° was performed with a laser beam of 633 nm. All experiments were done in triplicates and the average and standard deviation values were considered for plotting graphs. Dust free condition was maintained throughout the experiments.

The particle-size distribution and morphology of the liposomes were visually examined through a transmission electron microscope (TEM, HT7700, Hitachi). Concisely, carbon coated copper specimen grid with a mesh size of 200 was glow-discharged for 90 seconds. Four microliters of sample with liposomes was dropped on a copper grid and left for drying under dust free condition at room temperature for a week. TEM Images were captured and analyzed at 60 Kev acceleration voltage (DC voltage) using a CCD camera.

3.4.5. Agarose Gel Electrophoresis: The lipid-DNA complexation was assessed through a typical electrophoresis agarose gel assay. Cationic liposomes DOTAP:DOPE at lipid molar ratio 1:1 and DOTAP:DOPE:ATTA at lipid molar ratio of 1:1:1, were added with 0.3 µg of pDNA. N/P ratios of lipoplexes ranging from 1 to 15 were formulated by mixing of various amounts of liposome and a constant amount (0.3 µg) of pEGFP-C1 plasmid in de-ionized Milli-Q water. After 30 minutes of incubation at room temperature, the lipoplexes were added to the 0.8 % agarose gel which was pre-stained with DNA safe stain. The gel was subjected to electrophoresis for 20 min at a current of 140 V in Tris-borate EDTA (TBE) buffer. The DNA retention pattern was observed under UV light at 365 nm. In order to check the reduction responsive release of DNA form lipoplexes, dithiothreitol (DTT) was used as reducing agent. Lipoplexes at N/P ratios of 3 and 5 were initially prepared as mentioned above and incubated in PBS at pH 8.0 with 10 mM or 50 mM DTT. For the gel retardation assay with DTDA 2 µg and 3.4 µg of total lipid was complexed with 0.3 µg of DNA. Then, the complexes were incubated for another 3 h at 37° C. After the incubation, the lipoplexes were added to the 0.8 %

agarose gel which was pre-stained with DNA safe stain. The gel was subjected to electrophoresis for 20 min at a current of 140 V in TBE buffer.

3.4.6. Cell Experiments

HEL-299 and U87 cell lines were cultured and preserved in a CO_2 incubator (5 % CO_2) at 37 °C under moistened condition in MEM, complemented with 1% sodium pyruvate, 10% FBS and 100 μg/mL penicillin-streptomycin. HEK-293 cells and MDA-MB-231 were cultivated in DMEM, supplemented with 10% FBSand 100 μg/mL penicillin-streptomycin. PC3 cells and A549 were cultivated in Roswell Park Memorial Institute medium-1640 (RPMI-1640), added with 10% FBS and 100 μg/mL penicillin-streptomycin. The cells were continuously monitored for confluence throughout the duration of experiments. The medium was changed every two or three days, and sub-culture was done when the cells reached 90% confluence.

Cell viability. The cell viability of liposomes or lipoplexes was evaluated by MTT assay. The cytotoxicities of liposomes were examined for incubation with various concentrations of DTD 11 liposomes or DTDA 111 liposomes (0.5–100 μg of liposome/mL). HEK-293, HEL-299, PC3, U87, A549 and MDA-MB-231 cells at a density of 5×10^3/well were seeded in tissue culture plates (96-well) in their respective medium consisting 10% FBS. The relative cell viability of lipoplexes were examined at various N/P ratios (3-9) of DTD11/DNA lipoplexes or DTDA111/DNA lipoplexes at 48h of post-incubation at 37 °C. Two different pDNAs were used in this study to make lipoplexes and their corresponding lipoplexes were compared for cell viability. A control pEGFP plasmid and pTRAIL plasmid with anticancer properties were used to make lipoplexes. Lipofectamine/DNA complexes were prepared as per the manufacturer's protocol. The percentage of viable cells was estimated using a tetrazolium-based colorimetric technique by determining their mitochondrial reductase activity.[182]

In Vitro Transfection studies. In vitro transgene expression was done in HEK-293, HEL-299, U87, A549 and PC3 cells at a cell density of 5×10^4/well in 24-well plates and incubated in

their respective culture medium comprising 10% FBS in CO_2 incubator for 24 h prior to transfection. Lipoplexes with N/P ratios ranging from 3-9 were made using different amounts of DTD or DTDA based liposomes and a fixed DNA (pEGFP-C1 plasmid) amount of 1 μg to a final volume of 100 μL. After 30 minutes of incubation, the formed lipid/DNA complexes were added to well plates containing cells in MEM/RPMI/DMEM medium. The cells were then incubated with lipoplexes for 4h followed by the replacement of the medium with fresh complete-medium comprising 10 % FBS. The cells were further incubated for another 48 h of post-transfection. Expression of green fluorescent protein (GFP) was directly imaged using fluorescent microscopy (*Leica DMi8*; Leica Microsystems, Wetzlar, Germany). We have adopted a previously reported quantification method for the quantification of green fluorescence expression in various cell lines after transfection.[213, 232] Briefly, for individual experiment, at least three fields of view in each group were taken as fluorescence images. Subsequently, the fluorescence intensity of each corresponding image was semi-quantitated using ImageJ software (v1.51a, National Institute of Health, USA). Average and standard deviation of fluorescence intensity of each test group were calculated. Relative transfection efficiency was measured by comparing the fluorescence intensity of DTDA111 and Lipofectamine treated groups with DTD11 treated groups. Further, the percentage of GFP positive cells in each field of view has been calculated using the software by comparing the total number of cells with GFP expressing cells.[233]

3.4.7. Statistical analyses

Data were analyzed with the SigmaPlot 11.0 software (Systat Software, Inc, San Jose, CA) and presented as the mean ± SD of a minimum three individual experiments. Significant difference between individual groups was determined by performing t-test. Statistical differences between two groups were considered significant as per the following criteria: *$p < 0.05$, **$p < 0.01$ and ***$p < 0.001$.

SPECTRA

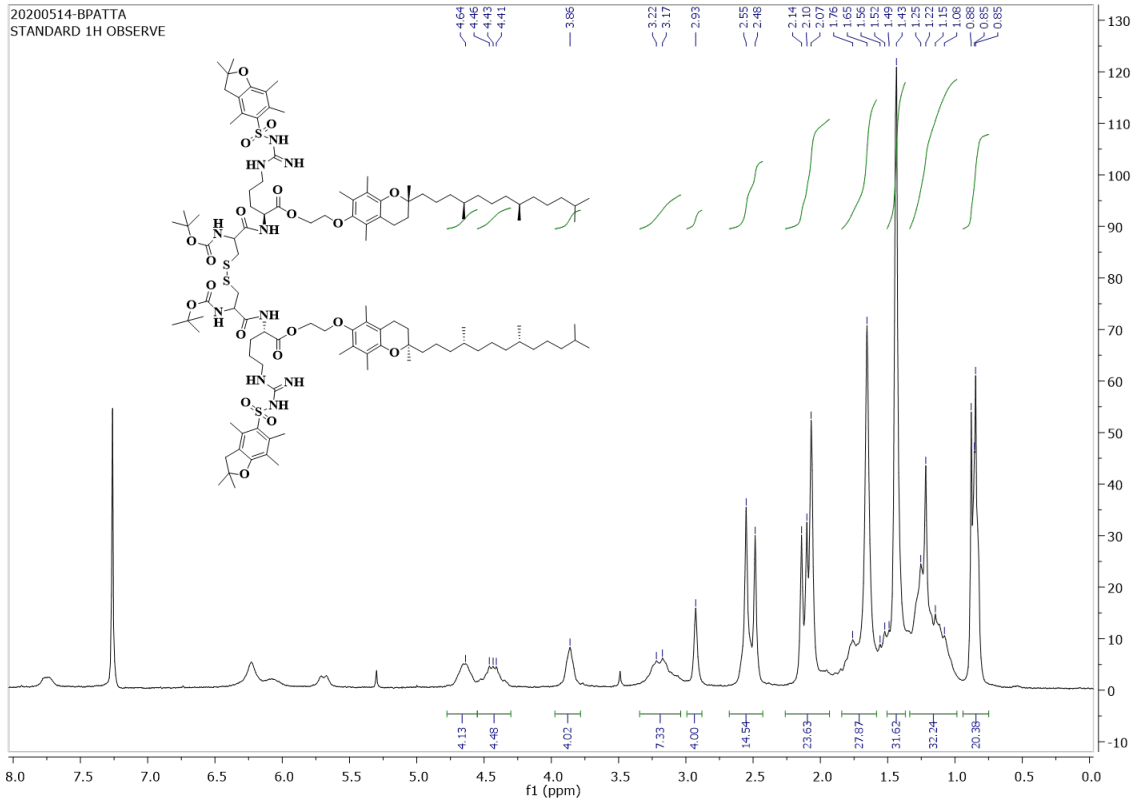

^{1}H NMR spectrum of BPATTA in $CDCl_3$

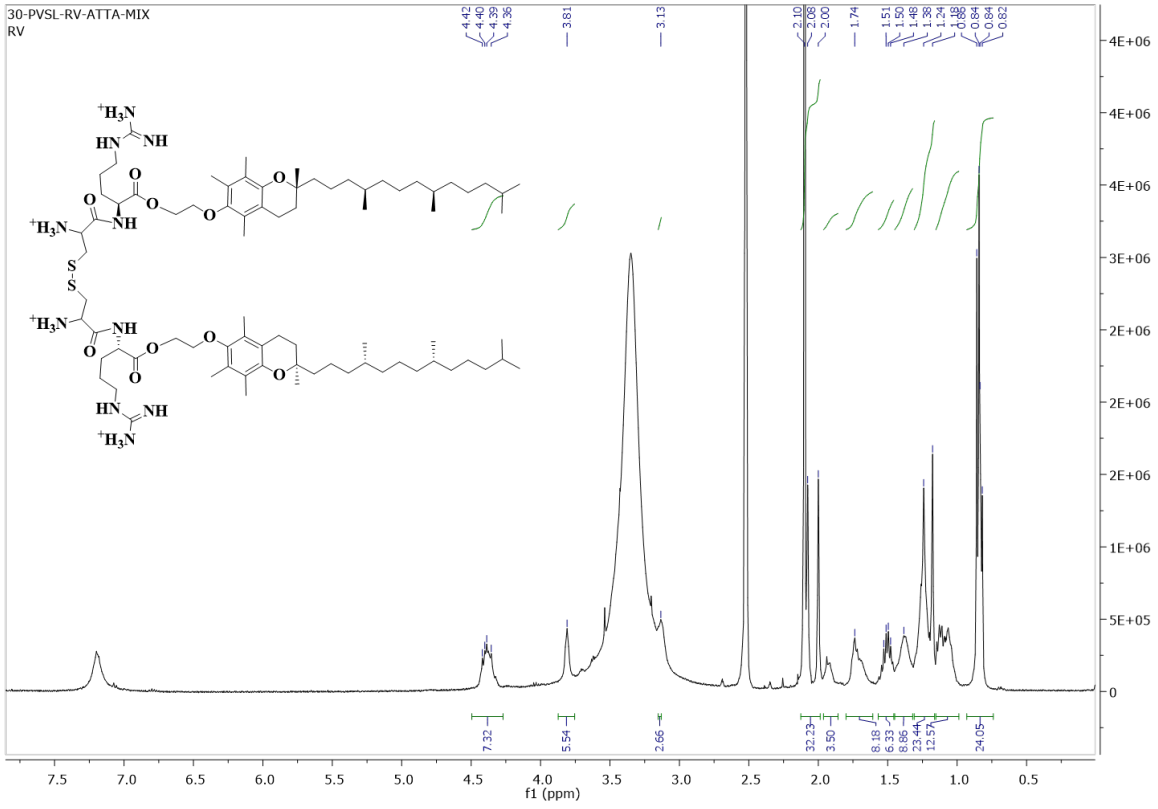

^{1}H NMR spectrum of ATTA in DMSO-D_6

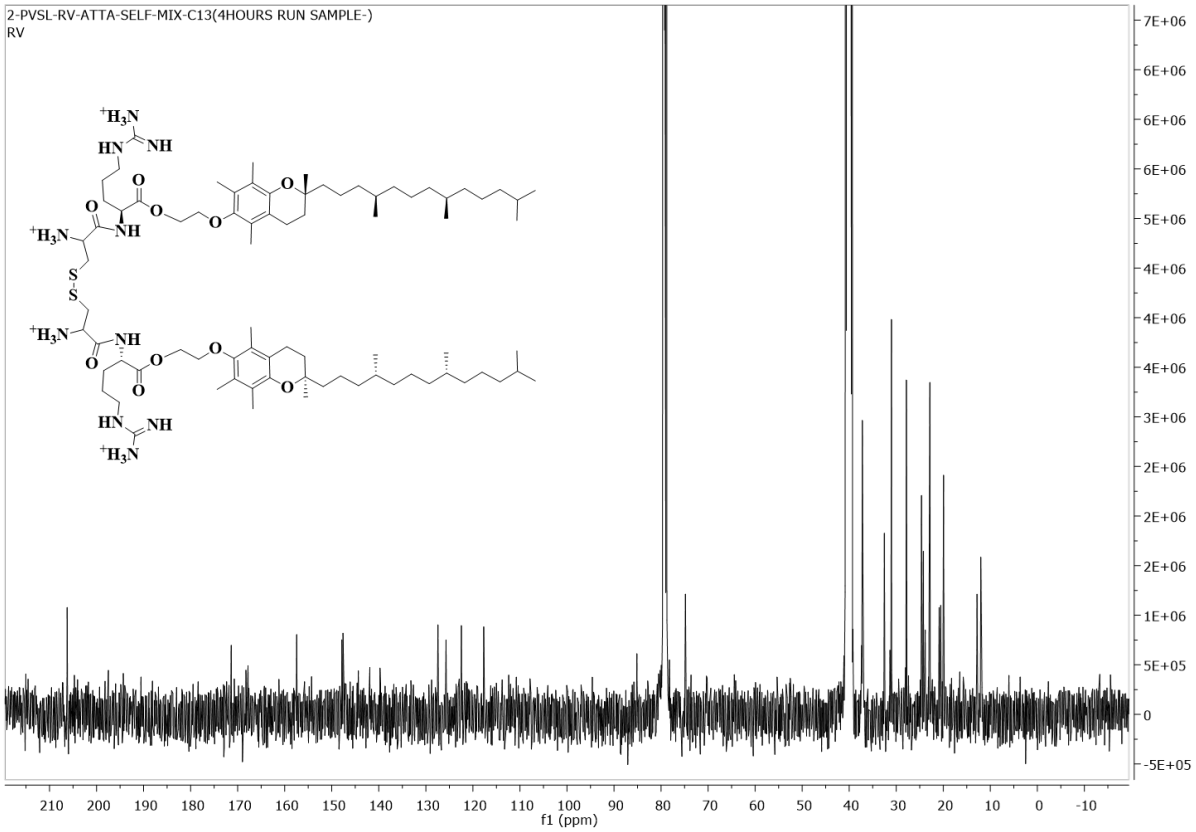

^{13}C NMR spectrum of ATTA in DMSO-D_6 + $CDCl_3$

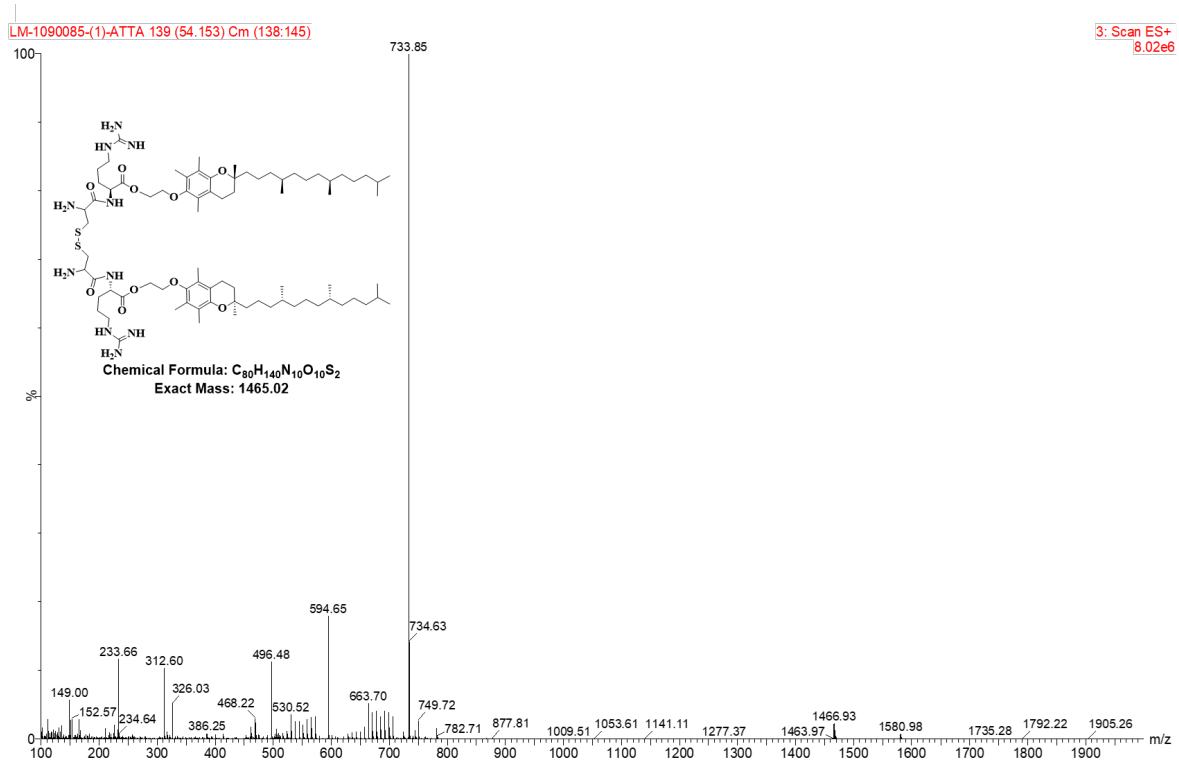

Mass spectrum of ATTA

CHAPTER IV

DOTAP INCORPORATED FORMULATIONS OF AMINOACID BASED CATIONIC LIPOSOMES FOR IMPROVED GENE TRANSFECTION

CHAPTER IV

DOTAP INCORPORATED FORMULATIONS OF AMINOACID BASED CATIONIC LIPOSOMES FOR IMPROVED GENE TRANSFECTION

4.1. INTRODUCTION

Liposomes have the potential to satisfy the qualities of perfect vectors since they are safe, contain natural lipids, and have a high degree of molecular and formulation diversity.[234] The problem with these liposomal vectors is that most of the liposomes are not as efficient as viral vectors in transfection. Thus, improving the efficiency of liposomes has been a major challenge since several years. Structural modifications on the cationic head groups,[119] incorporating cell penetrating peptides[120] and variations in hydrophobic chain lengths[121] are some of the strategies used for improved liposomal transfection. Although improvements were achieved, majority of these strategies have still outplayed by the transfection of commercial transfection reagents Lipofectamine 2000 (L2K) and Lipofectamine 3000 (L3K). L2k and L3k on the other hand cause significant cytotoxicity in variety of cell lines while transfecting. Thus, investigations on competent transfection reagents with better safety must be continued to improve cationic liposome-mediated gene delivery. A few of the previous reports emphasized the need to look at the modifications at formulation stages. Mixing different kinds of lipids, particularly varied by their hydrophobic domains, in liposomal formulations has shown synergistic enhancement in transfection.[235, 236] It was determined that manipulation of lipid carrier composition could be a useful strategy for improving delivery by changing their lipid-phase transition.[237] Therefore, along with structural variations of cationic lipids, formulation changes may hold promise to enhance transfection.

Amino acid based cationic lipids have long been considered as safe gene delivery vectors owing to their biocompatibility.[93, 238, 239] Development of amino acid based cationic lipids for higher transfection efficiency has been the subject of research for many researchers currently. Amino

acid based head groups are majorly beneficial for low cytotoxicity over the conventional quaternary ammonium head groups. On the other hand, quaternary ammonium based cationic lipid, 1,2-dioleoyl-3-trimethylammonium-propane (DOTAP) has been involved in many liposomal formulations which has proved to be a good transfection reagent.[240] However, its transfection efficiency was limited to a few easy to transfect cell lines such as HEK-293 and HEL-299. Its transfection in some of the aggressive cancer cell lines such as PC3 and A549 was found to be very poor. Our recent research has shown that the incorporation of an amino acid-based lipopeptide can improve DOTAP transfection efficiency in these cancer cell lines.[241] Taking cues from the past investigations, we intend to analyse various formulations of structurally different amino acid-based liposomes with DOTAP. **Chapter IV** demonstrates the development of new formulations using new amino acid based cationic lipids with DOTAP and compared with their individual liposomal formulations. The results indicate that formulations containing the new lipids and DOTAP are comparatively safer and better at transfection than L2K in specific cell lines.

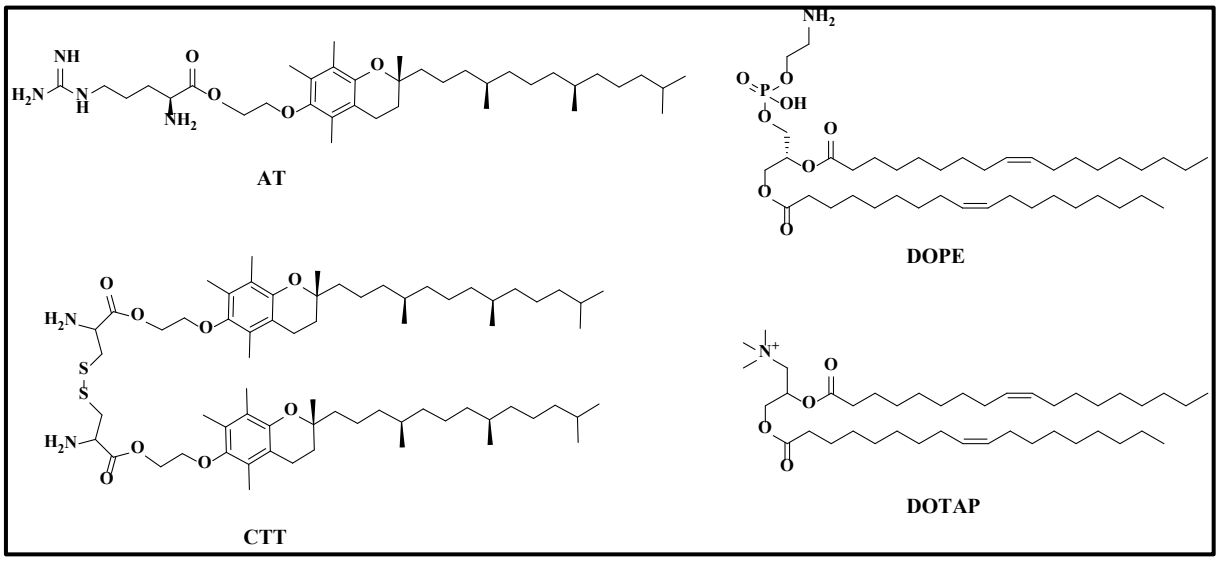

Figure 4.1: *Chemical structures of lipids used in the present study*

4.2. RESULTS AND DISCUSSION

4.2.1. Chemistry

One of the cationic lipids in the current study, arginine-tocopherol conjugated lipid (AT) was synthesized as per the previously described procedure.[238] Cystine-tocopherol conjugated dimeric lipid (CTT) was synthesized through the esterification of carboxylic acid ends of Cystine moiety by the reaction with 2-Tocopheryloxyethanol. De-protection of BOC groups using trifluoroacetic acid afforded positively charged cationic head group with trifluoroacetates as counter ions. Ionisation states and counter ions have significant effect on gene delivery capability of amino acid-based cationic lipids. It has been demonstrated that trifluoroacetates as counter ions have better effects on zeta potential and gene transfection than chloride ions. [160, 242] Both the cationic lipids vary by their amino acid head groups, besides dimeric structure of CTT in comparison with monomeric structure of AT. The synthetic intermediates and cationic lipid, CTT as shown in **Scheme 4.1** are characterised through ^{1}H, ^{13}C nuclear magnetic resonance (NMR) and electrospray ionization-mass spectrometry (ESI-MS). Chemical structures of cationic lipids (AT, CTT and DOTAP) and helper lipid, 1,2-dioleoyl-sn-glycerol-3-phosphoethanolamine (DOPE), used in this study were shown in **Figure 4.1.**

4.2.2. Preparation and Characterization of liposomes

Two aminoacid based cationic lipids, AT and CTT were used in this study to form liposomes with or without DOTAP. Four liposome formulations were prepared and studied, namely, CTTD (CTT:DOPE at 1:1 molar ratio), ATD (AT:DOPE at 1:1 molar ratio), DtATD (DOTAP:AT:DOPE at 1:1:1 molar ratio) and DtCTTD (DOTAP:CTT:DOPE at 1:1:1 molar ratio). Among the four liposomal formulations that were prepared, the lipid to lipid molar ratio was kept constant at one for uniformity. Our previous study using DOTAP in the formulation also revealed that Lipopeptide:DOPE:DOTAP at 1:1:1 ratio has resulted in stable particle sizes and efficient transfection.[241] Lipid formulations were characterized for particle size, surface

charge and morphology using dynamic light scattering (DLS) and transmission electron microscopy (TEM) techniques. Liposome's hydrodynamic diameters or particle sizes have a direct correlation to clearance of liposomes in blood, and thus can significantly affect the desired therapeutic outcome.[243] Earlier studies on drug delivery using liposomes revealed that, the smaller size of liposomes reduce the possibility of blood components to recognise these particles and avoid clearance.[244, 245] DLS sizes of the formulated co-liposome particles in deionized water media revealed the average hydrodynamic diameters, i.e. average particle sizes (**Figure 4.2A**). For all the liposomal formulations, the average size of the particles was found to be in the range of 100 nm – 180 nm. Among all, arginine bearing AT lipid with only DOPE in the formulation (ATD) attained maximum size followed by CTTD. Incorporation of DOTAP in the formulations apparently reduced the particle size as revealed by the sizes of DtATD and DtCTTD formulations. Regardless of its transfection efficiency, DOTAP is known form smaller sized liposomes.[240, 241, 246] DOTAP is thought to be inducing alterations at the membrane interface which may partially help in its electrostatic interactions. Previous molecular modelling studies have revealed that DOTAP forms a salt bridge with the phosphate groups of the helper lipids in the liposomes.[247] These physical interactions combined with membrane fluidity of DOTAP could be promoting size reduction of DOTAP incorporated liposomes.[246] Surface charges of liposomal formulations were determined through Zeta potential measurements. As shown in **Figure 4.2B**, the effect of DOTAP incorporation in the formulations was obvious with increased zeta potentials. DOTAP with positively charged quaternary ammonium head group was expected to enhance the surface charges of amino acid based liposomes. Although the morphology of the liposomes has limited effect on their efficacy, it is interesting to visualize their appearance. The morphology of liposomes modified by DOTAP were checked through TEM analysis which revealed the distinct morphologies attained by DtCTTD and DtATD. Although distinct, lamellar structures were seen for both DtATD and

DtCTTD liposomes. The representative TEM images of the DOTAP incorporated co-liposomal formulations are presented in **Figure 4.3**.

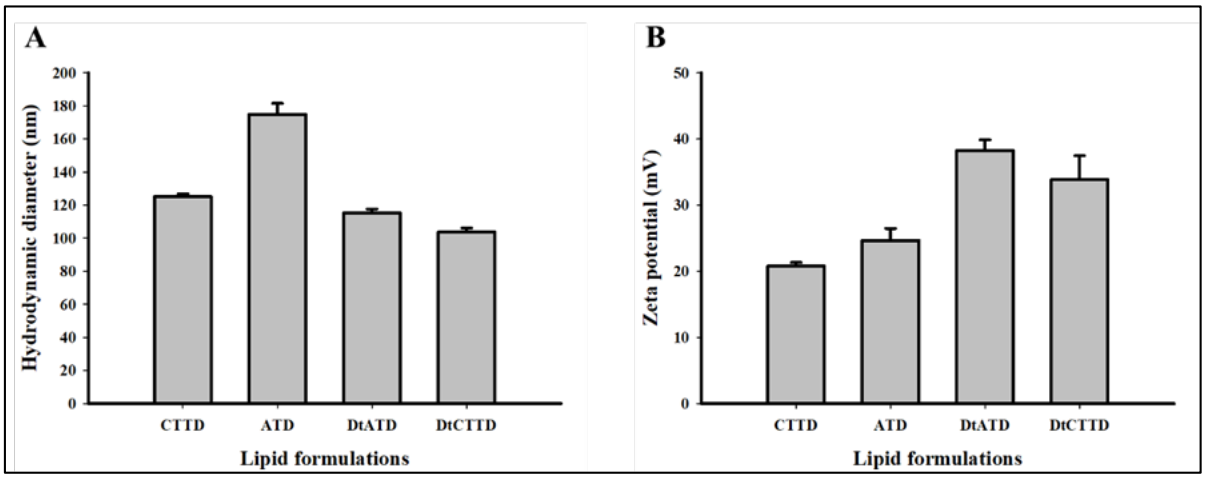

Figure 4.2: *Size and zeta potential of liposomal formulations. A) Hydrodynamic diameters of liposomes at different lipid molar ratios (n=3). B) Zeta potentials of liposomes at different lipid molar ratios (n=3).*

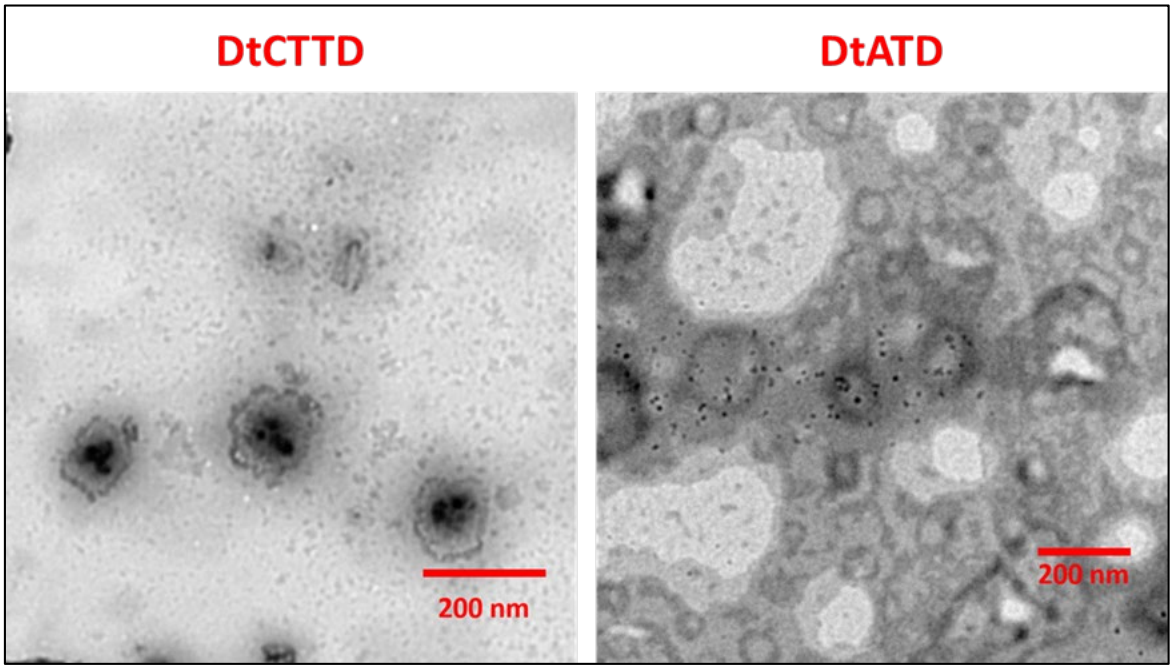

Figure 4.3: *Transmission electron microscopy (TEM) images of DOTAP incorporated formulations*, DtCTTD and DtATD.

4.2.3. Optimization of *in vitro* pEGFP gene transfection efficiency in HEK-293 cells.

The liposome-DNA complexes were prepared as described in the experimental section. Four types of liposomes (CTTD, ATD, DtATD and DtCTTD) were combined with pEGFP-C1

plasmid to form the corresponding lipoplexes. The prepared complexes were incubated with HEK-293 cells for transfection through the methods mentioned in experimental section. The gene delivery experiments revealed that cationic lipid AT-containing lipoplexes (ATD and DtATD) attained maximum transfection at N/P ratio of 5, while the cationic lipid CTT-containing lipoplexes (CTTD and DtCTTD) have shown their best transfection at N/P ratio of 9. This reiterates the fact that optimal N/P ratio for transfection depends on the lipid composition.[248]

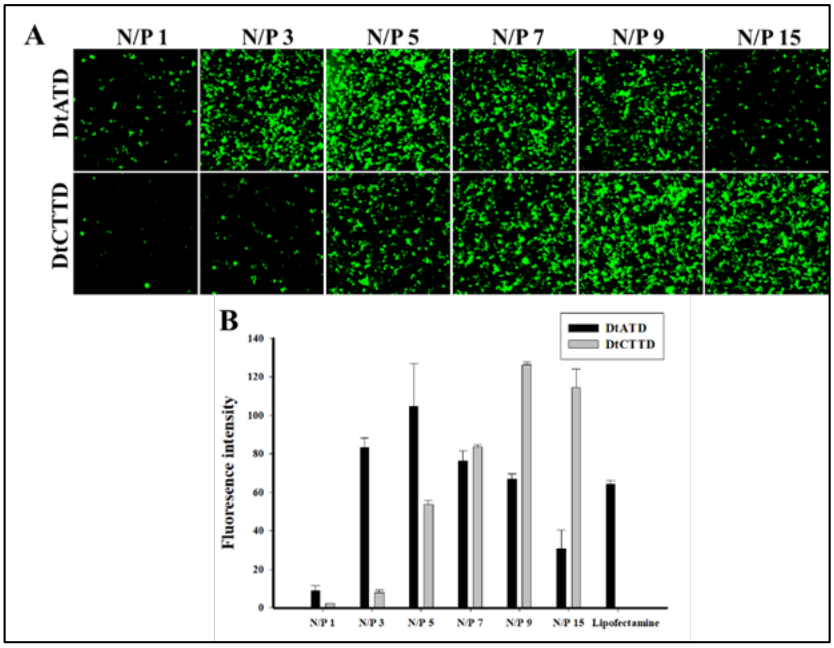

Figure 4.4: *Optimization of in vitro pEGFP gene transfection efficiency mediated by DOTAP incorporated formulations, DtATD and DtCTTD in HEK-293 cells. A) Representative fluorescence microscopy images after pEGFP gene transfection mediated by DtATD and DtCTTD at various N/P ratios ranging from 1 to 15. B) Fluorescence intensities of pEGFP transfected cells by various lipid formulations as quantified using ImageJ software (n=3).*

Figure 4.4A shows the representative fluorescence microscopy images of HEK-293 cells transfected with DOTAP-formulated lipid-DNA complexes while **Figure 4.4B** depicts their corresponding mean fluorescence intensities. It can be noted that the complexes of DtCTTD, at the N/P ratio of 9 exhibited superior transfection activity over other test formulations. Although DtATD has shown good transfection efficiency at N/P ratio of 5, it was less consistent when

compared with DtCTTD at N/P ratio of 9. The results suggest that, with high transfection activity at N/P ratio of 9, DtCTTD may have potential for efficient gene delivery even better than commercial transfection reagent, Lipofectamine.

4.2.4. Transfection activity in cancer cell lines

To check the efficiency of the newly formulated liposomes to transfect cancer cell lines, transfection experiments were performed in two cancer cell lines (PC3 and A549) using optimized N/P ratios of lipid-DNA complexes. For cytotoxicity and transfection experiments, 1µg of pDNA was complexed with calculated amount of liposome solution as per their N/P ratios. Four types of complexes based on ATD, DtATD, DtCTTD and Lipofectamine were compared in terms of their transfection efficiency. In case of PC3 cells (**Figure 4.5**), incorporation of DOTAP in CTTD liposomes has resulted in 3-fold increase in transfection efficiency. On the other hand, a slight increase in transfection efficiency was noted in DtATD in comparison with ATD. Interestingly, DOTAP-containing DtCTTD has resulted in 2-fold higher transfection efficiency than commercial transfection reagent, Lipofectamine. As shown in **Figure 4.6**, the transfection efficiency in A549 cell lines revealed that DtCTTD has better gene transfer ability among the tested lipid-DNA complexes. Having guanidine groups on the liposomal surface is a general strategy to improve transfection. Several studies have highlighted that arginine based liposomes have good transfection efficiency due to the presence of guanidine moieties.[160, 198, 238, 239] In both the cancer cell lines tested in the current study, arginine based liposomes, ATD and DtATD have decent transfection, which are however outplayed by DtCTTD. Although there was not much difference in transfection efficiency of DtATD and DtCTTD in HEK-293 cells at their optimal N/P ratios (**Figure 4.5**), notable difference was seen only in the tested cancer cell lines. The results indicate that, having cell penetrating molecules such as guanidines alone cannot be the determining factor to attain superior transfection in certain cell lines. The transfection of lipoplexes prepared by different cationic lipids varies

greatly among various cell lines. Along with the external properties of liposomes (size, surface charge, cell type), the intracellular transitions of lamellar to non-lamellar phases could also be playing a role in defining transfection activity of different combinations of liposomes.[249] As per the current results, the incorporation of DOTAP in liposomal formulations has apparently yielded superior transfection when compared with individual aminoacid based liposomes. Particularly, the combination of DOTAP+CTT+DOPE as denoted by DtCTTD has exhibited high transfection efficiency than all other tested formulations in PC3 and A549 cell lines.

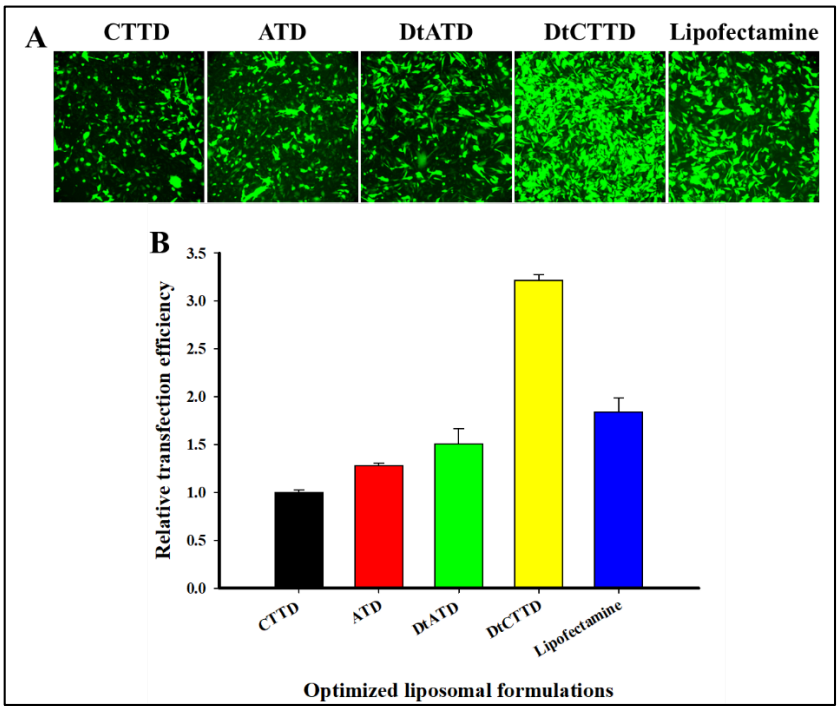

Figure 4.5: *In vitro pEGFP gene transfection efficiency mediated by optimized lipid-DNA complexes in PC3 cell line. A) Representative fluorescence microscopy images of PC3 cells after pEGFP gene transfection mediated by various formulations and Lipofectamine. B) Relative transfection efficiencies of various formulations and Lipofectamine, quantified from the fluorescence intensities of images (A) using ImageJ software.*

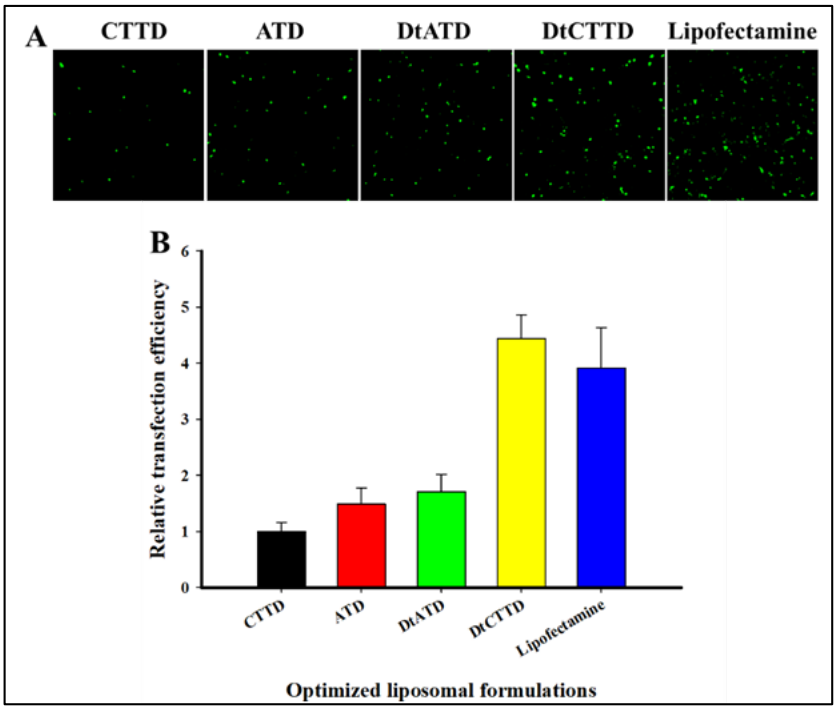

Figure 4.6: *In vitro pEGFP gene transfection efficiency mediated by optimized lipid-DNA complexes in A549 cell line. A) Representative fluorescence microscopy images of A549 cells after pEGFP gene transfection mediated by various formulations and Lipofectamine. B) Relative transfection efficiencies of various formulations and Lipofectamine, quantified from the fluorescence intensities of images (A) using ImageJ software.*

4.2.5. DNA Binding

Four types of liposomal formulations including both conventional (CTTD and ATD) and DOTAP incorporated (DtATD and DtCTTD), were tested for their DNA binding ability. Lipoplexes were made by similar procedures used for transfection studies. **Figure 4.7** reveals that, among the formulations without DOTAP (CTTD and ATD), ATD has shown superior binding ability with complete binding observed at N/P ratio of 3. It could be because the guanidium groups in ATD generated parallel Zwitter ionic hydrogen interactions (N–H+O–) with phosphate ions in DNA.[250] On the other hand, CTTD has achieved complete DNA retardation at N/P ratio of 9. DOTAP incorporated liposomes, however, have shown apparent enhanced DNA binding ability. Successful DNA retardation was seen for DtATD at N/P ratio of 1 while for DtCTTD, at N/P ratio of 3.

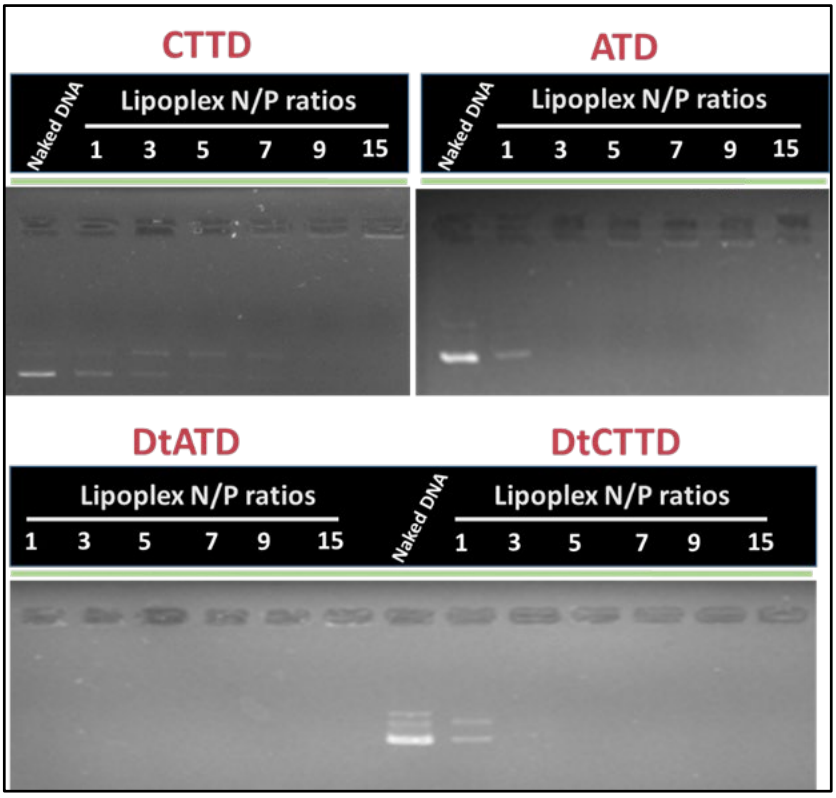

Figure 4.7: *DNA binding ability of four types of formulations. Gel retardation images were obtained after lipoplexes of CTTD, ATD, DtATD and DtCTTD at different N/P ratios ranging from 1 to 15 were electrophoresed on agarose gel.*

4.2.6. Cytotoxicity of lipid-DNA complexes

The MTT method could be used to assess the cytotoxicity of gene delivery materials. The relative percentage of cell viability of the three cell lines (HEK-293, PC3 and A549) after exposure to different lipid-DNA complexes at various N/P ratios is illustrated in **Figure 4.8.** Complexes without DOTAP (ATD-based complexes and CTTD based complexes) have shown negligible cytotoxicity in all the cell lines. Complexes of DOTAP incorporated liposomes (DtATD and DtCTTD), however were slightly toxic at high N/P ratio of 15 with 60 – 70 % cell viabilities. Across all the lipid-DNA complexes, the maximum N/P ratios used for optimized transfection was 9. The results of cell viability assays revealed that, except for DtCTTD in A549 cells, the transfection optimized lipid-DNA complexes were relatively non-toxic to the cell lines tested. On the hindsight, it was observed that all the complexes however, were much safer in comparison with Lipofectamine. The lower cytotoxicity of these liposomes could be attributed

to the nature of the aminoacid based lipids, as they are more biocompatible over quaternary ammonium based lipids, thus enhancing the cell tolerance to them.[156, 251] Also, it is learnt from previous reports that, the DOTAP:DOPE liposomes can be cytotoxic at high concentrations.[241, 252] Instead, the combination of aminoacid based lipids and DOTAP in the formulation can be helpful to regulate the toxicity.

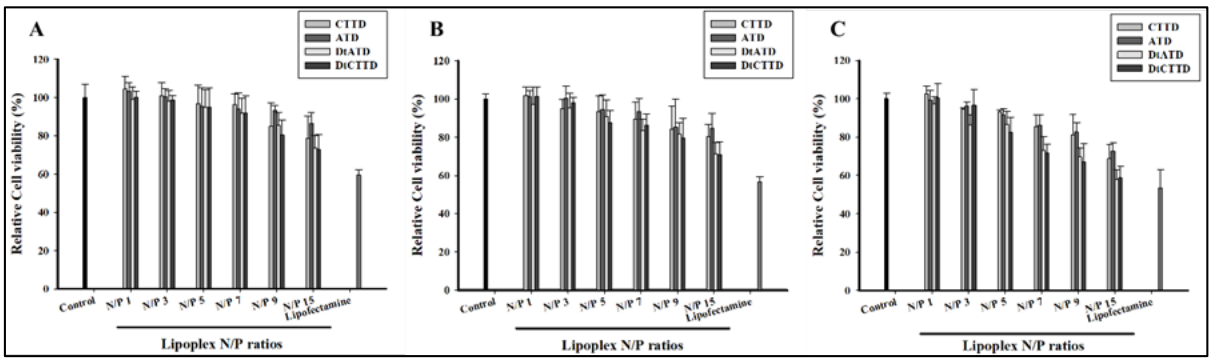

Figure 4.8: *Relative cell viabilities of lipid-DNA complexes of CTTD, ATD, DtATD and DtCTTD at different N/P ratios ranging from 1 to 15 in A) HEK-293, B) PC3 and C) A549 cell lines (n = 3).*

4.3. CONCLUSIONS

Two amonoacid based cationic lipids with either arginine or cystine in the head group were synthesized with α-tocopherol in the hydrophobic region of lipids. Co-liposomal formulations were made with various lipid compositions. Four liposomal formulations, broadly categorized into two types, i.e., aminoacid based liposomes without DOTAP (CTTD and ATD) and with DOTAP (DtATD and DtCTTD), were characterized for their physicochemical properties and DNA binding. DOTAP incorporated formulations (DtATD and DtCTTD) exhibited lower particles size, higher positive zeta potential and better DNA binding ability. Transfection optimized lipid-DNA complexes of DOTAP incorporated formulations had greater efficacy than their counterparts without DOTAP. Particularly, DtCTTD has shown superior transfection capability in PC3 and A549 cell lines in comparison with commercial transfection reagent, Lipofectamine. Additionally, all these new formulations are found to be less toxic than Lipofectamine. Taken together, the above findings may infer that these DOTAP

incorporated formulations derived from aminoacid based liposomes are promising tools for improving the transfection efficacy with low toxicity.

4.4. EXPERIMENTAL SECTION

4.4.1. Materials. N,N'-di-Boc-L-cystine **(**BOC-Cys-OH)$_2$, α-Tocopherol, 2-bromoethanol, 1,2-dio leoyl-3-trimethylammonium-propane (DOTAP), Fmoc-Arg(pbf)-OH and 1,2-dioleoyl-sn-glycerol-3-phosphoethanolamine (DOPE) were purchased from Sigma (Sigma-Aldrich Co., Ltd.). Invitrogen Life Technologies has supplied Lipofectamine2000. Unless mentioned otherwise, rest of the organic solvents and reagents i.e., methylene chloride (DCM), dimethyl formamide (DMF), piperidine, trifluoroacetic acid (TFA), N, N′ -dicyclohexylcarbodiimide (DCC), sodium hydroxide (NaOH), N-(3-dimethylaminopropyl)-N′-ethylcarbodiimide hydrochloride (EDC), 4-dimethylaminopyridine (DMAP), 1-hydroxybenzotriazole (HOBt), and methanol were acquired from Alfa Aesor, Sigma and Finar at their highest pure state which were used sans additional purification. Reaction evolvement was watched over silica gel thin-layer chromatography (TLC) plates (0.25 mm). Silica gel (60-120 or 100-200 mesh, Acme Synthetic Chemicals, India) was applied for column chromatography the separation of compounds. FT400MHz NMR (Varian) spectrometer was used to obtain spectral data (^{1}H and ^{13}C NMR). Mass analysis was carried out on a commercial ion trap LCQ mass spectrometer (Thermo Finnigan, SanJose, CA, U.S.) fitted with an ESI source. Fetal Bovine Serum (FBS), Dulbecco's Modified Eagle Medium (DMEM), Phosphate Buffer Saline (PBS), Roswell Park Memorial Institute (RPMI) 1640 and trypsin−EDTA solution were acquired from Invitrogen. MP Biomedicals has supplied 3-(4,5-Dimethylthiazol-2-yl)-2,5-diphenyl-tetrazolium bromide (MTT).

Scheme 4.1: Synthesis of Cationic Lipid CTT

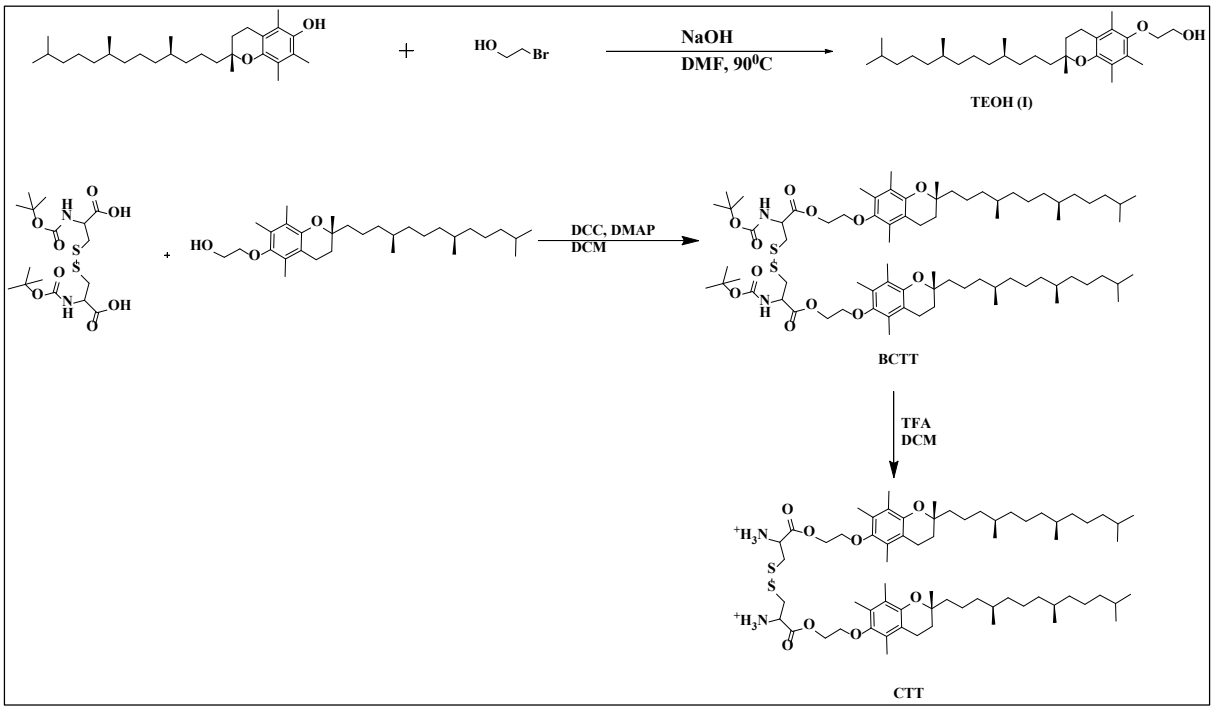

Reagents and solvents. *NaOH: Sodium hydroxide, DMF: N,N-Dimethylformamide, DCC: Dicyclohexylcarbodiimide, DMAP: 4-Dimethylaminopyridine, DCM: Dichloromethane, TFA: Trifluoroacetic acid.*

Synthesis. Arginine-tocopherol conjugated lipid, AT was synthesized as described in Chapter II.[238] Gemini-like cationic lipid with cystine linker, CTT was synthesized using the methods described in **Scheme 4.1**. Reaction intermediates and the final lipid were characterized by nuclear magnetic resonance (^{1}H and ^{13}C NMR) and mass spectrometry.

4.4.2. Synthesis of Gemini-like cationic lipid (CTT)

Synthesis of bis(tocopheryloxyethyl) 3,3'-disulfanediylbis(2-((tert-butoxycarbonyl)amino) propanoate) (BCTT).

Initially, 2-Tocopheryloxyethanol (TEOH) was synthesized and purified as per the method described in previous report.[238] Then sequentially, $(BOC\text{-}Cys\text{-}OH)_2$ (1.0 eq., 0.56 g,), TEOH (2.5 eq, 1.5 g), DMAP (0.3 eq., 0.047 g,) and DCC (3 eq., 0.78 g,) were added to 15 mL of dry DCM in a round bottom flask at 0 $^{\circ}$C. The reaction was maintained at 0 ^{0}C while stirring for 30 minutes followed by warming up to room temperature and continued stirring for another 24 h. the white precipitate formed during the reaction, Dicyclohexylurea (DCU), was filtered and the resultant filtrate

was subjected to vacuum for solvent evaporation. Ethyl acetate (EA, 50 mL) was added to the residue and washed thrice with water (3×50 mL). The collected organic layer was dried over sodium sulfate and concentrated. Further, the crude product was purified on column chromatography (7-12 % EA in Hexane) to give white coloured solid as desired product (BCTT). Yield: 1.23 g (72%). ^{1}H NMR [δ/ppm] (400 MHz, $CDCl_3$): 4.69 (t, 2H, 2 X –NH-**CH**(CH_2)-COO-), 4.49-4.40 (m, 4H, 2X –COO-**CH_2**-), 3.88-3.86 (t, 4H, 2X -CH_2-**CH_2**-O-), 3.22 (m, 4H, 2X –S-**CH_2**-), 2.57-2.54 (t, 4H, 2X –Ar-**CH_2**-), 2.16-2.07 (t, 18H, 6 X Ph–**CH_3**), 1.76-1.65 (m, 6H, 2X Ar–**CH_2**- (tocopherol), 2X –**CH**(CH_3)$_2$-), 1.54-1.45 (m, 8H, 2X –**CH_2**-, 4X –**CH**-), 1.38 (s, 18H, 6X –**CH_3** (BOC)), 1.25-1.07 (m, 38H, 2X –**CH_3**, 16 X –**CH_2**-) , 0.87-0.83 (m, 24H, 8 X –**CH_3**).

Synthesis of bis(tocopheryloxyethyl) 3,3'-disulfanediylbis(2-aminopropanoate) (CTT).

The amine-protecting BOC groups were removed by the action of 50 % trifluoroacetic acid (TFA) in DCM. BCTT (0.8 g, 0.59 mmol) was dissolved in 3 mL of DCM and 3 mL of TFA was added dropwise at 0° C. After adding TFA, the reaction temperature was gradually warmed up to room temperature with continued stirring for another 3 h. Afterwards, the TFA and DCM were evaporated with the help of vacuum evaporator and the resultant residue with crude product was washed thrice using EA to yield pure target product, CTT as brown waxy solid. Yield: 0.65 g (72%). ^{1}H NMR [δ/ppm] (400 MHz, $CDCl_3$): 4.51 (m, 6H, 2X NH_3^+-**CH**(CH_2)-COO-, 2X -COO-**CH_2**-), 3.84 (m, 4H, 2X -**CH2**-O-), 3.49 (m, 4H, 2X –S-**CH_2**-), 2.51 (t, 4H, 2X –Ar-**CH_2**-), 2.13-2.03 (m, 18H, 6 X Ph–**CH_3**), 1.75-1.66 (m, 4H, 2X Ar–**CH_2**- (tocopherol)), 1.55-1.48 (m, 6H, 2X –**CH_2**-, 2X –**CH**(CH_3)$_2$-) 1.45-1.07 (m, 42H, 4X –**CH**-, 16 X –**CH_2**-, 2X –**CH_3**), 0.87-0.83 (m, 24H, 8 X –**CH_3.** ^{13}C NMR [δ/ppm] (400 MHz, $CDCl_3$) 168.1, 148.1, 147.7, 127.5, 125.7, 122.9, 117.6, 96.8, 74.8, 73.7, 69.7, 62.4, 39.4, 37.6, 37.4, 37.3, 32.8, 29.7, 28.0, 24.8, 24.5, 23.5, 22.7, 22.6, 21.1, 20.6, 19.8, 19.7, 19.6. ESI-MS: m/z Calculated for $C_{68}H_{118}N_2O_8S_2$ $[M]^+$: 1152.82 Found: 1153.83.

4.4.3. Formulation of Liposomes and Lipoplexes. Four different liposomal formulations, namely CTTD, ATD, DtATD and DtCTTD were prepared with individual lipid components. CTTD represents the liposomes formed from equimolar mixture of individual lipids, CTT (denoted by CTT) and DOPE (denoted by D). Similarly, liposome formulation ATD was derived from equimolar mixture of lipids AT (denoted by AT) and DOPE, while addition of DOTAP (denoted by Dt, molar ratio equal to that of AT or CTT) to ATD and CTTD gives formulations DtATD and DtCTTD, respectively. All formulations were prepared by conventional thin film hydration method. Briefly, each individual lipid in chloroform solution were mixed in a Wheaton glass vial in required combinations as mentioned above. The chloroform solution was evaporated by a controlled flow of de-moisturized nitrogen gas. A thin film was made through this process, which was further dried for at least 3 hours under strong vacuum. The dried film was then hydrated by the addition of 2 mL of ion-free water (Milli-Q). Each lipid concentration after hydration was 0.5 mM, individually. The hydrated thin film was left overnight at room temperature. Subsequently, each vial with different liposomal formulations were subjected to recurrent vortex followed by bath sonication. The process results in turbid suspensions which comprises liposomal multi-lamellar vesicles. Lastly, these suspensions were subjected to probe sonication (pulse mode, 6 s on/off, 25% Amplitude) in an ice bath where homogenous colloidal solutions were obtained. All liposomal formulations were visibly transparent and stable until at least for a month with no aggregation when stored at 4 °C. No difference in size of the liposomes was noted within a month (data not shown). However, for consistency, liposomes were prepared freshly after every 30 days and stored under refrigerated condition until used for physicochemical and biological assays. For the lipoplex formation, each liposomal stock solution was added to pDNA at various N/P ratios. In detail, for gel electrophoresis analysis, each liposomal solution at various concentrations of lipids was diluted with sterile deionized water to 50 µL. This solution was added with 50 µL of DNA solution at 0.3 µg/50 µL concentration under mild vertex. This was followed by vigorous vertex

for another 30 seconds and incubation for 30 minutes. For transfection and cytotoxicity assay with lipoplexes, a similar procedure was used but the concentration of pDNA was 1 μg/50 μL to be added to the liposomes of required concentration to make desired N/P ratio of lipoplexes.

4.4.4. Particle Size and Zeta Potential Measurements

The particle hydrodynamic diameter and liposomal surface zeta potential was determined at 25° C by means of dynamic light scattering (DLS) using zeta-sizer (ELSZ-2000, Otsuka Electronics). Samples were diluted in deionized water which served as sample medium with viscosity of 0.89 and solution refractive index of 1.33. The instrument calibration was done by polystyrene nanospheres (−50 mV, 220 ± 6 nm). 90° scattering angle and a laser beam of 633 nm was used for the analysis. All the results were plotted as average and standard deviation of experiments in triplicates. The instrument and the samples were maintained at dust free environment throughout the experiments.

The morphology and distribution of the liposome particles was visualized by a transmission electron microscope (TEM, HT7700, Hitachi). In brief, TEM specimen grid with carbon coating and a mesh size of 200 was glow-discharged for 90 seconds. The liposomal sample was added on the grid as a drop (4 μL) and placed in a dust free environment at room temperature for drying. After 24 hours, 2 μL of 2 % phosphotungstic acid was added to the grid and dried at room temperature for 3 days before analysis. The images were obtained using CCD camera at 60 Kev acceleration voltage (DC voltage).

4.4.5. Agarose Gel Electrophoresis. The lipid binding to the DNA to make lipid-DNA complexes was monitored by a characteristic gel electrophoresis assay. Initially, lipoplexes were made through the procedure mentioned above. Lipoplexes after incubation of 30 minutes, were added to agarose gel (0.8 % in buffer) which was stained previously by DNA safe-stain. The electrophoresis was applied to the gel for 20 min with a current of 140 V in a Tris-borate

EDTA (TBE) buffer. The electrophoretic mobility pattern of DNA was witnessed under UV light (365 nm).

4.4.6. Cell Experiments

A549 (a human lung carcinoma cells) and PC-3 cells (a human prostate cancer cell line) were cultivated in RPMI-1640 medium, added with 10% FBS and 100 μg/mL penicillin-streptomycin. HEK-293 cells (a human embryonic kidney cell line) were cultivated in DMEM medium, supplemented with 10% FBS and 100 μg/mL penicillin-streptomycin. The confluence of the cells was continuously monitored throughout the experimental duration. The medium was replaced with fresh medium for every two or three days, and cells were sub-cultured when 90% confluence was reached.

In Vitro Transfection studies. Transgene expression of pEGFP transfected cells i*n vitro* was observed in HEK-293, PC-3 and A549 cells. Lipoplexes of N/P ratios stretching from 1-15 were prepared with different amounts of CTTD, ATD, DtATD and DtCTTD liposomes and a constant amount of pEGFP-C1 plasmid (1 μg/100 μL). Twenty four hours prior to the transfection, cells were seeded at a density of 5×10^4/well in 24 well plates. The seeded cells were incubated for 24 hours in their corresponding culture medium consisting of 10% FBS in CO_2 incubator, before adding transfection reagents. Prepared lipoplexes, after 30 minutes of incubation, were added to wells bearing cells in DMEM/RPMI medium. The 24-well plates were then transferred to CO_2 incubator and stored for 4 hours. Subsequently, the medium was replaced with fresh complete-medium consist of 10 % FBS. Following this, the well plates were transferred again to the incubator and incubated further for another 48 hours. With the help of fluorescent microscopy (*Leica DMi8*; Leica Microsystems, Wetzlar, Germany), the cells expressing green fluorescent protein (GFP) were directly imaged. Adopting a previously described quantification process, the green fluorescence expression was quantified in three cell lines 48 hours' post-transfection.[213, 241] Concisely, for separate experiment, a minimum of three

fields of view for each group were considered to capture fluorescence images. Afterwards, with the help of ImageJ software (v1.51a, National Institute of Health, USA), the fluorescence intensity of each image was semi-quantitated. For each group, a minimum of three fluorescence intensity values were averaged and presented along with their standard deviation. Measurement of relative transfection efficiency was carried out by relating the fluorescence intensity of each test group (ATD, DtATD, DtCTTD and Lipofectamine) with CTTD treated group.

Cell viability. The biocompatibility of the lipoplexes derived from liposomal formulations and pEGFP DNA was evaluated in terms of cell viability through the MTT assay. The lipoplexes were prepared in similar methods as per transfection studies. The cytotoxicity of lipoplexes was examined by incubating the cells with lipoplexes with various N/P ratios. HEK-293, PC-3 and A549 cells at a density of 5×10^4/well were initially transfected with the lipoplexes in triplicates as mentioned in transfection experiments. Total lipid concentration in each well as per the N/P ratios ranging from 1 to 15 were, 2.8 to 42 µg/mL for ATD, 3.9 to 58 µg/mL for CTTD, 5.4 to 80 µg/mL for DtCTTD and 4.2 to 64 µg/mL for DtATD. 48 hours after transfection, the wells were added with 500 µL of MTT (2.5mg/mL in PBS) and incubated in dark condition for another 4 to 5 hours. The plates were centrifuged for 20 minutes at 1600 rounds per minute. The supernatant was carefully removed and 1 mL of DMSO was added to each well. The contents in the well were dissolved by a gentle shaking. 100 µL from each well was taken and added to a new 96 well plate and measured the absorbance at 595 nm. The percentage of viable cells was calculated using the colorimetric technique.[253]

SPECTRA

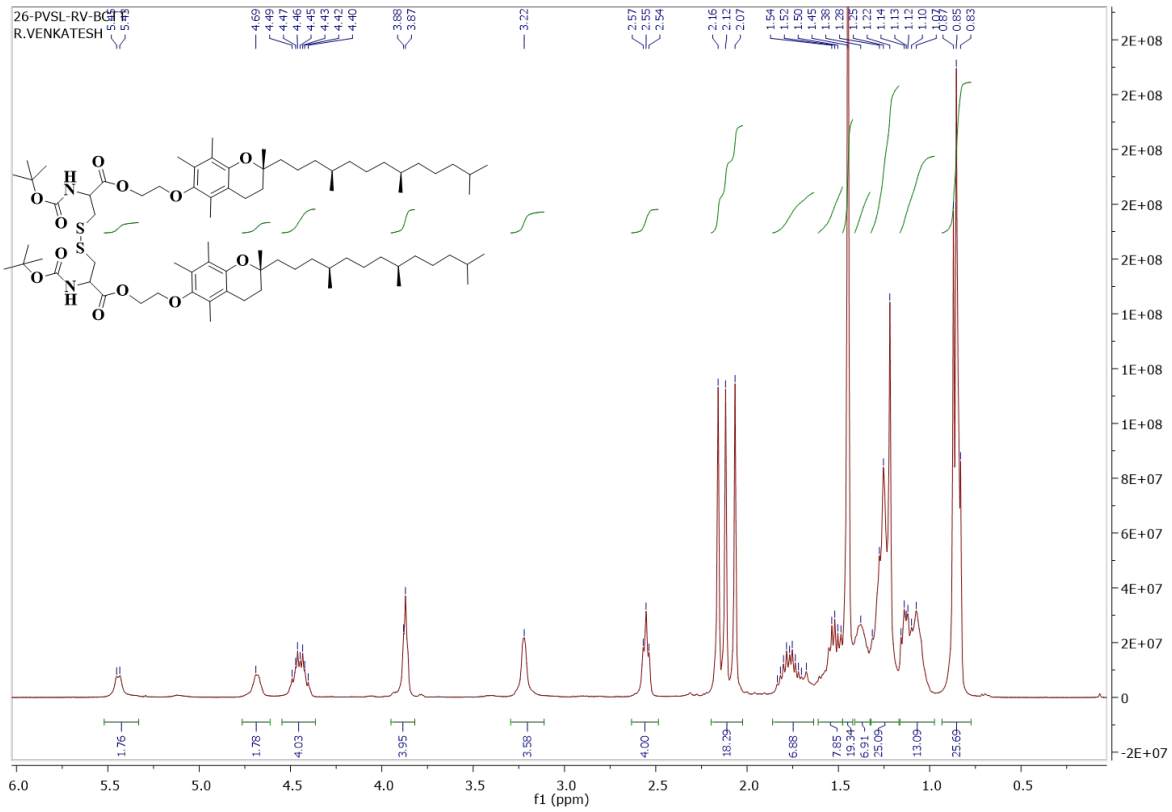

^{1}H NMR Spectrum of compound BCTT in $CDCl_3$

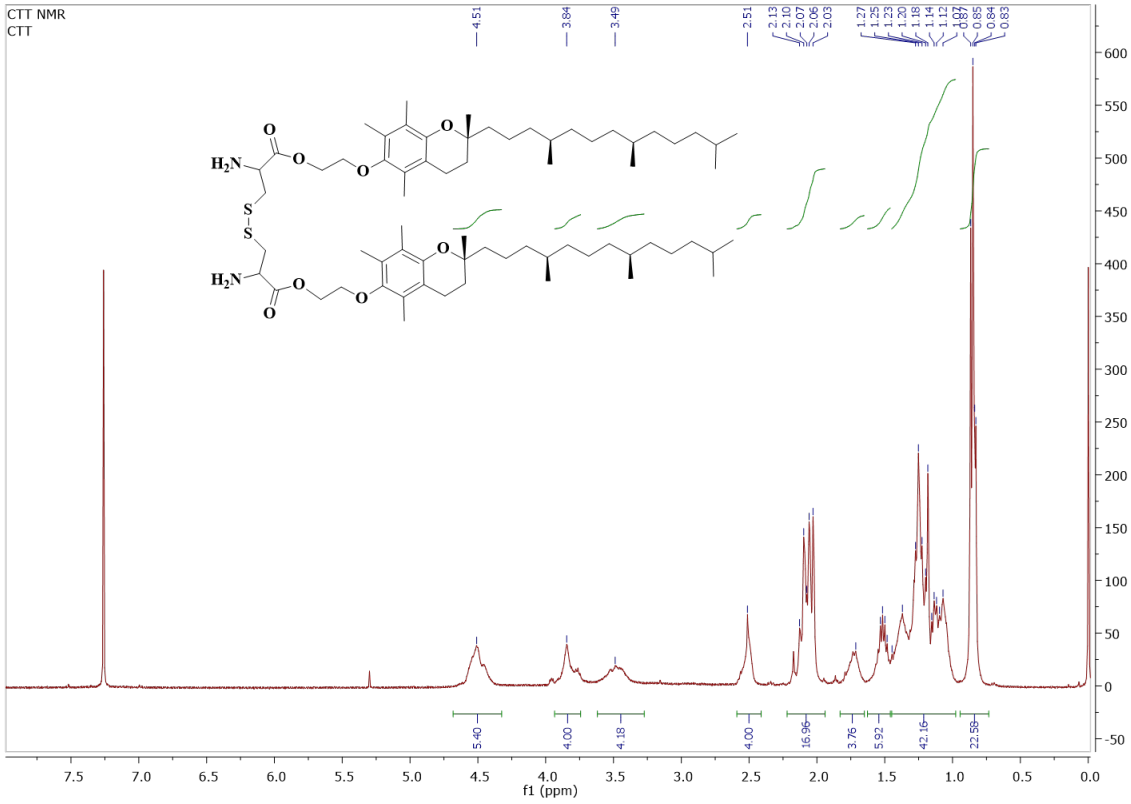

^{1}H NMR Spectrum of compound CTT in $CDCl_3$

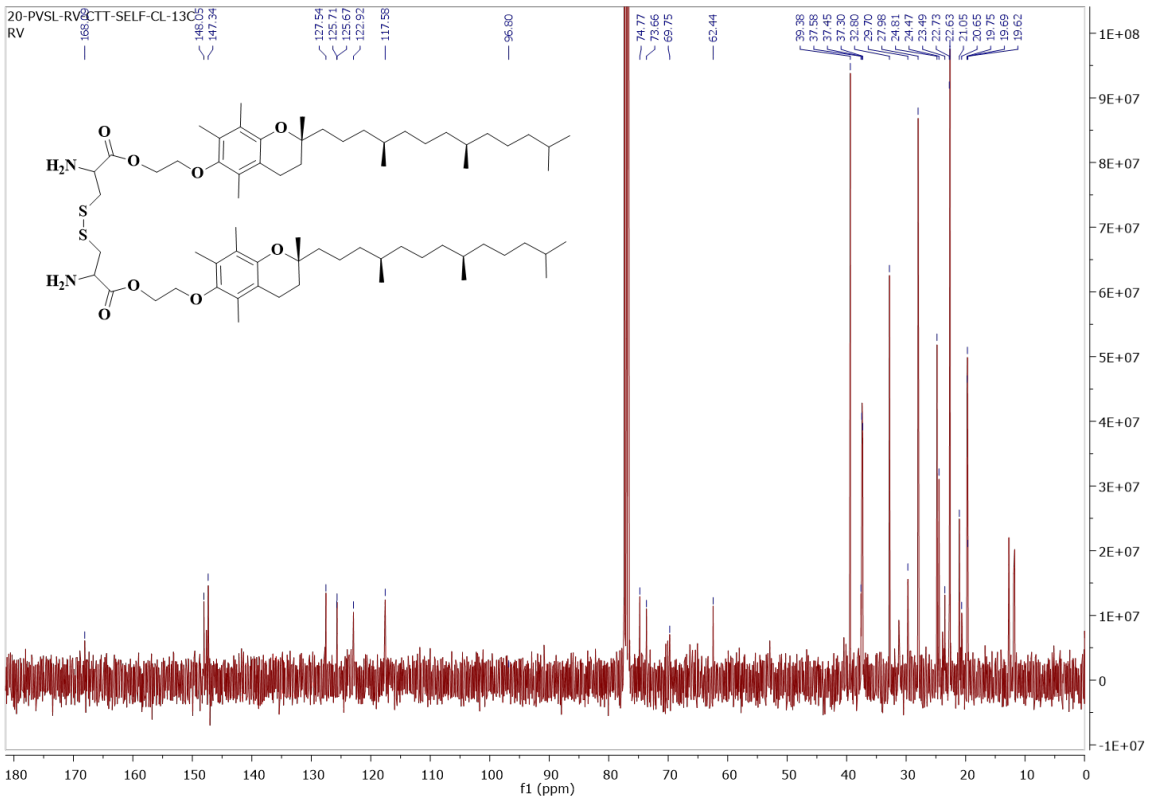

^{13}C NMR Spectrum of compound CTT in $CDCl_3$

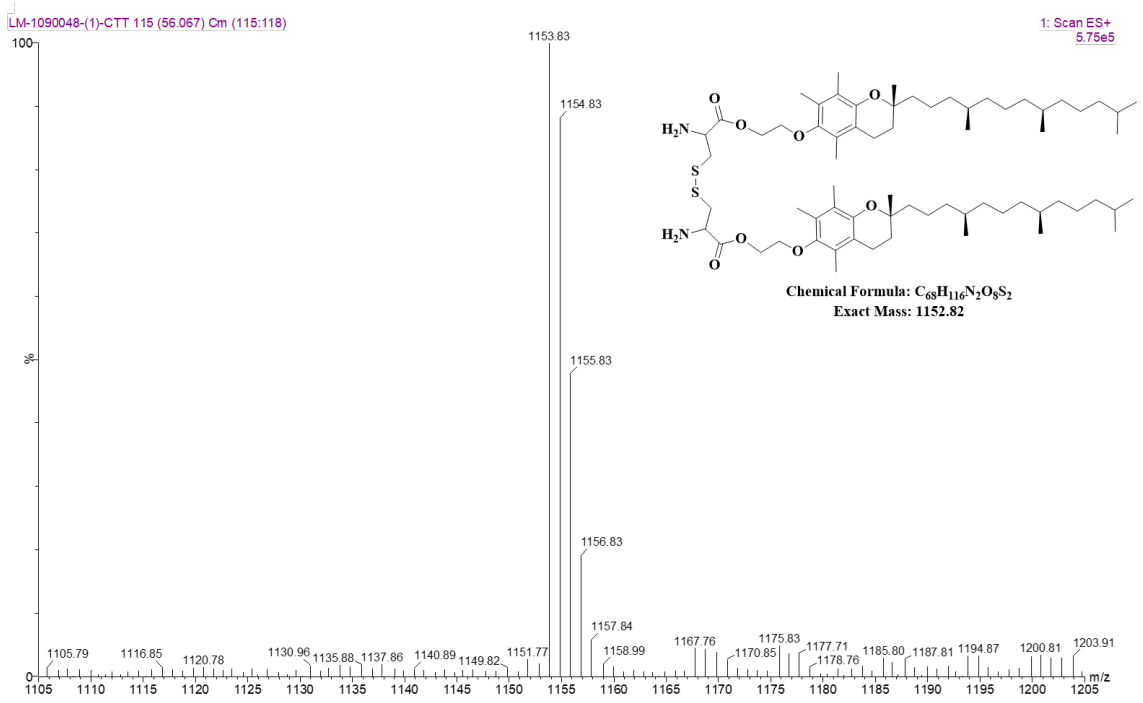

Mass spectrum of Compound CTT

CHAPTER V

α-TOCOPHEROL-CONJUGATED, OPEN CHAIN SUGAR-MIMICKING CATIONIC LIPIDS: DESIGN, SYNTHESIS AND IN VITRO GENE TRANSFECTION PROPERTIES

CHAPTER V

α-TOCOPHEROL-CONJUGATED, OPEN CHAIN SUGAR-MIMICKING CATIONIC LIPIDS: DESIGN, SYNTHESIS AND IN VITRO GENE TRANSFECTION PROPERTIES

5.1. INTRODUCTION

Gene-therapy has been evolved in to a prodigious therapeutic approach to address various medical ailments on-site. This relatively modern strategy has endorsed the utilization of numerous genetic materials implicated in a variety of biological processes, for diagnostic and therapeutic means.[43] Positive effects of gene therapy depend on the establishment of a benign gene delivery vector that effectively transfers genetic material into the cells.[254] Having known the potential immunological and production related disadvantages of viral delivery vectors, non-viral vectors have grabbed the central stage of research over the past few decades. Non-viral vectors are broadly categorised into, cationic lipids,[255] inorganic nanoparticles,[256, 257] polymers,[258] and dendrimers.[259, 260] Non-viral vectors are basically limited by transfection efficacy when compared with their viral counterparts and need special modules to overcome the biological barriers. As a consequence, there exist a continuing quest to develop and understand newer and better non-viral gene vectors. Nevertheless, non-viral vectors have numerous advantages, for instance, being biologically safer and having unlimited access to large scale production.[190] In the pool of non-viral gene carriers, cationic lipids are essentially sought after since they exhibit intriguing properties such as low cytotoxicity, no practical immunogenicity, accessibility for structural modifications, efficient complexation and condensation of nucleic acids.

Various structural units of cationic lipids, namely, head groups, linkers and hydrophobic anchoring groups, play their respective roles at several stages of gene delivery process. Head group moieties of cationic lipids are of particular interest, since they involve in binding to genetic materials through electrostatic interactions and further dictate transfection efficiency.[119]

In majority of the familiar cationic lipids, such as DOTMA, DOGAG and DOTAP, the head groups are quaternary ammonium groups.[55, 261] Introduction of hydroxyethyl functional groups on the quaternary ammonium head group has resulted in enhanced transfection efficacy. It was believed that hydrophilic hydroxyethyl functional groups in the head group region modulate the hydration level and inter-lipidic interaction of liposomes.[203, 261-263] It is also thought that the hydroxyl functionalities interact with DNA and the helper lipid through hydrogen bonding. Further, the interaction of water molecules with the hydroxyl functionalized complexes in aqueous medium, assist in stabilizing the lipid–DNA complexes and the bilayer structure.[119, 264] In other reports, presence of cationic lipids possessing α-tocopherol backbone and a helper lipid (DOPC or DOPE), displayed improvement in transfection efficacy by the increase in hydroxyethyl functional groups in the head group region.[92, 203] Based on these studies, it is evident that hydroxyl functional groups at the head group region are beneficial for transfection. Sugar alcohols, with abundant hydroxyl functional groups are probably the best choice to incorporate in lipid-based gene delivery systems. Initial reports in this direction to develop sugar-based liposomal gene delivery systems have demonstrated that, increased number of hydroxyl groups linked to the head group portion of the cationic glyco-lipids, bestowed the elevated transfection efficiency while reducing the cytotoxicity.[265] Interestingly, a few other reports including ours, have revealed that cationic glycolipids with either cyclic or open chain forms, are useful for targeted delivery towards liver cells.[200, 266, 267] Thus, it is important to design new sugar alcohol based cationic lipids and probe their effect on transfection and targeted delivery. In this context, we designed three new cationic lipid analogues as depicted in **Figure 5.1** with variations in the head group region and a common α-tocopherol based hydrophobic domain. α-Tocopherol as anchoring group has extensively contributed in liposomal gene delivery in the recent past, through its membrane solubility, biocompatibility and antioxidant nature.[98, 112, 268-270] A control lipid (TA) was initially synthesized with α-tocopherol as hydrophobic region and a cationic head group prone to substitution. Two sugar-

mimicking cationic lipids (TS1 and TS2) were synthesized by covalently conjugating 1,4 gluconic γ-lactone and ascorbic acid, respectively, to TA through their ring opening. The resultant cationic lipids with multiple hydroxyl functional groups close to the head group are probed for their liposomal formation and gene delivery properties.

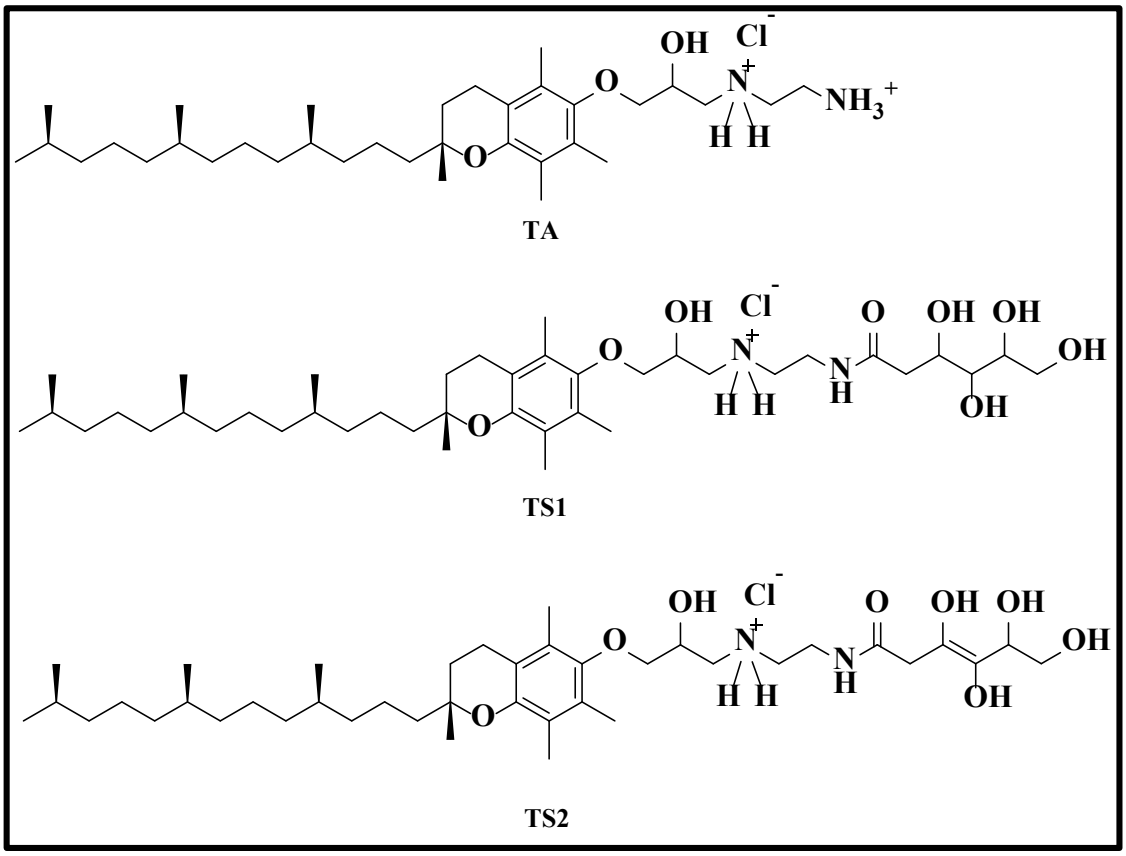

Figure 5.1: *Structures of synthesized cationic lipids (TA, TS1 and TS2) in this study*

5.2. RESULTS AND DISCUSSION

5.2.1. Synthesis of lipid derivatives

Synthetic methods followed for the synthesis of control lipid TA and polyhydroxy functionalized cationic lipids, TS1 and TS2 were shown in **Schemes 5.1, 5.2** and **5.3** respectively. α-tocopherol serves as a common hydrophobic domain in all the lipid derivatives that were synthesized. The three cationic lipids are varied by their hydrophilic head groups. The key intermediate α-tocopheryl 1-(2-aminoethyl) amino) propan-2-ol (TA) was synthesized initially in two steps. At first, α-tocopherol was allowed to react with epichlorohydrin under the action of tetrabutyl ammonium hydrogen sulphate and sodium hydroxide leading to the

formation of epoxide linked α-tocopherol as intermediate **1**. The epoxide ring was further opened up by the action of ethylenediamine under the reflux condition to give the intermediate **2** which was labelled and used as control lipid TA. The polyhydroxy functionalized cationic lipids, TS1 and TS2 were synthesized by the aminolysis of the corresponding lactones, 1,4 gluconic γ-lactone and ascorbic acid. The two lipids, TS1 and TS2 are varied only by the double bond in the head group region. Three cationic lipids were thoroughly characterized by ^{1}H NMR, ^{13}C NMR and ESI-MS spectral techniques which indicate the formation of given structures. ESI-HRMS analysis of final compounds TA, TS1 and TS2 further confirmed the formation of target molecules with accurate molecular weights.

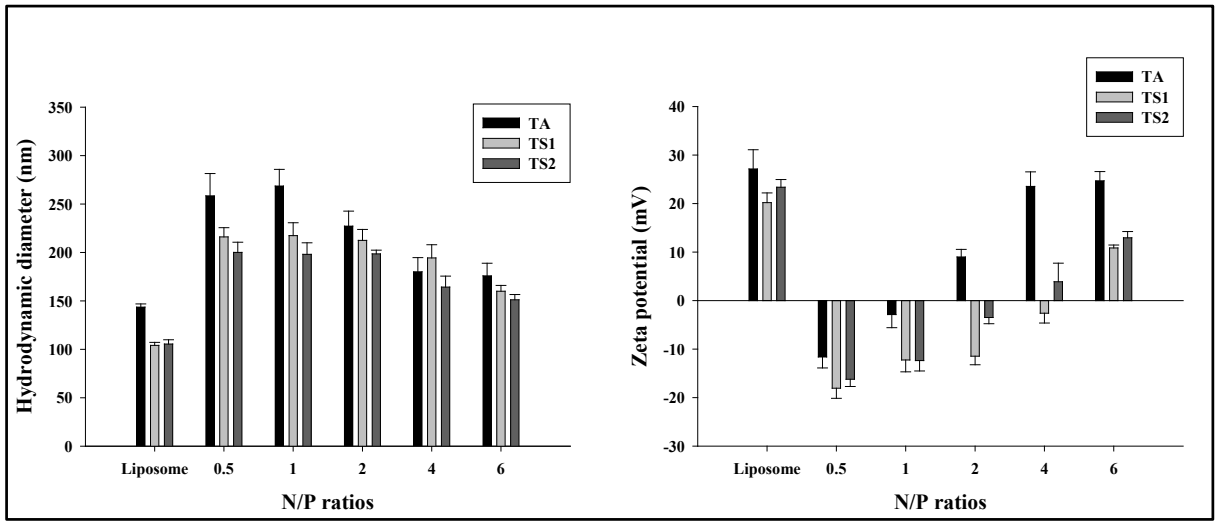

Figure 5.2: A) *Hydrodynamic diameters of liposome particles and their corresponding DNA complexes at N/P ratios ranging from 0.5 to 6, measured by the dynamic light scattering technique. Data represent mean ± SD (n = 3).* ***B)*** *Zeta potentials of liposome particles and their corresponding DNA complexes at N/P ratios ranging from 0.5 to 6, measured by the dynamic light scattering technique. Data represent mean ± SD (n = 3).*

5.2.2. Preparation and characterization of liposomes and lipoplexes.

Liposomes were prepared using the newly synthesized cationic lipids by mixing each of them with the helper lipid DOPC through the procedures mentioned in the experimental

section. Since the helper lipid is common in all the liposomal formulations derived from cationic lipids, TA, TS1 and TS2, their corresponding liposomes are called as TA, TS1 and TS2 from hereon. All the liposomes were visually transparent with no apparent aggregation after the sonication cycles. The lipid to co-lipid (DOPC) ratio in the current study was 1:1, which has shown best stability (verified by their hydrodynamic diameters) and uniformity of liposomes even after 8 weeks of storage. The ratios deviating from 1:1, have shown aggregation or layer formation after a week of storage at 4 ^{0}C. Storage stability of the liposomes has been one of the major problem hindering the effective application of liposomes for drug/gene delivery.[271, 272] Thus, in the current study, the optimally stable liposomal formulations were used for further experiments. Although, the uniformity of the liposomes was observed to be stable up to 8 weeks of storage at 4 ^{0}C, for the biological studies, fresh liposomes with no more than three weeks of storage were used. Lipoplexes were made by mixing appropriate amount of liposomes with pDNA under vortex condition at room temperature. Lipoplexes were characterised along with liposomes for their hydrodynamic size and surface zeta potentials. Zeta potential and size are the crucial physicochemical factors of the gene carrier particles, which considerably affect the *in-vitro* and/or *in-vivo* transfection efficacy.[273, 274] **Figure 5.2A** depicts the hydrodynamic diameters of liposomes as well as lipoplexes across N/P ratios of 0.5 to 6 as measured by dynamic light scattering (DLS) technique. The size of liposomes TS1 and TS2 were in the range of 100 nm, whereas the size of TA was slightly higher (≈140 nm). In general, liposomes with the particle diameters within the range of 50 to 200 nm are considered favourable for efficient delivery of therapeutics.[275] Upon complexation with pDNA, the size of the particles was increased. Nevertheless, as the N/P ratio increases, the size of the lipoplexes was reduced irrespective of the cationic lipid used. Apparently, the reduction in lipoplex size indicates the condensation of pDNA by liposomes. Then again, zeta potential on the surface of particles determines the binding interactions with pDNA. As shown in **Figure 5.2B**, all three liposomal particles possess positive zeta potentials which can bind to the negatively charged DNA. After

complexation with pDNA, the overall surface charges of lipoplexes converted from negative charge to positive charge as the N/P ratio increases. This is evidently due to the less amount of liposome available for the complete binding of DNA at low N/P ratios. Zeta potentials of all lipoplexes gradually increased by the addition of higher amount of liposomes while increasing N/P ratios facilitating better electrostatic interactions between lipid and DNA. The zeta potential values TS1/TS2 based liposomes and lipoplexes at each N/P ratio were appeared to be slightly lower than the TA based complexes, which is perhaps occurred due to the surface charge shielding by the partial negative charges on the hydroxy groups of TS1 and TS2, as reported previously.[276, 277] In addition to DLS, the liposomal characterization was also done using scanning electron microscopy (SEM). Although the size of the liposomes by SEM may not be accurate as it requires samples to be dried before analysis, basic understanding of particle morphology can be obtained by this technique. As it can be seen in **Figure 5.3, s**pherical morphologies were observed in the SEM images of liposomes made of TA, TS1 and TS2.

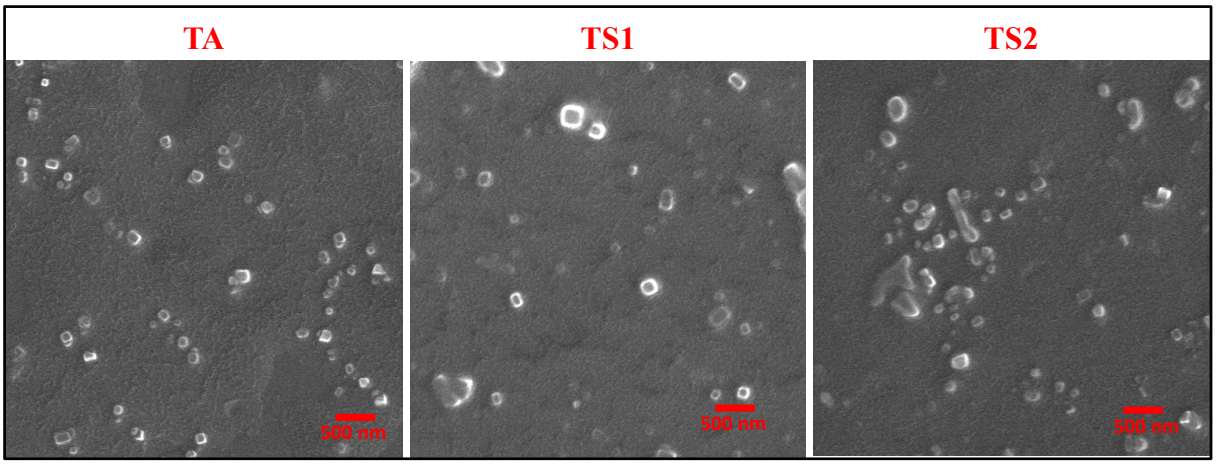

Figure 5.3: *Scanning electron microscope (SEM) images of TA, TS1 and TS2 based liposomes, respectively.*

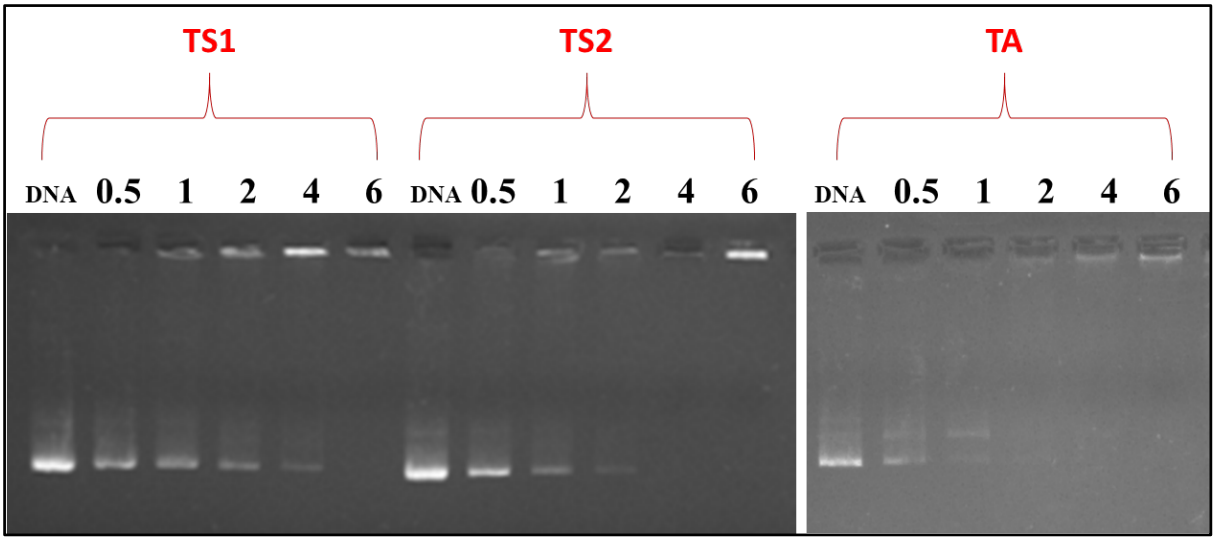

Figure 5.4: *Gel electrophoresis images of TS1, TS2 and TA derived DNA complexes at N/P ratios ranging from 0.5 to 6 as mentioned on top of each panel. Naked DNA served as a control indicated as 'DNA'.*

5.2.3. DNA binding study

With the purpose of assessing the ability of liposomes binding to DNA; TA, TS1 and TS2 were complexed with pEGFP-N3 plasmid and subjected to gel electrophoresis based on agarose gel. The electrophoretic mobility of DNA was visualized under UV light which determines the minimum N/P ratio necessary to completely inhibit DNA mobility from the complex. It can be observed from **Figure 5.4** that ~ >90% of DNA was bound to the TS1 at N/P ratio 4 while thorough binding was seen on N/P ratio 6. In case of TS2, thorough binding was noticed at the N/P ratio 4. However, TA has achieved complete DNA binding at the N/P ratio of 2 which can be explained by its higher zeta potential compared to TS1 and TS2. Moreover, the DNA binding results of the lipoplexes were in agreement with their size and zeta potential values where positive zeta potentials and lower sizes of the complexes were detected after complete DNA binding. Variations in the DNA binding capacities of functional materials is common as it can be collectively affected by the hydrophobic and electrostatic interactions.[278, 279]

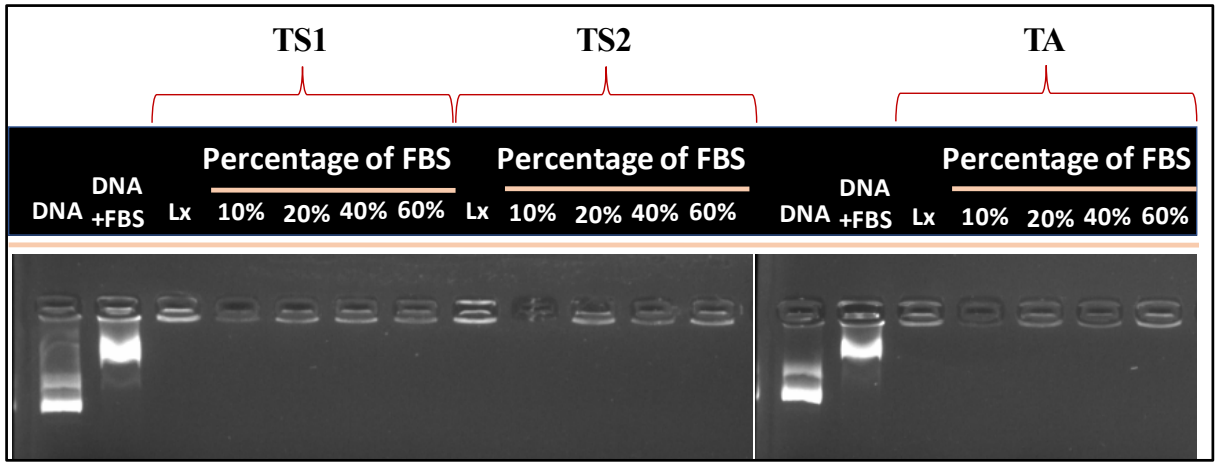

Figure 5.5: *Serum stability of lipoplexes after 3h of incubation in serum (FBS)-containing medium. Lx represents lipoplex of each formulation (TS1, TS2 and TA) at N/P ratio of 6. Naked DNA served as a control indicated as 'DNA'.*

Serum stability of the lipoplexes was assessed by incubating lipoplexes in various concentrations of serum containing medium. The release of free DNA after incubation was monitored using gel electrophoresis **(Figure 5.5)**. Interestingly, lipoplexes of TS1, TS2 and TA were all shown good DNA binding even after incubating at media with 60% of FBS. It was established that α-tocopherol based cationic lipids are generally exhibit good serum compatibility.[98, 99, 203] This effect could help to prevent the leakage of cargo from lipoplexes throughout the systemic circulation when administered into the body.[280, 281]

5.2.4. *In vitro* transfection biology

After determining the DNA binding abilities, the optimization of gene transfection efficacies of the complexes *in vitro* were first examined in HEK-293 cells using pEGFP-N3 plasmid as an example gene. **Figure 5.6A** exhibits the representative green fluorescence protein expression (GFP) of cells treated with various formulations at different N/P ratios. For cytotoxicity and transfection experiments, 1µg of pDNA was complexed with calculated amount of liposome solution as per their N/P ratios. Commercially obtained Lipofectamine 2000 served as the positive control. Sugar-mimicking polyhydroxy functionalised cationic lipids, TS1 and TS2, demonstrated higher GFP expression in comparison with simple cationic lipid TA. In addition, complexes of TS1 and TS2 at the N/P ratios 4 to 6 were demonstrated to

be of maximum potential to deliver pDNA in to the cell. However, the cationic lipid, TA was found to be not so competitive against the other two cationic lipids or the Lipofectamine in transfection efficiency. Introduction of sugar alcohols on the polymeric structures have been previously reported to enhance transfection efficiency and reduce cytotoxicity.[282] Reduction of charge density on the particles and caveolae-mediated endocytosis of sugar based non-viral gene vectors have been expected to be favouring the better gene transfection.[283-285] Quantitative fluorescence intensity and the percentage of GFP expressing cells as estimated by flow cytometry (**Figure 5.6B**) were in well accordance with visual microscopy images. The quantitative results were also revealed that both TS1 and TS2 at the N/P ratios of 4 and 6, respectively, were on par with Lipofectamine in transfecting HEK-293 cells.

Having determined the effective N/P ratios, we further evaluated the targeted transfection efficiency of synthesized lipids on a human liver cancer cell line (HEPG2). Out of the three lipid formulations, the lipid /pDNA complexes of TS1 have shown superior transfection compared to other formulations, even better than Lipofectamine (**Figure 5.7A**). Additionally, quantified fluorescence expression of the cells was also in agreement with the microscopy images (**Figure 5.7B**). Previous reports stated that, the abundance of hydroxyl functional groups on the delivery systems selectively stimulate caveolae-mediated endocytosis, which may be the deciding factor in defining transfection efficacy of sugar based gene delivery vectors.[277, 285] It was interesting to note that, the cationic lipid TS2, even though varied by a single double bond in its structure to TS1, has shown dramatic decline in efficiency of transfection. However, the transfection efficiencies of the new lipids were reversed in the case of U87.

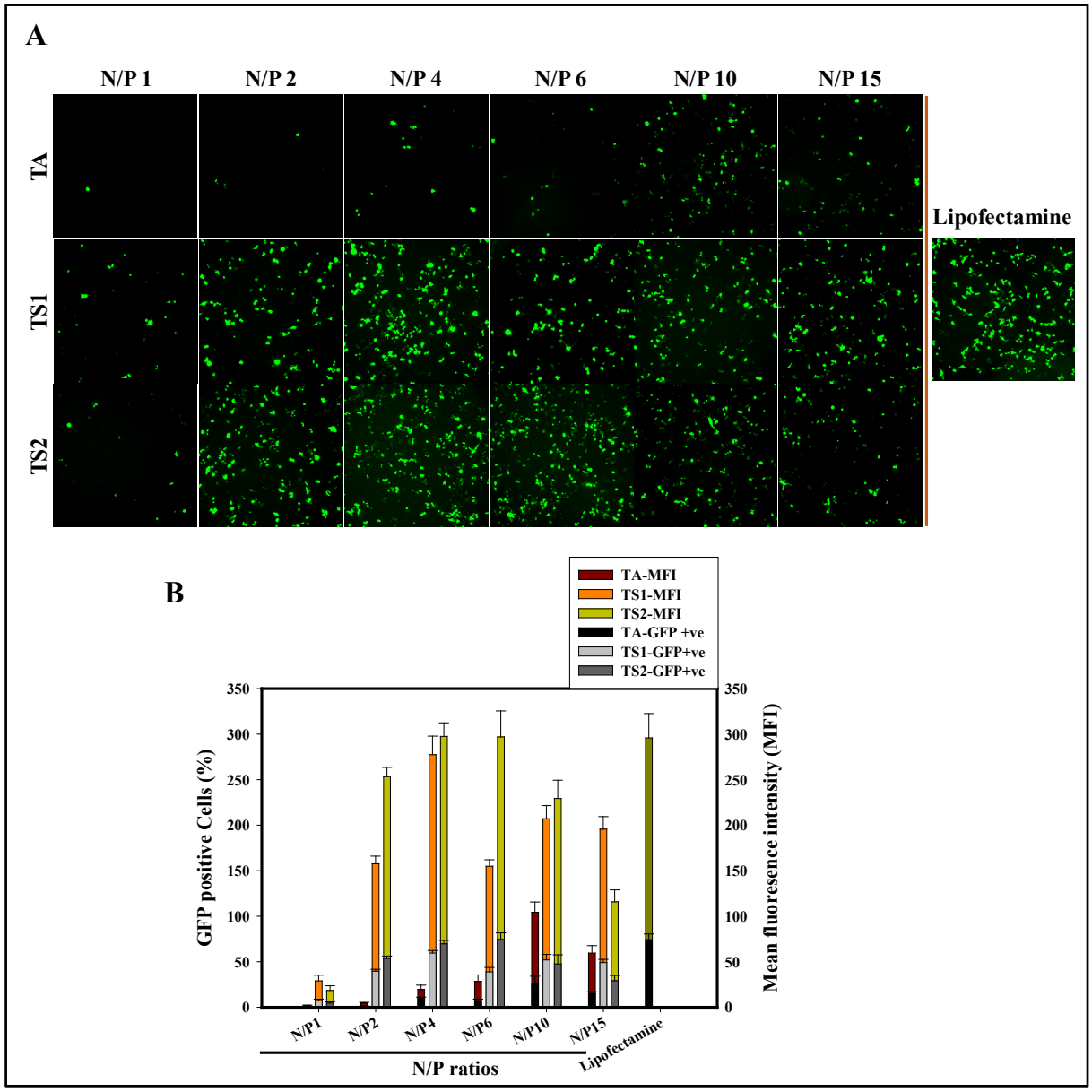

Figure 5.6: *Transfection in HEK-293 cells. A) Representative fluorescence microscopy images of HEK-293 cells after 48 h of transfection with various lipid/pEGFP DNA complexes at N/P ratios ranging from 1 to 15 and Lipofectamine. B) Mean fluorescence intensity and percentage of GFP expressed cells, quantified by flow cytometry.*

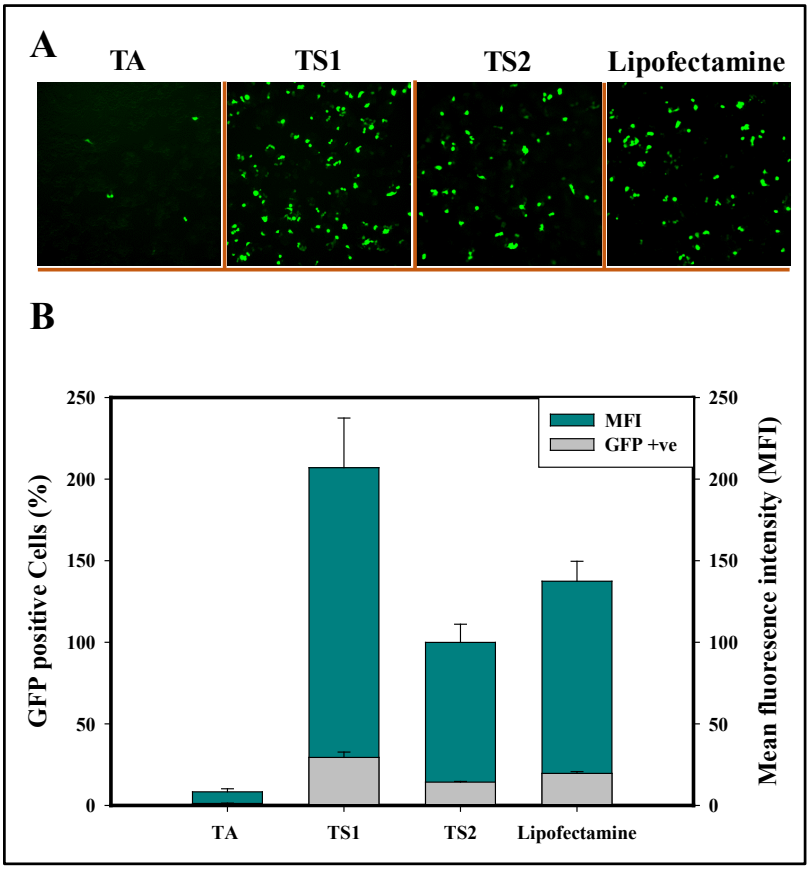

Figure 5.7: *Transfection in HEPG2 cells. A) Representative fluorescence microscopy images of HEK-293 cells after 48 h of transfection with various lipid/pEGFP DNA complexes at optimised N/P ratios and Lipofectamine. B) Mean fluorescence intensity and percentage of GFP expressed cells, quantified by flow cytometry.*

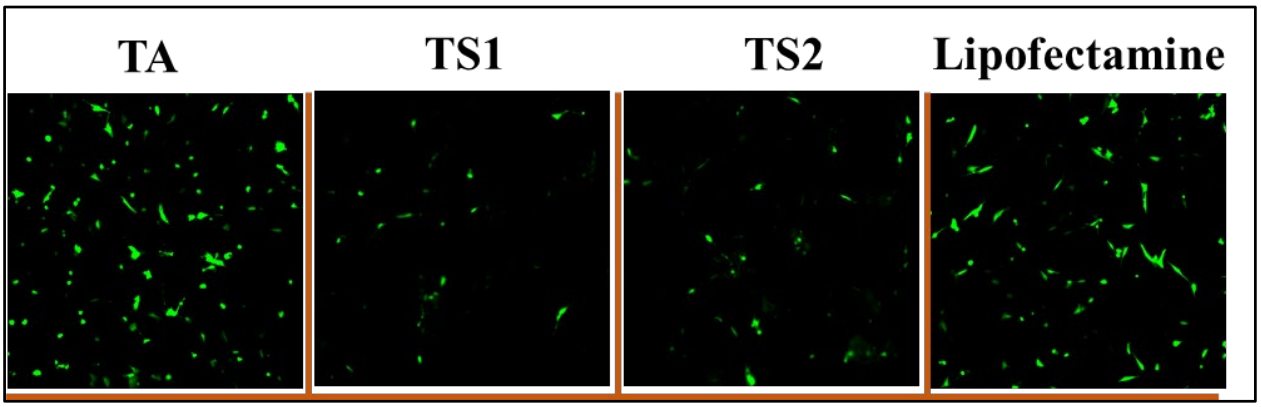

Figure 5.8: *Representative green fluorescence images of U87 cells transfected with optimised N/P ratios of TA, TS1, TS2 and Lipofectamine complexes, respectively.*

As it can be observed through inverted microscope images (**Figure 5.8**), the sugar alcohol conjugated lipids, TS1 and TS2 were essentially incompetent in transfecting U87 cells. Contrarily, TA has better transfection ability in U87 cells. The results point out that the

transfection efficiencies of sugar alcohol-based cationic lipids are cell-dependant and minute changes in the structure may results in variation in their gene delivery properties. Moreover, hepatocellular targeting ability of sugar-based cationic lipids has been highlighted by earlier studies.[200, 286] Thus, the results summarized from **Figure 5.6**, **5.7** and **5.8**, taken together, demonstrate that multi-hydroxy functionalised, sugar-based cationic lipid TS1, may have the potential to target the hepatocellular gene delivery.

5.2.5. Cellular internalization

Cellular internalization of lipoplexes was visualized with the help of rhodamine-PE labelled liposomes complexed with pCMV-SPORT-*β*-gal DNA, in HEK-293 cells. After incubating the cells with lipoplexes for 6 h, the internalization of the labelled lipoplexes was detected by confocal microscopy **(Figure 5.9)**. Cell nucleus was stained with 4′,6-diamidino-2-phenylindole (DAPI). Comparison of internalization of TA, TS1 and TS2-based lipoplexes was done using untreated cells as control. An apparently higher intensity of red fluorescence in the cells treated with sugar-based lipids, TS1 and TS2 than TA was noticed. The better cellular internalization of TS1 and TS2 is supposed to be a contributing aspect for their higher transfection efficiency as observed initially **(Figure 5.6 and 5.7)**.

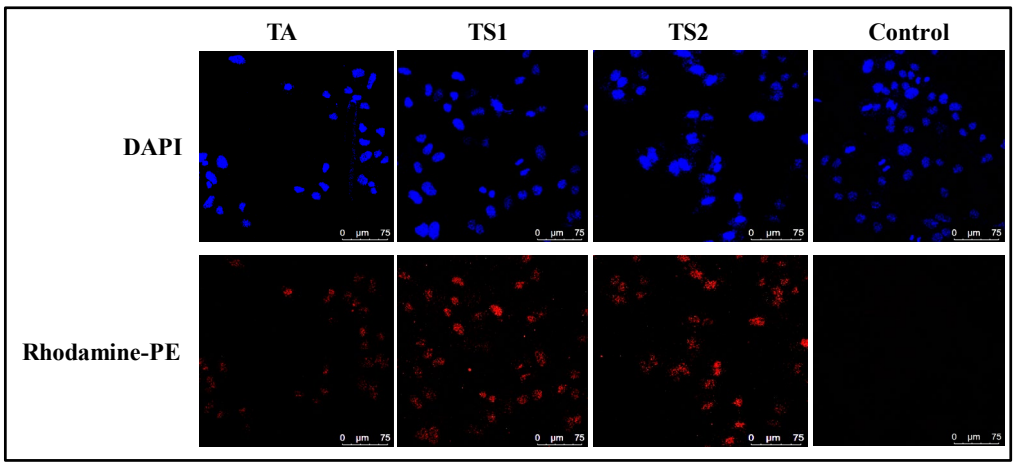

Figure 5.9: *Cellular uptake of rhodamine-PE labelled liposomes. CLSM images of HEK-293 cells after treatment with rhodamine-PE labelled liposomes of TA, TS1 and TS2, respectively. Untreated cells served as control. Blue: nuclei stained by DAPI; red: rhodamine-PE after internalization.*

5.2.6. Cytotoxicity analysis

An *in vitro* cytotoxicity assay with the three liopoplex systems against HEK-293 and HEPG2 cell lines was undertaken using an MTT based assay. The cytotoxicity experiments were executed in identical settings as done for transfection assays. With the cell viabilities close to 80 % or more, the lipids TS1 and TS2 are found to be least cytotoxic even at high N/P ratio of 15 (**Figure 5.10A and B**). However, the cell viabilities of TA-treated cells appear to be compromised at high N/P ratios in both cell lines (HEK-293 and HEPG2). Similarly, cytotoxicity of empty liposomes tested against HEK-293, HEPG2 and U87 cells, revealed that TS1 and TS2 are least toxic against these cell lines (**Figure 5.11**). Evidently, the poly hydroxyl functional groups on the lipids, TS1 and TS2, may have a role in improving their cell viabilities. Cytotoxicity of cationic liposomes is majorly depending on its surface positive charge. [287] In the case of sugar alcohol based cationic lipids, the overall positive charge of the complexes can be reduced by the presence of partially negative charge on the hydroxyl groups.[283] On the other hand, Hydroxyl groups on the head group region of liposomes, interact with the cell membrane through hydrogen bonding rather than electrostatic interactions.[262] All these factors taken together, enable sugar-alcohol based cationic lipids to be non-toxic delivery systems with cell-dependant transfection ability.

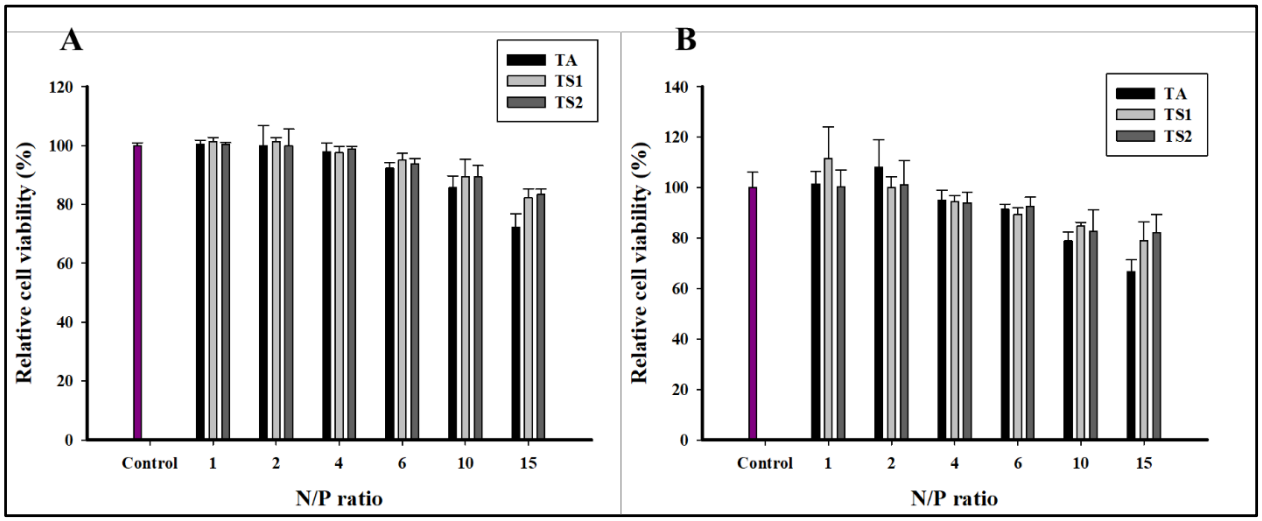

Figure 5.10: *MTT based cytotoxicity of lipid/pEGFP-DNA complexes at increasing N/P ratios ranging from 1 to 15, against A) HEK-293 and B) HEPG2 cells.*

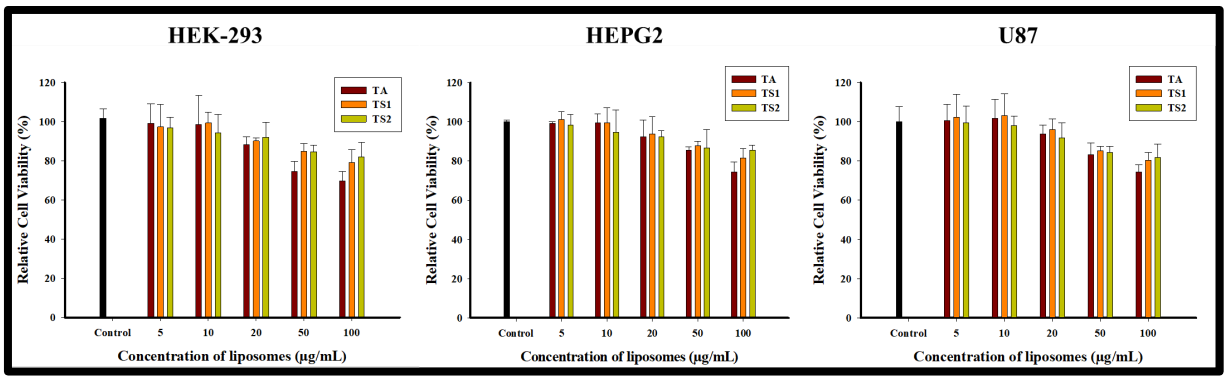

Figure 5.11: *MTT based cytotoxicity of increasing concentrations liposomes (5-100 µg/mL) against HEK-293, HEPG2 and U87 cells as mentioned in the figure.*

5.3. CONCLUSIONS

In summary, we have designed a new series of non-viral gene delivery vectors with either sugar-like head groups or not. Characterization of corresponding liposomes revealed that, lipids containing sugar like moieties attained smaller liposomal size and reduced cationic charge which in turn favoured low cytotoxicity of the sugar based cationic lipids. Sugar mimicking cationic lipids at optimised N/P ratios exhibited enhanced transfection, particularly in HEPG2 cell lines. On the other hand, minute structural changes such as inclusion of double bond in the head group, resulted in lower efficiency of the delivery system. However, sugar mimicking cationic lipids are found to be less toxic as compared with conventional delivery systems. Cationic lipid, TS1 with open chain sugar-like head group may have potential for hepatocellular targeted gene delivery.

Scheme 5.1*:*

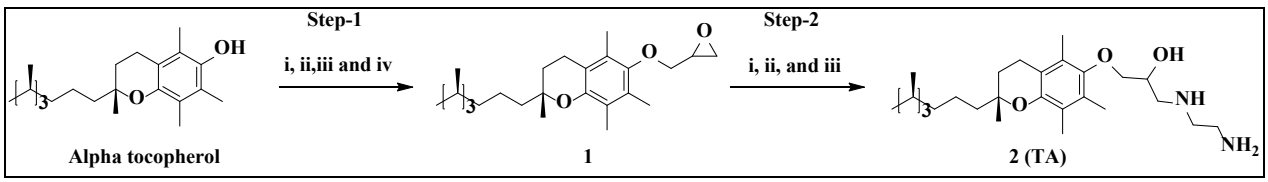

Reagents: Step1: *i) Epichlorohydrin, ii) NaOH solution, iii) tetrabutylammonium hydrogen sulfate, iv) Refluxed 16h,* ***Step2****: i) Ethylenediamine ii) Methanol, iii) Refluxed 16h*

Scheme 5.2:

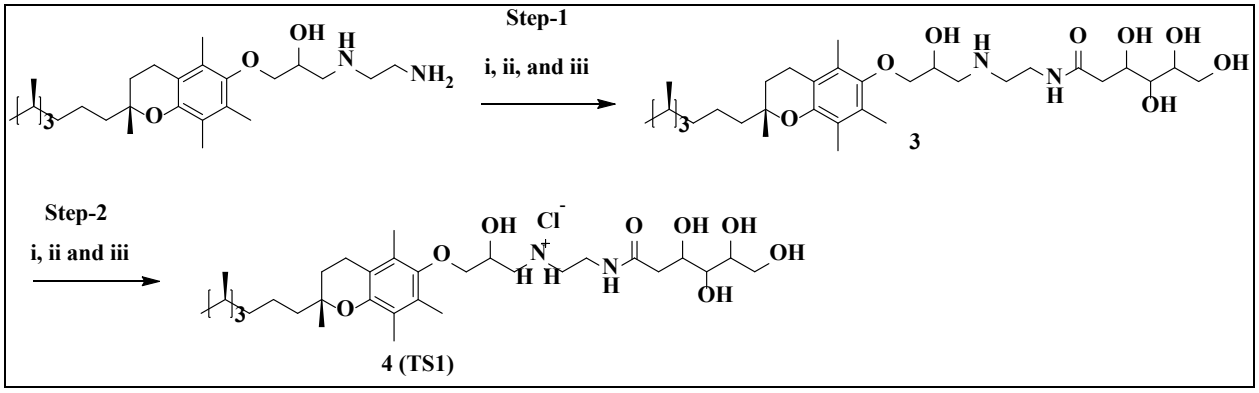

Reagents: Step1: *i) Methanol, ii) 1,4 gluconic γ-lactone, iii) Refluxed 16h,* ***Step2****: i) 6N HCl in Dioxane ii) RT 12h*

Scheme 5.3:

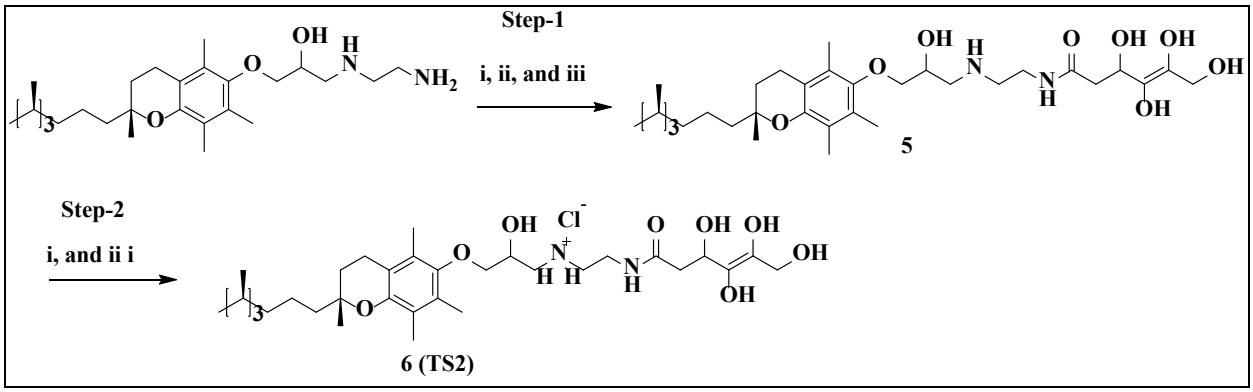

Reagents: Step1: *i) Methanol, ii) ascorbic acid, iii) Refluxed 16h,* ***Step2****: i) 6N HCl in Dioxane ii) RT 12h*

5.4. EXPERIMENTAL SECTION

5.4.1. General procedures and chemicals reagents

Mass spectrometry data were obtained using a commercial LCQ ion trap mass spectrometer (Thermo Finnigan, CA, U.S.) fitted by electron spray ionisation source. Nuclear Magentic resonance (NMR, $^{1}H/^{13}C$) spectra were acquired using a Varian FT-400 MHz NMR-spectrometer. Lipofectamine-2000 was procured from ThermoFisher Scientific. Epichlorohydrin, α-Tocopherol, 1,4 gluconic γ-lactone, ascorbic acid and 1,2-Dioleoyl-sn-glycero-3-phosphocholine (DOPC) were acquired from Sigma-Aldrich. pEGFP plasmid and the cell lines were generous gifts from Indian Institute of Chemical Technology (IICT, Hyderabad, India). Unless mentioned otherwise, different organic solvents such as dioxane,

methanol, chloroform, acetone, N, N-dimethylformamide (DMF), ethanol and methylene chloride (DCM) were acquired from Sigma-Aldrich and were used sans any further distillation. The development of the reactions was observed on aluminium plates with 0.25 mm silica gel using thin-layer chromatography technique. Purification of the compounds was done by column chromatography technique using silica gel matrix (200 and 60-120 mesh size. Acme Synthetic Chemicals, India). QExactive equipped High Resolution Mass Spectrometry (HRMS) (Thermo Scientific) was used for elemental analyses.

Synthesis of α-tocopheryl 1-(2-aminoethyl) amino) propan-2-ol (TA)

Initially, α-tocopheryl glycidyl ether (**1**) was synthesized as per the method described in our previous publication.[200] Then, α-tocopheryl glycidyl ether (0.486g, 1 mmol) was dissolved in dry methanol (10 mL) and was added with ethylenediamine (1.2 mmol). The mixture was refluxed for 16h. The progress of product formation was checked using TLC. After ensuring the consumption of compound **1**, the reaction mixture was concentrated with the help of rotary evapourator. The crude product was further refined using 60-120 mesh-sized silica-gel column chromatography (eluted with 15 % DCM in Methanol). The resultant target product was collected as a yellowish liquid (yield: 88 %, 0.4 g).

^{1}H NMR ($CDCl_3$, 400 MHz): δ/ppm = 5.52 (s, 2H, -NH_2, Broad), 4.09 (s, 1H, -NH Broad), 3.63 (m, 2H, -O-$\underline{CH_2}$-), 3.34 (m, 1H, -$\underline{CH}$-OH), 3.15 (t, 2H, NH-$\underline{CH_2}$-CH_2-NH_2), 2.89 (m, 2H, OH-$\underline{CH_2}$-NH-), 2.82 (t, 2H, NH-CH_2-$\underline{CH_2}$-NH_2), 2.52 (d, 2H, Ar-$\underline{CH_2}$-CH_2-), 2.09-2.03 (m, 9H, 3x –CH_3), 1.72 (m, 2H), 1.05–1.61 (m, 24H), 0.85 (s, 12H). **^{13}C NMR ($CDCl_3$, 400 MHz):** δ/ppm = 144.82, 127.30, 125.42, 122.12, 117.43, 117.11, 74.75, 74.35, 60.32, 57.43, 54.15, 50.34, 49.38, 49.28, 42.08, 41.18, 39.99, 37.25, 37.15, 30.82, 27.84, 24.66, 22.91,22.83, 22.50, 19.57, 18.24, 14.06, 12.56, 11.69, 11.62. **ESI-HRMS** Mass m/z: calc: 548. 48; found; [M^+]: 548.28520.

Synthesis of α-tocopheryl (E)-3,4,5,6-tetrahydroxy-N-(2-((2-hydroxy)-propyl)amino)ethyl)hex-4-enamide (3 and 4- TS1)

To a stirred solution of the α-tocopheryl 1-(2-aminoethyl) amino) propan-2-ol (200 mg, 19 mmol) in dry methanol, 1,4 gluconic γ-lactone (71 mg, 0.40 mmol) was added. The mixture of reactants was then stirred at reflux condition for 12 h. Subsequently, methanol was removed in vacuum. The crude was recrystallized from pentane and diethyl ether. Intermediate **3** appears as a light red solid. The yield of product was 87%. After purification, the intermediate **3** (100 mg, 0.141mmol) was dissolved in methanol (5 mL), chilled to 0 ˚C and added with HCl (1 N, 1 mL). The resultant mixture was continued stirring at room temperature overnight. Afterwards, the crude mixture was flushed with nitrogen to remove excess HCl which gave the target lipid as a hydrochloride salt. Further purification was done by washing with pentane in diethylether which offered the target lipid **4 (TS1)** as a pale yellowish semi solid (yield: 92%, TLC Rf = 0.2, 10% methanol in chloroform, one drop triethylamine).

^{1}H NMR ($CDCl_3$, 400 MHz):- δ/ppm = 8.5 (s, 1H, -CO-NH Broad), 4.5 (m, 2H, O-CH_2-), 4.05 (m, 2H, -CH(OH)-CH_2-OH), 3.75 (m, 4H, -OCH_2-CH-OH, -CH(OH)-CH(OH)-CH(OH), -CH(OH)-CH(OH)-CH(OH), -CH(OH)-CH(OH)-CH(OH)), 3.42-3.15 (m, 8H, NH-CH_2-CH_2-NH_2, 2H, -NH, Broad, OH-CH_2-NH-, Ar-CH_2-CH_2-), 2.43(m, 2H, -CONH-CH_2-CH-OH), 2.14 (t, 2H, NH-CH_2-CH_2-NH_2), 2.08 – 2.01 (m, 9H, Ar-CH_3), 1.66 (m, 2H), 1.4–1.13 (m, 24H), 0.85 (s, 12H). **^{13}C NMR ($CDCl_3$, 400 MHz):** δ/ppm = 174.16, 147.82, 127.30, 125.52, 122.21, 117.43, 117.11, 74.75, 60.32, 57.43, 54.14, 50.34,49.38, 49.28, 42.04, 41.18, 39.59, 39.24, 37.25, 30.80, 27.84, 24.66, 24.29, 22.91,22.81, 22.99, 22.50, 20.91, 19.57, 18.24, 12.56, 11.69, 11.62. **ESI-HRMS** Mass m/z: calc: 709.54; found; [M^+]: 709.53717.

Synthesis of α-tocopheryl 3,4,5,6-tetrahydroxy-N-(2-((2- propyl)amino)ethyl)hexanamide (5 and 6- TS2)

To a stirred solution of the α-tocopheryl 1-(2-aminoethyl) amino) propan-2-ol (200 mg, 19 mmol) in dry methanol, ascorbic acid (64 mg, 0.36 mmol) was supplemented. The mixture of reactants was then stirred at reflux condition for 12 h. Subsequently, methanol was removed

in vacuum. The crude was recrystallized from pentane and diethyl ether. Intermediate appears **5** as a white solid. The yield of product was 85%. After purification, the intermediate **5** (100 mg, 0.141 mmol) was dissolved in methanol (5 mL), chilled to 0 ˚C and added with HCl (1 N, 1 mL). The resultant mixture was continued stirring at room temperature overnight. Afterwards, the crude mixture was flushed with nitrogen to remove excess HCl which gave the target lipid as a hydrochloride salt. Further purification was done by washing with pentane in diehtylether which offered the target lipid **6 (TS2)** as a pale yellowish semi solid (yield 92%, TLC Rf = 0.2, 10% methanol in chloroform, one drop triethylamine).

^{1}H NMR ($CDCl_3$, 400 MHz):- δ/ppm = 8.54 (s, 1H, -CO-NH Broad), 4.68 (m, 2H, O-CH_2-), 4.45-4.39 (m, 2H, -CH(OH)-CH_2-OH), 4.26 (m, 2H, -CH(OH)-CH_2-OH , -O-CH_2-CH-OH), 4.23–4.13 (m, 2H, -CH_2-C(O)NH-), 3.85-3,81 (m, 2H, NHC(O)-CH_2-), 3.42-3.15 (m, 4H, NH-CH_2-CH_2-NH_2, OH-CH_2-NH-) 2.57 (t, 2H, Ar-CH_2-CH_2-), 2.35 (S, 2H, -NH_2, Broad), 2.03-1.95 (m, 9H, AR-CH_3), 1.80 (m, 2H), 1.54–1.10 (m, 24H), 0.87 (s, 12H). **^{13}C NMR ($CDCl_3$, 400 MHz):** δ/ppm = 171.91, 155.57, 147.89,147.02, 127.47, 125.62, 122.67, 117.39, 74.54, 72.61, 70.64, 66.33, 46.16, 39.38, 37.50, 37.42, 37.31, 32.80, 27.97, 24.81, 24.49, 22.37, 22.63, 19.75, 19.69, 14.12, 13.89, 12.55, 11.77, 11.59, 8.65. **ESI-HRMS** Mass m/z: calc: 706.57; found; [M^+]: 706.56737.

5.4.2. Lipoplex preparation and physicochemical characterization

Liposomes were developed through thin film hydration method as stated in previous reports.[157, 288] Briefly, Stock solutions of each cationic lipid and colipid (DOPC) were mixed at equimolar ratio (1:1) in a clean glass vial. The contents of the vial were dried by a gentle flow of nitrogen gas in order to form a tinny layer of lipid film on the walls of the vial. It was additionally dried using strong vacuum in order to eliminate any traces of solvent. The dried film in the vial was added with distilled and deionised water in order to hydrate the film. The contents were left overnight for hydration followed by vigorous shaking, bath sonication and finally probe

sonication yielded clear liposomal suspensions. Lipoplexes (Lipid/DNA complexes) were made by means of mixing various quantities of lipids to the DNA solution under vortex condition. The prepared complexes were used for further studies after incubation for about 30 minutes. Lipid/DNA complexes were prepared at increasing N/P ratios extending from 0.5 to 15. The size and the global surface charge (zeta potentials) of liposomes and their corresponding lipoplexes at all N/P ratios (0.5 to 6) were determined by photon correlation spectroscopy (PCS) on a Zetasizer 3000HSA (Malvern, U.K.). The particle hydrodynamic diameters were assessed in water medium with refractive index (RI) and viscosity of the sample at 1.59 and 0.89, respectively. The hydrodynamic diameters of neat liposomes and lipid/DNA complexes were assessed by the automated technique. The zeta potentials of the empty liposomes as well as lipid/DNA complexes were also measured under the following conditions: temperature, 25°C; dielectric constant, 79; viscosity, 0.89 cP; F (Ka), 1.50 (Smoluchowski). Analyses were done tenfold with the zero field correction. Hydrodynamic diameters and zeta potentials of all the liposome particles and lipoplexes were measured in triplicate through the zero field correction presented as their mean values with standard deviation. For SEM analysis, the liposomal solution in deionised water was dropped on coverslip attached to copper grid with carbon tape. The sample was dried before analysis. SEM analysis was performed on Apreo LoVac SEM (FEI).

5.4.3. DNA binding assay

Liposomes and pEGFP plasmid-DNA at various N/P ratios were mixed to check the DNA binding capability of developed liposomes. 0.8 % agarose gel, pre-stained with DNA safe stain (Invitrogen) was utilised to reveal the DNA binding capacity of newly developed liposomes. Addition of 0.3 μg of plasmid DNA to the varying concentrations of cationic liposomes under vortex, yielded lipoplexes of different N/P ratios. The prepared lipoplexes, after 30 min incubation at room temperature were loaded into the 0.8 % agarose gel immersed in TBE buffer (Tris-Borate-EDTA buffer). The gel electrophoresis was conducted at 140 V for

about 20 minutes. The pattern of DNA mobility was visualized using UV light at 365 nm. For the serum stability assay, lipoplexes after preparation and incubation for 30 min, were added to medium containing various percentage of FBS (10 - 60%, to a total volume of 100 μL). Then, these solution was further incubated for another 3 h, before subjecting to gel electrophoresis. The gel electrophoresis was conducted at 100 V for 30 minutes.

5.4.4. *In vitro* gene transfection analysis

HEK-293 and HepG2 cells were grown at 37 ^{0}C in Dulbecco's modified Eagle's medium (DMEM) comprising 10% FBS and incubated in CO_2 incubator at moistened environment with 5% CO_2. U87 cells were grown in Minimum Essential Media (MEM) and incubated at 37 ^{0}C in CO_2 incubator at humidified environment with 5% CO_2. Expression of pEGFP gene was monitored in HEK-293, HEPG2 and U87 cell lines. Cells density of seeded cells was 5×10^4/well in a 24-well plates which were raised in DMEM comprising 10% FBS for about 24 hours before assaying transfection. Lipoplexes of N/P ratios from 1 - 15 were made adding various amounts of TA, TS1 and TS2 derived liposome to a fixed DNA (pEGFP-C1 plasmid) amount of 1 μg to a total volume of 100 μL, which, upon 30 min of incubation were added into cells in the wells with medium. After 4h of incubation, a fresh complete-medium with 10 % FBS was added replacing the culture medium in the wells and the cells were left inside 5 % CO_2 incubator for about 48 h of post-transfection period. Directly, the visualization of green fluorescent protein expression (GFP) was carried out using fluorescence microscopy (*Leica DMi8*; Leica Microsystems, Wetzlar, Germany). For the quantification analysis, the HEK-293 and HEPG2 cells were dissociated by the addition of 1 × trypsin–EDTA (pre-diluted with PBS,100 μL per well) solution and re-suspended into PBS (400 μL/well). pEGFP expression of the cells was computed using a FACSCalibur flow cytometer instrument (Becton-Dickinson), with excitation at 488 nm using an argon ion laser and detected at 530nm. 10^4 cells of each treatment were considered to examine using the software, Cell Quest. Untreated cells

were considered as control group live cells for gate setting which subsequently gave the cut-off threshold to quantify the fluorescence intensity.

5.4.5. Cellular internalization study

The cells were seeded on coverslips (diameter of 18 x 18 mm) placed inside the wells of 6 well plate at a density of 3 x 10^5 cells per well and incubated in a CO_2 incubator at humidified atmosphere. After 24 hours, liposomes were labelled with rhodamine-PE and formed lipoplexes of optimal N/P ratios. The cells were treated with prepared lipoplexes and incubated at 37 ^oC under humidified environment with 5% CO_2. After 6 hours of incubation, the cells were washed twice with PBS (0.5 mL) and fixed with 4% paraformaldehyde for 10 minutes at room temperature, followed by washing with PBS again. The matched cells were counterstained with DAPI for 10 min at room temperature (300 nM in PBS). The coverslips were washed in PBS (0.5 mL) and then mounted on glass slides with 10 µL of vectashield. A confocal laser scanning microscope (Leica) was used to observe the fluorescence. The emission collection wavelengths for DAPI and rhodamine-PE tagged lipoplexes were 357-457 nm and 570-590 nm, respectively.

5.4.6. Cytotoxicity assay

The cytotoxicity of cationic liposomes (TA, TS1 and TS2) and their corresponding pEGFP derived lipoplexes was determined by reduction based cytotoxicity assays using MTT (3-(4,5-dimethylthiazol-2-yl)-2,5-diphenyltetrazolium Bromide). HEK-293, HEPG2 and U87 cells were sowed in 96-well tissue-culture plates along with their respective medium containing FBS (10%) at a density of 5×10^3/well. Various concentrations of TA-DOPC, TS1-DOPC and TS2-DOPC liposomes (5–100 µg of liposome/mL) in respective medium were added to the cells and incubated at 37 ^0C for 24 h. Upon incubation, 0.5mg/mL of MTT was fed to the wells and further incubated for another 4 h in dark. Then, the percentage of viable/live cells was measured by assessing their mitochondrial reductase activity with the help of a colorimetric

tetrazolium-based method.[289] Similarly, for the cytotoxicity of lipoplexes, HEK-293 and HEPG2 cells were grown in culture medium in a 24 well plate. Lipoplexes at various N/P ratios as used in transfection studies were added into the cells and incubated for 48 h post transfection. Total lipid concentration in each well as per the N/P ratios ranging from 1 to 15 were, 3.8 to 57 µg/mL for TA, 4.3 to 64 µg/mL for TS1 and 4.3 to 64 µg/mL for TS2.Percentage of viable cells was estimated after incubating the cells with MTT as mentioned above. Results were presented as percentage of viability = [value of treated cells – background value/ value of untreated cells –background value] x 100.

SPECTRA

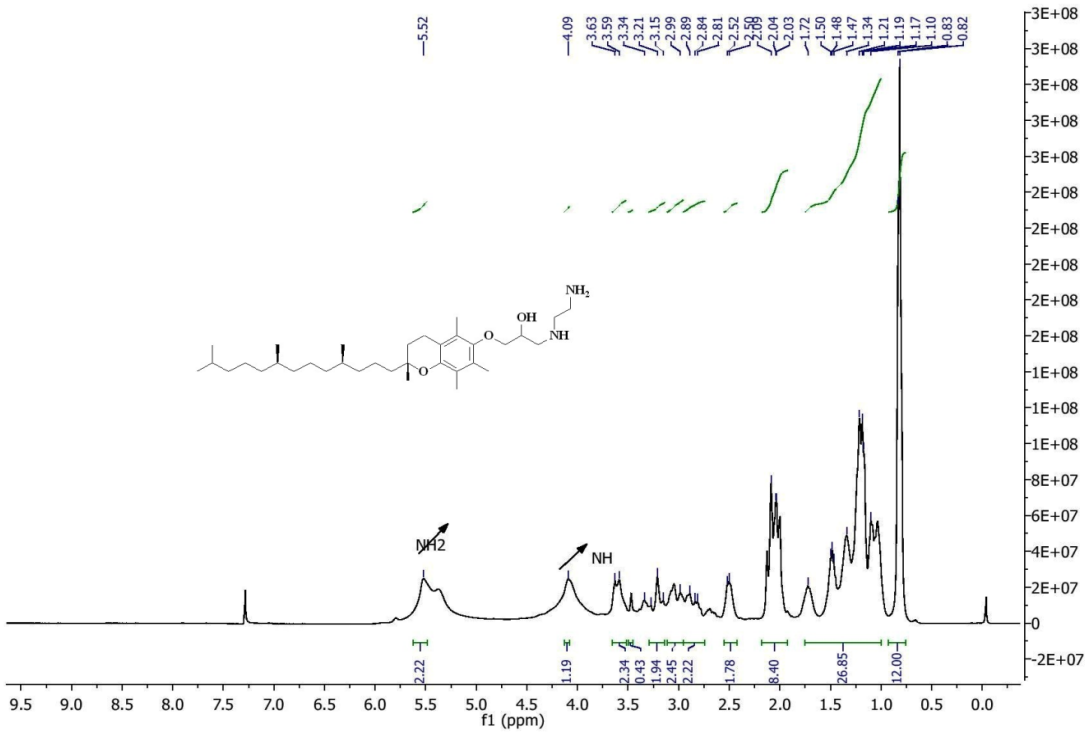

^{1}H NMR Spectra of Intermediate (Control Lipid) 2, Scheme 5.1

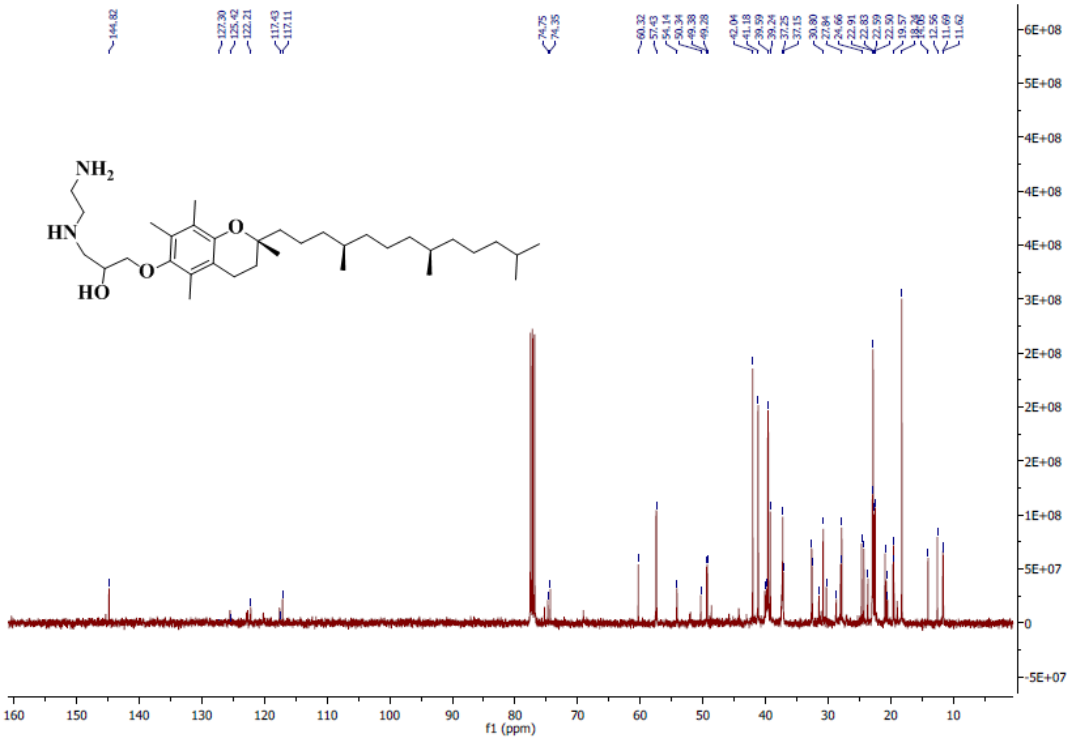

^{13}C NMR Spectra of (2) Control Lipid Scheme 5.1

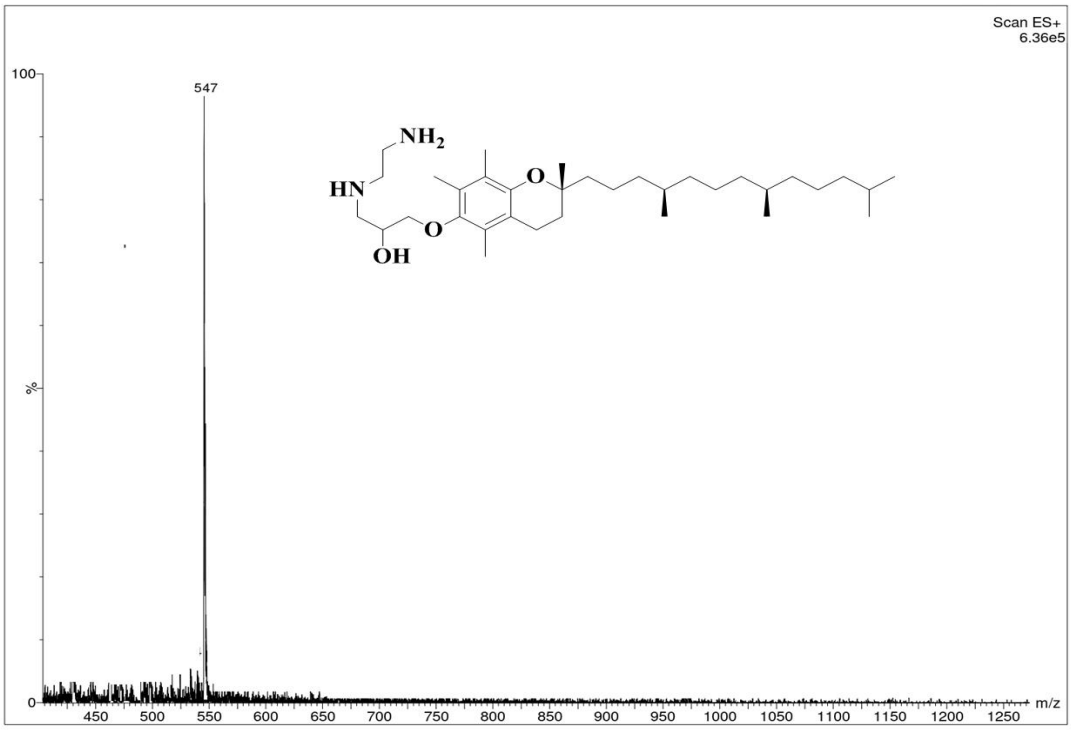

ESI-Mass Spectra of Intermediate 2, Scheme 5.1 (control lipid)

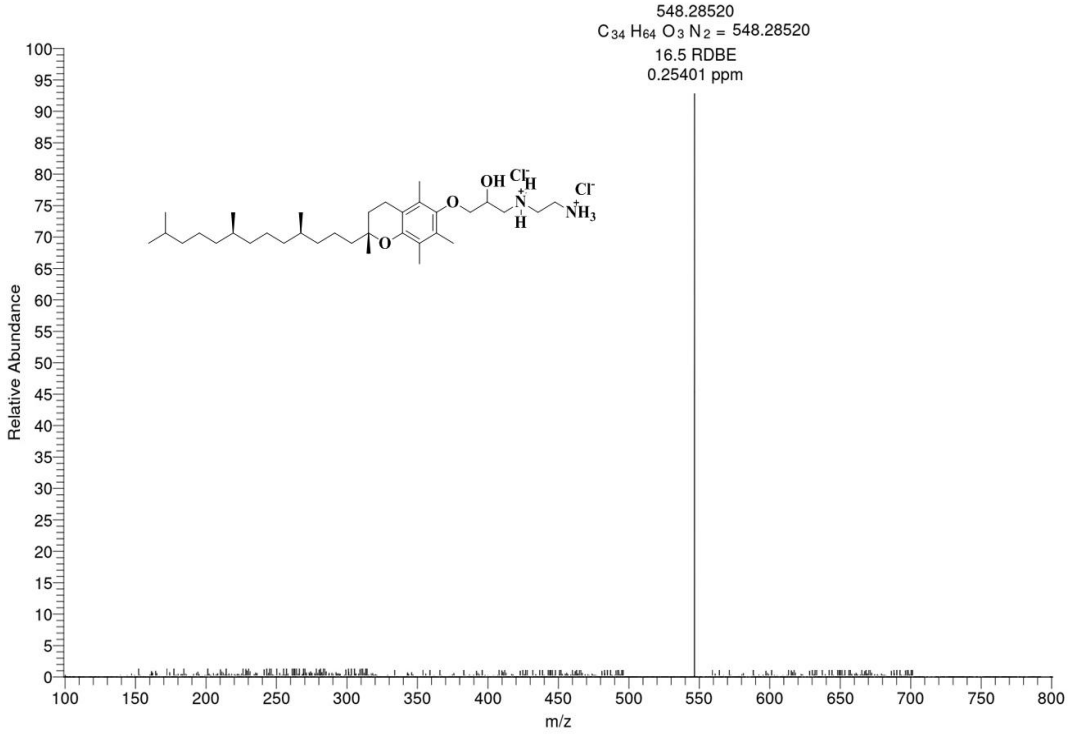

ESI-HRMS Mass of Toc-NH_2-NH_2 Scheme 5.1 (control lipid)

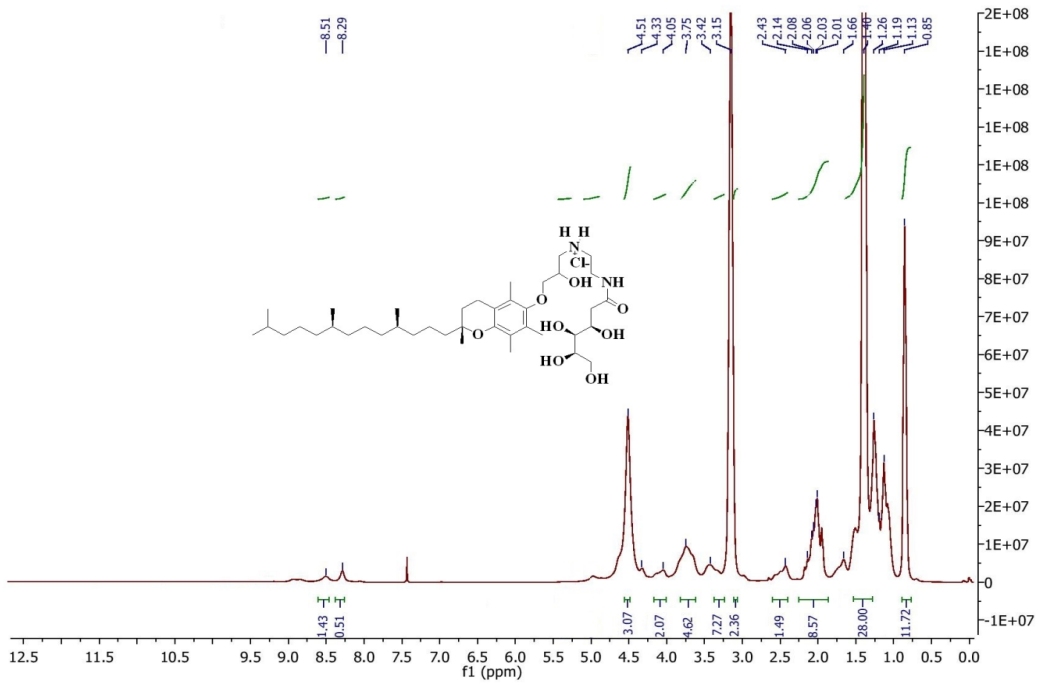

^{1}H NMR Spectra of Toc-open gluconic Lipid 4, Scheme 5.2

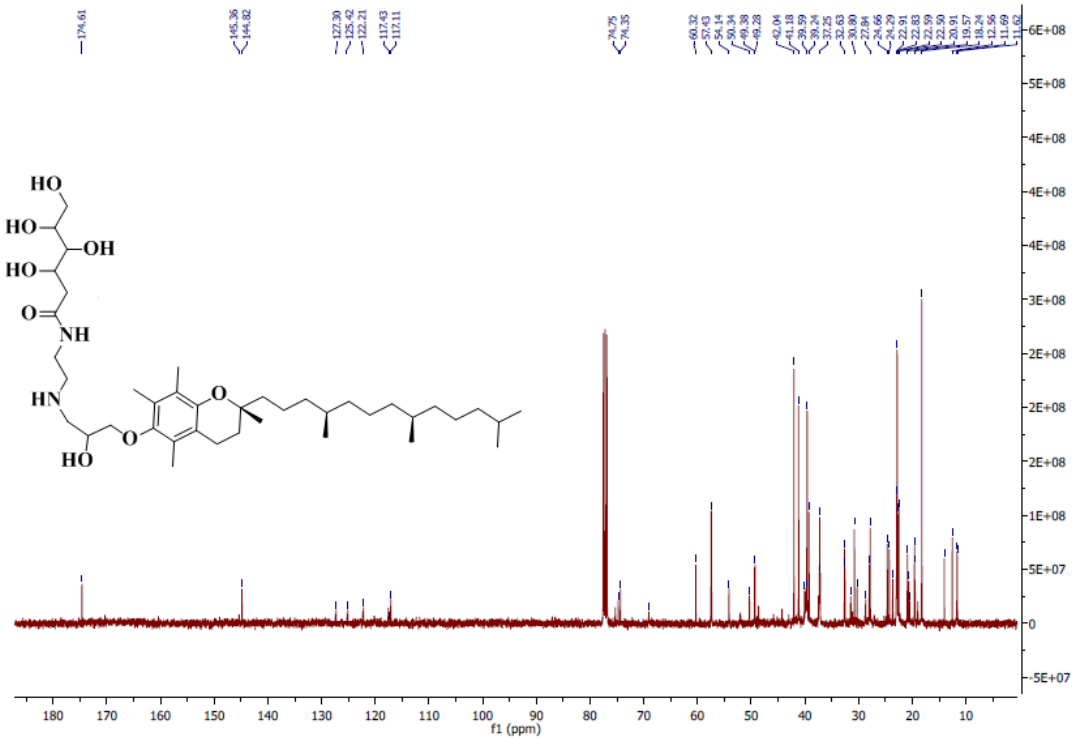

^{13}C NMR Spectra of Toc-open gluconic Lipid 4 Scheme 5.2

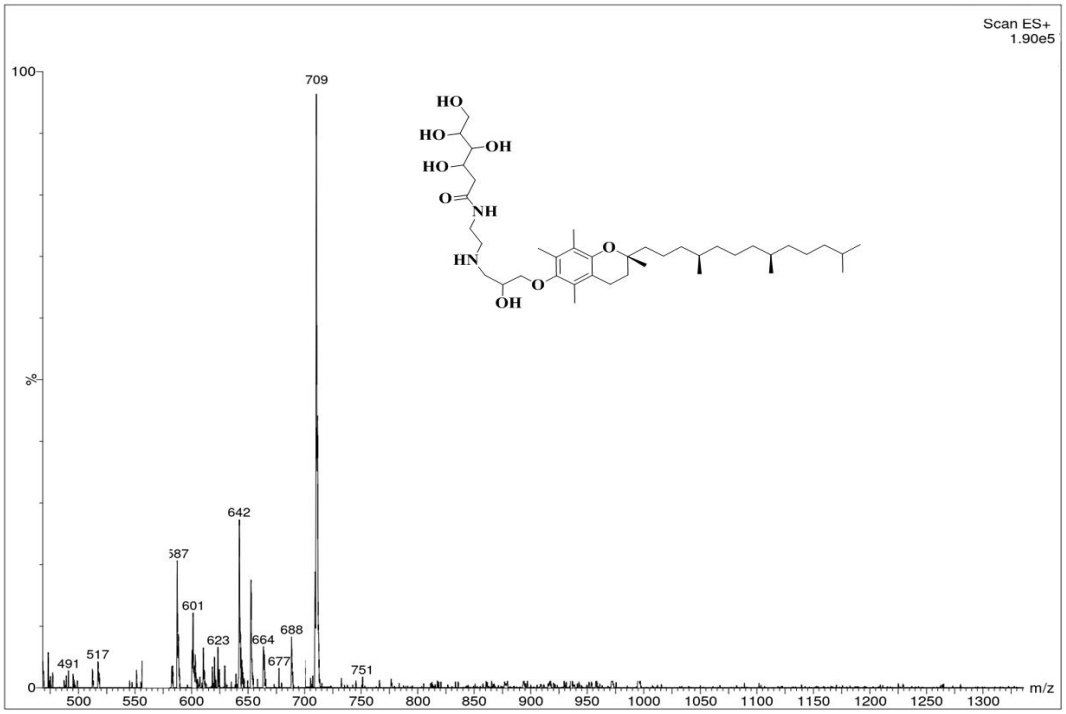

ESI-Mass Spectra of Toc-open gluconic Lipid 4 Scheme 5.2

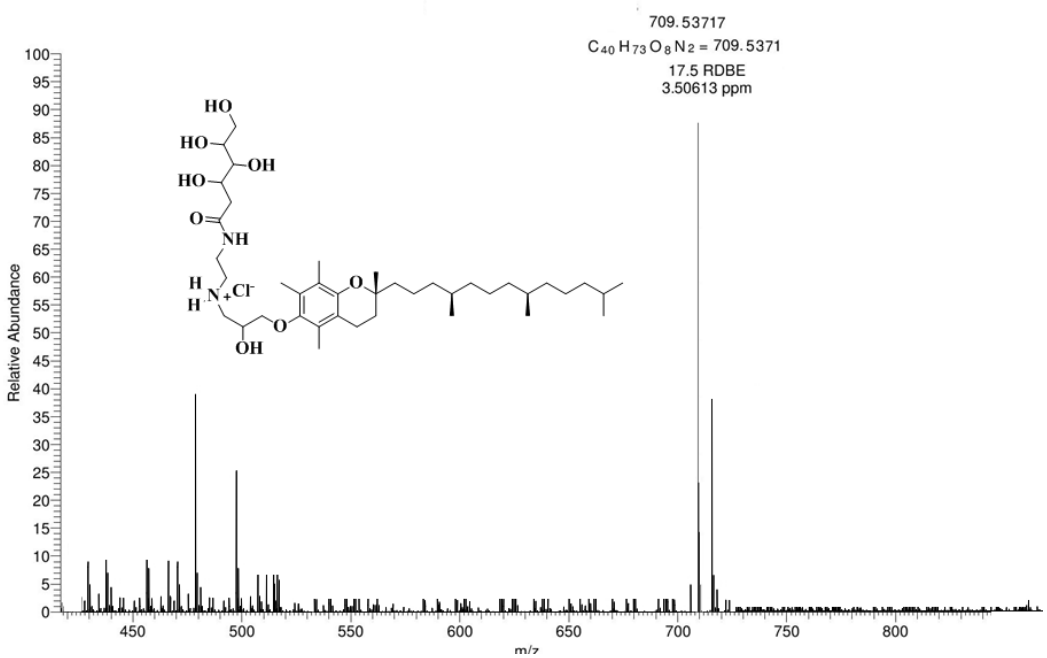

ESI-HRMS Mass of Toc-open gluconic Lipid 4 Scheme 5.2

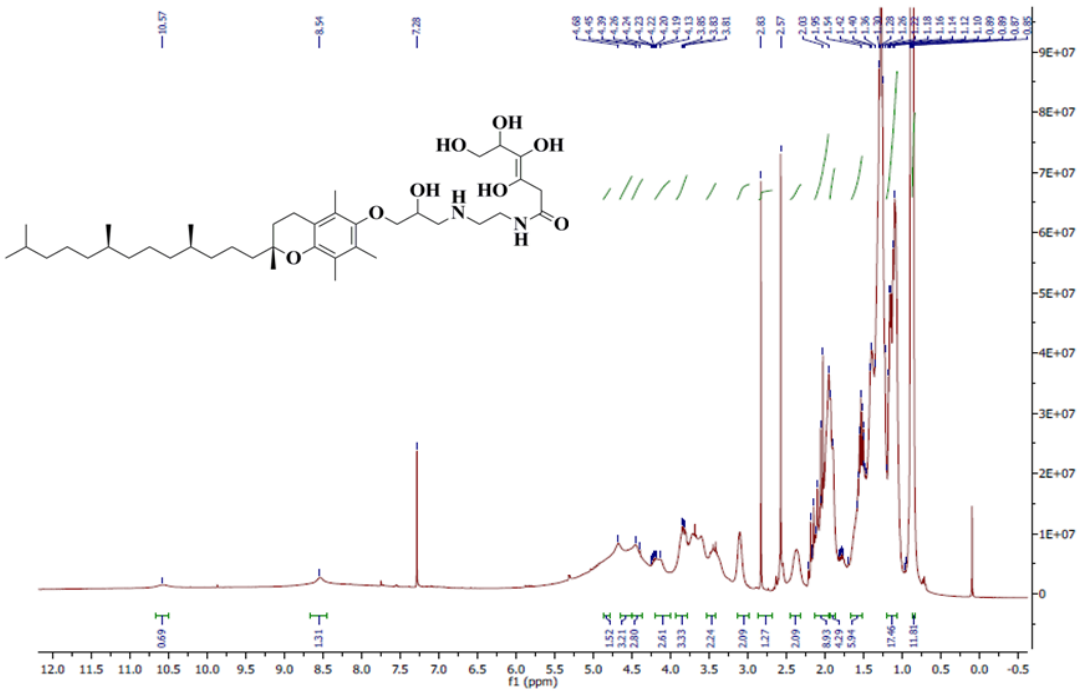

^{1}H NMR Spectra of Toc-open ascorbic acid Lipid 6, Scheme 5.3

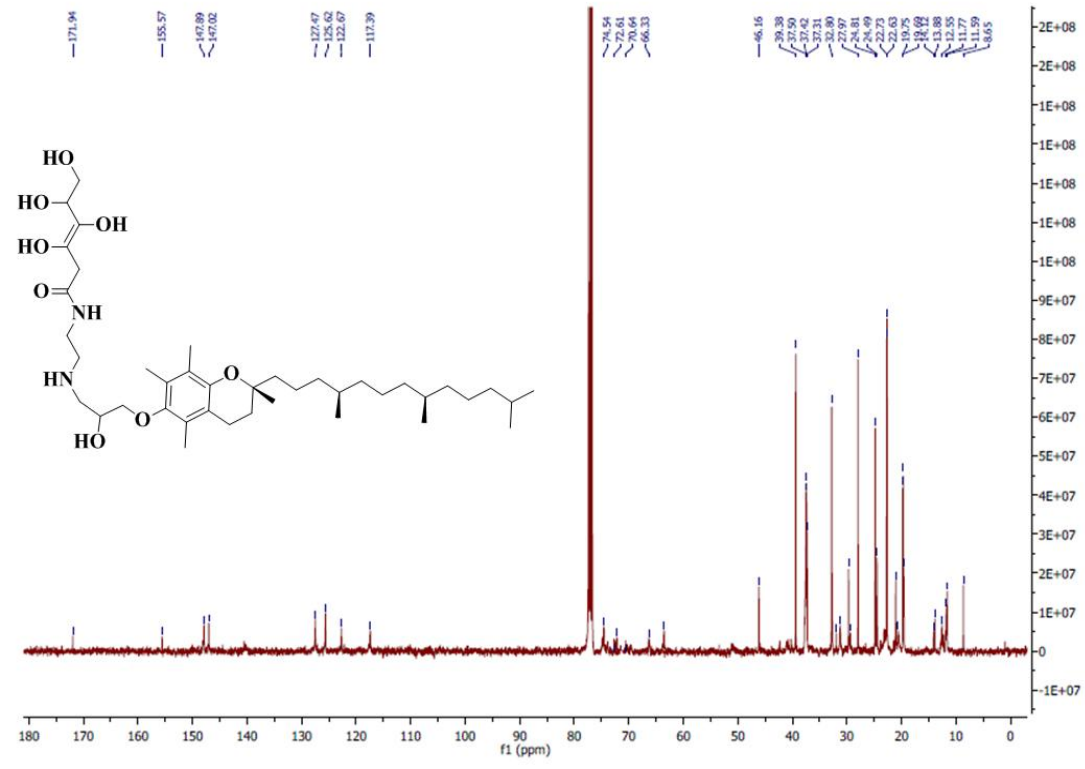

^{13}C NMR Spectra of Toc-open ascorbic acid Lipid 6 Scheme 5.3

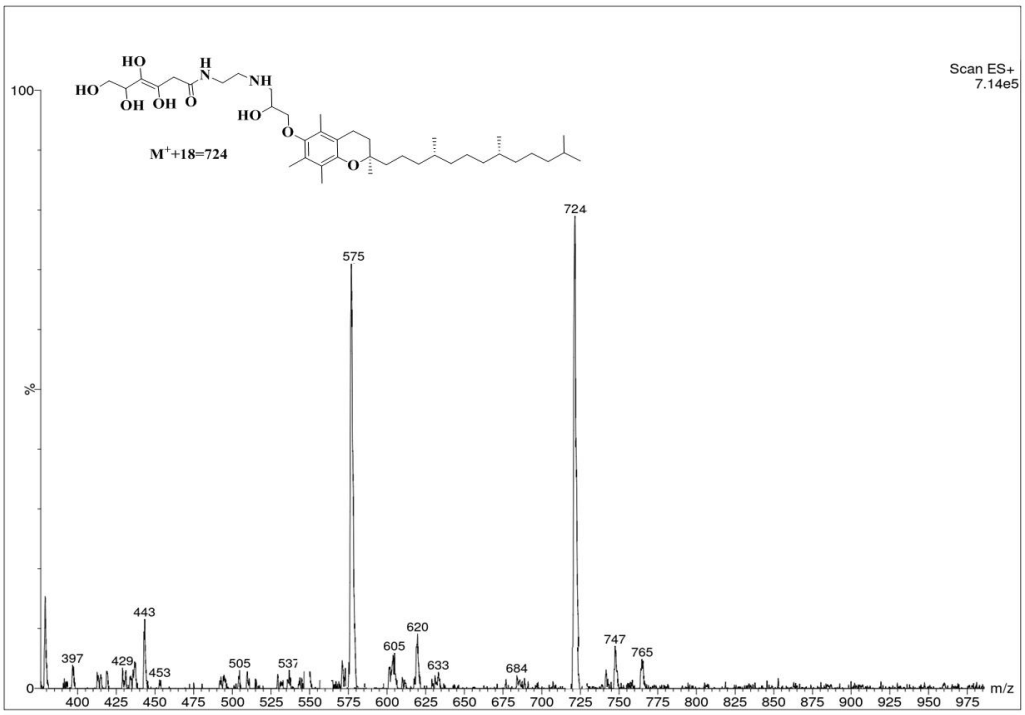

ESI-Mass Spectra of Toc-open ascorbic acid Lipid 6 Scheme 5.3

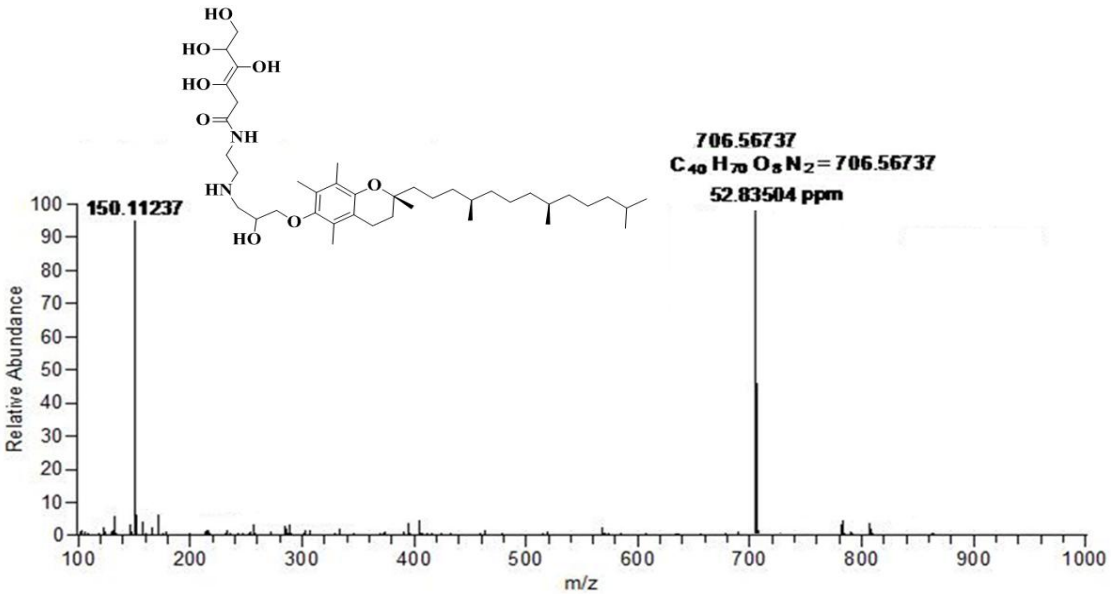

ESI-HRMS Mass of Toc-open ascorbic acid Lipid 6 Scheme 5.3

CHAPTER VI

SYNTHESIS OF NOVEL CATIONIC LIPIDS WITH FARNESOL AS A VERSATILE HYDROPHOBIC DOMAIN FOR POTENTIAL COMBINATORIAL GENE THERAPY

CHAPTER VI

SYNTHESIS OF NOVEL CATIONIC LIPIDS WITH FARNESOL AS A VERSATILE HYDROPHOBIC DOMAIN FOR POTENTIAL COMBINATORIAL GENE THERAPY

6.1. INTRODUCTION

Non-viral gene delivery has emerged as an attractive strategy in gene therapy due to its obvious advantages over its viral counterpart. Viral gene delivery systems are relatively better delivery vehicles, however, they suffer from a several drawbacks, such as the risk of potential recombination with wild-type viruses, intrinsic immunogenicity and minimal nucleic acid packaging capacity. Consequently, non-viral gene delivery systems have been put into action as safer and promising gene delivery platforms. Out of various non-viral vectors such as cationic lipids, polymers and dendrimers,[134, 290-296] utilization of cationic lipids as gene delivery systems has been considered to be more promising because of their diverse advantages, such as uncomplicated preparation, ease of reproducibility, biodegradability, and potential commercial value.[134]

A myriad of cationic lipids and their corresponding formulations have been reported in the last few decades are generally based on glycerol,[297, 298] cholesterol,[299-303] aliphatic hydrocarbon-tail[304, 305] or tocopherol[267, 306-309] as backbone. Despite numerous advantages of these cationic lipid systems for in vitro gene delivery, the performance of their nucleic acid therapies in clinical trials are far from satisfactory due to the complex biological setting in vivo.[310] However, substantial progress has been made to determine the specific barriers hindering the performance of cationic lipid vectors.[311] Evidently, the structural features of cationic lipids have major influence on DNA condensation and gene transfection properties. Design and synthesis of new cationic lipid vectors by means of alternative structural units are essential for the development of potential synthetic vehicles for gene delivery.

The configuration of the hydrophobic region in cationic lipid regulates the key factors in gene delivery. Factors such as phase transition temperature of liposome, fluidity of the bilayer, stability of liposomes, the endosomal escape, protection of DNA from nucleases, the release of DNA from lipoplex and the nuclear uptake are all influenced by the structure of hydrophobic moiety. On the other hand, hydrophobic domain also take part in determining the toxicity of lipid.[122] Thus, similar to other components of cationic lipids, the hydrophobic groups influence almost every step in the process of gene delivery. The majority of the cationic lipids developed so far contain one or two C18:1 oleyl chains.[312-315] Although single chain and triple chain lipids also reported in the literature, double chain lipids are established to be most effective in regulating transfection and cytotoxicity. However, the limitations of these cationic lipids are well documented. Studies on hydrocarbon chain length demonstrated that 14-carbon aliphatic chains serve the best for gene transfer compared to longer aliphatic chains.[291, 316] On the other hand, increase in unsaturation and branching of aliphatic chains resolved to be beneficial in transfection.[292, 317-319] In general, shorter chain length, unsaturation and branching on aliphatic chain are collectively bestows the better transfection properties to gene delivery vectors. In spite of these evidences, the research on cationic lipids fulfilling all these requirements is scarce. Over the years, major attention has been given to the head group evolution to enhance the gene delivery ability of cationic lipids. More exploration on the hydrophobic region seems necessary, in order to establish the competent gene delivery vectors.

Farnesol is a natural 15-carbon acyclic sesquiterpene alcohol with tri-unsaturated C12 aliphatic chain and branch like methyl groups adjacent to unsaturation. Structurally, farnesol appears to be interesting molecule to fabricate into cationic lipid with branched structure, short chain length, higher unsaturation than regular cationic lipids. Farnesol has been reported to inhibit tumor cell proliferation in vitro[123, 124] as well as in vivo.[124, 125] Additionally, pharmacological studies revealed that farnesol has chemo-preventative, anti-inflammatory antioxidant, analgesic and neuroprotective properties.[126-130, 320, 321] Over the past two decades,

several patents were registered studying the pharmaceutical potential of farnesol.[322] Given the wide variety of pharmoclogical applications coupled with its promising structural features, it's worthwhile to design farnesol based cationic lipids for gene delivery applications.

6.2. RESULTS AND DISCUSSION

The present investigation offers a new class of farnesol based cationic lipids with potential for carrying nucleic acids into desired cell lines. The cationic lipids of this work generally contain quaternary amine head groups with farnesol moiety as hydrophobic tail. The general molecular structure of newly designed cationic lipids in this work is given in **Figure 6.1.**

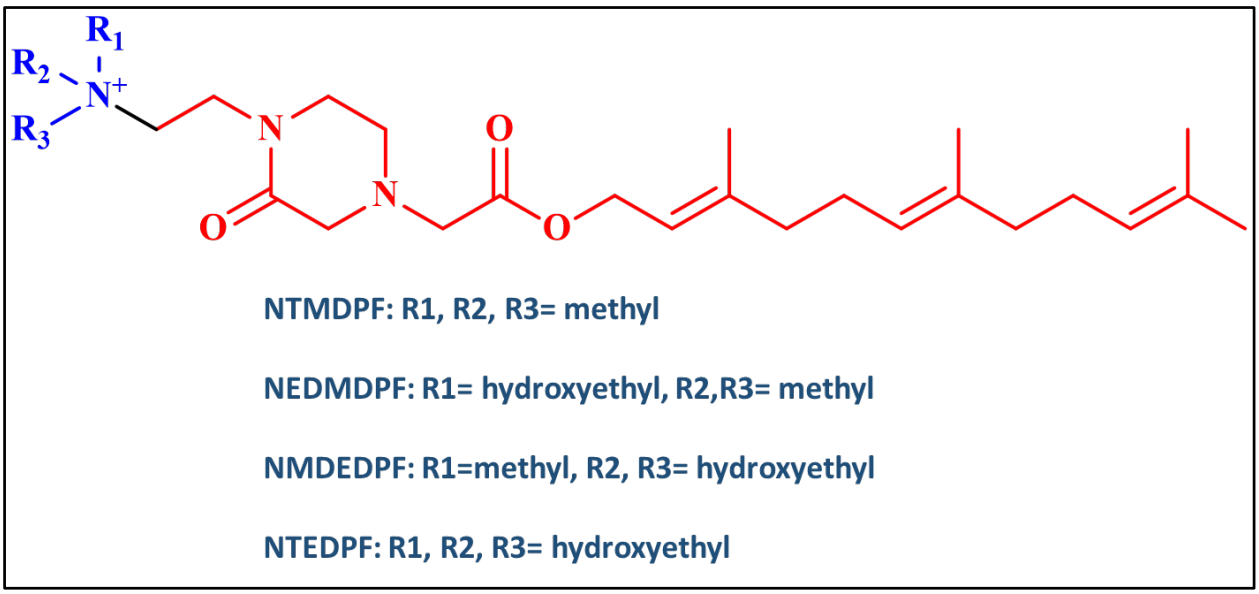

Figure 6.1: *General chemical structure of cationic lipids with farnesol-based tail group and quaternary ammonium head group connected through pyrazinone linker.*

Cationic head groups are designed by varying number of methyl or hydroxyethyl groups on a positively charged nitrogen atoms. The rationale for this design is to assess the effect of increasing or decreasing number of hydroxyethyl groups on cationic head which are known to be beneficial in transfection. The number of cationic charge on each final lipid is constant, however, only differing by the moieties attached to the cationic nitrogen. The cationic charge on the example lipids is independent of pH. Since farnesol structurally fulfilling basic

requirements of an ideal hydrophobic tail and quarternary ammonium based head groups are known to bind with DNA efficiently, the new cationic lipids described in the current chapter may provide new class of efficient gene delivery vectors.

6.2.1. Synthesis of active cationic head groups

As a prerequisite for gene delivery, hydrophilic cationic head groups are essential part of gene delivering cationic lipids. These hydrophilic head groups possess one or more positive charges, which involve in electrostatic interaction with negatively charged DNA, forming lipid-DNA complexes, also called as lipoplexes. Various types of head groups have been reported in the literature, such as, amines, quaternary ammoniums, aminoacids/peptides, heterocyclic headgroups, guanidiniums and some unusual head groups for correlating their structure with transfection activity.[119] Among these head groups, quaternary ammonium-based head groups are by far the most commonly used ones. Since the pioneering work of Felgner and co-workers in introducing first quaternary ammonium based lipid for gene delivery, numerous cationic lipids bearing quaternary ammonium head groups have been developed to transfect a wide variety of cell lines.[55, 303, 306, 323] Over the years, the research on quaternary ammonium head groups and their transfection activity has resolved that the existence of hydrophilic groups, precisely hydroxyl functional groups on cationic head is helpful in enhancing the transfection activity of lipids with quaternary ammonium head groups.[119] Our previous work on α-tocopherol based lipids, also reiterated that inclusion of hydroxyl functional groups in the head group region are beneficial for efficient gene delivery.[267, 306] Consequently, when new types of cationic lipids are being synthesized, it is essential to include structural variations involving hydroxyl functional croups. Accordingly, in our current work of designing new class of farnesol based cationic lipids, **Chapter VI** describes the synthesis of a series of lipids with or without hydroxyl groups on the cationic head. Active cationic head groups are synthesized initially

which can be readily reacted with hydrophobic groups. Synthesis of these head groups was explained in the experimental section and follows the reaction **schemes 6.1-6.3**.

Scheme 6.1:

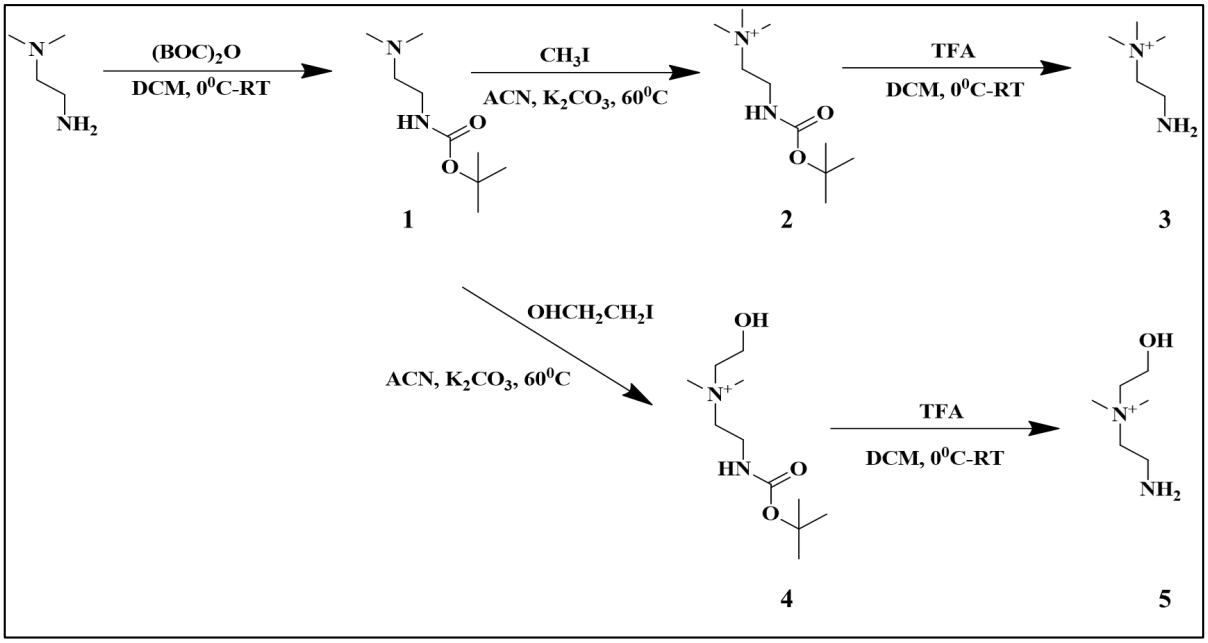

Reagents and solvents: *(BOC)2O: Di-tert-butyl dicarbonate, ACN: Acetonitrile, TFA: Trifluoroacetic acid, DCM: Dichloromethane*

All the cationic head groups were synthesized using ethylenediamine derivatives as starting materials. Protecting one of the free amine group with tert-Butyloxycarbonyl (Boc) group, the other amine was quaternized using methyl or hydroxyethyl halides.[324] Ethylenediamine derivatives with at least one free amine were reacted with $(BOC)_2O$ to give amine-protected ethylenediamine derivatives. Next step involved the quaternization of second amine group by the reaction of methyl iodide (**2, Scheme 6.1**) or iodoethanol (**4, Scheme 6.1**) or bromoethanol (**7, Scheme 6.2 and 10, Scheme 6.3**). Finally, removal of BOC groups by the action of TFA in DCM, has given active cationic head groups (**3, 5, 8 and 11**).

Scheme 6.2:

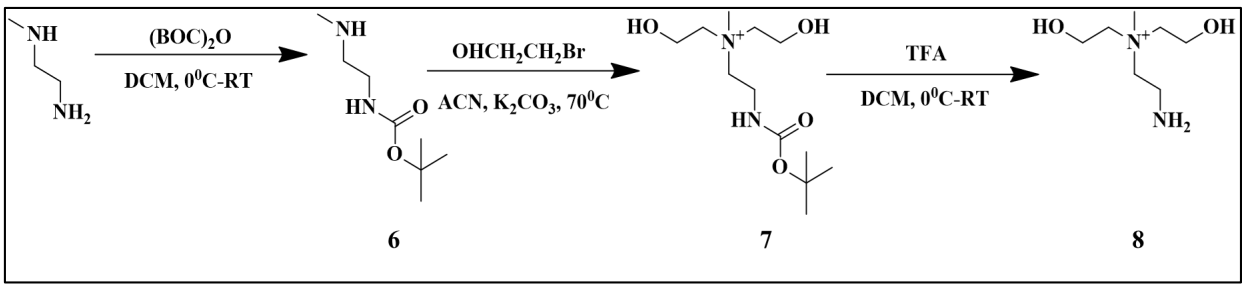

Scheme 6.3:

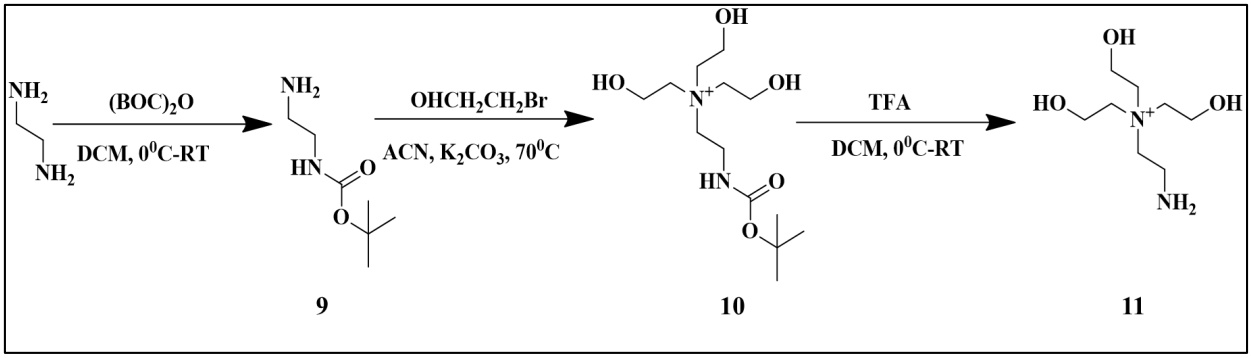

6.2.2. Synthesis of intermediate hydrophobic tail group

It has been resolved that, for cationic lipids to be effective gene carriers, the shorter hydrophobic chain length, unsaturation and branching on hydrophobic chain are beneficial.[292, 318, 319] However, studies of cationic lipids fulfilling all these parameters are scarce. Instead of moving towards chemical modifications of hydrophobic groups to incorporate above mentioned properties in cationic lipids, it may be worthy to look for naturally occurring biomolecules to fabricate into cationic lipids. In this direction, farnesol appears to be an attractive molecule with desirable chain length, unsaturation and branch-like structure. Thus, farnesol was used as a starting material to introduce new hydrophobic moiety into cationic liposomes. On the other hand, variety of biological functions of farnesol as highlighted by previous studies,[123-127, 325, 326] it is hypothesized that farnesol based cationic lipids can be used as gene delivery vehicles with intrinsic anticancer and antimicrobial properties.

To synthesize hydrophobic anchoring moiety, farnesol was treated with the bromoacetic acid in a typical solvent free reaction as reported previously,[327] with slight modifications. The resultant intermediate **12**, after purification was conjugated to 2-bromoethylamine in the presence of N,N-Diisopropylethylamine (DIPEA) to yield intermediate **13**.

Scheme 6.4:

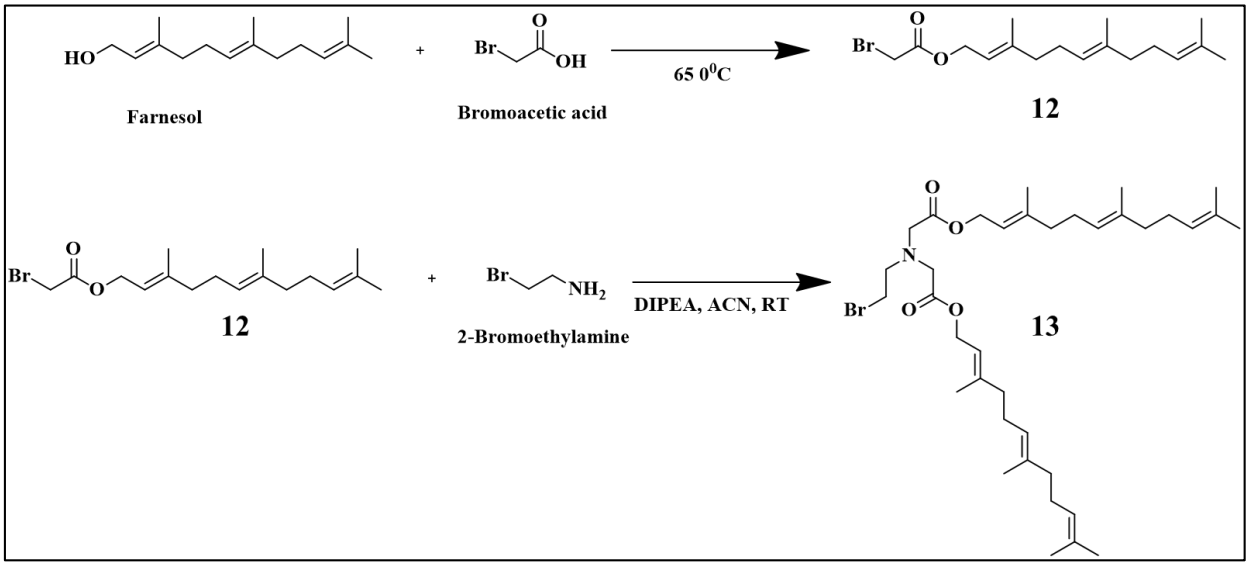

6.2.3. Conjugation of hydrophobic tail to the cationic head groups

The final cationic lipids of the present work were synthesized through the conjugation of active cationic head group to intermediate **13 (Scheme 6.5)**. The reaction proceeds through the formation of a piperazinone linker between the head group and hydrophobic tail group. Initially, the reaction may involve the N-alkylation of primary amine on the head group with bromoethylamine derived intermediate **13**. The secondary amine formed through this reaction may further react with at least one electrophilic carbonyl carbon present on the hydrophobic tail to give cyclization product. Overall, the basic structural units of the newly synthesized cationic lipids are, i) quaternary ammonium head group, ii) piperazinone linker and iii) farnesol-based hydrophobic anchoring group. It is hypothesized that, the inclusion of piperazinone in the skeletal structure of lipids might be beneficial for the purpose of drug delivery. Scaffolds involving piperazine derivatives are reportedly privileged structures for drug discovery and peptidomimetic research.[328-330] Particularly, the drug-like properties of 2-oxopiperazine (piperazinone) and the diketopiperazine scaffolds have been well documented in the literature.[331-334] Although, the gene delivery using piperazinone based structures has not been explored, it is intriguing to see their effect through gen delivery. The synthesized lipids (14, 15,

16 and 17), are potential gene delivery vectors with desirable properties to effectuate the physical and biological functions of their corresponding liposomes. Future studies would be focused on developing optimal liposomes using these cationic lipids and on studying their intracellular functions.

Scheme 6.5:

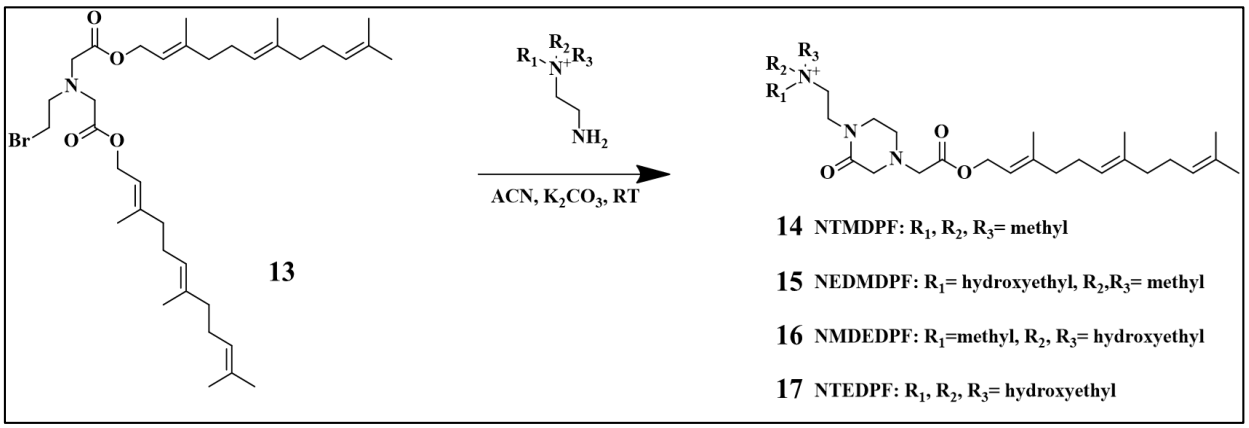

6.3. CONCLUSIONS

In summary, a new series of cationic lipids have been synthesized with farnesol-based hydrophobic anchoring group. The methods involved individual synthesis of cationic head group, intermediate hydrophobic tail and finally conjugation of both groups to give target lipids. Each lipid was differed with other through its cationic head group. Quaternary ammonium head groups with increasing number of hydroxyethyl functional moieties were linked to hydrophobic portion of lipid through piperazinone linkers. All the intermediate compounds were characterized by ^{1}H NMR and ESI-MS techniques. Final cationic lipids were characterised by ^{1}H, ^{13}C and ESI-MS techniques. The synthesized cationic lipids can be formulated into liposomes when mixed with helper lipids in aqueous medium. Future studies will be focussed on development of optimal liposomal formulations using the new farnesol based cationic lipids for gene delivery and on the study of their intracellular functions.

6.4. EXPERIMENTAL SECTION

The cationic lipids of the current investigation were synthesized by multistep reaction scheme as described as follows. The synthesis procedure can be divided into three broad segments, i.e., 1) Synthesis of active cationic head groups **(Scheme 6.1-6.3)**, 2) Synthesis of intermediate hydrophobic tail group **(Scheme 6.4)** and 3) Conjugation of hydrophobic tail to the cationic head groups **(Scheme 6.5)**.

6.4.1. Synthesis of active cationic head groups (Scheme 6.1-6.3)

*Synthesis of tert-butyl (2-(dimethylamino)ethyl)carbamate (**1, Scheme 6.1**)*

Di-tert-butyl dicarbonate (3.093 g, 14.4 mmol) was dissolved in dichloromethane (15 mL) and the solution was colled to 0 °C. A solution of N^1,N^1-dimethylethylenediamine (1.0 g, 11.3 mmol) in 10 mL of dichloromethane was added dropwise to the above solution at 0 °C. The mixture was warmed up to room temperature and continued to stir for 16 hours. The reaction mixture was washed trice with brine, dried over sodium sulphate and concentrated to give pure target product with 97 % yield. ^{1}H NMR (400 MHz, $CDCl_3$) δ/ppm: 3.70 (s, 1H), 3.22-3.18 (q, 2H), 2.40-2.37 (t, 2H), 2.22 (s, 6H), 1.44 (s, 9H)

*Synthesis of 2-((tert-butoxycarbonyl)amino)-N,N,N-trimethylethanaminium (**2, Scheme 6.1**)*

To a solution of tert-butyl (2-(dimethylamino)ethyl)carbamate (0.5 g, 2.6 mmol) in acetonitrile (10 mL), K2CO3 (0.732 g, 5.3 mmol) was added and the reaction mixture was stirred at room temperature for 30 min. Then, methyl iodide (0.25 mL, 3.9 mmol) was added to the above mixture and the reaction temperature was increased to reflux condition. The reaction was continued to stir under reflux condition for 24 hrs. Subsequently, the reaction temperature was decreased to room temperature and K2CO3 was filtered off. Organic solvent was removed under reduced pressure to yield an oily crude product. The crude was washed with diethyl ether for three times to yield the target product as white solid (yield, 93 %). ^{1}H NMR (400 MHz, $CDCl_3$) δ/ppm: 3.86-3.80 (m, 2H), 3.75-3.65 (m, 2H), 3.47 (s, 9H), 1.42 (s, 9H).

*Synthesis of 2-amino-N,N,N-trimethylethanaminium (**3, Scheme 6.1**)*

To a mixture of 2-((tert-butoxycarbonyl)amino)-N,N,N-trimethylethanaminium (0.76 g, 3.7 mmol) in dichloromethane (9 mL), trifluoroacetic acid (TFA) (1 mL) was added dropwise at 0 °C and the mixture was stirred for 30 min. After that, the reaction temperature was increased to room temperature and continuously stirred for another 3 hours. The solvent was evaporated under reduced pressure and the resultant oily crude was washed with diethyl ether thrice to give the target product as light yellow solid (yield, 80%). ^{1}H NMR (400 MHz, DMSO-D_6) δ/ppm: 3.22-3.18 (m, 2H), 3.05-2.85 (s, 9H), 2.38-2.28 (m, 2H); ESI-MS: calcd. for $C_5H_{15}N_2^+$: 103.12, found: 103.10 $[M + H]^+$.

*Synthesis of 2-((tert-butoxycarbonyl)amino)-N-(2-hydroxyethyl)-N,N-dimethylethanaminium **(4, Scheme 6.1)***

To a solution of tert-butyl (2-(dimethylamino)ethyl)carbamate (0.5 g,2.6 mmol) in acetonitrile (10 mL), K2CO3 (0.732 g, 5.3 mmol) was added and the reaction mixture was stirred at room temperature for 30 min. Then, Iodoethanol (0.413 mL, 5.3 mmol) was added to the above mixture and the reaction temperature was increased to reflux condition. The reaction was continued to stir under reflux condition for 24 hrs. Subsequently, the reaction temperature was decreased to room temperature and K2CO3 was filtered off. Organic solvent was removed under reduced pressure to yield an oily crude product. The crude was washed with diethyl ether for three times to yield the target product as oily liquid (yield, 87 %). ^{1}H NMR (400 MHz, $CDCl_3$) δ/ppm: 4.16-3.98 (m, 2H), 3.92-3.54 (m, 6H), 3.42 (s, 6H), 1.43 (s, 9H) $[M + H]^+$.

*Synthesis of 2-amino-N-(2-hydroxyethyl)-N,N-dimethylethanaminium (**5, Scheme 6.1**)*

To a mixture of 2-((tert-butoxycarbonyl)amino)-N-(2-hydroxyethyl)-N,N-dimethylethanaminium (0.8 g, 3.3 mmol.) in dichloromethane (9 mL), trifluoroacetic acid (TFA) (1 mL) was added dropwise at 0 °C and the mixture was stirred for 30 min. After that, the reaction temperature was increased to room temperature and continuously stirred for another 3 hours. The solvent was evaporated under reduced pressure and the resultant oily crude was

washed with diethyl ether thrice to give the target product as light yellow solid (yield, 93 %). ^{1}H NMR (400 MHz, D_2O) δ/ppm: 4.00-3.90 (t, 2H), 3.72-3.60 (m, 2H), 3.52-3.42 (m, 4H), 3.13 (s, 6H); ESI-MS: calcd. for $C_6H_{17}N_2O^+$: 133.13, found: 133.10 $[M + H]^+$.

*Synthesis of tert-butyl (2-(methylamino)ethyl)carbamate (**6, Scheme 6.2**)*

Di-tert-butyl dicarbonate (2.0 g, 9.2 mmol) was dissolved in dichloromethane (15 mL) and the solution was cooled to 0 °C. A solution of N-Methylethelenediamine (1.36 g, 18.33 mmol.) in 10 mL of dichloromethane was added dropwise to the above solution at 0 °C. The mixture was warmed up to room temperature and continued to stir for 16 hours. The reaction mixture was washed with brine, dried over sodium sulphate and filtered. The filtrate was concentrated to give pure product with 73 % yield. The resultant product was used without further purification. ^{1}H NMR (400 MHz, $CDCl_3$) δ/ppm: 3.38-3.32 (q, 2H), 3.30-3.26 (q, 2H), 2.88 (s, 3H), 1.47 (s, 9H); ESI-MS: calcd. for $C_8H_{18}N_2O_2$: 174.14, found: 175.10 $[M + H]^+$.

*Synthesis of 2-((tert-butoxycarbonyl)amino)-N,N-bis(2-hydroxyethyl)-N-methylethanaminium (**7, Scheme 6.2**)*

To a solution of tert-butyl (2-(methylamino)ethyl)carbamate (0.3 g, 1.7 mmol) in Acetonitrile (3 mL), K2CO3 (0.7 g, 5.1 mmol) was added and the reaction mixture was stirred at room temperature for 30 min. Then, Bromoethanol (0.64 g, 5.1 mmol) was added to the above mixture and the reaction temperature was increased to reflux condition. The reaction was continued to stir under reflux condition for 24 hrs. Subsequently, the reaction temperature was decreased to room temperature and K2CO3 was filtered off. Organic solvent was removed under reduced pressure to yield an oily crude product. The crude was washed with diethyl ether for three times to yield the target product as oily liquid (yield, 76 %). ^{1}H NMR (400 MHz, D_2O) δ/ppm: 4.08-4.00 (m, 4H), 3.75-3.62 (m, 4H), 3.62-3.57 (m, 2H), 3.56-3.53 (m, 2H), 3.20 (s, 3H), 1.42 (s, 9H); ESI-MS: calcd. for $C_{12}H_{27}N_2O_4$: 263.20, found: 285.20 $[M + Na]^+$.

*Synthesi of 2-amino-N,N-bis(2-hydroxyethyl)-N-methylethanaminium (8**, Scheme 6.2**)*

To a mixture of 2-((tert-butoxycarbonyl)amino)-N,N-bis(2-hydroxyethyl)-N-ethylethanaminium (0.2 g, 0.75 mmol) in dichloromethane (9 mL), trifluoroacetic acid (TFA) (1 mL) was added dropwise at 0 °C and the mixture was stirred for 30 min. After that, the reaction temperature was increased to room temperature and continuously stirred for another 3 hours. The solvent was evaporated under reduced pressure and the resultant oily crude was washed with diethyl ether thrice to give the target product as light yellow oil (yield, 90%). ^{1}H NMR (400 MHz, D_2O) δ/ppm: 4.04-3.98 (m, 4H), 3.93-3.89 (m, 2H), 3.84-3.80 (m, 2H), 3.72-3.69 (m, 2H), 3.64-3.62 (m, 2H), 3.23 (s, 3H); ESI-MS: calcd. for $C_7H_{19}N_2O_2^+$: 163.14, found: 163.10 $[M + H]^+$.

*Synthesis of tert-butyl (2-((2-hydroxyethyl)amino)ethyl)carbamate (**9, Scheme 6.3**)*

Di-tert-butyl dicarbonate (4.3g, 20 mmol) was dissolved in dichloromethane (15 mL) and the solution was cooled to 0 °C. A solution of ethelenediamine (12.02 g, 200 mmol) in 30 mL of dichloromethane was added dropwise to the above solution at 0 °C. The mixture was warmed up to room temperature and continued to stir for 16 hours The reaction mixture was washed with brine, dried over sodium sulphate and filtered. The filtrate was concentrated to give pure product with 78 % yield. The resultant product was used without further purification. ^{1}H NMR (400 MHz, $CDCl_3$) δ/ppm: 3.20-3.15 (q, 2H), 2.81-2.78 (t, 2H), 1.45 (s, 9H).

*Synthesis of 2-((tert-butoxycarbonyl)amino)-N,N,N-tris(2-hydroxyethyl)ethanaminium (**10, Scheme 6.3**)*

To a solution of tert-butyl (2-aminoethyl)carbamate (1.3 g, 8.12 mmol) in Acetonitrile (30 mL), K_2CO_3 (4.5 g, 32.5 mmol) was added and the reaction mixture was stirred at room temperature for 30 min. Then, Bromoethanol (4.06 g, 32.5 mmol) was added to the above mixture and the reaction temperature was increased to reflux condition. The reaction was continued to stir under reflux condition for 24 hrs. Subsequently, the reaction temperature was decreased to room temperature and K2CO3 was filtered off. Organic solvent was removed under reduced pressure to yield an oily crude product. The crude was washed with diethyl ether

for three times to yield the target product as oily liquid (yield, 66 %). ^{1}H NMR (400 MHz, D_2O) δ/ppm: 4.04-3.96 (m, 6H), 3.67-3.64 (t, 6H), 3.61-3.58 (m, 2H), 3.54-3.50 (m, 2H), 1.39 (s, 9H); ESI-MS: calcd. for $C_{13}H_{29}N_2O_5$: 293.21, found: 315.10 $[M + Na]^+$.

*Synthesis of 2-amino-N,N,N-tris(2-hydroxyethyl)ethanaminium (**11, Scheme 6.3)***

To a mixture of 2-((tert-butoxycarbonyl)amino)-N,N,N-tris(2-hydroxyethyl)ethanaminium (0.53 g, 1.7 mmol) in dichloromethane (9 mL), trifluoroacetic acid (TFA) (1 mL) was added dropwise at 0 °C and the mixture was stirred for 30 min. After that, the reaction temperature was increased to room temperature and continuously stirred for another 3 hours. The solvent was evaporated under reduced pressure and the resultant oily crude was washed with diethyl ether thrice to give the target product as light yellow oil (yield, 71%). ^{1}H NMR (400 MHz, D_2O) δ/ppm: 4.04-4.00 (m, 6H), 3.94-3.90 (m, 2H), 3.73-3.71 (m, 6H), 3.58-3.56 (m, 2H); ESI-MS: calcd. for $C_8H_{21}N_2O_3^+$: 193.15, found: 193.10 $[M + H]^+$.

6.4.2. Synthesis of intermediate hydrophobic tail group (Scheme 6.4)

*Synthesis of farnesyl 2-bromoacetate **(12, Scheme 6.4)***

Farnesol (5.0 g, 22.5 mmol) and bromoacetic acid (3.125 g, 22.5 mmol) were taken in round bottom flask and the mixture was stirred at 65 ºC for 22 hours under solvent free conditions. After that, Hexane was added to the reaction mixture and hexane layer was transferred to separating funnel. The residue was further washed with hexane twice and combined hexane layers were washed trice with water, separated, dried under sodium sulphate and concentrated under reduced pressure in a rotary evaporator. The resultant crude was further purified by silica gel column chromatography using 2 % Ethyl acetate in hexane as mobile phase which yielded pure farnesyl-2-bromoacetate in 82% isolated yield. ^{1}H NMR (400 MHz, $CDCl_3$) δ/ppm: 5.37-5.34 (t, 1H), 5.11-5.07 (t, 2H), 4.70-4.68 (d, 2H), 3.84 (s, 2H), 2.13-2.03 (m, 8H), 1.72-1.60 (m, 12 H); ESI-MS: calcd. for $C_{17}H_{27}BrO_2$: 342.12, found: 365.30 $[M + Na]^+$.

Synthesis of bis(farnesyl) 2,2'-((2-bromoethyl)azanediyl)diacetate ***(13, Scheme 6.4)***

2-Bromoethylamine (0.4 g, 1.9 mmol) in DMF (1 mL) was dropwise added to the mixture of Farnesyl 2-bromoacetate (2 g, 5.8 mmol) and DIPEA (1 g, 7.8 mmol) in DMF (2 mL). The mixture was stirred at room temperature overnight. Then, EA (100 mL) was added to the reaction mixture and washed with water (60 mL X 3) and with brine (60 mL X 2). The organic layer was dried over sodium sulphate and concentrated under reduced pressure in a rotary evaporator. The residue was subjected to silica gel column chromatography and the pure product was eluted with 2-3 % EA in hexane (yield, 49 %). ^{1}H NMR (400 MHz, $CDCl_3$) δ/ppm: 5.35-5.31 (t, 2H), 5.11-5.08 (t, 4H), 4.64-4.62 (d, 4H), 3.60 (s, 4H), 3.44-3.40 (t, 2H), 3.18-3.14 (t, 2H), 2.10-1.97 (m, 16H), 1.71-1.55 (m, 24H); ESI-MS: calcd. for $C_{36}H_{58}BrNO_4$: 647.35, found: 670.45 $[M + Na]^+$.

6.4.3. Conjugation of hydrophobic tail to the cationic head groups (Scheme 6.5).

Synthesis of N,N,N-trimethyl-2-(2-oxo-4-(2-oxo-2-((farnesyl)oxy)ethyl)piperazin-1-yl)ethanaminium ***(14, Scheme 6.5)***

bis(farnesyll) 2,2'-((2-bromoethyl)azanediyl)diacetate (0.1 g, 0.154 mmol) was dissolved in 1 mL of acetonitrile and K_2CO_3 (0.07 g, 0.46 mmol) was added. Then, 2-amino-N,N,N-trimethylethanaminium (0.067 g, 0.308 mmol) in 2 mL of acetonitrile was added dropwise. The reaction was stirred at room temperature for 24 hours. K_2CO_3 was filtered off using acetonitrile as solvent. Solvent was removed under reduced pressure and the resultant crude was washed with hexane. The residue was added with chloroform and filtered. Filtrate was concentrated to afford pure target lipid with 50 % yield. ^{1}H NMR (400 MHz, $CDCl_3$) δ/ppm: 5.35-5.31 (t, 1H), 5.11-5.07 (t, 2H), 4.66-4.64 (d, 2H), 4.14-4.11 (t, 2H), 3.91-3.89 (t, 2H), 3.72-3.69 (t, 2H), 3.45 (s, 9H), 3.35 (s, 2H), 3.31 (s, 2H), 2.97-2.94 (t, 2H), 2.10-1.96 (m, 8H), 1.71-1.60 (m, 12H); ^{13}C NMR (400 MHz, $CDCl_3$) δ/ppm: 169.58, 167.90, 143.14, 135.67, 131.34, 124.29, 117.66, 62.44, 61.80, 57.47, 56.49, 54.12, 49.30, 47.65, 40.83, 39.68, 39.54,

31.97, 26.71, 26.05, 25.69, 23.37, 17.69, 16.53, 16.03; ESI-MS: calcd. for $C_{26}H_{46}N_3O_3^+$: 448.35, found: 448.40 $[M]^+$.

Synthesis of 2-hydroxy-N,N-dimethyl-N-(2-(2-oxo-4-(2-oxo-2-((farnesyl)oxy)ethyl)piperazin-1-yl)ethyl)ethanaminium ***(15, Scheme 6.5)***

bis(farnesyll) 2,2'-((2-bromoethyl)azanediyl)diacetate (0.1 g, o,154 mmol) was dissolved in 1 mL of acetonitrile and K_2CO_3 (0.07 g, 0.46 mmol) was added. Then, 2-amino-N-(2-hydroxyethyl)-N,N-dimethylethanaminium (0.076 g, 0.308 mmol) in 2 mL of DMF was added dropwise. The reaction was stirred at room temperature for 24 hours. K_2CO_3 was filtered off using acetonitrile as solvent. Solvent was removed under reduced pressure and the resultant crude was washed with hexane. The residue was added with chloroform and filtered. Filtrate was concentrated to afford pure target lipid with 50 % yield. ^{1}H NMR (400 MHz, $CDCl_3$) δ/ppm: 5.34-5.31 (t, 1H), 5.11-5.07 (t, 2H), 4.65-4.63 (d, 2H), 4.16-4.12 (m, 2H), 3.90-3.86 (m, 3H), 3.80-3.72 (m, 2H), 3.62-3.58 (t, 2H), 3.39 (s, 6H), 3.33 (s, 2H), 3.31 (s, 2H), 3.16-3.14 (m, 2H), 2.93-2.91 (t, 2H), 2.10-1.96 (m, 8H), 1.71-1.60 (m, 12H); ^{13}C NMR (400 MHz, $CDCl_3$) δ/ppm: 169.68, 167.76, 143.13, 131.33, 124.29, 123.54, 123.36, 117.66, 66.31, 61.80, 61.12, 57.42, 56.44, 55.82, 52.57, 49.25, 47.62, 40.78, 39.68, 39.55, 31.96, 29.68, 26.71, 25.69, 23.37, 17.69, 16.53, 16.02; ESI-MS: calcd. for $C_{26}H_{46}N_3O_3^+$: 478.36, found: 478.40 $[M]^+$.

Synthesis of 2-hydroxy-N-(2-hydroxyethyl)-N-methyl-N-(2-(2-oxo-4-(2-oxo-2-((farnesyl)oxy)ethyl)piperazin-1-yl)ethyl)ethanaminium ***(16, Scheme 6.5)***

bis(farnesyll) 2,2'-((2-bromoethyl)azanediyl)diacetate (0.1 g, o,154 mmol) was dissolved in 1 mL of acetonitrile and K_2CO_3 (0.07 g, 0.46 mmol) was added. To this mixture 2-amino-N,N-bis(2-hydroxyethyl)-N-methylethanaminium (0.085 g, 0.308 mmol) in 2 mL of DMF was added dropwise. The reaction was stirred at room temperature for 24 hours. K_2CO_3 was filtered off using acetonitrile as solvent. Solvent was removed under reduced pressure and the resultant crude was washed with hexane. The residue was added with chloroform and filtered. Filtrate was concentrated to afford pure target lipid with 43 % yield. ^{1}H NMR (400

MHz, $CDCl_3$) δ/ppm: 5.34-5.31 (t, 1H), 5.11-5.09 (t, 2H), 4.64-4.62 (d, 2H), 4.16-4.14 (m, 4H), 4.07-4.03 (m, 2H), 3.66-3.65 (m, 2H), 3.58-3.50 (m, 11H), 2.92-2.87 (m, 2H), 2.17-1.97 (m, 8H), 1.68-1.53 (m, 12H); ^{13}C NMR (400 MHz, $CDCl_3$) δ/ppm: 171.25, 171.13, 142.87, 139.79, 135.52, 131.59, 131.34, 124.29, 123.54, 123.36, 117.63, 61.83, 61.59, 59.38, 57.79, 55.19, 51.47, 39.69, 39.55, 31.97, 29.69, 26.71, 26.57, 25.72, 25.68, 23.36, 17.69, 16.53, 16.02; ESI-MS: calcd. for $C_{28}H_{50}N_3O_5^+$: 508.37, found: 508.45 $[M]^+$.

Synthesis of 2-hydroxy-N,N-bis(2-hydroxyethyl)-N-(2-(2-oxo-4-(2-oxo-2-((farnesyl)oxy)ethyl)piperazin-1-yl)ethyl)ethanaminium ***(17, Scheme 6.5)***

bis(farnesyll) 2,2'-((2-bromoethyl)azanediyl)diacetate (0.1 g, 0.154 mmol) was dissolved in 1 mL of acetonitrile and K_2CO_3 (0.07 g, 0.46 mmol) was added. To this mixture 2-amino-N,N,N-tris(2-hydroxyethyl)ethanaminium (0.095 g, 0.308 mmol) in 2 mL of DMF was added dropwise. The reaction was stirred at room temperature for 24 hours. K_2CO_3 was filtered off using acetonitrile as solvent. Solvent was removed under reduced pressure and the resultant crude was washed with hexane. The residue was added with chloroform and filtered. Filtrate was concentrated to afford pure target lipid with 45 % yield. ^1H NMR (400 MHz, $CDCl_3$) δ/ppm: 5.34-5.31 (t, 1H), 5.11-5.07 (t, 2H), 4.66-4.61 (d, 2H), 4.16-4.06 (m, 6H), 3.96-3.90 (m, 2H), 3.80-3.60 (m, 12H), 3.50-3.38 (m, 2H), 3.29 (s, 2H), 2.86-2.84 (t, 2H), 2.09-1.97 (m, 8H), 1.76-1.59 (m, 12H); ^{13}C NMR (400 MHz, $CDCl_3$) δ/ppm: 161.93, 161.59, 143.13, 135.51, 131.31, 124.40, 123.57, 123.36, 62.04, 61.79, 57.29, 55.40, 39.69, 39.56, 31.96, 29.71, 26.72, 26.56, 26.25, 26.06, 25.68, 24.49, 23.36, 17.68, 16.46, 16.00; ESI-MS: calcd. for $C_{28}H_{50}N_3O_5^+$: 538.38, found: 538.45 $[M]^+$

SPECTRA

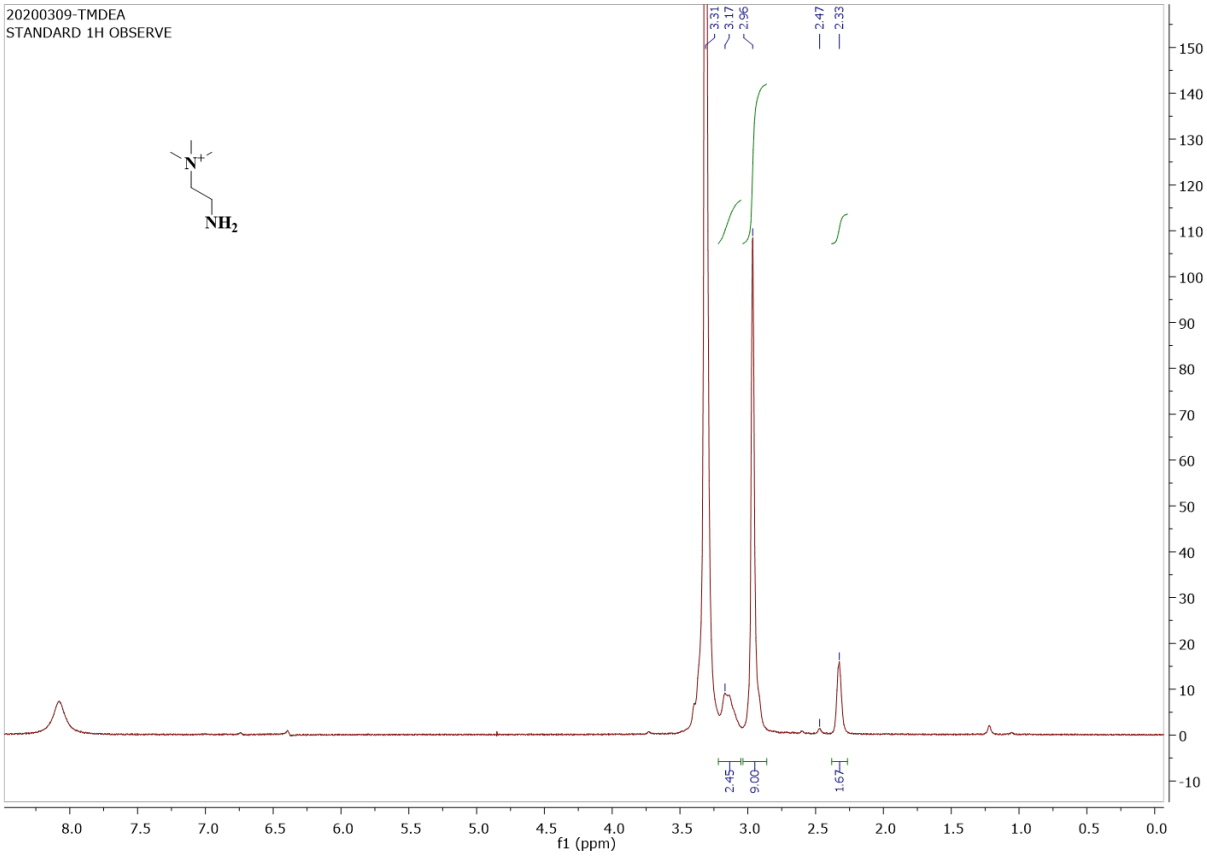

^{1}H NMR Spectrum of compound 3 in DMSO-D_6

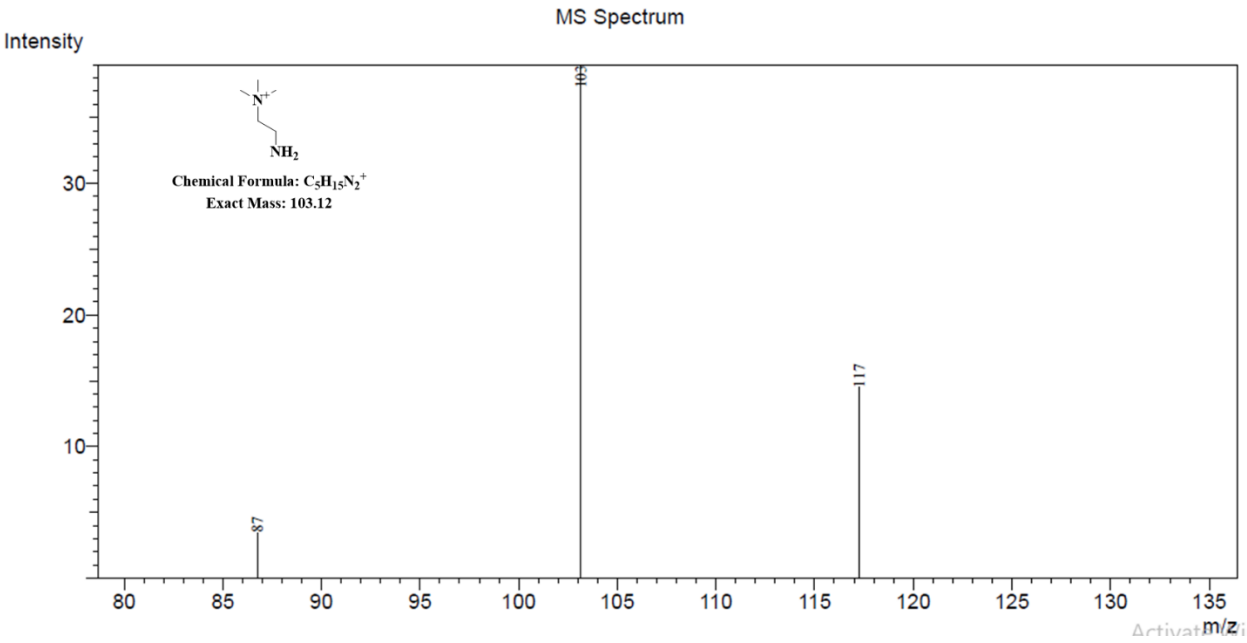

Mass spectrum of Compound 3

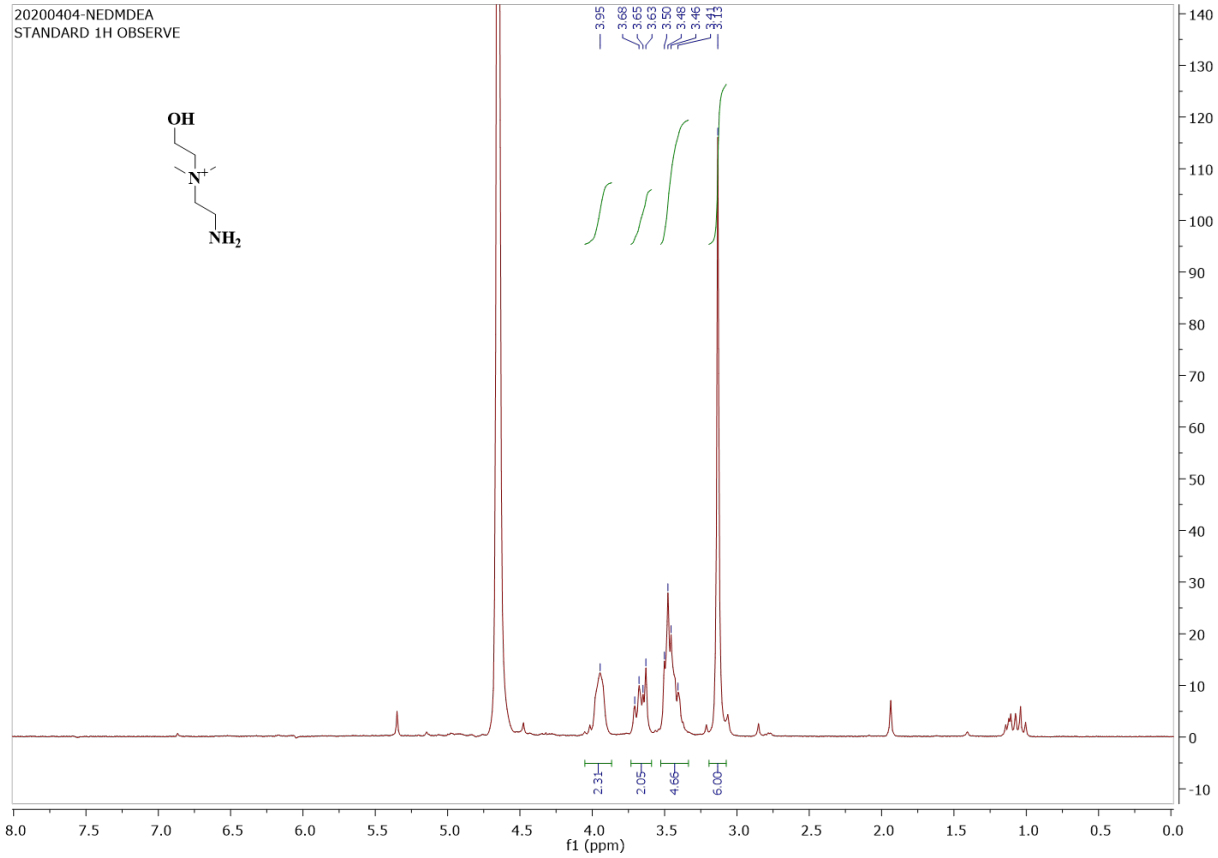

^{1}H NMR Spectrum of compound 5 in D_2O

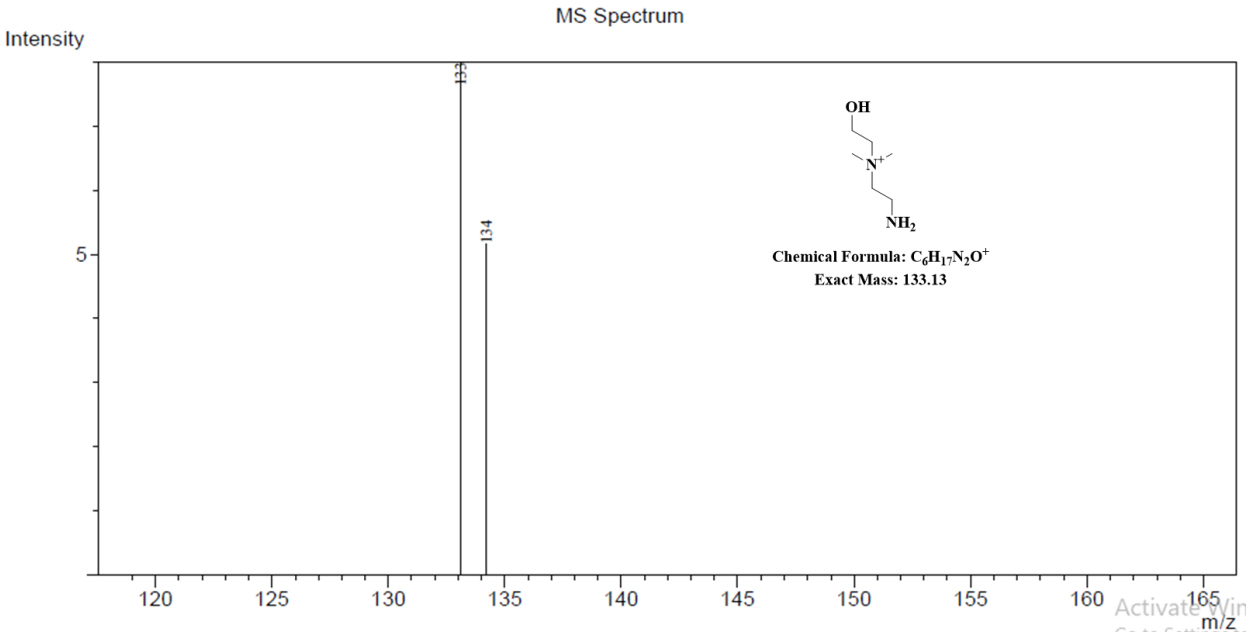

Mass spectrum of Compound 5

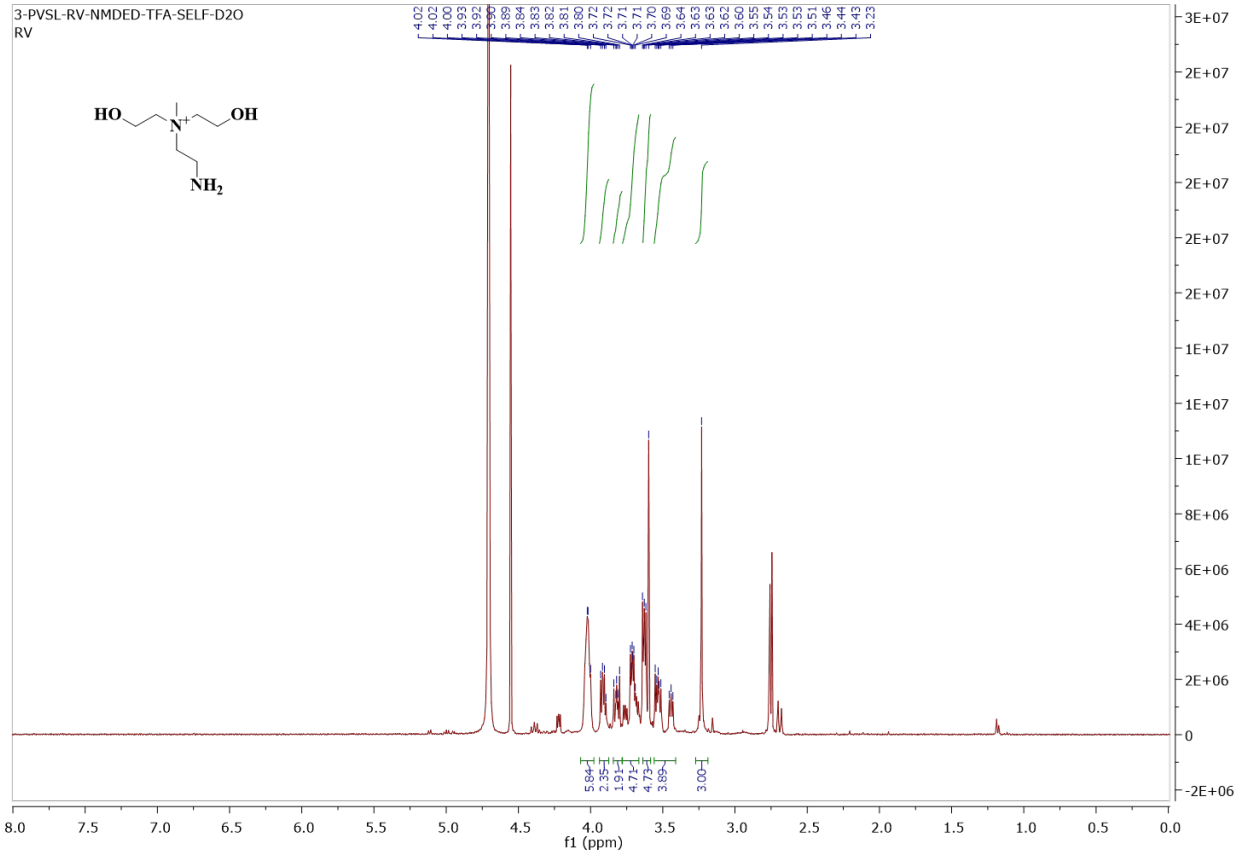

^{1}H NMR Spectrum of compound 8 in $CDCl_3$

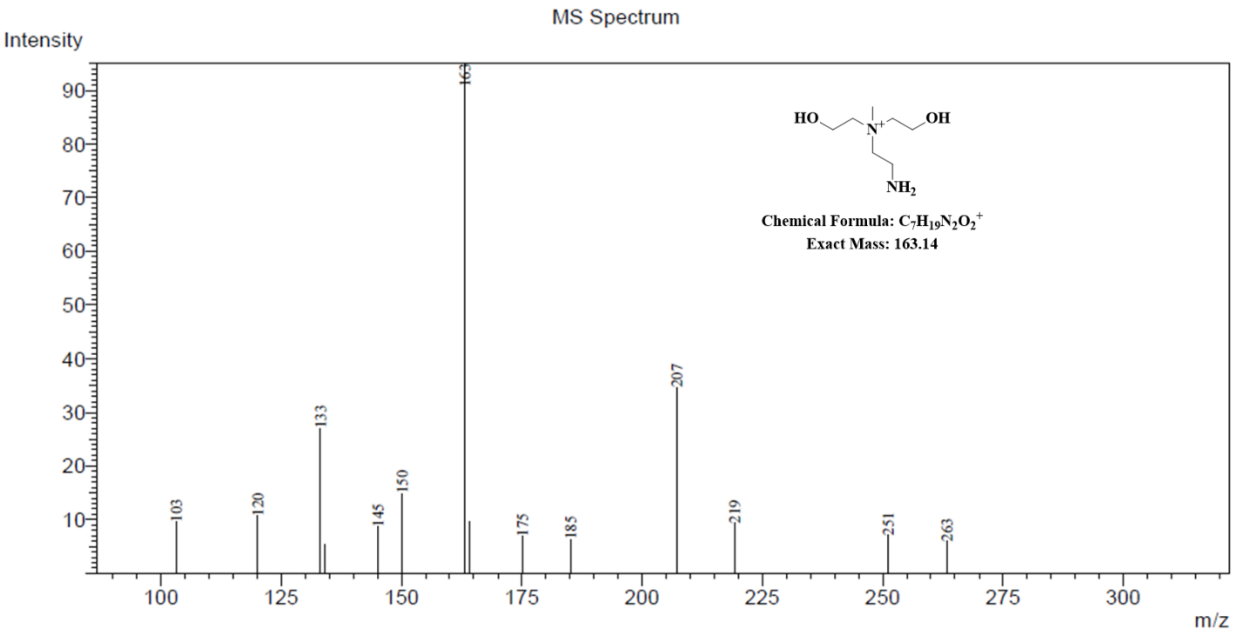

Mass spectrum of Compound 8

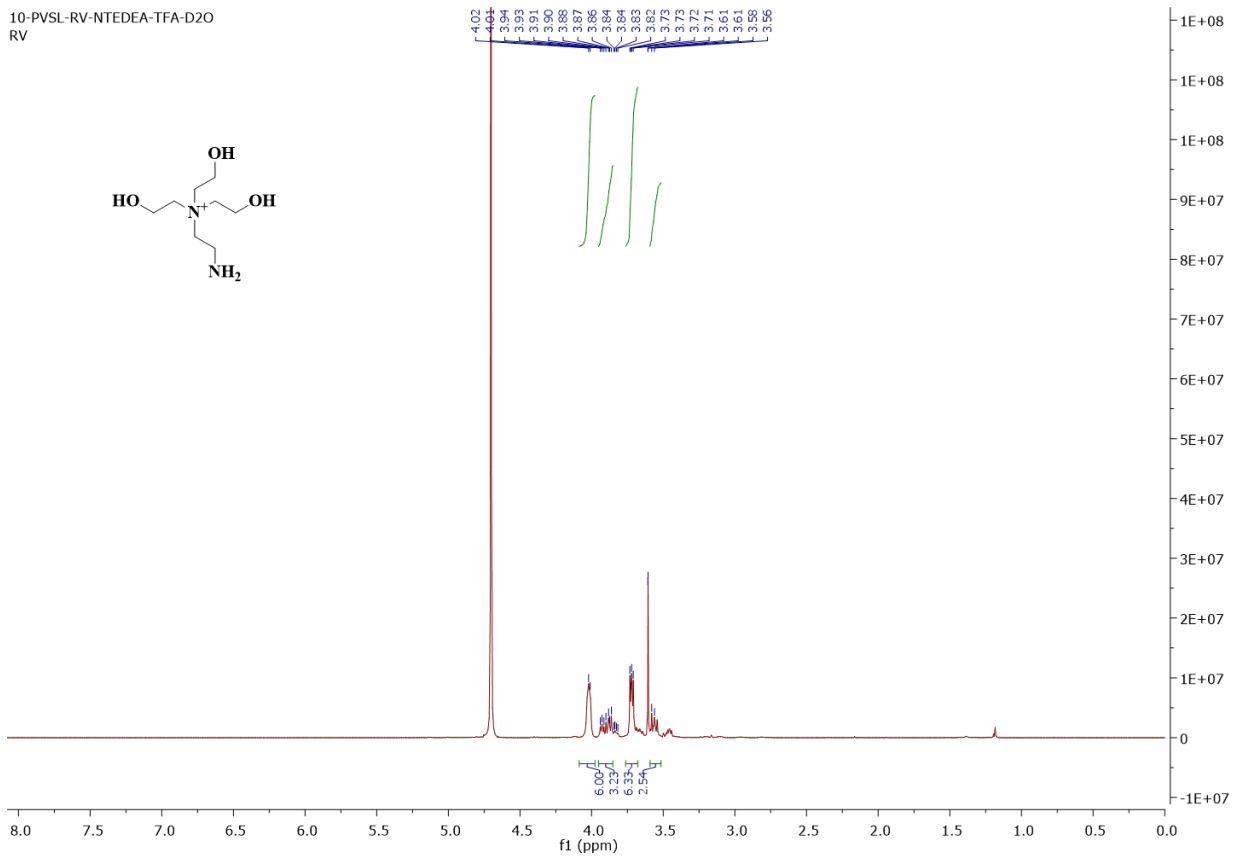

^{1}H NMR Spectrum of compound 11 in $CDCl_3$

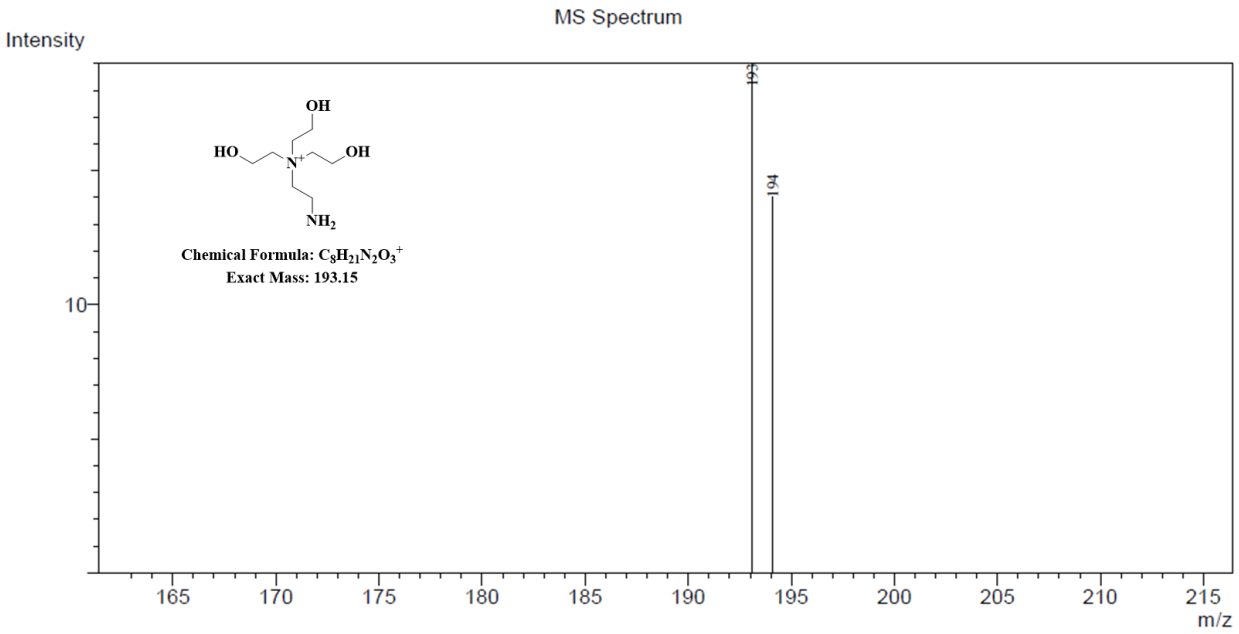

Mass spectrum of Compound 11

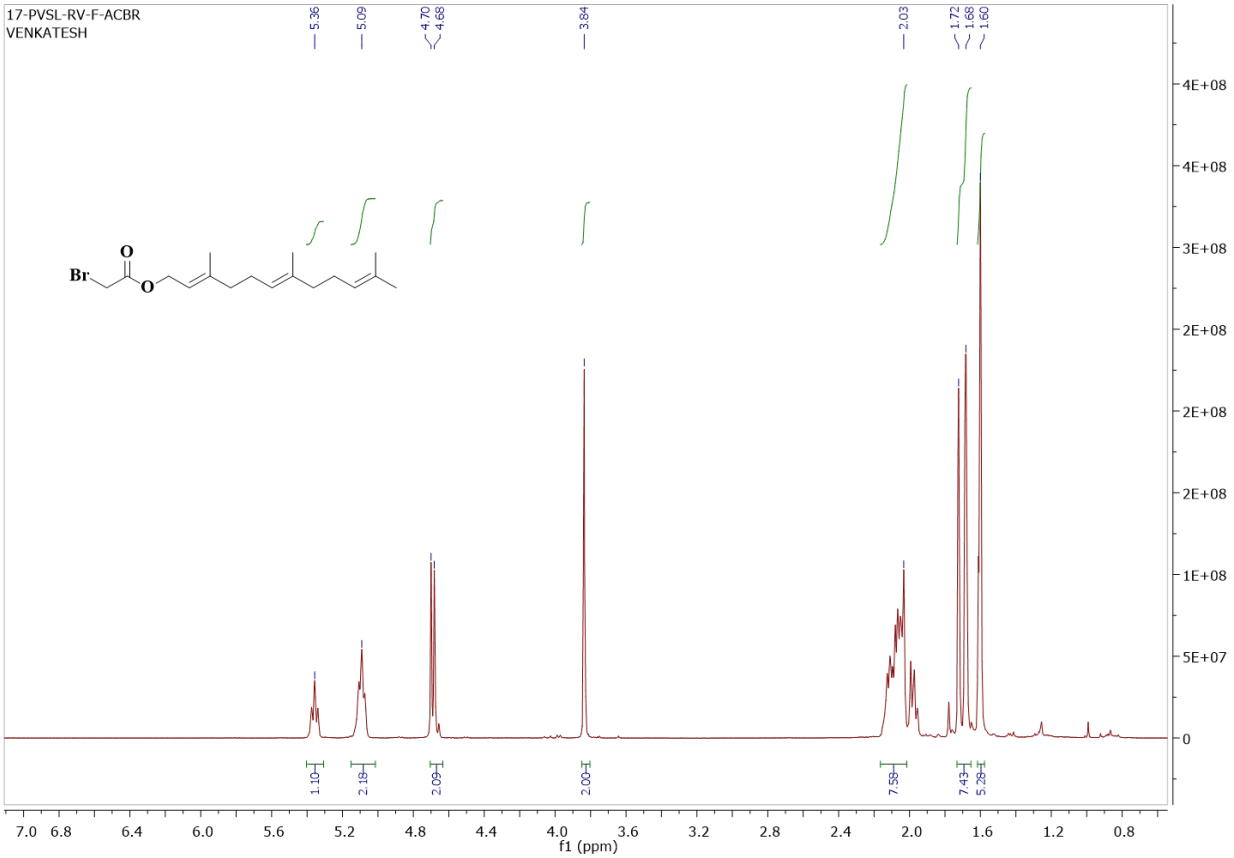

^{1}H NMR Spectrum of compound 12 in $CDCl_3$

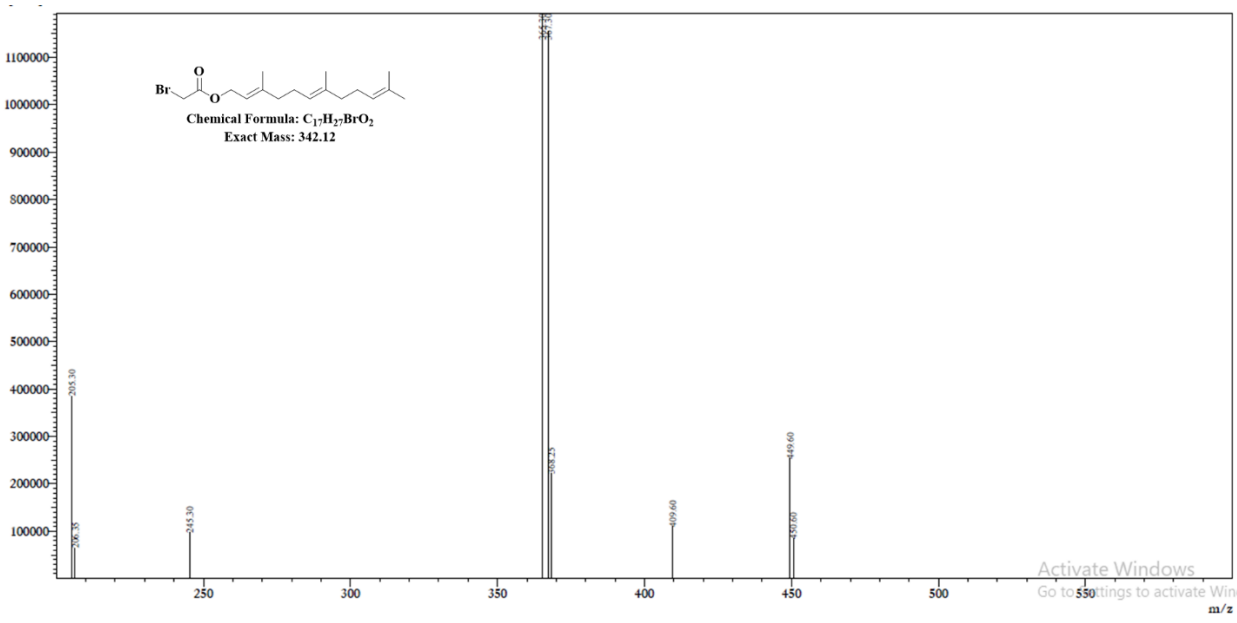

Mass spectrum of Compound 12

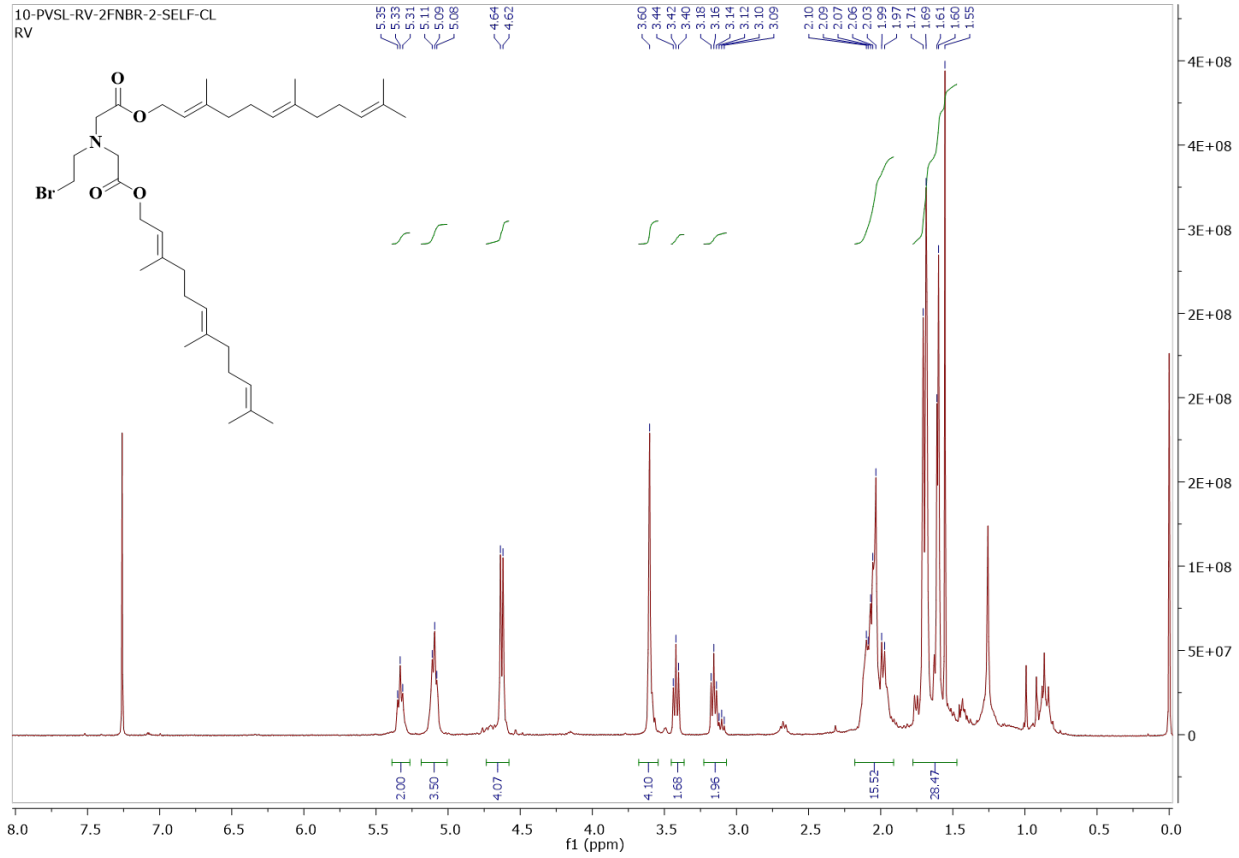

^{1}H NMR Spectrum of compound 13 in $CDCl_3$

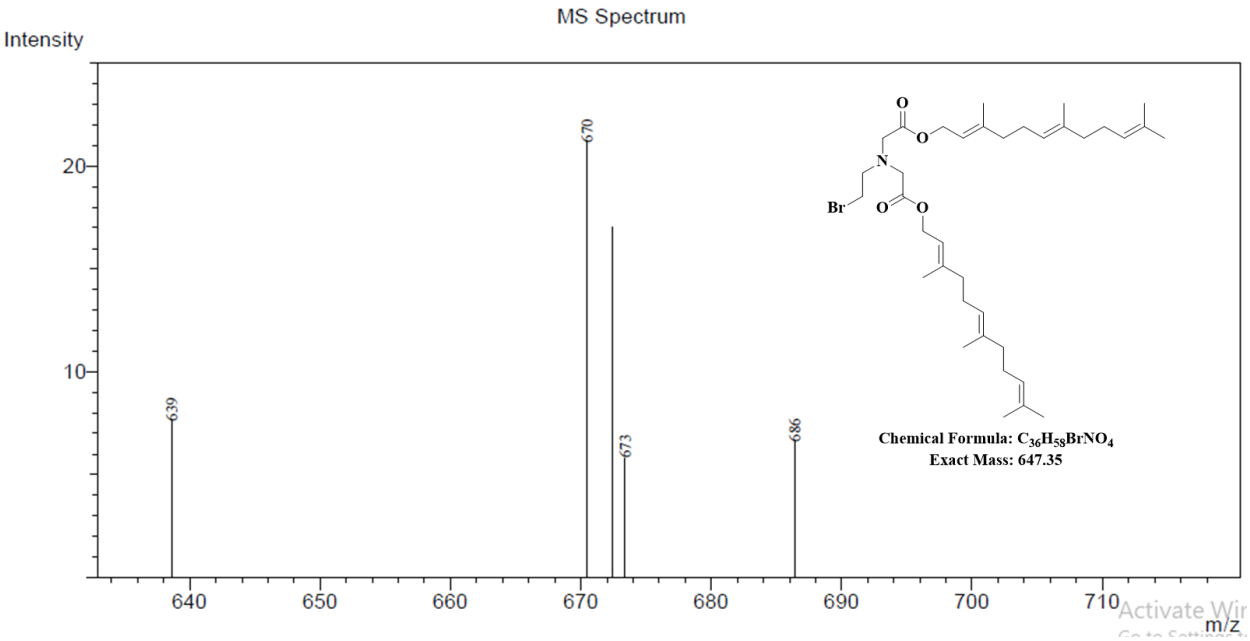

Mass spectrum of Compound 13

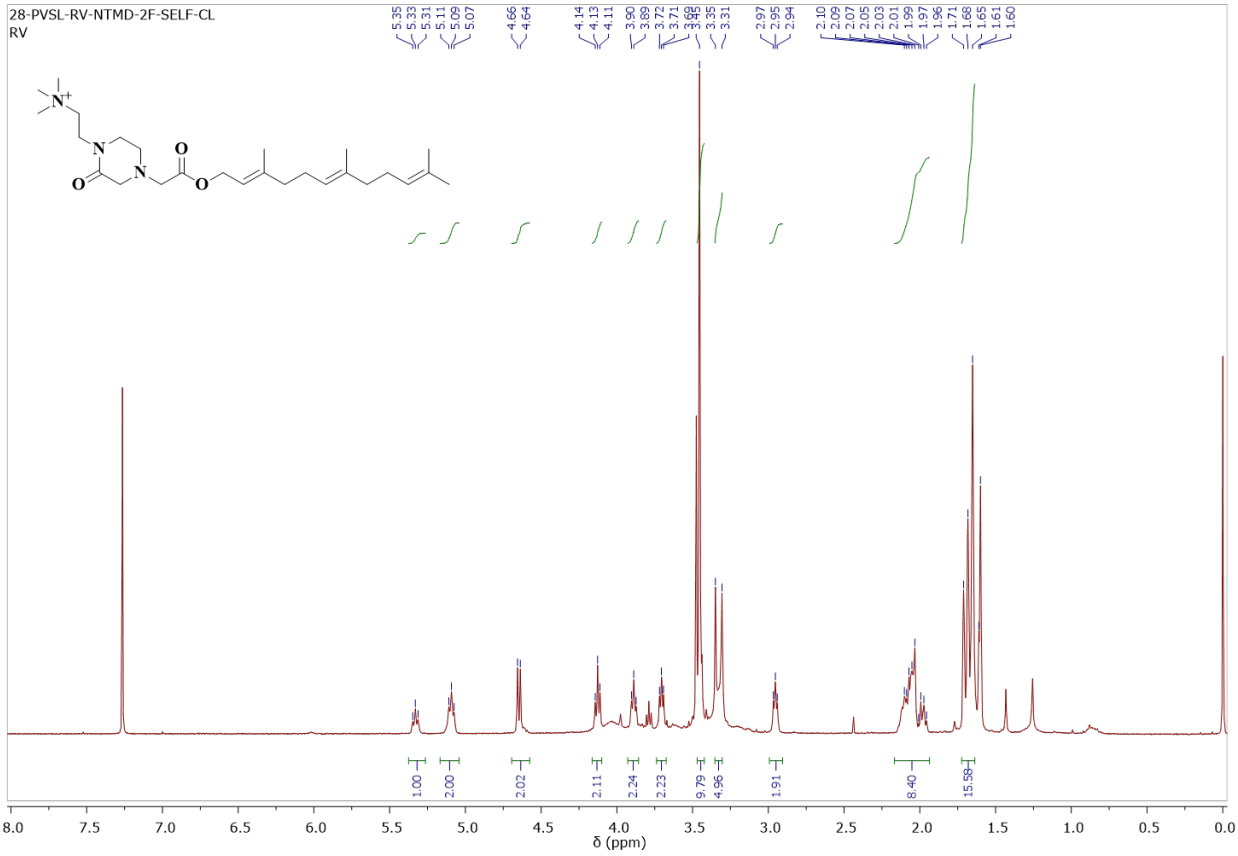

^{1}H NMR Spectrum of compound 14 in $CDCl_3$

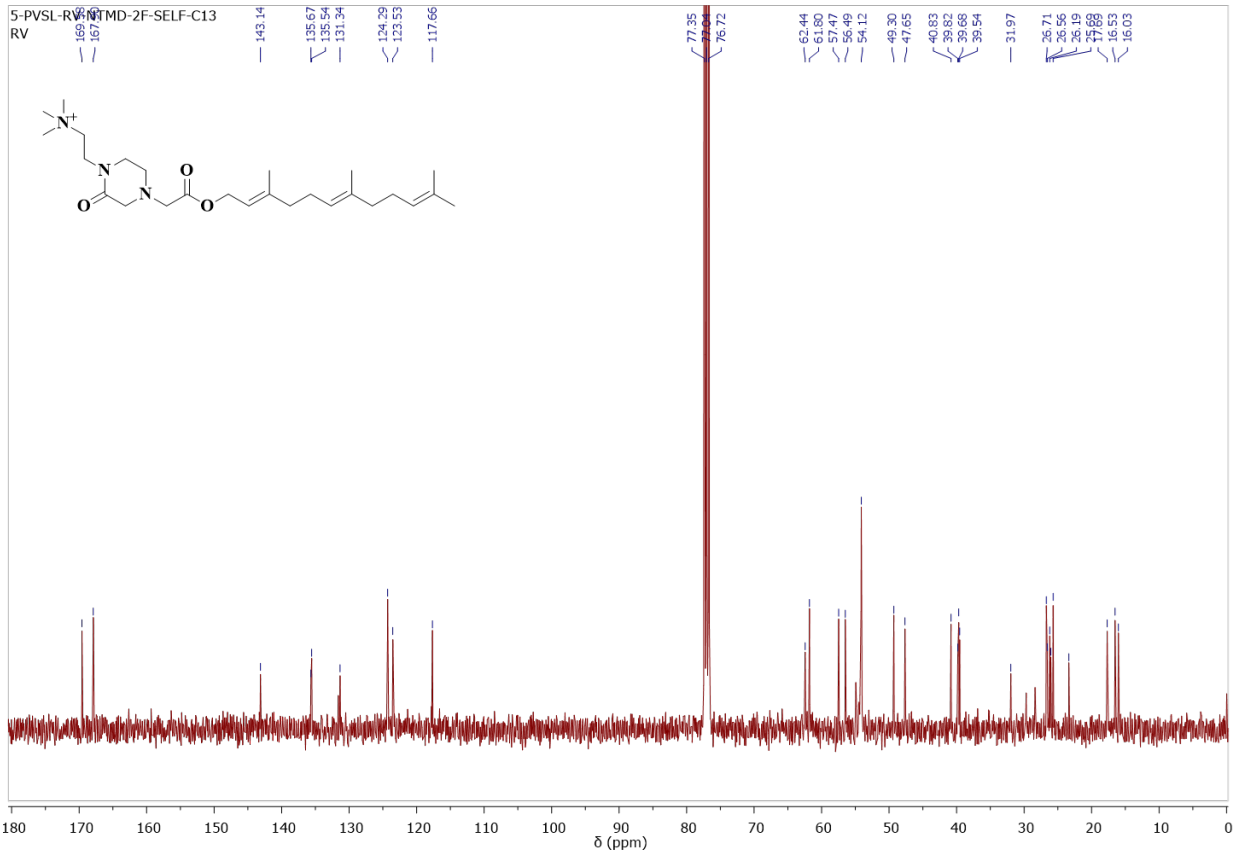

^{13}C NMR Spectrum of compound 14 in $CDCl_3$

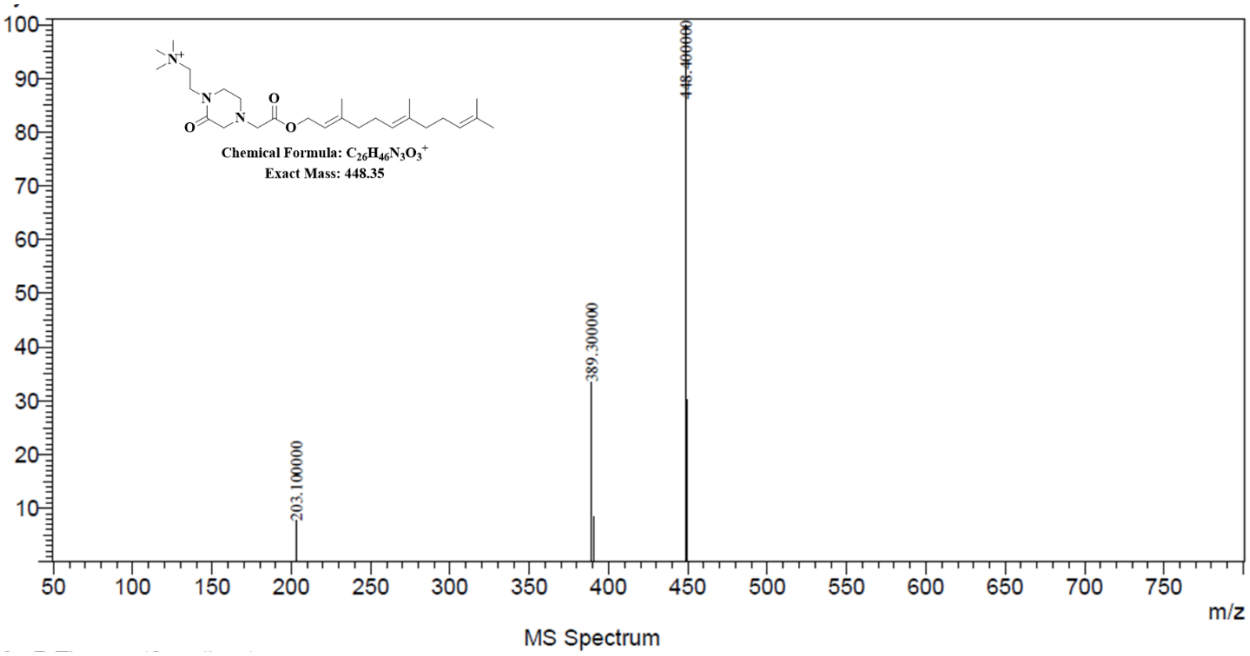

Mass spectrum of Compound 14

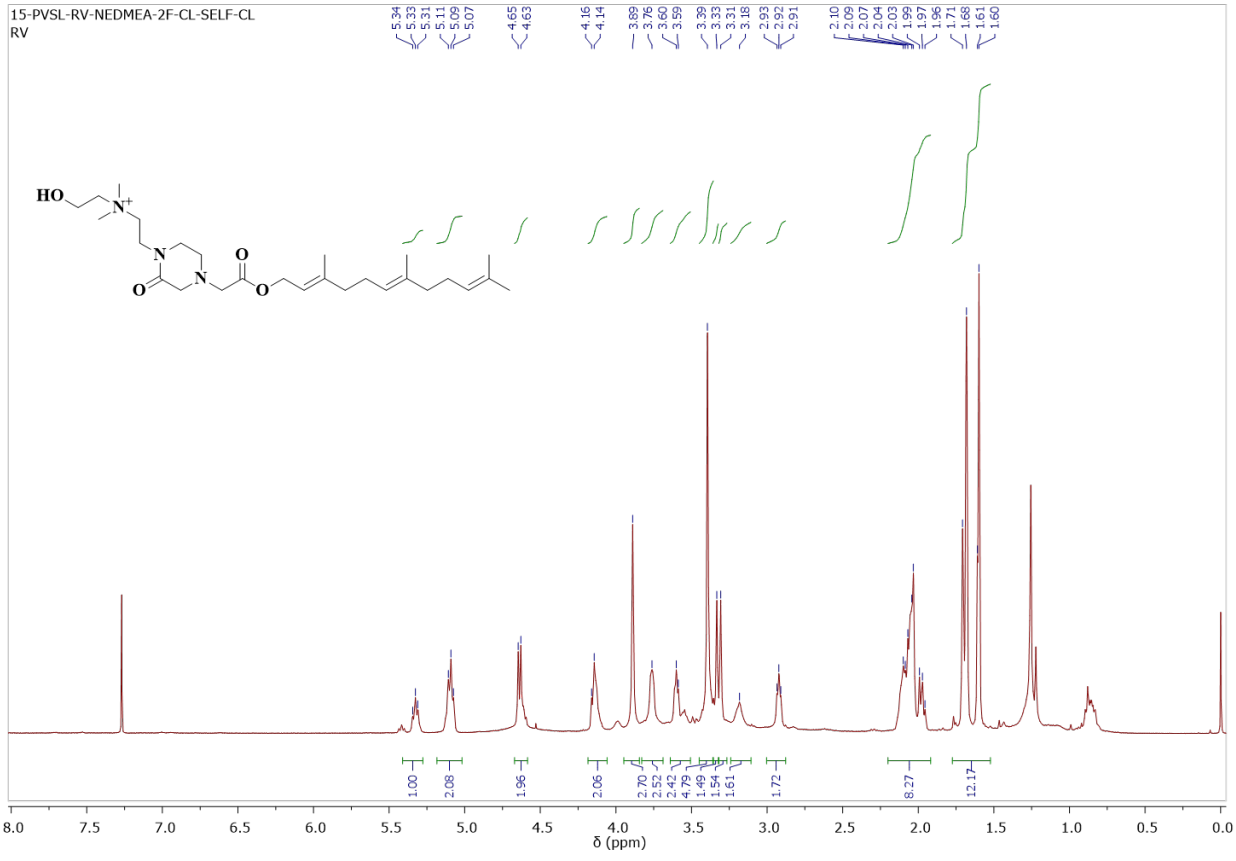

^{1}H NMR Spectrum of compound 15 in $CDCl_3$

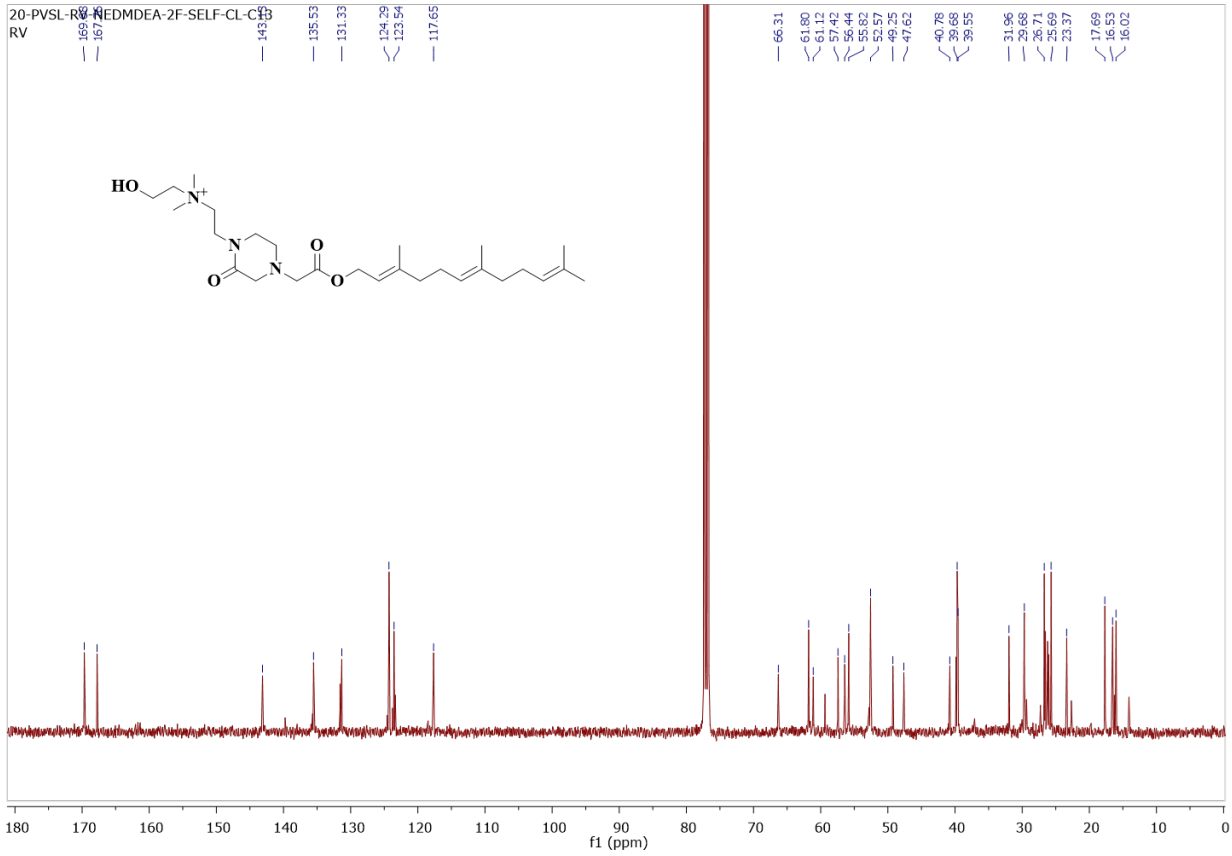

^{13}C NMR Spectrum of compound 15 in $CDCl_3$

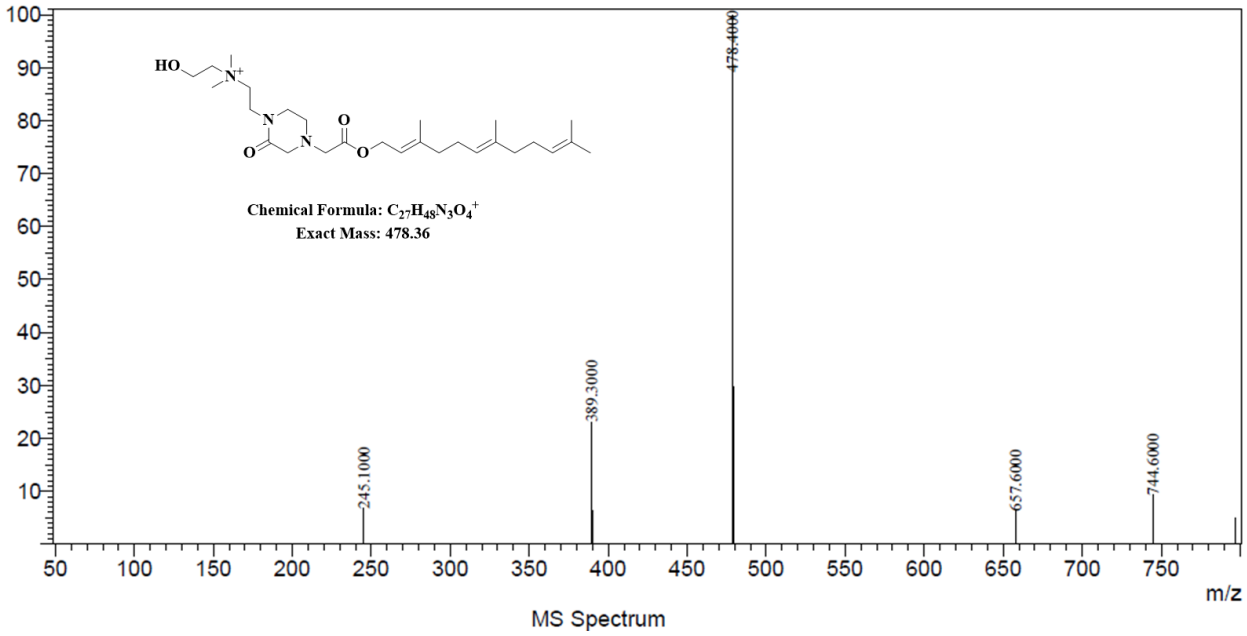

Mass spectrum of Compound 15

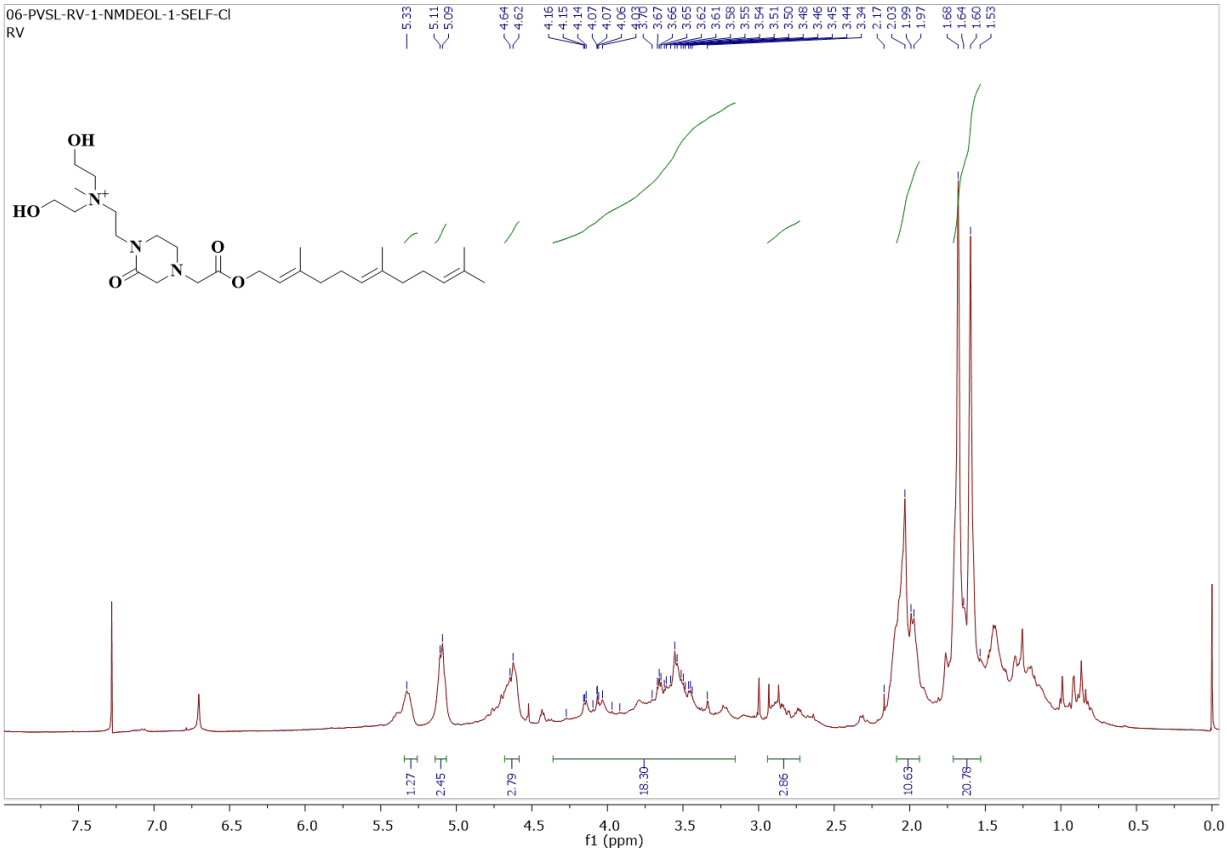

^{1}H NMR Spectrum of compound 16 in $CDCl_3$

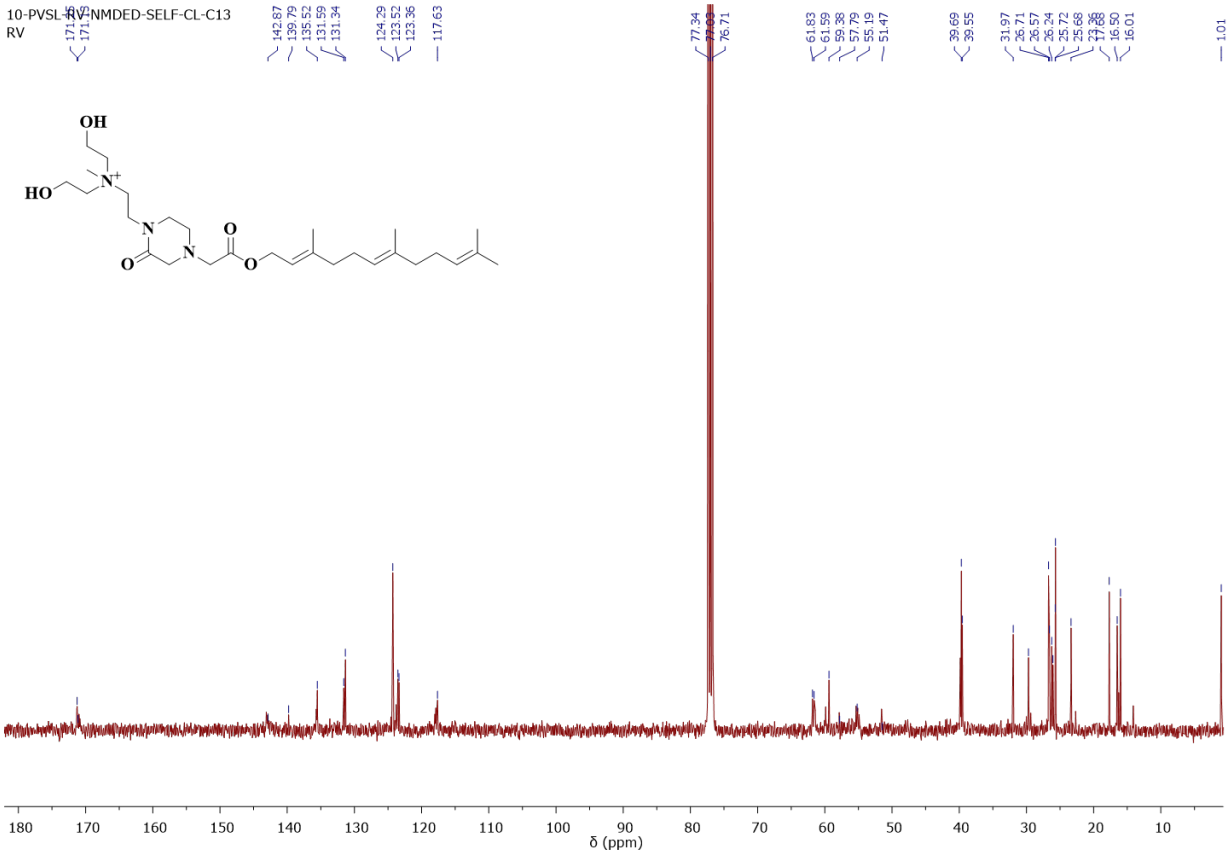

^{13}C NMR Spectrum of compound 16 in $CDCl_3$

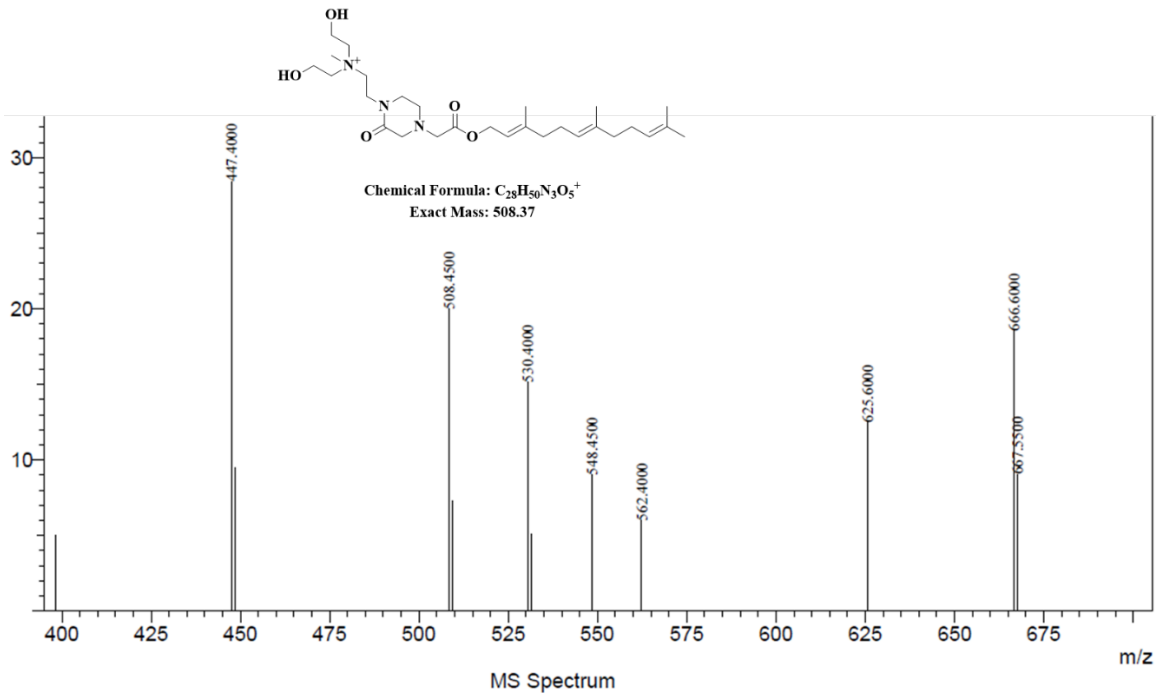

Mass spectrum of Compound 16

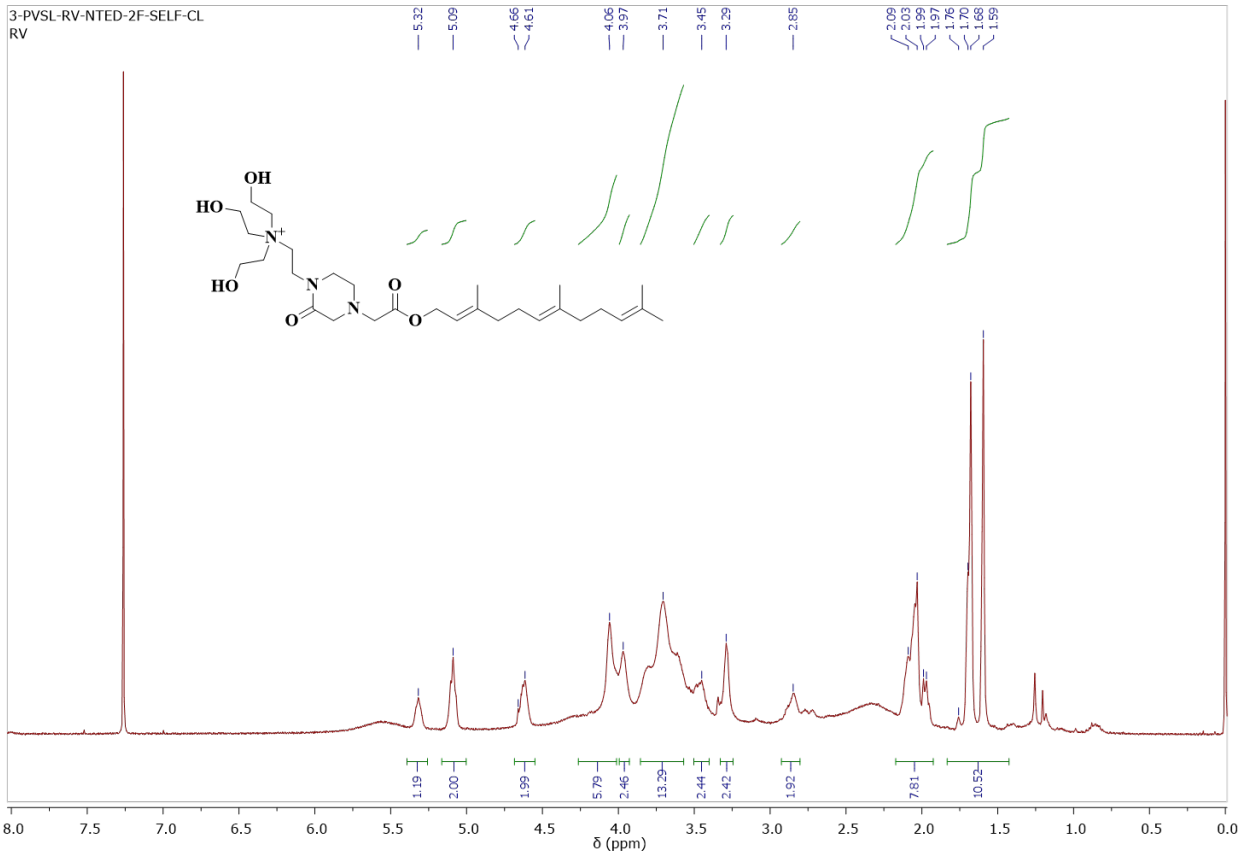

^{1}H NMR Spectrum of compound 17 in $CDCl_3$

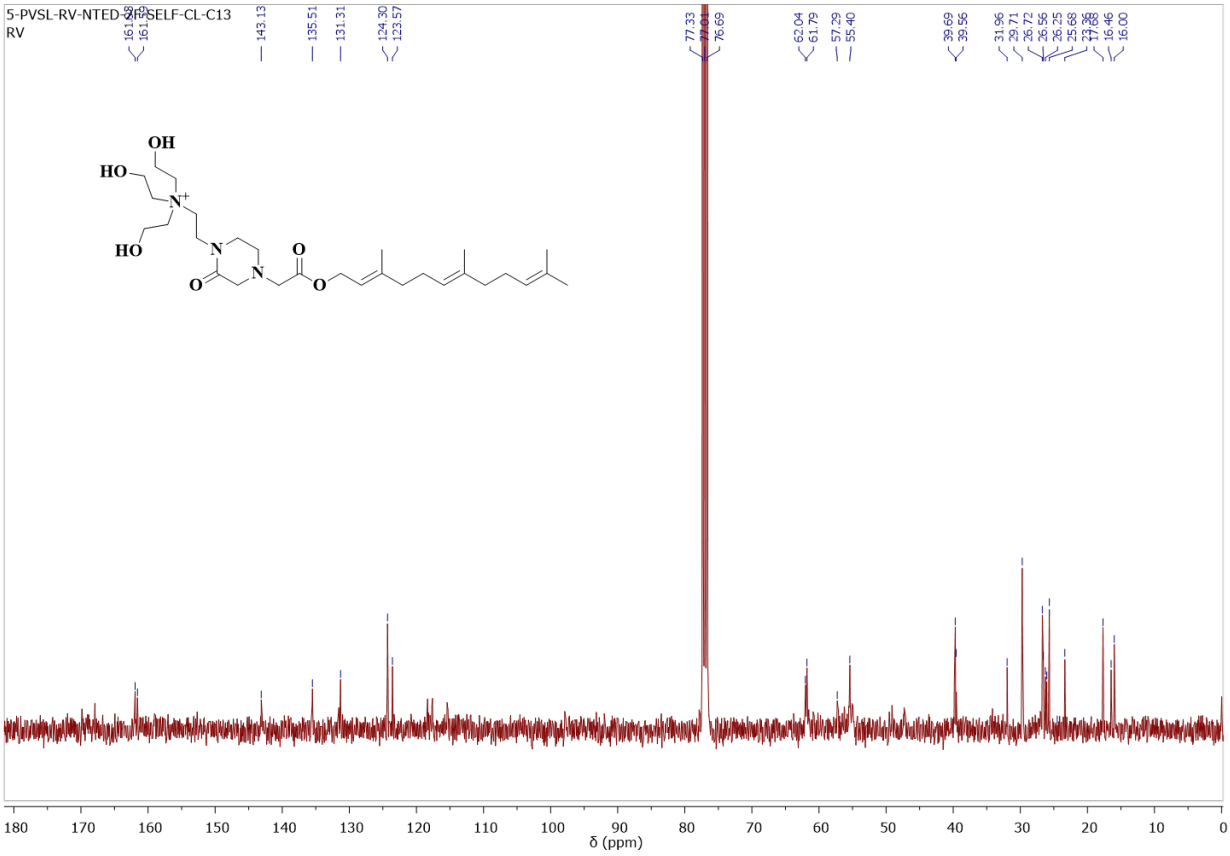

^{13}C NMR Spectrum of compound 17 in $CDCl_3$

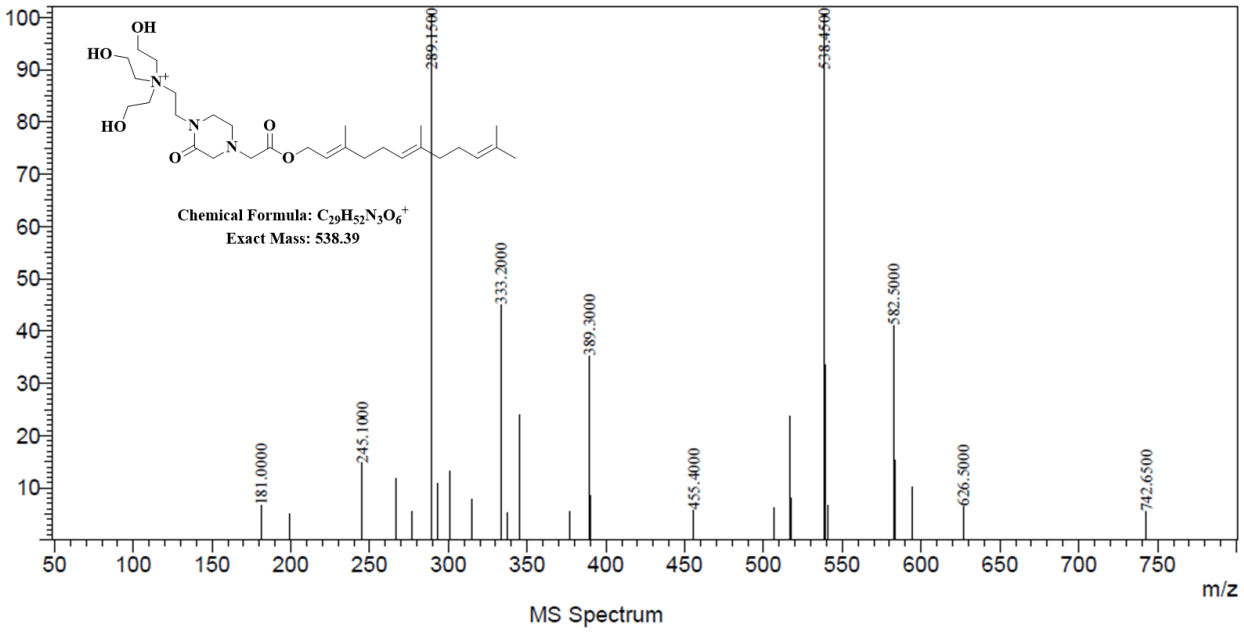

Mass spectrum of Compound 17

SUMMARY AND CONCLUSIONS

The vectors that can integrate the therapeutic gene at the disease location are critical to the success of gene therapy. The therapeutic impact is achieved by the delivered gene, either by producing therapeutic protein or by counteracting the faulty gene. Liposomal gene delivery is a well-established research subject that has drew the attention of a number of scientists who are working to produce efficient gene delivery vehicles based on cationic liposomes. Cationic liposomes have several advantages, including a low immunogenic response, the ability to modify their structure, and the ability to produce large quantities. However, the most effective cationic lipids have a low biosafety rating. Commercial liposomes such as Lipofectamine 2000 and 1,2-dioleoyl-3-trimethylammonium-propane (DOTAP), for example, have good transfection ability but high cytotoxicity. The use of bio-based natural molecules to make cationic liposomes appears to be a method that allows for high transfection without compromising safety. In this context, the present thesis illustrates, design, synthesis and *in vitro* gene transfer ability of several cationic lipids made up of biologically active molecules, such as, amino acids, peptides, sugar-mimicking molecules, vitamin E and farnesol.

Chapter II demonstrates the successful delivery of plasmid encoding tumor necrosis factor (TNF)-related apoptosis-inducing ligand (pTRAIL) using arginine- conjugated tocopherol lipid (AT) nanovesicles into glioblastoma cell lines. Another cationic lipid, glycine-conjugated tocopherol lipid (GT) having glycine in the head group region is also synthesized as a control lipid. Both lipid-derived liposomes effectively condensed the pDNA and the corresponding biomacromolecular assemblies (lipoplexes) are efficiently transfected into different cell lines. AT-based liposomes exhibit higher transfection efficacy in various cell lines, particularly selective in glioma cell lines. At an optimized N/P ratio, both the liposomal formulations show low cytotoxicity. AT-based lipoplexes have superior cellular uptake in U87 than the control lipid GT. The expression of TRAIL protein regulated death receptor and

apoptosis signaling pathway is assayed by western blot using transfection of AT-based/pTRAIL into U87 cell lines. Induction of apoptosis in U87 cells exposed to AT-based/pTRAIL plasmid is evaluated by MTT assay as well as Annexin V-Propidium iodide dual-staining assay. All results indicate that the developed AT-based/pTRAIL system offers a potentially safe and efficient therapeutic strategy for glioblastoma gene therapy.

Chapter III describes the design, synthesis and application of a novel cationic gemini lipopeptide for gene delivery. An ultrashort peptide, containing four amino acids, arginine-cysteine-cysteine-arginine, serves as cationic head group and two α-tocopherol moieties as hydrophobic anchoring groups. The new lipopeptide (ATTA) is formulated at different molar ratios into liposomes with conventional lipids, 1,2-dioleoyl-3-trimethylammonium-propane (DOTAP) and 1,2-dioleoyl-sn-glycerol-3-phosphoethanolamine (DOPE). The formulated liposomes are characterized and screened for better transfection efficiency. Transfection activity in multiple human cell lines from cancerous and non-cancerous origins, indicates that the inclusion of optimal ratio of ATTA in the liposomes substantially enhances transfection efficiency superior to a traditional liposome, DOTAP-DOPE. Cytotoxicity of ATTA-containing formulations against multiple cell lines indicates potentially distinct activity between cancer and non-cancer cell lines. Furthermore, lipoplexes of the ATTA-containing formulations with anticancer therapeutic gene, pTRAIL (plasmid encoding tumour necrosis factor-related apoptosis-inducing ligand), induce obviously more cytotoxicity than conventional formulations. The results indicate that arginine rich cationic lipopeptide appears to be a promising ingredient in gene delivery vector formulations to enhance transfection efficiency and cell selective cytotoxicity.

Chapter IV demonstrates the liposomal formulations of two newly synthesized amino acid based cationic lipids and commercial lipids, DOTAP and DOPE. Co-liposomal formulations were characterized for their physicochemical properties and DNA binding.

DOTAP incorporated formulations (DtATD and DtCTTD) exhibited lower particles size, higher positive zeta potential and better DNA binding ability. Transfection optimized lipid-DNA complexes of DOTAP incorporated formulations had greater efficacy than their counterparts without DOTAP. Particularly, DtCTTD has shown superior transfection capability in PC3 and A549 cell lines in comparison with commercial transfection reagent, Lipofectamine. Additionally, all these new formulations are found to be less toxic than Lipofectamine. Taken together, the above findings may infer that these DOTAP incorporated formulations derived from amino acid based liposomes are promising tools for improving the transfection efficacy with low toxicity.

Chapter V describes the synthesis of three new cationic lipid analogues with or without sugar-like multi-hydroxyl functional head groups. All of the lipid formulations were thoroughly characterized by means of DNA binding ability, size and zeta potential. Optimal N/P ratios of each lipid-DNA complex were elucidated by their transfection efficiency in HEK-293 cells. Sugar-mimicking cationic lipids, TS1 and TS2, exhibited superior transfection properties in HEPG2 cell line, whereas this property was reversed in the case of U87 cell line. The results point out that the transfection efficiencies of sugar alcohol-based cationic lipids are cell-dependant. Cytotoxicity of the lipid complexes through MTT based assay revealed that the sugar-mimicking cationic lipids are non-toxic towards the tested cell lines. In conclusion, the current paper adds knowledge on the sugar based cationic lipids and reiterates that these lipids could yield potential applications towards liver targeted gene delivery.

In Chapter VI, synthesis of a new series of cationic lipids with farnesol-based hydrophobic anchoring groups has been demonstrated. The methods involved individual synthesis of cationic head group, intermediate hydrophobic tail and finally conjugation of both groups to give target lipids. Each lipid was differed with other through its cationic head group. Quaternary ammonium head groups with increasing number of hydroxyethyl functional

moieties were linked to hydrophobic portion of lipid through piperazinone linkers. All the intermediate compounds were characterized by ^{1}H NMR and ESI-MS techniques. Final cationic lipids were characterised by ^{1}H, ^{13}C and ESI-MS techniques. The synthesized cationic lipids can be formulated into liposomes when mixed with helper lipids in aqueous medium. Future studies will be focussed on development of optimal liposomal formulations using the new farnesol based cationic lipids for gene delivery and on the study of their intracellular functions.

REFERENCES:

1. Staff, A. C., An introduction to gene therapy and its potential prenatal use. *Acta Obstet Gyn Scan* **2001,** *80* (6), 485-491.

2. Papanikolaou, E.; Bosio, A., The Promise and the Hope of Gene Therapy. *Frontiers in Genome Editing* **2021,** *3*.

3. Dunbar, C. E.; High, K. A.; Joung, J. K.; Kohn, D. B.; Ozawa, K.; Sadelain, M., Gene therapy comes of age. *Science* **2018,** *359* (6372).

4. Miller, A. D., Human gene therapy comes of age. *Nature* **1992,** *357* (6378), 455-60.

5. Anderson, W. F., Prospects for human gene therapy. *Science* **1984,** *226* (4673), 401-9.

6. Anderson, W. F., Gene therapy. The best of times, the worst of times. *Science* **2000,** *288* (5466), 627-9.

7. Goswami, R.; Subramanian, G.; Silayeva, L.; Newkirk, I.; Doctor, D.; Chawla, K.; Chattopadhyay, S.; Chandra, D.; Chilukuri, N.; Betapudi, V., Gene Therapy Leaves a Vicious Cycle. *Front Oncol* **2019,** *9*, 297.

8. Reed, J. C., Apoptosis-based therapies. *Nat Rev Drug Discov* **2002,** *1* (2), 111-21.

9. Somia, N.; Verma, I. M., Gene therapy: trials and tribulations. *Nat Rev Genet* **2000,** *1* (2), 91-9.

10. Ginn, S. L.; Amaya, A. K.; Alexander, I. E.; Edelstein, M.; Abedi, M. R., Gene therapy clinical trials worldwide to 2017: An update. *J Gene Med* **2018,** *20* (5), e3015.

11. Lebedeva, I. V.; Su, Z. Z.; Sarkar, D.; Fisher, P. B., Restoring apoptosis as a strategy for cancer gene therapy: focus on p53 and mda-7. *Semin Cancer Biol* **2003,** *13* (2), 169-178.

12. Griffith, T. S.; Stokes, B.; Kucaba, T. A.; Earel, J. K.; VanOosten, R. L.; Brincks, E. L.; Norian, L. A., TRAIL Gene Therapy: From Preclinical Development to Clinical Application. *Curr Gene Ther* **2009,** *9* (1), 9-19.

13. Fisher, P. B., Is mda-7/IL-24 a "magic bullet" for cancer? *Cancer Res* **2005,** *65* (22), 10128-10138.

14. Jia, L. T.; Chen, S. Y.; Yang, A. G., Cancer gene therapy targeting cellular apoptosis machinery. *Cancer Treat Rev* **2012,** *38* (7), 868-876.

15. Das, S. K.; Menezes, M. E.; Bhatia, S.; Wang, X. Y.; Emdad, L.; Sarkar, D.; Fisher, P. B., Gene Therapies for Cancer: Strategies, Challenges and Successes. *J Cell Physiol* **2015,** *230* (2), 259-271.

16. Vogelstein, B.; Lane, D.; Levine, A. J., Surfing the p53 network. *Nature* **2000,** *408* (6810), 307-10.

17. Matlashewski, G.; Lamb, P.; Pim, D.; Peacock, J.; Crawford, L.; Benchimol, S., Isolation and characterization of a human p53 cDNA clone: expression of the human p53 gene. *EMBO J* **1984,** *3* (13), 3257-62.

18. Wiman, K. G., The retinoblastoma gene: role in cell cycle control and cell differentiation. *FASEB J* **1993,** *7* (10), 841-5.

19. Shanker, M.; Jin, J.; Branch, C. D.; Miyamoto, S.; Grimm, E. A.; Roth, J. A.; Ramesh, R., Tumor suppressor gene-based nanotherapy: from test tube to the clinic. *J Drug Deliv* **2011,** *2011*, 465845.

20. Walczak, H.; Krammer, P. H., The CD95 (APO-1/Fas) and the TRAIL (APO-2L) apoptosis systems. *Exp Cell Res* **2000,** *256* (1), 58-66.

21. von Karstedt, S.; Montinaro, A.; Walczak, H., Exploring the TRAILs less travelled: TRAIL in cancer biology and therapy. *Nat Rev Cancer* **2017,** *17* (6), 352-366.

22. Graves, J. D.; Kordich, J. J.; Huang, T. H.; Piasecki, J.; Bush, T. L.; Sullivan, T.; Foltz, I. N.; Chang, W.; Douangpanya, H.; Dang, T.; O'Neill, J. W.; Mallari, R.; Zhao, X.; Branstetter, D. G.; Rossi, J. M.; Long, A. M.; Huang, X.; Holland, P. M., Apo2L/TRAIL and the death receptor 5 agonist antibody AMG 655 cooperate to promote receptor clustering and antitumor activity. *Cancer Cell* **2014,** *26* (2), 177-89.

23. Gibellini, D.; Borderi, M.; De Crignis, E.; Cicola, R.; Vescini, F.; Caudarella, R.; Chiodo, F.; Re, M. C., RANKL/OPG/TRAIL plasma levels and bone mass loss evaluation in antiretroviral naive HIV-1-positive men. *J Med Virol* **2007,** *79* (10), 1446-54.

24. Zhong, H. H.; Wang, H. Y.; Li, J.; Huang, Y. Z., TRAIL-based gene delivery and therapeutic strategies. *Acta Pharmacol Sin* **2019,** *40* (11), 1373-1385.

25. Truneh, A.; Sharma, S.; Silverman, C.; Khandekar, S.; Reddy, M. P.; Deen, K. C.; McLaughlin, M. M.; Srinivasula, S. M.; Livi, G. P.; Marshall, L. A.; Alnemri, E. S.; Williams, W. V.; Doyle, M. L., Temperature-sensitive differential affinity of TRAIL for its receptors. DR5 is the highest affinity receptor. *J Biol Chem* **2000,** *275* (30), 23319-25.

26. Wu, X.; Wang, S.; Li, M.; Wang, A.; Zhou, Y.; Li, P.; Wang, Y., Nanocarriers for TRAIL delivery: driving TRAIL back on track for cancer therapy. *Nanoscale* **2017,** *9* (37), 13879-13904.

27. Wu, S. Y.; Lopez-Berestein, G.; Calin, G. A.; Sood, A. K., RNAi therapies: drugging the undruggable. *Sci Transl Med* **2014,** *6* (240), 240ps7.

28. Giacca, M.; Zacchigna, S., Virus-mediated gene delivery for human gene therapy. *J Control Release* **2012,** *161* (2), 377-88.

29. Kootstra, N. A.; Verma, I. M., Gene therapy with viral vectors. *Annu Rev Pharmacol Toxicol* **2003,** *43*, 413-39.

30. Kay, M. A.; Glorioso, J. C.; Naldini, L., Viral vectors for gene therapy: the art of turning infectious agents into vehicles of therapeutics. *Nat Med* **2001,** *7* (1), 33-40.

31. Marshall, E., Gene therapy death prompts review of adenovirus vector. *Science* **1999,** *286* (5448), 2244-5.

32. Buckley, R. H., Gene therapy for SCID--a complication after remarkable progress. *Lancet* **2002,** *360* (9341), 1185-6.

33. Hacein-Bey-Abina, S.; Von Kalle, C.; Schmidt, M.; McCormack, M. P.; Wulffraat, N.; Leboulch, P.; Lim, A.; Osborne, C. S.; Pawliuk, R.; Morillon, E.; Sorensen, R.; Forster, A.; Fraser, P.; Cohen, J. I.; de Saint Basile, G.; Alexander, I.; Wintergerst, U.; Frebourg, T.; Aurias, A.; Stoppa-Lyonnet, D.; Romana, S.; Radford-Weiss, I.; Gross, F.; Valensi, F.; Delabesse, E.; Macintyre, E.; Sigaux, F.; Soulier, J.; Leiva, L. E.; Wissler, M.; Prinz, C.; Rabbitts, T. H.; Le Deist, F.; Fischer, A.; Cavazzana-Calvo, M., LMO2-associated clonal T cell proliferation in two patients after gene therapy for SCID-X1. *Science* **2003,** *302* (5644), 415-9.

34. Glover, D. J.; Lipps, H. J.; Jans, D. A., Towards safe, non-viral therapeutic gene expression in humans. *Nat Rev Genet* **2005,** *6* (4), 299-310.

35. Zu, H.; Gao, D., Non-viral Vectors in Gene Therapy: Recent Development, Challenges, and Prospects. *AAPS J* **2021,** *23* (4), 78.

36. Branski, L. K.; Pereira, C. T.; Herndon, D. N.; Jeschke, M. G., Gene therapy in wound healing: present status and future directions. *Gene Ther* **2007,** *14* (1), 1-10.

37. Young, J. L.; Dean, D. A., Electroporation-mediated gene delivery. *Adv Genet* **2015,** *89*, 49-88.

38. Dobson, J., Gene therapy progress and prospects: magnetic nanoparticle-based gene delivery. *Gene Therapy* **2006,** *13* (4), 283-287.

39. Seow, Y.; Wood, M. J., Biological Gene Delivery Vehicles: Beyond Viral Vectors. *Mol Ther* **2009,** *17* (5), 767-777.

40. Wang, Y.; Cui, H.; Li, K.; Sun, C.; Du, W.; Cui, J.; Zhao, X.; Chen, W., A magnetic nanoparticle-based multiple-gene delivery system for transfection of porcine kidney cells. *PLoS One* **2014,** *9* (7), e102886.

41. Newman, C. M.; Bettinger, T., Gene therapy progress and prospects: ultrasound for gene transfer. *Gene Ther* **2007,** *14* (6), 465-75.

42. Hengge, U. R.; Chan, E. F.; Foster, R. A.; Walker, P. S.; Vogel, J. C., Cytokine gene expression in epidermis with biological effects following injection of naked DNA. *Nat Genet* **1995,** *10* (2), 161-6.

43. Ramamoorth, M.; Narvekar, A., Non viral vectors in gene therapy- an overview. *J Clin Diagn Res* **2015,** *9* (1), GE01-6.

44. Park, J.; Lee, J.; Kwag, J.; Baek, Y.; Kim, B.; Yoon, C. J.; Bok, S.; Cho, S. H.; Kim, K. H.; Ahn, G. O.; Kim, S., Quantum Dots in an Amphiphilic Polyethyleneimine Derivative Platform for Cellular Labeling, Targeting, Gene Delivery, and Ratiometric Oxygen Sensing. *ACS Nano* **2015,** *9* (6), 6511-21.

45. Clapp, A. R.; Medintz, I. L.; Mauro, J. M.; Fisher, B. R.; Bawendi, M. G.; Mattoussi, H., Fluorescence resonance energy transfer between quantum dot donors and dye-labeled protein acceptors. *Journal of the American Chemical Society* **2004,** *126* (1), 301-310.

46. Huang, R. Y.; Liu, Z. H.; Weng, W. H.; Chang, C. W., Magnetic nanocomplexes for gene delivery applications. *J Mater Chem B* **2021,** *9* (21), 4267-4286.

47. Zare, H.; Ahmadi, S.; Ghasemi, A.; Ghanbari, M.; Rabiee, N.; Bagherzadeh, M.; Karimi, M.; Webster, T. J.; Hamblin, M. R.; Mostafavi, E., Carbon Nanotubes: Smart Drug/Gene Delivery Carriers. *Int J Nanomedicine* **2021,** *16*, 1681-1706.

48. Carvalho, A. M.; Cordeiro, R. A.; Faneca, H., Silica-Based Gene Delivery Systems: From Design to Therapeutic Applications. *Pharmaceutics* **2020,** *12* (7).

49. Zhang, B.; Ma, X. P.; Murdoch, W.; Radosz, M.; Shen, Y. Q., Bioreducible poly(amido amine)s with different branching degrees as gene delivery vectors. *Biotechnol Bioeng* **2013,** *110* (3), 990-998.

50. Schaffert, D.; Troiber, C.; Wagner, E., New sequence-defined polyaminoamides with tailored endosomolytic properties for plasmid DNA delivery. *Bioconjug Chem* **2012,** *23* (6), 1157-65.

51. Thanou, M.; Florea, B. I.; Geldof, M.; Junginger, H. E.; Borchard, G., Quaternized chitosan oligomers as novel gene delivery vectors in epithelial cell lines. *Biomaterials* **2002,** *23* (1), 153-9.

52. Kundu, P. P.; Sharma, V., Synthetic polymeric vectors in gene therapy. *Curr Opin Solid St M* **2008,** *12* (5-6), 89-102.

53. Gupta, B.; Levchenko, T. S.; Torchilin, V. P., Intracellular delivery of large molecules and small particles by cell-penetrating proteins and peptides. *Adv Drug Deliver Rev* **2005,** *57* (4), 637-651.

54. Haralambidis, J.; Duncan, L.; Tregear, G. W., The solid phase synthesis of oligonucleotides containing a 3′-peptide moiety. *Tetrahedron Letters* **1987,** *28* (43), 5199-5202.

55. Felgner, P. L.; Gadek, T. R.; Holm, M.; Roman, R.; Chan, H. W.; Wenz, M.; Northrop, J. P.; Ringold, G. M.; Danielsen, M., Lipofection: a highly efficient, lipid-mediated DNA-transfection procedure. *Proc Natl Acad Sci U S A* **1987,** *84* (21), 7413-7.

56. Brigham, K. L.; Meyrick, B.; Christman, B.; Berry, L. C., Jr.; King, G., Expression of a prokaryotic gene in cultured lung endothelial cells after lipofection with a plasmid vector. *Am J Respir Cell Mol Biol* **1989,** *1* (2), 95-100.

57. Innes, C. L.; Smith, P. B.; Langenbach, R.; Tindall, K. R.; Boone, L. R., Cationic liposomes (Lipofectin) mediate retroviral infection in the absence of specific receptors. *J Virol* **1990,** *64* (2), 957-61.

58. Brant, M.; Nachmansson, N.; Norrman, K.; Regnell, I.; Bredberg, A., Shuttle vector plasmid propagation in human peripheral blood lymphocytes facilitated by liposome-mediated transfection. *DNA Cell Biol* **1991,** *10* (1), 75-9.

59. Leventis, R.; Silvius, J. R., Interactions of mammalian cells with lipid dispersions containing novel metabolizable cationic amphiphiles. *Biochim Biophys Acta* **1990,** *1023* (1), 124-32.

60. Felgner, P. L.; Ringold, G. M., Cationic liposome-mediated transfection. *Nature* **1989,** *337* (6205), 387-8.

61. Zabner, J.; Fasbender, A. J.; Moninger, T.; Poellinger, K. A.; Welsh, M. J., Cellular and molecular barriers to gene transfer by a cationic lipid. *J Biol Chem* **1995,** *270* (32), 18997-9007.

62. Sternberg, B.; Sorgi, F. L.; Huang, L., New structures in complex formation between DNA and cationic liposomes visualized by freeze-fracture electron microscopy. *FEBS Lett* **1994,** *356* (2-3), 361-6.

63. Gershon, H.; Ghirlando, R.; Guttman, S. B.; Minsky, A., Mode of formation and structural features of DNA-cationic liposome complexes used for transfection. *Biochemistry* **1993,** *32* (28), 7143-51.

64. Safinya, C. R., Structures of lipid-DNA complexes: supramolecular assembly and gene delivery. *Curr Opin Struct Biol* **2001,** *11* (4), 440-8.

65. Simberg, D.; Weisman, S.; Talmon, Y.; Barenholz, Y., DOTAP (and other cationic lipids): chemistry, biophysics, and transfection. *Crit Rev Ther Drug Carrier Syst* **2004,** *21* (4), 257-317.

66. Farhood, H.; Serbina, N.; Huang, L., The role of dioleoyl phosphatidylethanolamine in cationic liposome mediated gene transfer. *Biochim Biophys Acta* **1995,** *1235* (2), 289-95.

67. Wattiaux, R.; Laurent, N.; Wattiaux-De Coninck, S.; Jadot, M., Endosomes, lysosomes: their implication in gene transfer. *Adv Drug Deliv Rev* **2000,** *41* (2), 201-8.

68. Parton, R. G.; Richards, A. A., Lipid Rafts and Caveolae as Portals for Endocytosis: New Insights and Common Mechanisms. *Traffic* **2003,** *4* (11), 724-738.

69. Perumal, O. P.; Inapagolla, R.; Kannan, S.; Kannan, R. M., The effect of surface functionality on cellular trafficking of dendrimers. *Biomaterials* **2008,** *29* (24-25), 3469-76.

70. Boleti, H.; Benmerah, A.; Ojcius, D. M.; Cerf-Bensussan, N.; Dautry-Varsat, A., Chlamydia infection of epithelial cells expressing dynamin and Eps15 mutants: clathrin-independent entry into cells and dynamin-dependent productive growth. *J Cell Sci* **1999,** *112 (Pt 10)*, 1487-96.

71. Martys, J. L.; Wjasow, C.; Gangi, D. M.; Kielian, M. C.; McGraw, T. E.; Backer, J. M., Wortmannin-sensitive trafficking pathways in Chinese hamster ovary cells. Differential effects on endocytosis and lysosomal sorting. *J Biol Chem* **1996,** *271* (18), 10953-62.

72. Li, D.; Li, P.; Li, G.; Wang, J.; Wang, E., The effect of nocodazole on the transfection efficiency of lipid-bilayer coated gold nanoparticles. *Biomaterials* **2009,** *30* (7), 1382-8.

73. Yamamoto, A.; Tagawa, Y.; Yoshimori, T.; Moriyama, Y.; Masaki, R.; Tashiro, Y., Bafilomycin A1 prevents maturation of autophagic vacuoles by inhibiting fusion between autophagosomes and lysosomes in rat hepatoma cell line, H-4-II-E cells. *Cell Struct Funct* **1998,** *23* (1), 33-42.

74. Xu, Y.; Szoka, F. C., Jr., Mechanism of DNA release from cationic liposome/DNA complexes used in cell transfection. *Biochemistry* **1996,** *35* (18), 5616-23.

75. Gao, X.; Huang, L., Cationic liposome-mediated gene transfer. *Gene Ther* **1995,** *2* (10), 710-22.

76. Hafez, I. M.; Maurer, N.; Cullis, P. R., On the mechanism whereby cationic lipids promote intracellular delivery of polynucleic acids. *Gene Ther* **2001,** *8* (15), 1188-96.

77. Ellens, H.; Bentz, J.; Szoka, F. C., Destabilization of phosphatidylethanolamine liposomes at the hexagonal phase transition temperature. *Biochemistry* **1986,** *25* (2), 285-94.

78. Tseng, W. C.; Haselton, F. R.; Giorgio, T. D., Mitosis enhances transgene expression of plasmid delivered by cationic liposomes. *Biochim Biophys Acta* **1999,** *1445* (1), 53-64.

79. Jans, D. A.; Chan, C. K.; Huebner, S., Signals mediating nuclear targeting and their regulation: application in drug delivery. *Med Res Rev* **1998,** *18* (4), 189-223.

80. Subramanian, A.; Ranganathan, P.; Diamond, S. L., Nuclear targeting peptide scaffolds for lipofection of nondividing mammalian cells. *Nat Biotechnol* **1999,** *17* (9), 873-7.

81. Sebestyen, M. G.; Ludtke, J. J.; Bassik, M. C.; Zhang, G.; Budker, V.; Lukhtanov, E. A.; Hagstrom, J. E.; Wolff, J. A., DNA vector chemistry: the covalent attachment of signal peptides to plasmid DNA. *Nat Biotechnol* **1998,** *16* (1), 80-5.

82. van der Woude, I.; Wagenaar, A.; Meekel, A. A.; ter Beest, M. B.; Ruiters, M. H.; Engberts, J. B.; Hoekstra, D., Novel pyridinium surfactants for efficient, nontoxic in vitro gene delivery. *Proc Natl Acad Sci U S A* **1997,** *94* (4), 1160-5.

83. Byk, G.; Dubertret, C.; Escriou, V.; Frederic, M.; Jaslin, G.; Rangara, R.; Pitard, B.; Crouzet, J.; Wils, P.; Schwartz, B.; Scherman, D., Synthesis, activity, and structure--activity relationship studies of novel cationic lipids for DNA transfer. *J Med Chem* **1998,** *41* (2), 229-35.

84. Hofland, H. E.; Shephard, L.; Sullivan, S. M., Formation of stable cationic lipid/DNA complexes for gene transfer. *Proc Natl Acad Sci U S A* **1996,** *93* (14), 7305-9.

85. Aissaoui, A.; Martin, B.; Kan, E.; Oudrhiri, N.; Hauchecorne, M.; Vigneron, J. P.; Lehn, J. M.; Lehn, P., Novel cationic lipids incorporating an acid-sensitive acylhydrazone linker: synthesis and transfection properties. *J Med Chem* **2004,** *47* (21), 5210-23.

86. Gao, H.; Hui, K. M., Synthesis of a novel series of cationic lipids that can act as efficient gene delivery vehicles through systematic heterocyclic substitution of cholesterol derivatives. *Gene Ther* **2001,** *8* (11), 855-63.

87. Misra, S. K.; Munoz-Ubeda, M.; Datta, S.; Barran-Berdon, A. L.; Aicart-Ramos, C.; Castro-Hartmann, P.; Kondaiah, P.; Junquera, E.; Bhattacharya, S.; Aicart, E., Effects of a delocalizable cation on the headgroup of gemini lipids on the lipoplex-type nanoaggregates directly formed from plasmid DNA. *Biomacromolecules* **2013,** *14* (11), 3951-63.

88. Gao, X.; Huang, L., A novel cationic liposome reagent for efficient transfection of mammalian cells. *Biochem Biophys Res Commun* **1991,** *179* (1), 280-5.

89. Aberle, A. M.; Tablin, F.; Zhu, J.; Walker, N. J.; Gruenert, D. C.; Nantz, M. H., A novel tetraester construct that reduces cationic lipid-associated cytotoxicity. Implications for the onset of cytotoxicity. *Biochemistry* **1998,** *37* (18), 6533-40.

90. Miller, A. D., Cationic Liposomes for Gene Therapy. *Angewandte Chemie International Edition* **1998,** *37* (13-14), 1768-1785.

91. Kumar, V. V.; Singh, R. S.; Chaudhuri, A., Cationic transfection lipids in gene therapy: Successes, set-backs, challenges and promises. *Curr Med Chem* **2003,** *10* (14), 1297-1306.

92. Kedika, B.; Patri, S. V., Design, synthesis, and in vitro transfection biology of novel tocopherol based monocationic lipids: a structure-activity investigation. *J Med Chem* **2011,** *54* (2), 548-61.

93. Zheng, L. T.; Yi, W. J.; Su, R. C.; Liu, Q.; Zhao, Z. G., Reducible Amino Acid Based Cationic Lipids as Highly Efficient and Serum-Tolerant Gene Vectors. *Chempluschem* **2016,** *81* (1), 125-134.

94. Kumar, K.; Maiti, B.; Kondaiah, P.; Bhattacharya, S., alpha-Tocopherol derived lipid dimers as efficient gene transfection agents. Mechanistic insights into lipoplex internalization and therapeutic induction of apoptotic activity. *Org Biomol Chem* **2015,** *13* (8), 2444-52.

95. Menger, F. M.; Keiper, J. S., Gemini Surfactants. *Angew Chem Int Ed Engl* **2000,** *39* (11), 1906-1920.

96. Bajaj, A.; Paul, B.; Kondaiah, P.; Bhattacharya, S., Structure-activity investigation on the gene transfection properties of cardiolipin mimicking gemini lipid analogues. *Bioconjug Chem* **2008,** *19* (6), 1283-300.

97. Misra, S. K.; Naz, S.; Kondaiah, P.; Bhattacharya, S., A cationic cholesterol based nanocarrier for the delivery of p53-EGFP-C3 plasmid to cancer cells. *Biomaterials* **2014,** *35* (4), 1334-46.

98. Kumar, K.; Maiti, B.; Kondaiah, P.; Bhattacharya, S., Efficacious gene silencing in serum and significant apoptotic activity induction by survivin downregulation mediated by new cationic gemini tocopheryl lipids. *Mol Pharm* **2015,** *12* (2), 351-61.

99. Kedika, B.; Patri, S. V., Synthesis and gene transfer activities of novel serum compatible reducible tocopherol-based cationic lipids. *Mol Pharm* **2012,** *9* (5), 1146-62.

100. Kumar, K.; Barran-Berdon, A. L.; Datta, S.; Munoz-Ubeda, M.; Aicart-Ramos, C.; Kondaiah, P.; Junquera, E.; Bhattacharya, S.; Aicart, E., A delocalizable cationic headgroup together with an oligo-oxyethylene spacer in gemini cationic lipids improves their biological activity as vectors of plasmid DNA. *J Mater Chem B* **2015,** *3* (8), 1495-1506.

101. Fuhrhop, J. H.; Wang, T., Bolaamphiphiles. *Chem Rev* **2004,** *104* (6), 2901-37.

102. Blume, A.; Drescher, S.; Graf, G.; Kohler, K.; Meister, A., Self-assembly of different single-chain bolaphospholipids and their miscibility with phospholipids or classical amphiphiles. *Adv Colloid Interface Sci* **2014,** *208*, 264-78.

103. Jain, N.; Arntz, Y.; Goldschmidt, V.; Duportail, G.; Mely, Y.; Klymchenko, A. S., New unsymmetrical bolaamphiphiles: synthesis, assembly with DNA, and application for gene delivery. *Bioconjug Chem* **2010,** *21* (11), 2110-8.

104. Khan, M.; Ang, C. Y.; Wiradharma, N.; Yong, L. K.; Liu, S.; Liu, L.; Gao, S.; Yang, Y. Y., Diaminododecane-based cationic bolaamphiphile as a non-viral gene delivery carrier. *Biomaterials* **2012,** *33* (18), 4673-80.

105. Patil, S. P.; Kim, S. H.; Jadhav, J. R.; Lee, J. H.; Jeon, E. M.; Kim, K. T.; Kim, B. H., Cancer-specific gene silencing through therapeutic siRNA delivery with B vitamin-based nanoassembled low-molecular-weight hydrogelators. *Bioconjug Chem* **2014,** *25* (8), 1517-25.

106. Obata, Y.; Suzuki, D.; Takeoka, S., Evaluation of cationic assemblies constructed with amino acid based lipids for plasmid DNA delivery. *Bioconjug Chem* **2008,** *19* (5), 1055-63.

107. Jiang, Q.; Yue, D.; Nie, Y.; Xu, X.; He, Y.; Zhang, S.; Wagner, E.; Gu, Z., Specially-Made Lipid-Based Assemblies for Improving Transmembrane Gene Delivery: Comparison of Basic Amino Acid Residue Rich Periphery. *Mol Pharm* **2016,** *13* (6), 1809-21.

108. Muripiti, V.; Brijesh, L.; Rachamalla, H. K.; Marepally, S. K.; Banerjee, R.; Patri, S. V., alpha-Tocopherol-ascorbic acid hybrid antioxidant based cationic amphiphile for gene delivery: Design, synthesis and transfection. *Bioorg Chem* **2019,** *82*, 178-191.

109. Traber, M. G.; Atkinson, J., Vitamin E, antioxidant and nothing more. *Free Radic Biol Med* **2007,** *43* (1), 4-15.

110. Duhem, N.; Danhier, F.; Preat, V., Vitamin E-based nanomedicines for anti-cancer drug delivery. *J Control Release* **2014,** *182*, 33-44.

111. Gosangi, M.; Rapaka, H.; Ravula, V.; Patri, S. V., Evolution of New "Bolaliposomes" using Novel alpha-Tocopheryl Succinate Based Cationic Lipid and 1,12-Disubstituted Dodecane-Based Bolaamphiphile for Efficient Gene Delivery. *Bioconjug Chem* **2017,** *28* (7), 1965-1977.

112. Kamra, M.; Maiti, B.; Dixit, A.; Karande, A. A.; Bhattacharya, S., Tumor Chemosensitization through Oncogene Knockdown Mediated by Unique alpha-Tocopherylated Cationic Geminis. *Biomacromolecules* **2019,** *20* (4), 1555-1566.

113. Grippo, L. D.; Reidel, I. G.; Garcia, M. I.; Streu, A.; Muller, D. M.; Veaute, C. M., Gemini lipopeptides as vaccine adjuvants: a new role for these versatile carriers. *Clin Exp Vaccine Res* **2020,** *9* (2), 159-163.

114. Neubauer, D.; Jaskiewicz, M.; Bauer, M.; Olejniczak-Keder, A.; Sikorska, E.; Sikora, K.; Kamysz, W., Biological and Physico-Chemical Characteristics of Arginine-Rich Peptide Gemini Surfactants with Lysine and Cystine Spacers. *Int J Mol Sci* **2021,** *22* (7).

115. Roberts, K. D.; Azad, M. A.; Wang, J.; Horne, A. S.; Thompson, P. E.; Nation, R. L.; Velkov, T.; Li, J., Antimicrobial Activity and Toxicity of the Major Lipopeptide

Components of Polymyxin B and Colistin: Last-line Antibiotics against Multidrug-Resistant Gram-negative Bacteria. *ACS Infect Dis* **2015,** *1* (11), 568-575.

116. Neubauer, D.; Jaskiewicz, M.; Sikorska, E.; Bauer, S. B. M.; Kapusta, M.; Narajczyk, M.; Kamysz, W., Effect of Disulfide Cyclization of Ultrashort Cationic Lipopeptides on Antimicrobial Activity and Cytotoxicity. *Int J Mol Sci* **2020,** *21* (19).

117. Damen, M.; Aarbiou, J.; van Dongen, S. F.; Buijs-Offerman, R. M.; Spijkers, P. P.; van den Heuvel, M.; Kvashnina, K.; Nolte, R. J.; Scholte, B. J.; Feiters, M. C., Delivery of DNA and siRNA by novel gemini-like amphiphilic peptides. *J Control Release* **2010,** *145* (1), 33-9.

118. Zheng, Y.; Guo, Y. J.; Li, Y. T.; Wu, Y.; Zhang, L. H.; Yang, Z. J., A novel gemini-like cationic lipid for the efficient delivery of siRNA. *New J Chem* **2014,** *38* (10), 4952-4962.

119. Zhi, D.; Zhang, S.; Cui, S.; Zhao, Y.; Wang, Y.; Zhao, D., The headgroup evolution of cationic lipids for gene delivery. *Bioconjug Chem* **2013,** *24* (4), 487-519.

120. Di Pisa, M.; Chassaing, G.; Swiecicki, J. M., When cationic cell-penetrating peptides meet hydrocarbons to enhance in-cell cargo delivery. *J Pept Sci* **2015,** *21* (5), 356-369.

121. Nantz, M. H.; Dicus, C. W.; Hilliard, B.; Yellayi, S.; Zou, S. M.; Hecker, J. G., The Benefit of Hydrophobic Domain Asymmetry on the Efficacy of Transfection as Measured by in Vivo Imaging. *Mol Pharmaceut* **2010,** *7* (3), 786-794.

122. Zhi, D.; Zhang, S.; Wang, B.; Zhao, Y.; Yang, B.; Yu, S., Transfection efficiency of cationic lipids with different hydrophobic domains in gene delivery. *Bioconjug Chem* **2010,** *21* (4), 563-77.

123. He, L.; Mo, H.; Hadisusilo, S.; Qureshi, A. A.; Elson, C. E., Isoprenoids suppress the growth of murine B16 melanomas in vitro and in vivo. *J Nutr* **1997,** *127* (5), 668-74.

124. Burke, Y. D.; Stark, M. J.; Roach, S. L.; Sen, S. E.; Crowell, P. L., Inhibition of pancreatic cancer growth by the dietary isoprenoids farnesol and geraniol. *Lipids* **1997,** *32* (2), 151-6.

125. Burke, Y. D.; Ayoubi, A. S.; Werner, S. R.; McFarland, B. C.; Heilman, D. K.; Ruggeri, B. A.; Crowell, P. L., Effects of the isoprenoids perillyl alcohol and farnesol on apoptosis biomarkers in pancreatic cancer chemoprevention. *Anticancer Res* **2002,** *22* (6A), 3127-34.

126. Yazlovitskaya, E. M.; Melnykovych, G., Selective farnesol toxicity and translocation of protein kinase C in neoplastic HeLa-S3K and non-neoplastic CF-3 cells. *Cancer Lett* **1995,** *88* (2), 179-83.

127. Ong, T. P.; Heidor, R.; de Conti, A.; Dagli, M. L.; Moreno, F. S., Farnesol and geraniol chemopreventive activities during the initial phases of hepatocarcinogenesis involve similar actions on cell proliferation and DNA damage, but distinct actions on apoptosis, plasma cholesterol and HMGCoA reductase. *Carcinogenesis* **2006,** *27* (6), 1194-203.

128. Qamar, W.; Sultana, S., Farnesol ameliorates massive inflammation, oxidative stress and lung injury induced by intratracheal instillation of cigarette smoke extract in rats: an initial step in lung chemoprevention. *Chem Biol Interact* **2008,** *176* (2-3), 79-87.

129. Khan, R.; Sultana, S., Farnesol attenuates 1,2-dimethylhydrazine induced oxidative stress, inflammation and apoptotic responses in the colon of Wistar rats. *Chem Biol Interact* **2011,** *192* (3), 193-200.

130. Shahnouri, M.; Abouhosseini Tabari, M.; Araghi, A., Neuropharmacological properties of farnesol in Murine model. *Iran J Vet Res* **2016,** *17* (4), 259-264.

131. Delmondes, G. D.; Lemos, I. C. S.; Dias, D. D.; Da Cunha, G. L.; Araujo, I. M.; Barbosa, R.; Coutinho, H. D. M.; Felipe, C. F. B.; Barbosa, J. M.; De Lima, N. T. R.; De Menezesa, I. R. A.; Kerntopf, M. R., Pharmacological applications of farnesol (C15H26O): a patent review. *Expert Opin Ther Pat* **2020,** *30* (3), 227-234.

132. Naldini, L., Gene therapy returns to centre stage. *Nature* **2015,** *526* (7573), 351-60.

133. Mahato, R. I.; Rolland, A.; Tomlinson, E., Cationic lipid-based gene delivery systems: pharmaceutical perspectives. *Pharm Res* **1997,** *14* (7), 853-9.

134. Zhi, D.; Bai, Y.; Yang, J.; Cui, S.; Zhao, Y.; Chen, H.; Zhang, S., A review on cationic lipids with different linkers for gene delivery. *Adv Colloid Interface Sci* **2018,** *253*, 117-140.

135. Lv, H.; Zhang, S.; Wang, B.; Cui, S.; Yan, J., Toxicity of cationic lipids and cationic polymers in gene delivery. *J Control Release* **2006,** *114* (1), 100-9.

136. Tang, F.; Hughes, J. A., Synthesis of a single-tailed cationic lipid and investigation of its transfection. *J Control Release* **1999,** *62* (3), 345-58.

137. Liu, D.; Hu, J.; Qiao, W.; Li, Z.; Zhang, S.; Cheng, L., Synthesis of carbamate-linked lipids for gene delivery. *Bioorg Med Chem Lett* **2005,** *15* (12), 3147-50.

138. Suh, M. S.; Shim, G.; Lee, H. Y.; Han, S. E.; Yu, Y. H.; Choi, Y.; Kim, K.; Kwon, I. C.; Weon, K. Y.; Kim, Y. B.; Oh, Y. K., Anionic amino acid-derived cationic lipid for siRNA delivery. *J Control Release* **2009,** *140* (3), 268-76.

139. Fu, C.; Qian, K.; Fu, A., Arginine-modified carbon dots probe for live cell imaging and sensing by increasing cellular uptake efficiency. *Mater Sci Eng C Mater Biol Appl* **2017,** *76*, 350-355.

140. Rothbard, J. B.; Jessop, T. C.; Lewis, R. S.; Murray, B. A.; Wender, P. A., Role of membrane potential and hydrogen bonding in the mechanism of translocation of guanidinium-rich peptides into cells. *J Am Chem Soc* **2004,** *126* (31), 9506-7.

141. Preusser, M.; de Ribaupierre, S.; Wohrer, A.; Erridge, S. C.; Hegi, M.; Weller, M.; Stupp, R., Current concepts and management of glioblastoma. *Ann Neurol* **2011,** *70* (1), 9-21.

142. Khoury, O.; Ghazale, N.; Stone, E.; El-Sibai, M.; Frankel, A. E.; Abi-Habib, R. J., Human recombinant arginase I (Co)-PEG5000 [HuArgI (Co)-PEG5000]-induced arginine depletion is selectively cytotoxic to human glioblastoma cells. *J Neurooncol* **2015,** *122* (1), 75-85.

143. Syed, N.; Langer, J.; Janczar, K.; Singh, P.; Lo Nigro, C.; Lattanzio, L.; Coley, H. M.; Hatzimichael, E.; Bomalaski, J.; Szlosarek, P.; Awad, M.; O'Neil, K.; Roncaroli, F.; Crook, T., Epigenetic status of argininosuccinate synthetase and argininosuccinate lyase modulates autophagy and cell death in glioblastoma. *Cell Death Dis* **2013,** *4*, e458.

144. Pilanc-kudlek, P.; Cyranowski, S.; Wojnicki, K.; Ochocka, N.; Grzybowski, M.; Stanczak, P.; Pomper, P.; Blaszczyk, R.; Golebiowski, A.; Dobrzanski, P.; Kaminska, B., Novel arginase inhibitor alone and in combination with an immune check point inhibitor reduces tumour growth in murine experimental gliomas. *Ann Oncol* **2019,** *30*.

145. Ashkenazi, A.; Pai, R. C.; Fong, S.; Leung, S.; Lawrence, D. A.; Marsters, S. A.; Blackie, C.; Chang, L.; McMurtrey, A. E.; Hebert, A.; DeForge, L.; Koumenis, I. L.; Lewis, D.; Harris, L.; Bussiere, J.; Koeppen, H.; Shahrokh, Z.; Schwall, R. H., Safety and antitumor activity of recombinant soluble Apo2 ligand. *J Clin Invest* **1999,** *104* (2), 155-62.

146. Hellwig, C. T.; Rehm, M., TRAIL signaling and synergy mechanisms used in TRAIL-based combination therapies. *Mol Cancer Ther* **2012,** *11* (1), 3-13.

147. LeBlanc, H. N.; Ashkenazi, A., Apo2L/TRAIL and its death and decoy receptors. *Cell Death Differ* **2003,** *10* (1), 66-75.

148. Srivastava, R. K., TRAIL/Apo-2L: mechanisms and clinical applications in cancer. *Neoplasia* **2001,** *3* (6), 535-46.

149. Wang, S.; El-Deiry, W. S., TRAIL and apoptosis induction by TNF-family death receptors. *Oncogene* **2003,** *22* (53), 8628-33.

150. Ashkenazi, A.; Dixit, V. M., Apoptosis control by death and decoy receptors. *Curr Opin Cell Biol* **1999,** *11* (2), 255-60.

151. Griffith, T. S.; Lynch, D. H., TRAIL: a molecule with multiple receptors and control mechanisms. *Curr Opin Immunol* **1998,** *10* (5), 559-63.

152. Liu, Q.; Su, R. C.; Yi, W. J.; Zheng, L. T.; Lu, S. S.; Zhao, Z. G., pH and reduction dual-responsive dipeptide cationic lipids with alpha-tocopherol hydrophobic tail for efficient gene delivery. *Eur J Med Chem* **2017,** *129*, 1-11.

153. Muripiti, V.; Rachamalla, H. K.; Banerjee, R.; Patri, S. V., alpha-Tocopherol-based cationic amphiphiles with a novel pH sensitive hybrid linker for gene delivery. *Org Biomol Chem* **2018,** *16* (16), 2932-2946.

154. Dong, H.; Pang, L.; Cong, H.; Shen, Y.; Yu, B., Application and design of esterase-responsive nanoparticles for cancer therapy. *Drug Deliv* **2019,** *26* (1), 416-432.

155. Yuba, E.; Nakajima, Y.; Tsukamoto, K.; Iwashita, S.; Kojima, C.; Harada, A.; Kono, K., Effect of unsaturated alkyl chains on transfection activity of poly(amidoamine) dendron-bearing lipids. *J Control Release* **2012,** *160* (3), 552-60.

156. Yi, W. J.; Zheng, L. T.; Su, R. C.; Liu, Q.; Zhao, Z. G., Amino acid-based cationic lipids with alpha-tocopherol hydrophobic tail for efficient gene delivery. *Chem Biol Drug Des* **2015,** *86* (5), 1192-202.

157. Gosangi, M.; Mujahid, T. Y.; Gopal, V.; Patri, S. V., Effects of heterocyclic-based head group modifications on the structure–activity relationship of tocopherol-based lipids for non-viral gene delivery. *Organic & Biomolecular Chemistry* **2016,** *14* (28), 6857-6870.

158. Moss, K. H.; Popova, P.; Hadrup, S. R.; Astakhova, K.; Taskova, M., Lipid Nanoparticles for Delivery of Therapeutic RNA Oligonucleotides. *Mol Pharm* **2019,** *16* (6), 2265-2277.

159. Gerile, G.; Ganbold, T.; Li, Y. Z.; Baigude, H., Head group configuration increases the biocompatibility of cationic lipids for nucleic acid delivery. *Journal of Materials Chemistry B* **2017,** *5* (28), 5597-5607.

160. Sarker, S. R.; Aoshima, Y.; Hokama, R.; Inoue, T.; Sou, K.; Takeoka, S., Arginine-based cationic liposomes for efficient in vitro plasmid DNA delivery with low cytotoxicity. *Int J Nanomedicine* **2013,** *8*, 1361-75.

161. Albaugh, V. L.; Pinzon-Guzman, C.; Barbul, A., Arginine-Dual roles as an onconutrient and immunonutrient. *J Surg Oncol* **2017,** *115* (3), 273-280.

162. Pavlyk, I.; Rzhepetskyy, Y.; Jagielski, A. K.; Drozak, J.; Wasik, A.; Pereverzieva, G.; Olchowik, M.; Kunz-Schugart, L. A.; Stasyk, O.; Redowicz, M. J., Arginine deprivation affects glioblastoma cell adhesion, invasiveness and actin cytoskeleton organization by impairment of beta-actin arginylation. *Amino Acids* **2015,** *47* (1), 199-212.

163. Cheng, C. T.; Qi, Y.; Wang, Y. C.; Chi, K. K.; Chung, Y.; Ouyang, C.; Chen, Y. R.; Oh, M. E.; Sheng, X.; Tang, Y.; Liu, Y. R.; Lin, H. H.; Kuo, C. Y.; Schones, D.; Vidal, C.

M.; Chu, J. C.; Wang, H. J.; Chen, Y. H.; Miller, K. M.; Chu, P.; Yen, Y.; Jiang, L.; Kung, H. J.; Ann, D. K., Arginine starvation kills tumor cells through aspartate exhaustion and mitochondrial dysfunction. *Commun Biol* **2018,** *1*, 178.

164. Neuhaus, B.; Tosun, B.; Rotan, O.; Frede, A.; Westendorf, A. M.; Epple, M., Nanoparticles as transfection agents: a comprehensive study with ten different cell lines. *RSC Advances* **2016,** *6* (22), 18102-18112.

165. Wang, Y. T.; Wang, M. M.; Chen, H.; Liu, H. M.; Zhang, Q.; Cheng, Y. Y., Fluorinated dendrimer for TRAIL gene therapy in cancer treatment. *Journal of Materials Chemistry B* **2016,** *4* (7), 1354-1360.

166. Wang, G.; Zhu, D.; Zhou, Z.; Piao, Y.; Tang, J.; Shen, Y., Glutathione-Specific and Intracellularly Labile Polymeric Nanocarrier for Efficient and Safe Cancer Gene Delivery. *ACS Appl Mater Interfaces* **2020,** *12* (13), 14825-14838.

167. Kwon, O. S.; Jung, J. H.; Shin, E. A.; Park, J. E.; Park, W. Y.; Kim, S. H., Epigallocatechin-3-Gallate Induces Apoptosis as a TRAIL Sensitizer via Activation of Caspase 8 and Death Receptor 5 in Human Colon Cancer Cells. *Biomedicines* **2020,** *8* (4).

168. Wang, K.; Kievit, F. M.; Jeon, M.; Silber, J. R.; Ellenbogen, R. G.; Zhang, M. Q., Nanoparticle-Mediated Target Delivery of TRAIL as Gene Therapy for Glioblastoma. *Adv Healthc Mater* **2015,** *4* (17), 2719-2726.

169. Kang, J.; Kisenge, R. R.; Toyoda, H.; Tanaka, S.; Bu, J.; Azuma, E.; Komada, Y., Chemical sensitization and regulation of TRAIL-induced apoptosis in a panel of B-lymphocytic leukaemia cell lines. *Br J Haematol* **2003,** *123* (5), 921-32.

170. Goklany, S.; Lu, P.; Godeshala, S.; Hall, A.; Garrett-Mayer, E.; Voelkel-Johnson, C.; Rege, K., Delivery of TRAIL-expressing plasmid DNA to cancer cells in vitro and in vivo using aminoglycoside-derived polymers. *J Mater Chem B* **2019,** *7* (44), 7014-7025.

171. Lacal, J.; Andera, L., Choline kinase inhibitors synergize with TRAIL in the treatment of colorectal tumors and overcomes TRAIL resistance. *Cancer Translational Medicine* **2016,** *2* (6).

172. Sandra, F.; Hendarmin, L.; Nakao, Y.; Nakamura, N.; Nakamura, S., TRAIL cleaves caspase-8, -9 and -3 of AM-1 cells: a possible pathway for TRAIL to induce apoptosis in ameloblastoma. *Tumour Biol* **2005,** *26* (5), 258-64.

173. Sun, X. M.; MacFarlane, M.; Zhuang, J.; Wolf, B. B.; Green, D. R.; Cohen, G. M., Distinct caspase cascades are initiated in receptor-mediated and chemical-induced apoptosis. *J Biol Chem* **1999,** *274* (8), 5053-60.

174. Zauli, G.; Milani, D.; Rimondi, E.; Baldini, G.; Nicolin, V.; Grill, V.; Secchiero, P., TRAIL activates a caspase 9/7-dependent pathway in caspase 8/10-defective SK-N-SH neuroblastoma cells with two functional end points: induction of apoptosis and PGE2 release. *Neoplasia* **2003,** *5* (5), 457-66.

175. Seol, D. W.; Li, J.; Seol, M. H.; Park, S. Y.; Talanian, R. V.; Billiar, T. R., Signaling events triggered by tumor necrosis factor-related apoptosis-inducing ligand (TRAIL): caspase-8 is required for TRAIL-induced apoptosis. *Cancer Res* **2001,** *61* (3), 1138-43.

176. Thorburn, A., Death receptor-induced cell killing. *Cell Signal* **2004,** *16* (2), 139-44.

177. Micheau, O.; Merino, D., Controlling TRAIL-mediated caspase-3 activation. *Leukemia* **2004,** *18* (10), 1578-80.

178. Sun, X.; Cui, M.; Wang, D.; Guo, B.; Zhang, L., Tumor necrosis factor-related apoptosis inducing ligand overexpression and Taxol treatment suppresses the growth of cervical cancer cells in vitro and in vivo. *Oncol Lett* **2018,** *15* (4), 5744-5750.

179. Ferri, P.; Angelino, D.; Gennari, L.; Benedetti, S.; Ambrogini, P.; Del Grande, P.; Ninfali, P., Enhancement of flavonoid ability to cross the blood-brain barrier of rats by co-administration with alpha-tocopherol. *Food Funct* **2015,** *6* (2), 394-400.

180. Kuo, Y. C.; Chen, C. L.; Rajesh, R., Optimized liposomes with transactivator of transcription peptide and anti-apoptotic drugs to target hippocampal neurons and prevent tau-hyperphosphorylated neurodegeneration. *Acta Biomater* **2019,** *87*, 207-222.

181. Liu, J.; Feng, M.; Liang, D.; Yang, J.; Tang, X., Vitamin E-Labeled Polyethylenimine for in vitro and in vivo Gene Delivery. *Biomacromolecules* **2016,** *17* (10), 3153-3161.

182. Lo, Y. L.; Chou, H. L.; Liao, Z. X.; Huang, S. J.; Ke, J. H.; Liu, Y. S.; Chiu, C. C.; Wang, L. F., Chondroitin sulfate-polyethylenimine copolymer-coated superparamagnetic iron oxide nanoparticles as an efficient magneto-gene carrier for microRNA-encoding plasmid DNA delivery. *Nanoscale* **2015,** *7* (18), 8554-65.

183. Liu, W.; Lo, Y. L.; Hsu, C.; Wu, Y. T.; Liao, Z. X.; Wu, W. J.; Chen, Y. J.; Kao, C.; Chiu, C. C.; Wang, L. F., CS-PEI/Beclin-siRNA Downregulate Multidrug Resistance Proteins and Increase Paclitaxel Therapeutic Efficacy against NSCLC. *Mol Ther Nucleic Acids* **2019,** *17*, 477-490.

184. Lo, Y. L.; Tsai, M. F.; Soorni, Y.; Hsu, C.; Liao, Z. X.; Wang, L. F., Dual Stimuli-responsive Block Copolymers with Adjacent Redox- and Photo-cleavable Linkages for Smart Drug Delivery. *Biomacromolecules* **2020**.

185. Kuo, Y. C.; Chang, Y. H.; Rajesh, R., Targeted delivery of etoposide, carmustine and doxorubicin to human glioblastoma cells using methoxy poly(ethylene

glycol)poly(epsiloncaprolactone) nanoparticles conjugated with wheat germ agglutinin and folic acid. *Mater Sci Eng C Mater Biol Appl* **2019,** *96*, 114-128.

186. Yang, J. T.; Kuo, Y. C.; Chen, I. Y.; Rajesh, R.; Lou, Y. I.; Hsu, J. P., Protection against Neurodegeneration in the Hippocampus Using Sialic Acid- and 5-HT-Moduline-Conjugated Lipopolymer Nanoparticles. *ACS Biomater Sci Eng* **2019,** *5* (3), 1311-1320.

187. Amer, M. H., Gene therapy for cancer: present status and future perspective. *Mol Cell Ther* **2014,** *2*, 27.

188. Husain, S. R.; Han, J.; Au, P.; Shannon, K.; Puri, R. K., Gene therapy for cancer: regulatory considerations for approval. *Cancer Gene Ther* **2015,** *22* (12), 554-63.

189. Zhou, Z.; Liu, X.; Zhu, D.; Wang, Y.; Zhang, Z.; Zhou, X.; Qiu, N.; Chen, X.; Shen, Y., Nonviral cancer gene therapy: Delivery cascade and vector nanoproperty integration. *Adv Drug Deliv Rev* **2017,** *115*, 115-154.

190. Yin, H.; Kanasty, R. L.; Eltoukhy, A. A.; Vegas, A. J.; Dorkin, J. R.; Anderson, D. G., Non-viral vectors for gene-based therapy. *Nat Rev Genet* **2014,** *15* (8), 541-55.

191. Zhao, Y. N.; Piao, Y. Z.; Zhang, C. M.; Jiang, Y. M.; Liu, A.; Cui, S. H.; Zhi, D. F.; Zhen, Y. H.; Zhang, S. B., Replacement of quaternary ammonium headgroups by tri-ornithine in cationic lipids for the improvement of gene delivery in vitro and in vivo. *J. Mater. Chem. B* **2017,** *5* (39), 7963-7973.

192. Miller, J. B.; Kos, P.; Tieu, V.; Zhou, K.; Siegwart, D. J., Development of Cationic Quaternary Ammonium Sulfonamide Amino Lipids for Nucleic Acid Delivery. *ACS Appl Mater Interfaces* **2018,** *10* (3), 2302-2311.

193. Jones, C. H.; Chen, C. K.; Ravikrishnan, A.; Rane, S.; Pfeifer, B. A., Overcoming nonviral gene delivery barriers: perspective and future. *Mol Pharm* **2013,** *10* (11), 4082-98.

194. Wan, Y.; Dai, W.; Nevagi, R. J.; Toth, I.; Moyle, P. M., Multifunctional peptide-lipid nanocomplexes for efficient targeted delivery of DNA and siRNA into breast cancer cells. *Acta Biomater* **2017,** *59*, 257-268.

195. Liang, H.; Bi, Q.; Hu, A.; Chen, X.; Jin, R.; Song, X.; Ke, B.; Barz, M.; Nie, Y., A nitroreductase and glutathione responsive nanoplatform for integration of gene delivery and near-infrared fluorescence imaging. *Chem Commun (Camb)* **2020,** *56* (51), 6949-6952.

196. Chen, X.; Yang, J.; Liang, H.; Jiang, Q.; Ke, B.; Nie, Y., Disulfide modified self-assembly of lipopeptides with arginine-rich periphery achieve excellent gene transfection efficiency at relatively low nitrogen to phosphorus ratios. *J Mater Chem B* **2017,** *5* (7), 1482-1497.

197. Ravula, V.; Lo, Y.-L.; Wu, Y.-T.; Chang, C.-W.; Patri, S. V.; Wang, L.-F., Arginine-tocopherol bioconjugated lipid vesicles for selective pTRAIL delivery and subsequent apoptosis induction in glioblastoma cells. *Materials Science and Engineering: C* **2021,** *126*.

198. Zhou, Y.; Han, S.; Liang, Z.; Zhao, M.; Liu, G.; Wu, J., Progress in arginine-based gene delivery systems. *J Mater Chem B* **2020,** *8* (26), 5564-5577.

199. Song, S. J.; Lee, S.; Lee, Y.; Choi, J. S., Enzyme-responsive destabilization of stabilized plasmid-lipid nanoparticles as an efficient gene delivery. *Eur J Pharm Sci* **2016,** *91*, 20-30.

200. Muripiti, V.; Lohchania, B.; Marepally, S. K.; Patri, S. V., Hepatocellular targeted alpha-tocopherol based pH sensitive galactosylated lipids: design, synthesis and transfection studies. *Medchemcomm* **2018,** *9* (2), 264-274.

201. Li, D.; Zhang, R.; Liu, G.; Kang, Y.; Wu, J., Redox-Responsive Self-Assembled Nanoparticles for Cancer Therapy. *Adv Healthc Mater* **2020,** *9* (20), e2000605.

202. Thomas, R. G.; Surendran, S. P.; Jeong, Y. Y., Tumor Microenvironment-Stimuli Responsive Nanoparticles for Anticancer Therapy. *Front Mol Biosci* **2020,** *7*, 610533.

203. Maiti, B.; Kamra, M.; Karande, A. A.; Bhattacharya, S., Transfection efficiencies of alpha-tocopherylated cationic gemini lipids with hydroxyethyl bearing headgroups under high serum conditions. *Org Biomol Chem* **2018,** *16* (11), 1983-1993.

204. Ma, L. L.; Tang, Q.; Liu, M. X.; Liu, X. Y.; Liu, J. Y.; Lu, Z. L.; Gao, Y. G.; Wang, R., [12]aneN3-Based Gemini-Type Amphiphiles with Two-Photon Absorption Properties for Enhanced Nonviral Gene Delivery and Bioimaging. *ACS Appl Mater Interfaces* **2020,** *12* (36), 40094-40107.

205. Gosangi, M.; Ravula, V.; Rapaka, H.; Patri, S. V., alpha-Tocopherol-anchored gemini lipids with delocalizable cationic head groups: the effect of spacer length on DNA compaction and transfection properties. *Org Biomol Chem* **2021**.

206. Grippo, L. D.; Reidel, I. G.; García, M. I.; Streu, A.; Müller, D. M.; Veaute, C. M., Gemini lipopeptides as vaccine adjuvants: a new role for these versatile carriers. *Clinical and Experimental Vaccine Research* **2020,** *9* (2).

207. Zheng, Y.; Guo, Y.; Li, Y.; Wu, Y.; Zhang, L.; Yang, Z., A novel gemini-like cationic lipid for the efficient delivery of siRNA. *New J. Chem.* **2014,** *38* (10), 4952-4962.

208. Ma, X. F.; Sun, J.; Qiu, C.; Wu, Y. F.; Zheng, Y.; Yu, M. Z.; Pei, X. W.; Wei, L.; Niu, Y. J.; Pang, W. H.; Yang, Z. J.; Wang, J. C.; Zhang, Q., The role of disulfide-bridge on the activities of H-shape gemini-like cationic lipid based siRNA delivery. *J Control Release* **2016,** *235*, 99-111.

209. Li, Y.; Jarvis, R.; Zhu, K.; Glass, Z.; Ogurlu, R.; Gao, P.; Li, P.; Chen, J.; Yu, Y.; Yang, Y.; Xu, Q., Protein and mRNA Delivery Enabled by Cholesteryl-Based Biodegradable Lipidoid Nanoparticles. *Angew Chem Int Ed Engl* **2020,** *59* (35), 14957-14964.

210. Netto, L. E. S.; Stadtman, E. R., The Iron-Catalyzed Oxidation of Dithiothreitol Is a Biphasic Process: Hydrogen Peroxide Is Involved in the Initiation of a Free Radical Chain of Reactions. *Archives of Biochemistry and Biophysics* **1996,** *333* (1), 233-242.

211. Grant, N.; Wu, H.; Zhang, H., Reduction-Controlled Release of Organic Nanoparticles from Disulfide Cross-linked Porous Polymer. *Industrial & Engineering Chemistry Research* **2013,** *53* (1), 246-252.

212. Lee, Y.; Thompson, D. H., Stimuli-responsive liposomes for drug delivery. *Wiley Interdiscip Rev Nanomed Nanobiotechnol* **2017,** *9* (5).

213. Qin, B.; Yuan, X.; Jiang, M.; Yin, H.; Luo, Z.; Zhang, J.; Zhu, C.; Li, X.; Shi, Y.; Luo, L.; Du, Y.; You, J., Targeting DNA to the endoplasmic reticulum efficiently enhances gene delivery and therapy. *Nanoscale* **2020,** *12* (35), 18249-18262.

214. Brock, R., The uptake of arginine-rich cell-penetrating peptides: putting the puzzle together. *Bioconjug Chem* **2014,** *25* (5), 863-8.

215. Alhakamy, N. A.; Nigatu, A. S.; Berkland, C. J.; Ramsey, J. D., Noncovalently associated cell-penetrating peptides for gene delivery applications. *Ther Deliv* **2013,** *4* (6), 741-57.

216. Taylor, R. E.; Zahid, M., Cell Penetrating Peptides, Novel Vectors for Gene Therapy. *Pharmaceutics* **2020,** *12* (3).

217. Schneider, A. F. L.; Wallabregue, A. L. D.; Franz, L.; Hackenberger, C. P. R., Targeted Subcellular Protein Delivery Using Cleavable Cyclic Cell-Penetrating Peptides. *Bioconjugate Chemistry* **2019,** *30* (2), 400-404.

218. Dowaidar, M.; Abdelhamid, H. N.; Hallbrink, M.; Zou, X.; Langel, U., Graphene oxide nanosheets in complex with cell penetrating peptides for oligonucleotides delivery. *Biochim Biophys Acta Gen Subj* **2017,** *1861* (9), 2334-2341.

219. Abdelhamid, H. N.; Dowaidar, M.; Langel, Ü., Carbonized chitosan encapsulated hierarchical porous zeolitic imidazolate frameworks nanoparticles for gene delivery. *Microporous and Mesoporous Materials* **2020,** *302*.

220. Abdelhamid, H. N.; Dowaidar, M.; Hällbrink, M.; Langel, Ü., Gene delivery using cell penetrating peptides-zeolitic imidazolate frameworks. *Microporous and Mesoporous Materials* **2020,** *300*.

221. Gabas, I. M.; Nielsen, P. E., Effective Cellular Delivery of Antisense Peptide Nucleic Acid by Conjugation to Guanidinylated Diaminobutanoic Acid-Based Peptide Dendrons. *Biomacromolecules* **2020,** *21* (2), 472-483.

222. Jiang, Q.; Chen, X.; Liang, H.; Nie, Y.; Jin, R.; Barz, M.; Yue, D.; Gu, Z., Multistage rocket: integrational design of a prodrug-based siRNA delivery system with sequential release for enhanced antitumor efficacy. *Nanoscale Advances* **2019,** *1* (2), 498-507.

223. Tseng, W.-C.; Haselton, F. R.; Giorgio, T. D., Transfection by Cationic Liposomes Using Simultaneous Single Cell Measurements of Plasmid Delivery and Transgene Expression. *Journal of Biological Chemistry* **1997,** *272* (41), 25641-25647.

224. Armas, F.; Pacor, S.; Ferrari, E.; Guida, F.; Pertinhez, T. A.; Romani, A. A.; Scocchi, M.; Benincasa, M., Design, antimicrobial activity and mechanism of action of Arg-rich ultra-short cationic lipopeptides. *PLoS One* **2019,** *14* (2), e0212447.

225. Sikorska, E.; Stachurski, O.; Neubauer, D.; Maluch, I.; Wyrzykowski, D.; Bauer, M.; Brzozowski, K.; Kamysz, W., Short arginine-rich lipopeptides: From self-assembly to antimicrobial activity. *Biochim Biophys Acta Biomembr* **2018,** *1860* (11), 2242-2251.

226. Makovitzki, A.; Avrahami, D.; Shai, Y., Ultrashort antibacterial and antifungal lipopeptides. *Proc Natl Acad Sci U S A* **2006,** *103* (43), 15997-6002.

227. Huang, W.; Seo, J.; Willingham, S. B.; Czyzewski, A. M.; Gonzalgo, M. L.; Weissman, I. L.; Barron, A. E., Learning from host-defense peptides: cationic, amphipathic peptoids with potent anticancer activity. *PLoS One* **2014,** *9* (2), e90397.

228. Domalaon, R.; Findlay, B.; Ogunsina, M.; Arthur, G.; Schweizer, F., Ultrashort cationic lipopeptides and lipopeptoids: Evaluation and mechanistic insights against epithelial cancer cells. *Peptides* **2016,** *84*, 58-67.

229. Wu, Y. S.; Ngai, S. C.; Goh, B. H.; Chan, K. G.; Lee, L. H.; Chuah, L. H., Anticancer Activities of Surfactin and Potential Application of Nanotechnology Assisted Surfactin Delivery. *Front Pharmacol* **2017,** *8*, 761.

230. Shai, Y., Mode of action of membrane active antimicrobial peptides. *Biopolymers* **2002,** *66* (4), 236-48.

231. Xie, M.; Liu, D.; Yang, Y., Anti-cancer peptides: classification, mechanism of action, reconstruction and modification. *Open Biol* **2020,** *10* (7), 200004.

232. Ployon, S.; Belloir, C.; Bonnotte, A.; Lherminier, J.; Canon, F.; Morzel, M., The membrane-associated MUC1 improves adhesion of salivary MUC5B on buccal cells. Application to development of an in vitro cellular model of oral epithelium. *Arch Oral Biol* **2016,** *61*, 149-55.

233. Lojk, J.; Cibej, U.; Karlas, D.; Sajn, L.; Pavlin, M., Comparison of two automatic cell-counting solutions for fluorescent microscopic images. *J Microsc* **2015,** *260* (1), 107-16.

234. Lasic, D. D., Novel applications of liposomes. *Trends Biotechnol* **1998,** *16* (7), 307-21.

235. Wang, L.; MacDonald, R. C., New strategy for transfection: mixtures of medium-chain and long-chain cationic lipids synergistically enhance transfection. *Gene Ther* **2004,** *11* (17), 1358-62.

236. Wang, L.; Koynova, R.; Parikh, H.; MacDonald, R. C., Transfection activity of binary mixtures of cationic o-substituted phosphatidylcholine derivatives: the hydrophobic core strongly modulates physical properties and DNA delivery efficacy. *Biophys J* **2006,** *91* (10), 3692-706.

237. Koynova, R.; Wang, L.; MacDonald, R. C., Synergy in lipofection by cationic lipid mixtures: superior activity at the gel-liquid crystalline phase transition. *J Phys Chem B* **2007,** *111* (27), 7786-95.

238. Ravula, V.; Lo, Y. L.; Wu, Y. T.; Chang, C. W.; Patri, S. V.; Wang, L. F., Arginine-tocopherol bioconjugated lipid vesicles for selective pTRAIL delivery and subsequent apoptosis induction in glioblastoma cells. *Materials Science & Engineering C-Materials for Biological Applications* **2021,** *126*.

239. Sanchez-Arribas, N.; Martinez-Negro, M.; Villar, E. M.; Perez, L.; Aicart, E.; Taboada, P.; Guerrero-Martinez, A.; Junquera, E., Biocompatible Nanovector of siRNA Consisting of Arginine-Based Cationic Lipid for Gene Knockdown in Cancer Cells. *ACS Appl Mater Interfaces* **2020,** *12* (31), 34536-34547.

240. Kim, B. K.; Hwang, G. B.; Seu, Y. B.; Choi, J. S.; Jin, K. S.; Doh, K. O., DOTAP/DOPE ratio and cell type determine transfection efficiency with DOTAP-liposomes. *Biochim Biophys Acta* **2015,** *1848* (10 Pt A), 1996-2001.

241. Ravula, V.; Lo, Y.-L.; Wang, L.-F.; Patri, S. V., Gemini Lipopeptide Bearing an Ultrashort Peptide for Enhanced Transfection Efficiency and Cancer-Cell-Specific Cytotoxicity. *ACS Omega* **2021,** *6* (35), 22955-22968.

242. Sarker, S. R.; Arai, S.; Murate, M.; Takahashi, H.; Takata, M.; Kobayashi, T.; Takeoka, S., Evaluation of the influence of ionization states and spacers in the thermotropic phase behaviour of amino acid-based cationic lipids and the transfection efficiency of their assemblies. *Int J Pharm* **2012,** *422* (1-2), 364-73.

243. Andar, A. U.; Hood, R. R.; Vreeland, W. N.; Devoe, D. L.; Swaan, P. W., Microfluidic Preparation of Liposomes to Determine Particle Size Influence on Cellular Uptake Mechanisms. *Pharm Res-Dordr* **2014,** *31* (2), 401-413.

244. Nagayasu, A.; Uchiyama, K.; Kiwada, H., The size of liposomes: a factor which affects their targeting efficiency to tumors and therapeutic activity of liposomal antitumor drugs. *Adv Drug Deliv Rev* **1999,** *40* (1-2), 75-87.

245. Drummond, D. C.; Meyer, O.; Hong, K.; Kirpotin, D. B.; Papahadjopoulos, D., Optimizing liposomes for delivery of chemotherapeutic agents to solid tumors. *Pharmacol Rev* **1999,** *51* (4), 691-743.

246. Campbell, R. B.; Balasubramanian, S. V.; Straubinger, R. M., Phospholipid-cationic lipid interactions: influences on membrane and vesicle properties. *Biochim Biophys Acta* **2001,** *1512* (1), 27-39.

247. Zuidam, N. J.; Barenholz, Y., Electrostatic parameters of cationic liposomes commonly used for gene delivery as determined by 4-heptadecyl-7-hydroxycoumarin. *Biochim Biophys Acta* **1997,** *1329* (2), 211-22.

248. Lechanteur, A.; Sanna, V.; Duchemin, A.; Evrard, B.; Mottet, D.; Piel, G., Cationic Liposomes Carrying siRNA: Impact of Lipid Composition on Physicochemical Properties, Cytotoxicity and Endosomal Escape. *Nanomaterials (Basel)* **2018,** *8* (5).

249. Koynova, R.; Wang, L.; MacDonald, R. C., An intracellular lamellar-nonlamellar phase transition rationalizes the superior performance of some cationic lipid transfection agents. *Proc Natl Acad Sci U S A* **2006,** *103* (39), 14373-8.

250. Li, L.; Nie, Y.; Zhu, R.; Shi, S.; Luo, K.; He, B.; Yang, Y.; Yang, J.; Gu, Z., Preparation and gene delivery of alkaline amino acids-based cationic liposomes. *Arch Pharm Res* **2008,** *31* (7), 924-31.

251. Obata, Y.; Ciofani, G.; Raffa, V.; Cuschieri, A.; Menciassi, A.; Dario, P.; Takeoka, S., Evaluation of cationic liposomes composed of an amino acid-based lipid for neuronal transfection. *Nanomed-Nanotechnol* **2010,** *6* (1), 70-77.

252. Zhao, Y.; Zhang, S.; Zhang, Y.; Cui, S.; Chen, H.; Zhi, D.; Zhen, Y.; Zhang, S.; Huang, L., Tri-peptide cationic lipids for gene delivery. *J Mater Chem B* **2015,** *3* (1), 119-126.

253. Lo, Y. L.; Chou, H. L.; Liao, Z. X.; Huang, S. J.; Ke, J. H.; Liu, Y. S.; Chiu, C. C.; Wang, L. F., Chondroitin sulfate-polyethylenimine copolymer-coated superparamagnetic iron oxide nanoparticles as an efficient magneto-gene carrier for microRNA-encoding plasmid DNA delivery. *Nanoscale* **2015,** *7* (18), 8554-8565.

254. Li, S.; Huang, L., Nonviral gene therapy: promises and challenges. *Gene Ther* **2000,** *7* (1), 31-4.

255. Karmali, P. P.; Chaudhuri, A., Cationic liposomes as non-viral carriers of gene medicines: Resolved issues, open questions, and future promises. *Medicinal Research Reviews* **2007,** *27* (5), 696-722.

256. Loh, X. J.; Lee, T. C.; Dou, Q.; Deen, G. R., Utilising inorganic nanocarriers for gene delivery. *Biomater Sci* **2016,** *4* (1), 70-86.

257. Muripiti, V.; Gondru, R.; Patri, S. V., Review of Zinc(II) Scaffolds: Efficient Role in Gene Delivery. *ChemistrySelect* **2020,** *5* (25), 7638-7647.

258. Pack, D. W.; Hoffman, A. S.; Pun, S.; Stayton, P. S., Design and development of polymers for gene delivery. *Nat Rev Drug Discov* **2005,** *4* (7), 581-93.

259. Franiak-Pietryga, I.; Ziemba, B.; Messmer, B.; Skowronska-Krawczyk, D., Dendrimers as Drug Nanocarriers: The Future of Gene Therapy and Targeted Therapies in Cancer. In *Dendrimers - Fundamentals and Applications*, 2018.

260. Wang, D.; Zhao, T.; Zhu, X.; Yan, D.; Wang, W., Bioapplications of hyperbranched polymers. *Chem Soc Rev* **2015,** *44* (12), 4023-71.

261. Fichert, T.; Regelin, A.; Massing, U., Synthesis and transfection properties of novel non-toxic monocationic lipids. Variation of lipid anchor, spacer and head group structure. *Bioorg Med Chem Lett* **2000,** *10* (8), 787-91.

262. Banerjee, R.; Das, P. K.; Srilakshmi, G. V.; Chaudhuri, A.; Rao, N. M., Novel Series of Non-Glycerol-Based Cationic Transfection Lipids for Use in Liposomal Gene Delivery1,†. *Journal of Medicinal Chemistry* **1999,** *42* (21), 4292-4299.

263. Rajesh, M.; Sen, J.; Srujan, M.; Mukherjee, K.; Sreedhar, B.; Chaudhuri, A., Dramatic influence of the orientation of linker between hydrophilic and hydrophobic lipid moiety in liposomal gene delivery. *J Am Chem Soc* **2007,** *129* (37), 11408-20.

264. Narang, A. S.; Thoma, L.; Miller, D. D.; Mahato, R. I., Cationic lipids with increased DNA binding affinity for nonviral gene transfer in dividing and nondividing cells. *Bioconjug Chem* **2005,** *16* (1), 156-68.

265. Banerjee, R.; Mahidhar, Y. V.; Chaudhuri, A.; Gopal, V.; Rao, N. M., Design, synthesis, and transfection biology of novel cationic glycolipids for use in liposomal gene delivery. *J Med Chem* **2001,** *44* (24), 4176-85.

266. Mukthavaram, R.; Marepally, S.; Venkata, M. Y.; Vegi, G. N.; Sistla, R.; Chaudhuri, A., Cationic glycolipids with cyclic and open galactose head groups for the selective targeting of genes to mouse liver. *Biomaterials* **2009,** *30* (12), 2369-84.

267. Muripiti, V.; Lohchania, B.; Ravula, V.; Manturthi, S.; Marepally, S.; Velidandi, A.; Patri, S. V., Dramatic influence of the hydroxy functionality of azasugar moiety in the head

group region of tocopherol-based cationic lipids on in vitro gene transfection efficacies. *New Journal of Chemistry* **2021,** *45* (2), 615-627.

268. Ravula, V.; Lo, Y. L.; Wu, Y. T.; Chang, C. W.; Patri, S. V.; Wang, L. F., Arginine-tocopherol bioconjugated lipid vesicles for selective pTRAIL delivery and subsequent apoptosis induction in glioblastoma cells. *Mater Sci Eng C Mater Biol Appl* **2021,** *126*, 112189.

269. Muripiti, V.; Mujahid, T. Y.; Boddeda, V. H. V.; Tiwari, S.; Marepally, S. K.; Patri, S. V.; Gopal, V., Structure-activity relationship of serotonin derived tocopherol lipids. *Int J Pharm* **2019,** *554*, 134-148.

270. Gosangi, M.; Ravula, V.; Rapaka, H.; Patri, S. V., alpha-Tocopherol-anchored gemini lipids with delocalizable cationic head groups: the effect of spacer length on DNA compaction and transfection properties. *Org Biomol Chem* **2021,** *19* (20), 4565-4576.

271. Leitgeb, M.; Knez, Z.; Primozic, M., Sustainable technologies for liposome preparation. *J Supercrit Fluid* **2020,** *165*.

272. Bochot, A.; Fattal, E., Liposomes for intravitreal drug delivery: A state of the art. *J Control Release* **2012,** *161* (2), 628-634.

273. Liu, R.; Gan, L.; Yang, X.; Xu, H., Chitosan as a condensing agent induces high gene transfection efficiency and low cytotoxicity of liposome. *Journal of Bioscience and Bioengineering* **2011,** *111* (1), 98-103.

274. Tao, J.; Ding, W. F.; Che, X. H.; Chen, Y. C.; Chen, F.; Chen, X. D.; Ye, X. L.; Xiong, S. B., Optimization of a cationic liposome-based gene delivery system for the application of miR-145 in anticancer therapeutics. *Int J Mol Med* **2016,** *37* (5), 1345-54.

275. Patil, Y. P.; Jadhav, S., Novel methods for liposome preparation. *Chem Phys Lipids* **2014,** *177*, 8-18.

276. Islam, M. A.; Yun, C. H.; Choi, Y. J.; Shin, J. Y.; Arote, R.; Jiang, H. L.; Kang, S. K.; Nah, J. W.; Park, I. K.; Cho, M. H.; Cho, C. S., Accelerated gene transfer through a polysorbitol-based transporter mechanism. *Biomaterials* **2011,** *32* (36), 9908-24.

277. Park, T. E.; Kang, B.; Kim, Y. K.; Zhang, Q.; Lee, W. S.; Islam, M. A.; Kang, S. K.; Cho, M. H.; Choi, Y. J.; Cho, C. S., Selective stimulation of caveolae-mediated endocytosis by an osmotic polymannitol-based gene transporter. *Biomaterials* **2012,** *33* (29), 7272-81.

278. He, C.; Wang, S.; Liu, M.; Zhao, C.; Xiang, S.; Zeng, Y., Design, synthesis and in vitro evaluation ofd-glucose-based cationic glycolipids for gene delivery. *Organic & Biomolecular Chemistry* **2016,** *14* (5), 1611-1622.

279. Xiao, F.; Chen, Z.; Wei, Z.; Tian, L., Hydrophobic Interaction: A Promising Driving Force for the Biomedical Applications of Nucleic Acids. *Advanced Science* **2020,** *7* (16).

280. Mady, M. M.; Ghannam, M. M., Stability of anionic liposomes in serum and plasma. *Afr J Pharm Pharmaco* **2011,** *5* (16), 1898-1905.

281. Chen, Z. J.; Yang, S. C.; Liu, X. L.; Gao, Y.; Dong, X.; Lai, X.; Zhu, M. H.; Feng, H. Y.; Zhu, X. D.; Lu, Q.; Zhao, M.; Chen, H. Z.; Lovell, J. F.; Fang, C., Nanobowl-Supported Liposomes Improve Drug Loading and Delivery. *Nano Lett* **2020,** *20* (6), 4177-4187.

282. Hong, S. J.; Ahn, M. H.; Sangshetti, J.; Arote, R. B., Sugar alcohol-based polymeric gene carriers: Synthesis, properties and gene therapy applications. *Acta Biomater* **2019,** *97*, 105-115.

283. Hong, S. J.; Ahn, M. H.; Sangshetti, J.; Choung, P. H.; Arote, R. B., Sugar-based gene delivery systems: Current knowledge and new perspectives. *Carbohydr Polym* **2018,** *181*, 1180-1193.

284. Ren, X.; Liu, L.; Zhou, Y.; Zhu, Y.; Zhang, H.; Zhang, Z.; Li, H., Nanoparticle siRNA against BMI-1 with a Polyethylenimine-Laminarin Conjugate for Gene Therapy in Human Breast Cancer. *Bioconjug Chem* **2016,** *27* (1), 66-73.

285. Choi, S. I.; Maeng, Y. S.; Kim, T. I.; Lee, Y.; Kim, Y. S.; Kim, E. K., Lysosomal trafficking of TGFBIp via caveolae-mediated endocytosis. *PLoS One* **2015,** *10* (4), e0119561.

286. Mukthavaram, R.; Marepally, S.; Venkata, M. Y.; Vegi, G. N.; Sistla, R.; Chaudhuri, A., Cationic glycolipids with cyclic and open galactose head groups for the selective targeting of genes to mouse liver. *Biomaterials* **2009,** *30* (12), 2369-2384.

287. Smistad, G.; Jacobsen, J.; Sande, S. A., Multivariate toxicity screening of liposomal formulations on a human buccal cell line. *Int J Pharm* **2007,** *330* (1-2), 14-22.

288. Bangham, A. D.; Hill, M. W.; Miller, N. G. A., Preparation and Use of Liposomes as Models of Biological Membranes. In *Methods in Membrane Biology*, 1974; pp 1-68.

289. Pagé, M.; Bejaoui, N.; Cinq-Mars, B.; Lemieux, P., Optimization of the tetrazolium-based colorimetric assay for the measurement of cell number and cytotoxicity. *International Journal of Immunopharmacology* **1988,** *10* (7), 785-793.

290. Srinivas, R.; Samanta, S.; Chaudhuri, A., Cationic amphiphiles: promising carriers of genetic materials in gene therapy. *Chem Soc Rev* **2009,** *38* (12), 3326-38.

291. Zhao, Y. N.; Qureshi, F.; Zhang, S. B.; Cui, S. H.; Wang, B.; Chen, H. Y.; Lv, H. T.; Zhang, S. F.; Huang, L., Novel gemini cationic lipids with carbamate groups for gene delivery. *J Mater Chem B* **2014,** *2* (19), 2920-2928.

292. Shi, J.; Yu, S.; Zhu, J.; Zhi, D.; Zhao, Y.; Cui, S.; Zhang, S., Carbamate-linked cationic lipids with different hydrocarbon chains for gene delivery. *Colloids Surf B Biointerfaces* **2016,** *141*, 417-422.

293. Englezou, P. C.; Sapet, C.; Demoulins, T.; Milona, P.; Ebensen, T.; Schulze, K.; Guzman, C. A.; Poulhes, F.; Zelphati, O.; Ruggli, N.; McCullough, K. C., Self-Amplifying Replicon RNA Delivery to Dendritic Cells by Cationic Lipids. *Mol Ther Nucleic Acids* **2018,** *12*, 118-134.

294. Oliveira, A. V.; Rosa da Costa, A. M.; Silva, G. A., Non-viral strategies for ocular gene delivery. *Mater Sci Eng C Mater Biol Appl* **2017,** *77*, 1275-1289.

295. Li, L.; He, Z. Y.; Wei, X. W.; Wei, Y. Q., Recent advances of biomaterials in biotherapy. *Regen Biomater* **2016,** *3* (2), 99-105.

296. Wang, M.; Cheng, Y., The effect of fluorination on the transfection efficacy of surface-engineered dendrimers. *Biomaterials* **2014,** *35* (24), 6603-13.

297. Liu, D.; Qiao, W.; Li, Z.; Chen, Y.; Cui, X.; Li, K.; Yu, L.; Yan, K.; Zhu, L.; Guo, Y.; Cheng, L., Structure-function relationship research of glycerol backbone-based cationic lipids for gene delivery. *Chem Biol Drug Des* **2008,** *71* (4), 336-44.

298. Behr, J. P.; Demeneix, B.; Loeffler, J. P.; Perez-Mutul, J., Efficient gene transfer into mammalian primary endocrine cells with lipopolyamine-coated DNA. *Proc Natl Acad Sci U S A* **1989,** *86* (18), 6982-6.

299. Sheng, R.; Luo, T.; Li, H.; Sun, J.; Wang, Z.; Cao, A., Cholesterol-based cationic lipids for gene delivery: contribution of molecular structure factors to physico-chemical and biological properties. *Colloids Surf B Biointerfaces* **2014,** *116*, 32-40.

300. Bajaj, A.; Kondiah, P.; Bhattacharya, S., Design, synthesis, and in vitro gene delivery efficacies of novel cholesterol-based gemini cationic lipids and their serum compatibility: a structure-activity investigation. *J Med Chem* **2007,** *50* (10), 2432-42.

301. Radchatawedchakoon, W.; Thongbamrer, C.; Konbamrung, W.; Khattawee, P.; Sakee, U.; Roobsoong, W.; Sattabongkot, J.; Opanasopit, P.; Yingyongnarongkul, B. E., The effect of polar headgroups and spacer length on the DNA transfection of cholesterol-based cationic lipids. *RSC Med Chem* **2020,** *11* (2), 212-224.

302. Ju, J.; Huan, M. L.; Wan, N.; Qiu, H.; Zhou, S. Y.; Zhang, B. L., Novel cholesterol-based cationic lipids as transfecting agents of DNA for efficient gene delivery. *Int J Mol Sci* **2015,** *16* (3), 5666-81.

303. Medvedeva, D. A.; Maslov, M. A.; Serikov, R. N.; Morozova, N. G.; Serebrenikova, G. A.; Sheglov, D. V.; Latyshev, A. V.; Vlassov, V. V.; Zenkova, M. A., Novel cholesterol-based cationic lipids for gene delivery. *J Med Chem* **2009,** *52* (21), 6558-68.

304. Venkata Srilakshmi, G.; Sen, J.; Chaudhuri, A.; Ramadas, Y.; Madhusudhana Rao, N., Anchor-dependent lipofection with non-glycerol based cytofectins containing single 2-hydroxyethyl head groups. *Biochim Biophys Acta* **2002,** *1559* (2), 87-95.

305. Sen, J.; Chaudhuri, A., Design, syntheses, and transfection biology of novel non-cholesterol-based guanidinylated cationic lipids. *J Med Chem* **2005,** *48* (3), 812-20.

306. Kedika, B.; Patri, S. V., Design, Synthesis, and in Vitro Transfection Biology of Novel Tocopherol Based Monocationic Lipids: A Structure-Activity Investigation. *Journal of Medicinal Chemistry* **2011,** *54* (2), 548-561.

307. Muripiti, V.; Mujahid, T. Y.; Boddeda, V. H. V.; Tiwari, S.; Marepally, S. K.; Patri, S. V.; Gopal, V., Structure-activity relationship of serotonin derived tocopherol lipids. *Int J Pharmaceut* **2019,** *554*, 134-148.

308. Gosangi, M.; Rapaka, H.; Ravula, V.; Patri, S. V., Evolution of New "Bolaliposomes" using Novel alpha-Tocopheryl Succinate Based Cationic Lipid and 1,12-Disubstituted Dodecane-Based Bolaamphiphile for Efficient Gene Delivery. *Bioconjugate Chem* **2017,** *28* (7), 1965-1977.

309. Gosangi, M.; Mujahid, T. Y.; Gopal, V.; Patri, S. V., Effects of heterocyclic-based head group modifications on the structure-activity relationship of tocopherol-based lipids for non-viral gene delivery. *Org Biomol Chem* **2016,** *14* (28), 6857-6870.

310. Buck, J.; Grossen, P.; Cullis, P. R.; Huwyler, J.; Witzigmann, D., Lipid-Based DNA Therapeutics: Hallmarks of Non-Viral Gene Delivery. *ACS Nano* **2019,** *13* (4), 3754-3782.

311. Liu, C.; Zhang, L.; Zhu, W.; Guo, R.; Sun, H.; Chen, X.; Deng, N., Barriers and Strategies of Cationic Liposomes for Cancer Gene Therapy. *Mol Ther Methods Clin Dev* **2020,** *18*, 751-764.

312. Loisel, S.; Floch, V.; Le Gall, C.; Ferec, C., Factors influencing the efficiency of lipoplexes mediated gene transfer in lung after intravenous administration 1 *. *J Liposome Res* **2001,** *11* (2-3), 127-38.

313. Fletcher, S.; Ahmad, A.; Perouzel, E.; Heron, A.; Miller, A. D.; Jorgensen, M. R., In vivo studies of dialkynoyl analogues of DOTAP demonstrate improved gene transfer efficiency of cationic liposomes in mouse lung. *J Med Chem* **2006,** *49* (1), 349-57.

314. Wang, B.; Zhao, R. M.; Zhang, J.; Liu, Y. H.; Huang, Z.; Yu, Q. Y.; Yu, X. Q., Rigid aromatic linking moiety in cationic lipids for enhanced gene transfection efficiency. *Eur J Med Chem* **2017,** *136*, 585-595.

315. Tassler, S.; Pawlowska, D.; Janich, C.; Dobner, B.; Wolk, C.; Brezesinski, G., Lysine-based amino-functionalized lipids for gene transfection: the influence of the chain composition on 2D properties. *Phys Chem Chem Phys* **2018,** *20* (10), 6936-6944.

316. Koynova, R.; Tenchov, B.; Wang, L.; Macdonald, R. C., Hydrophobic moiety of cationic lipids strongly modulates their transfection activity. *Mol Pharm* **2009,** *6* (3), 951-8.

317. Zuhorn, I. S.; Oberle, V.; Visser, W. H.; Engberts, J. B. F. N.; Bakowsky, U.; Polushkin, E.; Hoekstra, D., Phase behavior of cationic amphiphiles and their mixtures with helper lipid influences lipoplex shape, DNA translocation, and transfection efficiency. *Biophys J* **2002,** *83* (4), 2096-2108.

318. Zhou, H.; Yang, J.; Du, Y.; Fu, S.; Song, C.; Zhi, D.; Zhao, Y.; Chen, H.; Zhang, S.; Zhang, S., Novel carbamate-linked quaternary ammonium lipids containing unsaturated hydrophobic chains for gene delivery. *Bioorg Med Chem* **2018,** *26* (12), 3535-3540.

319. Martin, B.; Sainlos, M.; Aissaoui, A.; Oudrhiri, N.; Hauchecorne, M.; Vigneron, J. P.; Lehn, J. M.; Lehn, P., The design of cationic lipids for gene delivery. *Curr Pharm Des* **2005,** *11* (3), 375-94.

320. Silva, J. C.; de Moraes Alcantara, L. F.; Dias Soares, J. M.; e Silva, M. G.; de Lavor, É. M.; Andrade, V. M.; dos Passos Menezes, P.; de Souza Araújo, A. A.; Leite, L. H. I.; de Menezes, I. R. A.; Scotti, L.; Scotti, M. T.; Oliveira, R. C. M.; Quintans, J. S. S.; Silva Almeida, J. R. G.; Quintans-Júnior, L. J., Docking, characterization and investigation of β-cyclodextrin complexed with farnesol, an acyclic sesquiterpene alcohol, produces orofacial antinociceptive profile in experimental protocols. *Process Biochemistry* **2017,** *62*, 193-204.

321. Santhanasabapathy, R.; Sudhandiran, G., Farnesol attenuates lipopolysaccharide-induced neurodegeneration in Swiss albino mice by regulating intrinsic apoptotic cascade. *Brain Res* **2015,** *1620*, 42-56.

322. Delmondes, G. A.; Santiago Lemos, I. C.; Dias, D. Q.; Cunha, G. L. D.; Araujo, I. M.; Barbosa, R.; Coutinho, H. D. M.; Felipe, C. F. B.; Barbosa-Filho, J. M.; Lima, N. T. R.; De Menezes, I. R. A.; Kerntopf, M. R., Pharmacological applications of farnesol (C15H26O): a patent review. *Expert Opin Ther Pat* **2020,** *30* (3), 227-234.

323. Kim, B. K.; Bae, Y. U.; Doh, K. O.; Hwang, G. B.; Lee, S. H.; Kang, H.; Seu, Y. B., The synthesis of cholesterol-based cationic lipids with trimethylamine head and the effect of spacer structures on transfection efficiency. *Bioorg Med Chem Lett* **2011,** *21* (12), 3734-7.

324. Saha, A.; Panda, S.; Paul, S.; Manna, D., Phosphate bioisostere containing amphiphiles: a novel class of squaramide-based lipids. *Chem Commun (Camb)* **2016,** *52* (60), 9438-41.

325. Nowacka, M.; Kowalewska, A.; Kręgiel, D., Farnesol-Containing Macromolecular Systems for Antibiofilm Strategies. *Surfaces* **2020,** *3* (2), 197-210.

326. Derengowski, L. S.; De-Souza-Silva, C.; Braz, S. V.; Mello-De-Sousa, T. M.; Bao, S. N.; Kyaw, C. M.; Silva-Pereira, I., Antimicrobial effect of farnesol, a Candida albicans quorum sensing molecule, on Paracoccidioides brasiliensis growth and morphogenesis. *Ann Clin Microbiol Antimicrob* **2009,** *8*, 13.

327. Bhadani, A.; Rane, J.; Veresmortean, C.; Banerjee, S.; John, G., Bio-inspired surfactants capable of generating plant volatiles. *Soft Matter* **2015,** *11* (15), 3076-3082.

328. Tošovská, P.; Arora, P. S., Oligooxopiperazines as Nonpeptidic α-Helix Mimetics. *Organic Letters* **2010,** *12* (7), 1588-1591.

329. Patchett, A. A.; Nargund, R. P., Chapter 26. Privileged structures — An update. 2000; pp 289-298.

330. Kim, J.; Lee, W. S.; Koo, J.; Lee, J.; Park, S. B., Synthesis and library construction of privileged tetra-substituted Delta5-2-oxopiperazine as beta-turn structure mimetics. *ACS Comb Sci* **2014,** *16* (1), 24-32.

331. Kitamura, S.; Fukushi, H.; Miyawaki, T.; Kawamura, M.; Konishi, N.; Terashita, Z.; Naka, T., Potent dibasic GPIIb/IIIa antagonists with reduced prolongation of bleeding time: synthesis and pharmacological evaluation of 2-oxopiperazine derivatives. *J Med Chem* **2001,** *44* (15), 2438-50.

332. Valdivielso, A. M.; Ventosa-Andres, P.; Tato, F.; Fernandez-Ibanez, M. A.; Pappos, I.; Tsopanoglou, N. E.; Garcia-Lopez, M. T.; Gutierrez-Rodriguez, M.; Herranz, R., Highly functionalized 2-oxopiperazine-based peptidomimetics: an approach to PAR1 antagonists. *Eur J Med Chem* **2013,** *70*, 199-224.

333. Kounde, C. S.; Yeo, H. Q.; Wang, Q. Y.; Wan, K. F.; Dong, H.; Karuna, R.; Dix, I.; Wagner, T.; Zou, B.; Simon, O.; Bonamy, G. M. C.; Yeung, B. K. S.; Yokokawa, F., Discovery of 2-oxopiperazine dengue inhibitors by scaffold morphing of a phenotypic high-throughput screening hit. *Bioorg Med Chem Lett* **2017,** *27* (6), 1385-1389.

334. Herrero, S.; Garcia-Lopez, M. T.; Latorre, M.; Cenarruzabeitia, E.; Del Rio, J.; Herranz, R., 2-Oxopiperazine-based gamma-turn conformationally constrained peptides: synthesis of CCK-4 analogues. *J Org Chem* **2002,** *67* (11), 3866-73.

List of Publications

1. "Arginine-tocopherol bioconjugated lipid vesicles for selective pTRAIL delivery and subsequent apoptosis induction in glioblastoma cells" **Ravula,** Y.L. Lo, Y.T. Wu, C.W. Chang, S.V. Patri*, L.F. Wang* **Materials Science and Engineering: C, 126 (2021) 112189**
2. "Enhancing the Transfection Efficiency and Cancer-cell-specific Cytotoxicity by Novel Cationic Gemini Lipopeptide Bearing an Ultrashort Peptide" **V. Ravula,** Y.L. Lo, L.F. Wang*, S.V. Patri* **ACS Omega, 6 (2021) 35, 22955–22968**
3. "α-Tocopherol conjugated open sugar based cationic amphiphiles for gene delivery" **V. Ravula,** V. Muripiti, M. Shireesha, S.V. Patri* **ChemistrySelect (Accepted)**
4. "α-Tocopherol-anchored gemini lipids with delocalizable cationic head groups: the effect of spacer length on DNA compaction and transfection properties" M. Gosangi, **V. Ravula,** H. Rapaka, S.V. Patri* **Organic & Biomolecular Chemistry, 19 (2021) 4565-4576;**
5. "Dramatic influence of the hydroxy functionality of azasugar moiety in the head group region of tocopherol-based cationic lipids on in vitro gene transfection efficacies" V. Muripiti, B. Lohchania, **V. Ravula,** S. Manturthi, S. Marepally, A. Velidandi, S. V. Patri* **New Journal of Chemistry 45 (2021) 615-627**
6. **"**A simple reversed-phase HPLC method for the estimation of dimethylarginines and homocysteine in plasma and serum**" V. Ravula**, S. Annapurna Singh* **Separation Science Plus, 1 (2018), 404-410**
7. "Effect of arginine:lysine and glycine:methionine intake ratios on dyslipidemia and selected biomarkers implicated in cardiovascular disease: A study with hypercholesterolemic rats" **R. Venkatesh,** K. Srinivasan, S. Annapurna Singh* **Biomedicine & Pharmacotherapy, 91 (2017) 408-414**
8. "Evolution of new "bolaliposomes" using novel α-tocopheryl succinate based cationic lipid and 1, 12-disubstituted dodecane-based bolaamphiphile for efficient gene delivery" M. Gosangi, H. Rapaka, **V. Ravula**, S.V. Patri* **Bioconjugate Chemistry, 28 (2017) 1965-1977**

Patent

1. Process for preparing arnesol-based cationic lipids for carrying nucleic acids in to desired cell lines, Patri Srilakshmi V., **Ravula Venkatesh**, AU Patent, 2021106376.

CURRICULUM VITAE

Mr. VENKATESH RAVULA

Present: Department of Chemistry,
National Institute of Technology Warangal, Telangana, India. PIN-506004
Residence: H.No: 1-117/1/4/A, Inugurthy, Kesamudram, Warangal
Telangana, India. PIN-506112
+91-9741138928
venkatesh.ravula6@gmail.com,
Web link: http://scholar.google.com/citations?user=1d6WuJQAAAAJ&hl=en
Gender: Male | Date of Birth: 03-06-1989 | Nationality: Indian
Languages knew: Telugu, Hindi, Kannada and English | Marital Status: SINGLE

PROFILE

Ph.D. at National Institute of Technology (NIT) Warangal, with more than seven years of experience in conducting high-level research majoring in bioorganic and medicinal chemistry. Significant research publications and international work experience in the field of **synthesis of organic molecules for biomedical applications**.

EDUCATION

- **Doctor of Philosophy (August 2016 – October 2021)**

  Department of Chemistry, National Institute of Technology (NIT) Warangal, India

  Specialization: Bioorganic and Medicinal Chemistry

  Thesis Title: "Synthesis, Formulation and Biological Evaluation of Novel Cationic Lipid Bio-conjugates for Potential Therapeutic Gene Delivery"

- **Master of Science (5 years Integrated, September 2007 – November 2012)**

  Kakatiya University, Warangal, Telangana, India

  Specialization: Organic Chemistry

  Master's research Project: "Synthesis of Alkynyl Ketones and Their Michael Adducts" at CSIR-Indian Institute of Chemical Technology, Hyderabad

RESEARCH INTERESTS

- Organic Synthesis
- Peptide synthesis
- Medicinal Chemistry
- Biomaterials and drug delivery

RESEARCH EXPERIENCE

- **Doctoral Research Scholar: August 2016 – Present**

  Department of Chemistry, National Institute of Technology (NIT) Warangal, India

- **Research Intern**: **October 2019 – December 2020**
  Department of Medicinal and Applied Chemistry, Kaohsiung Medical University, Kaohsiung, Taiwan.
- **Research Intern**: **December 2017 – May 2018**
  Department of Medicinal and Applied Chemistry, Kaohsiung Medical University, Kaohsiung, Taiwan.
- **Project Research Fellow**: **July 2013 – July 2016**
  Department of Protein Chemistry and Technology, CSIR-Central Food Technological Research Institute, Mysuru, India

TEACHING EXPERIENCE

- Assisted in the smooth conduction of Organic Chemistry Laboratory to the undergraduate students at NIT Warangal for four years.
- Assisted in guiding M.Sc. students during their final semester research projects in the Department of Chemistry, NIT Warangal.

ACADEMIC ACHIEVEMENTS

- Qualified in All India level Graduate Aptitude Test in Engineering (GATE) – 2012
- Qualified in All India level Graduate Aptitude Test in Engineering (GATE) – 2016
- Selected for research internship awarded by Kaohsiung medical University, Taiwan, and Taiwan Experience Education Program (TEEP@India) during December, 2017 – May, 2018.
- Selected for research internship awarded by Kaohsiung medical University, Taiwan, and Taiwan Experience Education Program (TEEP@AsiaPLUS) during October, 2019 – December, 2020.

RESEARCH SKILLS

- Having experience in synthesis and purification of wide range of organic molecules, cationic lipids, peptides, peptide-lipid conjugates and biopolymers.
- Expertise in operating a wide variety of instruments for purification and characterization of organic molecules viz. HPLC, GPC, NMR, Mass and IR spectroscopy.
- Well versed with culturing, maintenance and cryopreservation of cells; Transfection, cellular uptake, Cytotoxicity assays and immunocytochemistry.
- Familiar with UV-Vis, SEM, TEM, DLS, confocal microscopy and flow cytometry.

COMPUTER SKILLS

Proficient in using a variety of software (Chem office, MestReNova, MestReC, Mendeley Reference Manager, Endnote, Origin 8.0 and 8.5, SigmaPlot 11.0 to 14.5, Microsoft Office, Adobe Photoshop 7.0, etc.) for a broad range of data measurement, plotting, analyses and publication writings.

Place: Warangal
Date: 15th November 2021

(Venkatesh Ravula)